Regulation of human cardiac fibroblast function by specific microRNAs

Christopher James Trevelyan

Submitted in accordance with the requirements for the degree of Doctor of Philosophy

The University of Leeds

Faculty of Medicine and Health

Leeds Institute of Cardiovascular and Metabolic Medicine

November, 2022

Funded by the British Heart Foundation

The candidate confirms that the work submitted is his own and that appropriate credit has been given where reference has been made to the work of others.

Acknowledgements

I would like to take this opportunity to say a huge thank you to my supervisor, Dr Neil Turner for his support, guidance, and advice throughout the last 3 years. His teachings as a supervisor have undoubtedly helped me to become a better scientist and his attention to detail has been invaluable in the improvement of the many drafts of this thesis. I would also like to thank him for providing logic and calm during stressful moments and entertaining my excited emails after quickly constructing graphs of PCR results on the train home.

I would also like to say thank you to my co-supervisor Dr Karen Forbes for providing an ear and for offering unique perspectives for the direction of this project. Your straight-forward no-nonsense approach at getting things done was often much needed during the times that I had often overcomplicated my own work. This project would not have been as successful if it was not for your expertise in microRNAs and proteomics.

Thank you to my PGRT, Dr Karen Porter for a seemingly never-ending supply of cardiac fibroblasts, for enthusiasm and advice in the support of my fellowship interview and always being a source of knowledge and encouragement for all things personal development for PhD students in LICAMM.

I would like to thank, the members of the Turner lab, Leander and Michael for their technical support, knowledge and experience and providing an audience for venting about the joys of culturing human cells, in the lab group meetings. I would also like to thank Karen Hemmings for being a fountain of knowledge on practical skills and all things cardiac cells. I would also like to thank Dr Andrew Smith, Sotirios Papaspyros, and the Leeds General Infirmary theatre team for providing a supply of human myocardium tissue for cell isolation at a time of dire straits and lack of cells and thank you to Dr Amanda Maccannell and Professor Lee Roberts for their expertise on mitochondrial experiments. Finally, I would also like to thank all members of the LICAMM community, without who this would not have been possible. This includes everyone from the PhD students to the postdocs and to the SOT who make the things happen so that the science can take place, especially thanks to Julie, Val, Alan, Kay, and Ping.

I would also like to thank all the friends I have made in LICAMM throughout this time, and I will miss our coffee breaks, lunches, socials, and pep talks to keep going when every experiment is failing, thanks especially to Hannah, Abbie, Lauren, Kirsten, Ash, Eva, Mike, Sabina, Sam, Jacob, Michael, Jane L and Jane B.

Thank you to The British Heart Foundation for funding my PhD studentship. This funding and the money they raise in charitable donations is essential for saving and improving lives and the importance of the research cannot be overstated.

I would like to say a final thank you to my parents Elaine and Adrian. Thank you for being so supportive and motivating without expecting or asking for anything. You have been my greatest support system to turn the last 3 (and the other 25) years into a massive success and you have only pushed me to do what you know I am capable of, thank you.

Abstract

Background

Cardiac fibroblasts are pivotal regulators of cardiac function and cardiovascular disease, by sensing and responding to cardiac injury through release of proinflammatory cytokines, synthesising proteins for wound repair and promoting hypertrophy through paracrine signalling. Cardiac fibroblast behaviour and gene/protein expression can be regulated by microRNAs (miRNAs); short noncoding RNAs that perform post-transcriptional regulation by binding to target messenger RNAs (mRNAs). MiR-21a, -214, -224 and -30d were modulated in a mouse model of heart failure and are regulated by p38α MAP kinase expression. The hypothesis is that these miRNAs play important roles in regulating cardiac fibroblast behaviour and expression, relevant to cardiac remodelling.

Methods and Results

MiR-21a, -214, -224 and -30d were differentially expressed in multiple *in vivo* models of cardiac dysfunction. RT-PCR confirmed expression of each miRNA in mouse cardiac fibroblast fractions and cultured mouse and human cardiac fibroblasts. Analysis of relevant stimuli and p38 inhibition revealed important mechanisms of miRNA regulation. Transfection with pre-miRs (overexpression) or anti-miRs (inhibition) modulated expression of important cardiac remodelling mRNAs. A tandem-mass-tagging (TMT) proteomics screen of miR-214 and -30d overexpression in human cardiac fibroblasts predicted that miR-30d significantly regulates activation of protein translation. MiR-214 significantly modulated mitochondrial dysfunction, confirmed by a citrate synthase assay for mitochondrial integrity and decreased gene/protein expression of the mitochondrial fusion protein, MFN2. MiR-214 upregulated the expression of the lysyl oxidase family suggesting modulation of collagen cross-linking. Furthermore, miR-214 decreased gene/protein expression of the mechanosensitive cation channel PIEZO1, decreasing PIEZO1-specific signalling in human cardiac fibroblasts.

Conclusion

This study found that miR-21a, -214, -224 and -30d regulate human cardiac fibroblasts. MiR-214 significantly dysregulated mitochondrial function and inhibited function of PIEZO1-mediated intracellular calcium signalling. Improved understanding of the roles these miRNAs play *in vivo* is necessary to understand how binding of mRNA targets may regulate cardiac fibroblasts in cardiac remodelling.

Table of contents

List of Tables

List of Figures

Abbreviations

ACTA2 Smooth muscle alpha (α)-2 actin

AD Alzheimer's disease

ADAMTS A disintegrin and metalloproteinase with thrombospondin motif

AMI Acute myocardial infarction

AF Atrial fibrillation

Ang II Angiotensin II

AP-1 Activator protein 1

ASO Antisense oligonucleotide

AST Aspartate aminotransferase

ATP Adenosine triphosphate

BMP1 Bone morphogenic protein 1

cTnI Cardiac troponin

Ca2+ Calcium

CAD Coronary artery disease

CDK Cyclin-dependent kinase

CF Cardiac fibroblast

CK-MB Creatinine kinase-MB

CM Cardiomyocyte

COL1A1 Collagen, type I, alpha I

COL1A2 Collagen, type I, alpha II

COL3A1 Collagen, type III, alpha I

C_T Cycle threshold

CVD Cardiovascular disease

DAMP Danger associated molecular pattern

DDR2 Discoidin domain receptor tyrosine kinase 2

DMEM Dulbecco’s modified Eagle’s medium

DMSO Dimethyl sulfoxide

DTNB 5', 5'-Dithiobis 2-nitrobenzoic acid

EC Endothelial cell

ECM Extracellular matrix

EF Ejection fraction

EIF Eukaryotic initiation factor

ELISA Enzyme linked immuno-sorbent assay

ER Endoplasmic reticulum

ERK Extracellular signal-regulated kinase

ETC Electron transport chain

FAK Focal adhesion kinase

FGF Fibroblast growth factor

FCS Foetal calf serum

FMT Fibroblast to myofibroblast transition

GAPDH Glyceraldehyde-3-phosphate dehydrogenase

HF Heart failure

HFpEF Heart failure with preserved ejection fraction

HFrEF Heart failure with reduced ejection fraction

HMGB1 High mobility group box 1

IL Interleukin

IPA Ingenuity pathway analysis

IRAK3 Interleukin 1 receptor associated kinase 3

ISO Isoproterenol

KO Knockout

LAD Left anterior descending

LDH Lactate dehydrogenase

LOX Lysyl oxidase

MnSOD Manganese superoxide dismutase

MACS Magnetic antibody cell separation

MAPK Mitogen-activated protein kinase

MI Myocardial infarction

MiRNA MicroRNA

MFN2 Mitofusin 2

MMP Matrix metalloproteinase

MRNA Messenger RNA

MyoFb Myofibroblast

MYH6 Myosin Heavy Chain 6

MYH11 Myosin Heavy Chain 11

NDUF NADH-ubiquinone oxidoreductase protein

NF-κB Nuclear factor kappa B

NLR Nucleotide-binding oligomerization domain–like receptors

NYHA New York Heart Association

PAD Peripheral artery disease

PBS Phosphate-buffered saline

PCR Polymerase chain reaction

PDGFRA Platelet derived growth factor receptor alpha

PECAM1 Platelet endothelial cell adhesion molecule 1

PDCD4 Programmed cell death 4

PRRs Pattern recognition receptors

PI3K Phosphoinositide-3-kinase

PTEN Phosphatase and tensin homolog

RAAS Renin angiotensin aldosterone system

ROS Reactive oxygen species

RT Reverse transcription

qRT-PCR Real-time quantitative reverse transcription polymerase chain reaction

S100A4 S100 Calcium Binding Protein A4

SBS Salt buffered saline

SDS Sodium dodecyl sulphate

SEM Standard error of the mean

SFM Serum free media

siRNA short interfering RNA

SMC Smooth muscle cell

SNS Sympathetic nervous system

STRING Search Tool for the Retrieval of Interacting Genes/Proteins

SDH Succinate dehydrogenase

TAC Transverse aortic constriction

TGF-β Transforming growth factor-beta

TIMP Tissue inhibitor of metalloproteinase

TLR Toll-like receptor

TMT Tandem mass tagging

TNC Tenascin C

THY1 Thy-1 membrane glycoprotein

TNF Tumour necrosis factor

α-SMA Alpha smooth muscle actin

Publications and Communications

Publications

Co-author:

AMIN, M. M. J., **TREVELYAN, C. J.** & TURNER, N. A. 2021. MicroRNA-214 in Health and Disease. **Cells**, 10.

TAYLOR, H. A., SIMMONS, K. J., CLAVANE, E. M., **TREVELYAN, C. J.**, BROWN, J. M., PRZEMYŁSKA, L., WATT, N. T., MATTHEWS, L. C. & MEAKIN, P. J. 2022. PTPRD and DCC Are Novel BACE1 Substrates Differentially Expressed in Alzheimer's Disease: A Data Mining and Bioinformatics Study. **Int J Mol Sci**, 23.

D'ALESSANDRO, E., SCAF, B., MUNTS, C., VAN HUNNIK, A., **TREVELYAN, C. J.**, VERHEULE, S., SPRONK, H. M. H., TURNER, N. A., TEN CATE, H., SCHOTTEN, U. & VAN NIEUWENHOVEN, F. A. 2021. Coagulation Factor Xa Induces Proinflammatory Responses in Cardiac Fibroblasts via Activation of Protease-Activated Receptor-1. **Cells**, 10.

Communications

Poster presentations:

Investigating The Regulation Of Human Cardiac Fibroblast Behaviour By Micro-RNA-214 In The Context Of Pathological Cardiac Remodelling. **Christopher J. Trevelyan**, Leander Stewart, Karen E. Porter, Karen Forbes, Neil A. Turner. The British Society for Cardiovascular Research (BSCR), Autumn Meeting (2022).

Regulation of human cardiac fibroblast behaviour by specific microRNAs in the pathological cardiac remodelling process. **Christopher J. Trevelyan**, Leander Stewart, Karen Hemmings, Karen Forbes and Neil A. Turner. The 28th Northern Cardiovascular Research Group (NCRG) Meeting, The University of Bradford (2021).

Chapter 1 Introduction

1.1 Cardiovascular Disease

Cardiovascular disease (CVD) is a class of diseases that concern the heart and the blood vessels and is both the leading cause of premature death and the leading cause of mortality worldwide. With 17.9 million deaths per annum, CVD can be divided into four main types which includes; coronary artery disease (CAD), cerebrovascular disease, peripheral artery disease (PAD) and aortic atherosclerosis (Kim, 2021). These types can be even further divided into disease subtypes such as hypertension, congenital heart disease, myocarditis, and valvular heart disease. Common risk factors are hereditary or environmental such as cigarette smoking, obesity, genetic factors and ageing (Francula-Zaninovic and Nola, 2018). CVD can also be referred to as a disease of socioeconomic disparity and deprivation, with a correlation between CVD mortality rates and deprivation and higher rates of risk factors such as obesity in areas of higher deprivation (Schultz et al., 2018). In the UK where 168,000 people die each year from CVD (47,000 of which are classed as premature) (ONS, 2021), the financial cost is substantial, costing the UK economy £9 billion each year. This thesis will be primarily focused on the myocardium and how cardiac fibroblasts (CFs) influence pathology in this area.

1.1.1 Cellular Composition of the Heart

The mammalian heart is comprised of cardiomyocytes (CMs), CFs, endothelial cells (ECs), peri-vascular cells including smooth muscle cells (SMCs) and immune cells. The majority of the volume of the heart is comprised of the CMs (~80% of the heart) but all the cells have important roles in regulating cardiac homeostasis (Zhou and Pu, 2016). The cellular composition of the heart differs between atrial and ventricular tissue (Lim, 2020). Atrial tissues are comprised of 30.1% CMs, 24.3% CFs, 17.1% peri-vascular cells, 12.2% ECs and 10.4% immune cells and ventricular tissues are composed of 49.2% CMs, 21.2% peri-vascular cells, 15.5% CFs, 7.8% ECs and 5.3% immune cells. Cells of the same type also show different transcriptional signatures depending on if they are atrial or ventricular which is an important consideration for any research. The CMs are contractile and excitable cells that express sarcomeric proteins and contract due to electrical stimulation that arises from specialised pacemaker cells (Keepers et al., 2020). CMs can undergo hypertrophy whereby the cells increase in size, sarcomeres undergo reorganisation and protein synthesis is enhanced and sustained hypertrophy throughout the heart can manifest as pathology and subsequently clinically relevant changes (Frey et al., 2004). ECs are able to regulate blood flow, vascular permeability and angiogenesis and paracrine signalling has been detected between ECs and CMs where ECs can stimulate hypertrophy in CMs and CMs can stimulate angiogenesis by

ECs (Lother et al., 2018). CFs have been described as primary nodal regulators of cardiac remodelling in the heart and are responsible for the regulation of extracellular matrix (ECM) turnover and wound healing (Bretherton et al., 2020). Many of CF behaviours are mediated by activation and transition to a myofibroblast (MyoFb) phenotype where CFs are capable of detecting danger associated molecular patterns (DAMPs) such as TNFα, IL-1, IL-6 and TGFβ and responding by changes in specific cell behaviours including proliferation, migration, invasion and synthesis of ECM proteins such as collagen, matrix metalloproteinase (MMPs) and tissue inhibitors of matrix metalloproteinases (TIMPs) (Porter and Turner, 2009). Issues arise however following events such as myocardial infarction (MI) when CFs and MyoFbs persist (Turner and Porter, 2013) and this persistence with continuous proliferation, anti-apoptotic signalling, continual synthesis of ECM proteins and increased ECM turnover can drive pathological fibrosis, leading to arrhythmias, myocardial stiffness and progression to heart failure (HF). Potential therapeutics to target cardiac remodelling would therefore involve selectively inhibiting adverse pathological remodelling but allowing essential CF behaviours such as wound healing and scar formation to occur (van Nieuwenhoven and Turner, 2013).

1.1.2 Myocardial Infarction

Acute MI (AMI), often referred to as heart attack, is most often caused by a cessation of blood flow to the myocardium, resulting in necrosis of CMs. The coronary arteries supply blood to the myocardium and thus a blockage means that oxygen supply to the CMs is impeded and it is this lack of oxygen that results in CM death (Chiong et al., 2011). The impact of CM death is emphasised by the fact that CMs are terminally differentiated and cannot undergo significant cell proliferation in the same way that other cell types in the body can (Gong et al., 2021). The initiating cause of this inadequate blood supply, or ischaemia, is atherosclerosis. The arteries are comprised of three general layers: the tunica intima (innermost layer), tunica media (middle layer) and tunica adventitia (outermost layer). It is the tunica intima that is implicated in the pathology of atherosclerosis which is now commonly regarded as a disease of inflammation (Milutinović et al., 2020). Atherosclerosis is the accumulation of fatty and fibrous material, eventually leading to formation of an atherosclerotic plaque (or atheroma) which is dynamic and changes over time with further accumulation of lipid material, cholesterol, calcium mineral, connective tissue and inflammatory cells (Rafieian-Kopaei et al., 2014). Atherosclerosis can lead to ischemia via two distinct routes at this point, either advanced atherosclerosis can lead to a narrowing of the arterial lumen and impeding blood flow (which are the symptoms of angina), or the formation of a thrombus (blood clot) can occur which similarly occludes the lumen and leads to ischemia (Badimon et al., 2012). MI then occurs, which triggers a multitude of signalling cascades with the initial aim of salvage and reparation of the myocardium. These events can be divided into two main phases: the inflammatory

phase and the reparative (proliferative) phase. The inflammatory phase begins with leukocyte infiltration via impaired vascular EC integrity, necrosis, and autophagy of CMs and ECM damage. It is cell death and ECM damage that leads to the release of damage-associated molecular patterns (DAMPs) which are pro-inflammatory and activate cells of the immune system and CFs (Turner, 2016). This signalling occurs via binding of DAMPs, such as interleukin (IL) 1-alpha (IL-1α) and high mobility group box 1 (HMGB1) to responsive pattern recognition receptors (PRRs) found on the infiltrating leukocytes as well as some other pre-existing cell types, including CFs (Turner, 2014). The most common of these PRRs are membrane-bound toll like receptors (TLRs), IL-1 receptor (IL-1R) and intracellular nucleotide-binding oligomerization domain–like receptors (NLRs). Downstream of receptor activation, there is activation of mitogen activated protein kinases (MAPKs) (serine/threonine protein kinases of which there are five types) and the transcription factor nuclear factor kappa B (NF-κB) (Turner, 2011). The consequence of this signalling cascade is the transcription, synthesis and release of pro-inflammatory cytokines, chemokines, and cell-adhesion molecules, all of which are also released and expressed by CFs (Turner et al., 2011). Pro-inflammatory cytokine release further propagates cell activation in the same way the initiating inflammatory signals do, whereas chemokines and cell-adhesion molecules enable cell migration and recruitment to distinct areas related to the damage. Proinflammatory cytokines include tumour necrosis factor alpha (TNFα), IL-1β and the pleiotropic cytokine IL-6, which has pro-inflammatory, pro-fibrotic and pro-hypertrophic properties. Chemokines include CXCL and CCL families which each attract neutrophils and monocytes respectively. Cell-adhesion molecules are made up of four families which include immunoglobulin-like adhesion molecules, integrins, cadherins and selectins. The ongoing recruitment and invasion of leukocytes leads to amplification of the inflammatory response with digestion of necrotic cell debris and apoptotic cells and dynamic change in ECM composition. Dynamic changes in the ECM include the synthesis and release of MMPs (for which macrophages and CFs are the main source) and the activation of MMPs which can be induced for example by the release of reactive oxygen species (ROS). At around seven days post-infarction, the second phase of MI then begins. Following inflammation, proper “clean up” is then driven to facilitate progression to wound healing and repair. CFs are the main drivers of wound healing. Necrotic CMs are engulfed and then replaced with a fibrotic scar which involves the synthesis and release of different subtypes of collagen by CFs. CFs are then capable of contracting collagen fibres to maintain the integrity of the scar during healing and activation of CFs to drive this process is essential in reducing the possible size of the scar. Neutrophils begin to express mediators such as lipoxins and annexin A1 which regulate the inflammatory response with the overall outcome being a reduction in neutrophil migration, apoptosis, and phagocytosis of existing neutrophils by macrophages. These macrophages are also found to polarise to the

M2 phenotype which is associated with the release of anti-inflammatory cytokines and drive both fibrosis and proliferation. Such anti-inflammatory mediators include IL-10 and transforming growth factor beta (TGF-β) as well as intracellular molecular stop signals such as interleukin 1 receptor associated kinase 3 (IRAK3) (Prabhu and Frangogiannis, 2016).

1.1.3 Heart Failure

HF is a clinical presentation and a disease syndrome that occurs when the heart is no longer capable of meeting the body's oxygen needs. Symptoms of HF include but are not limited to; shortness of breath, fatigue and lethargy and oedema. A comprehensive definition of HF is that there are structural and/or functional pathologies that prevent the ventricle(s) from effectively filling with blood (diastole) or ejecting blood (systole) (Murphy et al., 2020). There are several underlying causes to HF, including those that are mentioned here such as MI and cardiac remodelling, however it is not clear cut, and it is often a multitude of causal factors that contribute to HF, also including increased pressure overload, excessive neuro-humoral stimulation, and genetic abnormalities. Clinicians will diagnose HF based on whether there is preserved ejection fraction (HFpEF) or reduced ejection fraction (HFrEF). HFpEF is characterised by a thickened left ventricular wall but with an ejection fraction (EF) of over 50% whereas HFrEF is typified by a normal left ventricular mass/end-diastolic volume ratio but an increased left ventricular cavity (Bhuiyan and Maurer, 2011). The New York Heart Association (NYHA) has a functional classification for HF which is made of four classes. Class I is asymptomatic with no limitations to physical activity. Class II is asymptomatic at rest, but ordinary physical activity will become symptomatic. Class III is symptomatic at less than ordinary activity. Finally, class IV is when patients cannot carry on any physical activity and are symptomatic at rest (Association, 2017). Similarly, there are biological markers (biomarkers) which are expressed and are used as diagnostic and prognostic indicators in HF, with each biomarker being indicative of specific events. For example, the presence in the blood of noradrenaline and angiotensin II (Ang-II) are neurotransmitters and hormones associated with HF, whereas cardiac troponins and myosin light-chain kinase I are associated with myocardial injury and there are ECM specific proteins such as MMPs and TIMPs which are dysregulated during ECM remodelling (Polyakova et al., 2021).

1.2 Cardiac Remodelling

Cardiac remodelling is a term used to describe the genetic, cellular, structural, and functional changes that occur in the heart and can be either pathological, because of cardiac load or injury, or physiological (including exercise and pregnancy induced cardiac remodelling). Presenting clinically as changes in size, shape and function, the course and extent of cardiac remodelling are generally regarded as prognostic for the development of HF in part because

of ventricular dysfunction. Figure 1.1 is a graphical display of the triggers of remodelling and the resultant cardiac remodelling that occurs. More specifically, clinical diagnosis takes into account seven main criteria, some of which have been aforementioned in the events following MI, they include a change in cavity diameter, mass, geometry, scarring, fibrosis and immunological and inflammatory infiltrate (Azevedo et al., 2016). The most common hallmark is that of left ventricular remodelling, occurring in what is generally regarded as the chronic phase of MI, after the initial inflammatory and reparative phases and when repair mechanisms can become aberrant and deleterious. Alteration in the tension across the myocardium occurs during cardiac remodelling. Tensile strength is altered between remaining live CMs which undergo increased hypertrophy to compensate for the loss in myocyte cell number. This is also altered by CFs through a transitional switch to a MyoFB phenotype. This phenotype shows increased expression of the protein alpha smooth muscle actin (α-SMA) and the subsequent contraction of the collagenous scar (Shinde et al., 2017). If the increased wall stresses are not balanced then structural changes occur such as progressive dilatation (when the ventricular chambers enlarge), recruitment of border zone myocardium into the fibrotic scar, and an overall reduction in cardiac output (Jackson et al., 2003).

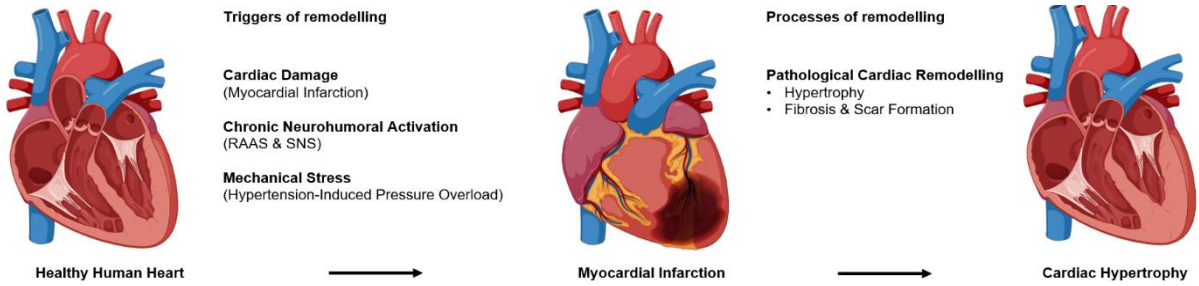

Figure 1.1 The triggers and processes of cardiac remodelling. The triggers of cardiac remodelling include cardiac damage through events such as myocardial infarction, chronic neurohumoral activation (such as the renin aldosterone angiotensin system (RAAS) and the sympathetic nervous system (SNS). In the acute phase, this can have the appearance of scarring, but hypertrophy and fibrosis (including scar formation) can further result in pathological cardiac remodelling. Created with BioRender.com.

1.2.1 Cardiac Fibrosis

Fibrosis is a pathology that can occur in multiple organ types and is typified by an excessive production of ECM components. Fibrosis itself is usually a consequence of programmed repair. Higher levels and more seriously implicating fibrosis is found in the disease of diabetes mellitus which has consequences for cardiovascular health (Wight and Potter-Perigo, 2011). Irrespective, cardiac fibrosis is a necessary response for repair and wound healing, especially in the case of MI where the loss of CMs presents a need to repair the myocardium. The repair takes the form of a collagen-based scar, which lacks contractility in comparison to the previous healthy myocardium but serves the purpose of replacing necrotic tissue (Frangogiannis, 2020). Central key players to this process are the CFs. These cells are the source of proteins known as ECM proteins, of which there are different types with contrasting and opposing roles. The synthesis and secretion of these ECM proteins however is mediated by differing signals and it is in the reparative phase of MI, as aforementioned, that the balance of ECM synthesis and secretion is tilted. The fibrotic scar that replaces CMs in MI is predominantly made up of type III collagen which is laid down first and then replaced with type I collagen which is primarily deposited by CFs (Daseke et al., 2020). Although scar formation is necessary for repair and survival following MI, there are consequences for homeostasis and normal functioning of the heart. Firstly, fibrotic scars in the heart have increased tensile strength compared to the healthy myocardium and this tension impacts contractility (both systolic and diastolic), with collagen cross linking meaning that flexible contraction is impaired and cardiac output is diminished. Secondly, the replacement of CMs with fibrous tissue interrupts gap junction signalling between CMs across the myocardium. The consequence of this interruption is that electrical conductance throughout the heart is impeded, and the cardiac action potential is affected, with a correlation between the amount and type of fibrosis and the presence of certain cardiac dysrhythmias (Albert, 2004). Similarly, the amount of fibrosis present is a commonly used prognostic indicator for a patient's probability to go on and experience HF, the inability of the heart to meet the body's oxygen demands. Indeed, a correlation exists between cardiac fibrosis and predisposition to both HFrEF and HFpEF (Sweeney et al., 2020). Reparative fibrosis is not the only kind of fibrosis however, with another type called interstitial (or reactive) fibrosis involving excessive ECM deposition in the myocardial interstitium. This is more diffuse and consequently, the myocardium responds by undergoing myocardial or CM hypertrophy as a compensatory mechanism to preserve cardiac output (Díez et al., 2020). The two types of fibrosis, therefore, result in a thickening of the myocardium, particularly in the left ventricle, with a loss of contractility and flexibility which leads to a worse prognosis in the development of HF.

1.2.2 Extracellular Matrix

The ECM is a highly organised network of macromolecules, each with different biological functions, supporting cells and tissue in an organ specific manner (Frantz et al., 2010). The different cell types within a tissue are integrated within the ECM and the network provides not only structural support but also provides a network to sequester growth factors and bioactive molecules so that autocrine signalling and paracrine signalling between cells is facilitated (Barcellos-Hoff and Bissell, 1989). The ECM is not a static entity and is instead dynamic, with communication between it and the cells it supports being bilateral and the activity of specific cells affects the makeup of the ECM, and vice versa. Similarly, environmental stimuli can induce ECM changes, for example injury or force. Different tissues have differing ECM compositions which depends upon the function that it serves. A commonality among these networks however is that they are generally made up of collagens, elastin, glycoproteins, and proteoglycans. Each of these ECM proteins act alone and in combination with activities such as protein degradation, protease inhibition (causing ECM turnover) and signalling mechanisms to cells in the ECM (Yue, 2014).

The major proteins of the ECM are collagens. The structure of collagens is well known to contain a triple helix and they can form either homodimers or heterodimers which are identifiable by specific α-chains (Xu et al., 2010). The specific type of collagens that are important in the ECM of the myocardium, as well as in other tissues, are fibrillar collagens and one of their important properties in the myocardium and in the fibrotic scar specifically is the ability to withstand tension. There are also post-translational modifications of collagen that lead to stabilisation, one such being crosslinking between collagens molecules which is catalysed by an important family of enzymes called the lysyl oxidases (LOX), of which there are five members called: LOX, LOXL1, LOXL2, LOXL3 and LOXL4 (Siegel and Fu, 1976). Other important proteins in the processing of fibrillar collagen include metalloproteinases that are part of the A Disintegrin And Metalloproteinase with Thrombospondin motif (ADAMTS) and bone morphogenic protein 1 (BMP1) families which are responsible for removal of the propeptide domains of collagen (Rosell-García et al., 2019). Most collagen fibres in the myocardium consist of collagen types I and III and each are synthesised by CFs (de Souza, 2002). As well as providing mechanistic structure and the basis for CM alignment to prevent ventricular dilatation, collagens are vital components of the fibrotic scar formed in MI wound healing (Lindsey et al., 2015). The production and organisation of collagens are therefore necessary for the architecture, shape, and structure of the ECM.

CFs are also capable of the synthesis and release of MMPs (Turner and Porter, 2012), ADAMs, TIMPs and other proteases such as elastase (Fan et al., 2012). The MMP family in

humans is made up of twenty three members and are a mixture of membrane bound (MT-MMPs) and soluble secreted proteins (Nagase et al., 2006). They are secreted in an inactive, zymogen form and require activation before they can catalyse reactions. Activation can occur in the form of signals such as oxygen free radicals (produced during events such as ischemia and reperfusion injury) and the angiotensin converting enzyme (ACE). Their primary role is catalysing the breakdown of other ECM proteins and their activity is regulated by inflammatory signals such as those that occur following an MI. MMPs are named after their requirement on zinc for activity and calcium for stability. Three MMPs that are particularly important in the pathology of cardiac remodelling are MMP2, MMP3 and MMP9 and are all produced by CFs as well as other cells such as macrophages (Turner and Porter, 2012). MMP2 is also known as gelatinase-A and is a secreted MMP that catalyses the breakdown of both collagen I and III. The post-MI levels of MMP2 are increased in the plasma and infarct because of CM and CF stimulation and HF patients show a four-fold increase in MMP2 expression in comparison to controls (DeLeon-Pennell et al., 2017). MMP3 (stromelysin 1), also a secreted MMP, catalyses the breakdown of collagen II, IX, X and XI (Cui et al., 2017). MMP3 is secreted by both CFs and macrophages and is capable of activating other MMPs such as MMP1, MMP7 and MMP9 which makes it an upstream MMP activator (Cui et al., 2017). MMP9 (gelatinase-B) similarly is a secreted MMP that breaks down collagens IV and V and circulating levels of MMP9 are increased at day one post-MI and remain elevated until day seven in mice (DeLeon-Pennell et al., 2017). A correlation has been demonstrated associating increased MMP9 levels with larger left ventricular volumes and greater left ventricular dysfunction post-MI, making it an important biomarker in cardiac remodelling (Sundström et al., 2004).

In the same way that there are signalling mechanisms that exist to stimulate MMP release and activity in cardiac remodelling, there are also signalling mechanisms for the release and activity of TIMPs which act to inhibit MMPs. This activation and inhibition of MMPs and TIMPs respectively, resulting in the turnover of ECM, is an orchestrated process and in the healthy human heart, CFs drive this process as essential for the proper maintenance of the structure and function of the heart (Arpino et al., 2015). During aberrant cardiac remodelling however, activation of CFs and transitioning to the MyoFb phenotype can result in a dysregulation of ECM turnover, resulting in an imbalance in the deposition of ECM proteins (Nielsen et al., 2019). This increased deposition of proteins such as fibrillary collagens results in some of the pathologies such as increased left ventricular thickness as aforementioned. Deviations in the balance of MMP and TIMP activity has been observed in several cardiovascular pathologies, including; MI, viral myocarditis, dilated cardiomyopathy and pressure-overload induced HF (Wang et al., 2002) (Pauschinger et al., 2004). In general, this dysregulation is characterised by an increase in MMP secretion and activity and a decrease in TIMP secretion and activity.

There are four members of the TIMP family, named: TIMP1, TIMP2, TIMP3 and TIMP4 (Brew and Nagase, 2010). They inhibit the activity of the MMPs by binding to their active site and therefore preventing substrate binding. Interestingly, TIMPs also exhibit activity on CFs and subsequently the ECM, independent of their inhibitory activity on MMPs.

1.3 Cardiac Fibroblasts

CFs are a cell-type found in the heart that play a pivotal role in the healthy functioning heart as well as in CVD (van Nieuwenhoven and Turner, 2013). Once thought to be passive players in adverse cardiac remodelling, CFs are now known to be drivers of pathological remodelling, driven through dysregulation of their usual actions (Humeres and Frangogiannis, 2019). In the healthy heart, CFs function by regulating ECM turnover, producing ECM proteins such as MMPs and TIMPs and providing structural support to the heart, helping to define the arrangement and stability of the heart's chambers (Turner and Porter, 2012). When CFs function like this, they are said to be at resting, or quiescent, state. When myocardial injury occurs, a phenotypic switch is triggered whereby CFs undergo a fibroblast to MyoFB transition (FMT) (Hall et al., 2021). Myocardial injury includes acute events such as MI or equally they can be chronic, for example, chronic neurohumoral activation (such as sustained activation of the renin-angiotensin-aldosterone system (RAAS) or sympathetic nervous system (SNS)), mechanical stress (such as hypertension-induced pressure overload) or type 2 diabetes mellitus (T2DM) where chronic activation of MyoFBs and increased expression of *COL1A1* mRNA is observed (Sedgwick et al., 2014). After FMT occurs, MyoFbs are responsible for two distinct roles which are; driving cardiac fibrosis and scar formation through deposition of type I and III collagen and stimulating CM hypertrophy through paracrine signalling, including secretion of IL-6 family cytokines (Bageghni et al., 2018) (Kakkar and Lee, 2010). Although once thought to be the most abundant cell type in the heart, lineage tracing means we now know that CFs make up only ~11% of all cells in the heart (although the number of CFs increases in both aging and disease) (Ivey and Tallquist, 2016). It is the primary nodal role of the CFs, interacting with the cellular components of the heart (in CMs) and non-cellular components (in the ECM) that underpin the importance of the CF.

1.3.1 Cardiac Fibroblast Behaviours

The phenotypic behaviours of CFs (displayed in Figure 1.2), just like the ECM that they regulate, are dynamic and their functions enhance, adapt, and become dysregulated through the lifetime of an organism by ageing or through disease. One of these important behaviours is proliferation. Cell proliferation is a highly coordinated process and increased proliferation is associated with differentiation. For CFs specifically, proliferation is an important mediator of cardiac fibrosis (Hall et al., 2021). Whereas cardiac fibrosis is usually associated with negative

implications, the ability of CFs to proliferate and undergo enhanced proliferation is necessary for survival following AMI so that there are enough CFs to release ECM proteins and promote wound healing. In fact, the rate of proliferation is often used as a measure of the activation of CFs (Olson et al., 2005). Olson et al., (2005) demonstrated that the proliferation of CFs is dependent upon activation of both MEK and ERK1/2 and that Ang II (released during events such as RAAS activation) induces activation of these molecules. Even though increased proliferation of CFs is the basis for the transition and expansion of a MyoFb phenotype (which will be covered subsequently), proliferation is required for the proper repair of wounds in the myocardium (Ma et al., 2017b). An important consideration however is the implication of genetic variability to CF proliferation, especially when using CF proliferation as a measure of activation or of cardiac fibrosis. Park et al. (2018) found that rates of CF proliferation do not necessarily correlate with extent of fibrosis (whereas CF activation and differentiation to MyoFbs did) suggesting that CF proliferation as a behaviour is more than just pathological.

Migration is a pivotal CF behavioural process in the acute response to MI and the longer-term chronic implications of pathological remodelling. The action of cytokines such as IL-1β on CFs has been demonstrated to induce migration by Mitchell et al. (2007) by activation of the three MAPK subfamilies (extracellular signal-regulated kinases, c-Jun NH(2)-terminal kinases, and p38), a process that was reversible by pharmacological inhibition of each MAPK subfamily. Migration of CFs into the infarct area, from where necrotic CMs have been cleared, is essential for proper repair and survival. Distinct regulators of fibroblast migration are not fully understood, however suggested mediators include 5-lipoxygenase (5-LOX), cardiotrophin-1, TGFβ and fibroblast growth factors (FGFs) (Freed et al., 2011). The environment through which the CFs migrate to the infarct zone (the ECM) is dynamic and has plasticity. The secretion of matrix degrading enzymes such as MMPs is therefore an essential mediator of this movement and similarly, it is therefore important that CFs produce matricellular proteins to maintain stability of the myocardium, such as tenascin-C (TNC). Just as important as it is for CFs to migrate to the infarct zone when they are required, it is important that their migration is arrested when they arrive there. Therefore, anti-migratory inhibitory signals exist for this reason. CXCL10/interferon-γ-inducible protein (IP)-10 is a cysteine X cysteine (CXC) chemokine that is increased in the infarcted myocardium and inhibits FGF induced CF migration (Bujak et al., 2009). The relationship between CFs and CMs as co-communicators in the heart is also evident in the induction of CF migration. It was demonstrated by Shi et al. (2017) that metabolites of hypoxic CMs, including TNF-α and IL1-β, can induce CF migration and this migration can conversely be inhibited through treatment with anti-TNF-α and anti-IL1-β antibodies. Each of these behaviours are important and necessary to heal the injured heart but can become dysregulated and harmful after differentiation to the MyoFb phenotype.

1.3.2 Fibroblast to Myofibroblast Differentiation

The transition to MyoFb is characterised by a change in protein expression that means MyoFBs become proliferative and contractile cells that are hyper-synthetic for ECM proteins. Such proteins that are used to characterise MyoFBs include vimentin, fibronectin and most importantly, α-SMA (Baum and Duffy, 2011). Although MyoFbs express α-SMA (*ACTA2* gene), they do not express other SMC markers such as smooth muscle myosin heavy chain (SM-MHC; *MYH11* gene) (Souders et al., 2009a). Another important distinction of MyoFBs is that they are particularly responsive to proinflammatory cytokines which as aforementioned are increased in the pathological remodelling heart. Such cytokines include but are not limited to; TNFα, IL-1, IL-6 TGF-β and the vasoactive peptide angiotensin II (Ang II) (Van Linthout et al., 2014). MyoFbs are not sensitive to only chemical mediators of remodelling however, with other signals including changes in stretch and tension (which can be replicated *in vitro* using specialised plates) and ischemia and reperfusion which involves the restriction of oxygen and then the rapid influx and reperfusion of oxygen which can lead to the production of reactive oxygen species (ROS) known to induce cell damage (Li et al., 2022b).

CFs and MyoFbs are both responsive to stimuli of cardiac dysfunction. Response occurs through altered synthesis and release of ECM proteins such as collagen, fibronectin, MMPs and TIMPs and pleiotropic cytokines such as IL-6 (Souders et al., 2009a). This response has been shown to affect electrophysiology. CFs in coculture with CMs have been shown to alter the electrophysiological properties of CMs while also exhibiting membrane potential fluctuations themselves (Hall et al., 2021). Following MI, CFs show increased sensitivity to mechanical stretch, demonstrated through altered resting potential and mechanically induced potential and such alterations can result in post-MI arrhythmias (Kamkin et al., 2003). Mechanosensitive ion channels, therefore, such as those belonging to the Piezo family of proteins, are of interest in CFs due to their ability to respond to membrane tension (Blythe et al., 2019) (Stewart and Turner, 2021).

Another important distinction of MyoFbs is their localisation, proliferation, and migration in the remodelling heart. Unlike skin fibroblasts, which after wound repair undergo apoptosis, cardiac MyoFBs persist and are found localised to the mature infarct scar (Darby et al., 2014). Although MyoFbs participate in the initial wound healing process, which is vital for cardiac function and survival, their persistence in this area of the heart becomes detrimental. This is due to dysregulation of ECM turnover leading to fibrosis. In fact, MyoFBs, unlike CFs, are not actually found in the healthy myocardium but their persistence is necessary for continues remodelling to maintain scar viability (Kim et al., 2018).

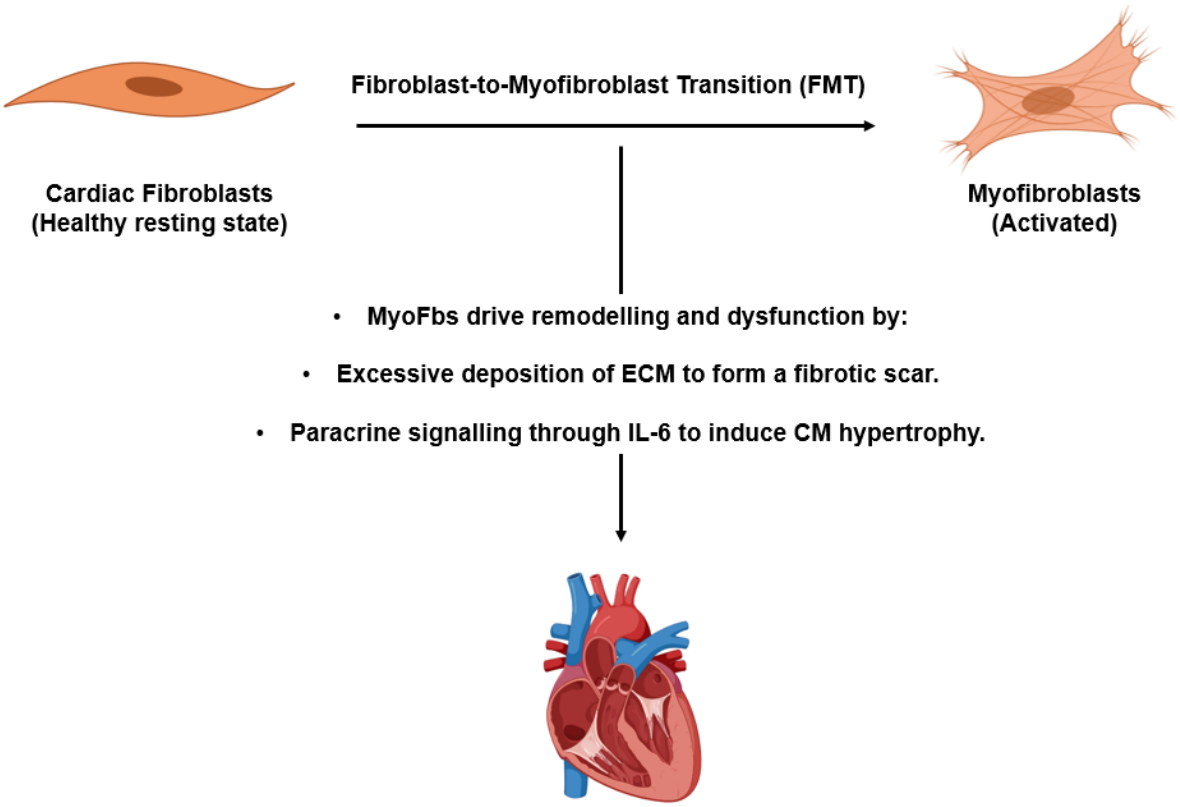

Figure 1.2 The role of myofibroblasts in the development of cardiac remodelling and dysfunction after transition and activation. Cardiac fibroblasts are at a quiescent and healthy resting state in the heart until fibroblast-to-MyoFb transition (FMT) occurs where their phenotype changes to that of an active MyoFb. MyoFbs then drive remodelling through excessive deposition of extracellular matrix or induction of CM hypertrophy through paracrine signalling, for example with the secretion of IL-6. Created with BioRender.com.

1.4 Mitochondrial Dysfunction

Mitochondria are subcellular organelles that drive the generation of adenosine triphosphate (ATP) and therefore are important for the healthy functioning of all cells and subsequently, tissues, organs, and homeostasis (Javadov et al., 2020). Mitochondrial dysfunction is any abnormality in the mitochondrial structure or activity that compromises its proper functioning. This dysfunction can take the form of; issues with maintenance of the electrical or chemical potential of the inner mitochondrial membrane, alterations with proper functioning of the electron transport chain (ETC), or decreases in the transport of metabolites into the mitochondria (Nicolson, 2014). Metabolic or environmental stress can cause damage to the mitochondria and cause dysfunction, but there are responses to stress in the form of mitochondrial fission or mitochondrial fusion (Youle and van der Bliek, 2012). Fission, which is also required for the generation of new mitochondria, can help to break down and remove damaged mitochondria and result in apoptosis of cells in response to stress. Fusion on the other hand involves the combination of partially damaged mitochondria in a process called complementation. Fusion between mitochondrial outer membranes is mediated by two proteins called mitofusins, either MFN1 or MFN2. In addition, MFN2 specifically is also integral for endoplasmic reticulum (ER) to mitochondrial tethering (Liu and Zhu, 2017). This tethering is essential for various processes including, phospholipid synthesis and exchange, calcium transfer, regulation of fission and apoptosis.

Mitochondrial dysfunction has been identified in numerous forms of CVD, including but not limited to; atherosclerosis, ischemia–reperfusion injury, HF, and hypertension (Poznyak et al., 2020). Dysfunction of the mitochondria most likely causes either a lack of energy or uncontrolled release of ROS in these cases. In fact, mitochondrial dysfunction has been suggested as a player in the development of apoptosis, inflammation, and fibrosis, all of which are hallmarks of cardiac remodelling. There has been increasing research to discern the role of the mitochondria in the progression of fibrosis and suggestions that mitochondrial dysfunction actively contributes to this. The heart is an example of a high oxygen consuming organ and is sensitive to any changes in mitochondrial function. The impact of ROS in the myocardium is far reaching (Siwik and Colucci, 2004). For example, ROS can activate the MAPKs and stress activated kinases such as p38 MAPKs and JNKs in both CMs and CFs. Pivotally, it has also been found that ROS can activate MMPs post-transcriptionally and similarly, decreasing the levels of TIMPs and collagen synthesis to result in a balance leading to ECM degradation and myocardial remodelling. In fact, Zhang et al. (2002) demonstrated that MMP-2 activation specifically was dependent upon the release of ROS which is regulated by the activity of manganese superoxide dismutase (MnSOD), an enzyme capable of preventing mitochondrial dysfunction by detoxifying ROS. It has also been shown by Li et al.

(2011) that hypoxia-induced release of ROS leads to activation of NF-κB signalling which similarly then leads to MMP-2 activation. It could be hypothesised therefore that CFs, given their active role in regulating the ECM, could be influenced by the onset of mitochondrial dysfunction. There is currently a lack of research concerning mitochondrial dysfunction in CFs despite this rationale. In fact, miRNAs have been found to play active roles in the regulation of ROS production in the field of senescence research (Catanesi et al., 2020). This has suggested a role for miRNAs in responding to ageing and then regulating gene expression related to ROS production and has been the basis for much research in neurodegenerative diseases such as Alzheimer's disease (AD). In relation to this project however, miR-214 particularly has been demonstrated as an inhibitor of MFN2 in the disease of acute kidney injury (AKI) (Yan et al., 2020). It was therefore found that ischemia-reperfusion injury in the kidneys results in an overexpression of miR-214 and that contributes to mitochondrial fragmentation, renal tubular cell death, and ischemic acute kidney injury. It would therefore be interesting to investigate whether any of the miRNA's part of this investigation, play a role in the regulation of mitochondrial dysfunction, in human CFs.

1.5 MicroRNAs

MicroRNAs (miRNAs) are non-coding RNAs that are around 22 nucleotides (nt) in length and regulate gene expression by preventing the translation of messenger RNA (mRNA) into protein (O'Brien et al., 2018). They primarily exhibit their effects by targeting the 3' untranslated region (UTR) of mRNA either by perfect or imperfect complementary binding, although binding to the 5' UTR as well as gene promoters has also been reported (Liu et al., 2018). The human genome encodes around 2,600 miRNAs and they are estimated to regulate around one third of the mRNAs (O'Brien et al., 2018). MiRNAs are vital for development and health, however they are also associated with human disease such as cancer, CVD, diabetes, and neurodegenerative disease. Associations with these diseases has been demonstrated on a functional level where miRNAs prevent protein translation leading to downstream changes leading to disease but also as biomarkers where the levels of miRNAs are expressed at higher or lower levels in disease compared to healthy controls. Importantly, miRNAs can act within the cells they are transcribed as well as on other cells by circulating extracellular miRNAs can be measured as biomarkers.

1.5.1 Biogenesis of microRNAs

The main pathway for miRNA biogenesis is the canonical pathway (summarised in Figure 1.3). The first step is transcription of primary miRNAs (pri-miRs) and subsequent processing into precursor miRNAs (pre-miRs) by a collection of proteins known as the microprocessor complex. This complex is made up of an RNA binding protein called DiGeorge Syndrome

Critical Region 8 (DGCR8) and a ribonuclease III enzyme called Drosha. Pri-miRs contain a characteristic hairpin as part of their structure which forms a pri-miR duplex. However, upon recognition and binding by DGCR8, Drosha catalyses the cleavage of the hairpin which ultimately results in the generation of a pre-miR. The next processing occurs in the cytoplasm and transport here is facilitated by an exportin 5 (XPO5)/RanGTP complex. The pre-miR is processed to remove the terminal loop which produces a mature miRNA duplex, and this step is catalysed by an RNase III endonuclease called Dicer. A key result of this processing is the directionality of the miRNA strand that is produced by Dicer. The directionality refers to whether the strand arises from the 5' end or 3' end of the pre-miRNA hairpin where each of these strands are referred to as 5p and 3p respectively. Finally, the strands may be loaded into the Argonaute (AGO) family of proteins which help mediate RNA targeting of both siRNA and miRNA. Another important pathway for miRNA biogenesis that should be considered is the non-canonical pathway. The non-canonical pathway can be broadly defined as miRNA biogenesis that is independent of either Drosha or DGCR8 and appears to have a bias for 3p strand biogenesis (Stavast and Erkeland, 2019).

The loaded miRNA strand and AGO in combination, make up the miRNA-induced silencing complex (miRISC) which mediates silencing of RNA by different means depending on the complementarity and target specificity of the complex. The miRISC binds to complementary sequences on mRNA which are known as miRNA response elements (MREs). If there is a perfect binding and full complementarity between miRNA and MRE then AGO2 becomes catalytically active and cleaves and degrades the mRNA. This process involves the RISC driving the miRNA towards the 3' UTR or 5' UTR (in the case of non-canonical seed sequences where miRNAs can bind to the coding regions of mRNAs) of mRNA targets. Upon binding, the mRNA is still stable but its translation into protein by the ribosome is inhibited either by preventing elongation or by causing an already bound ribosome to "drop off" from the mRNA. This is the primary cause of post-transcriptional gene regulation by miRNAs, with the degradation of the mRNA being a secondary step that occurs once translation has already been inhibited.

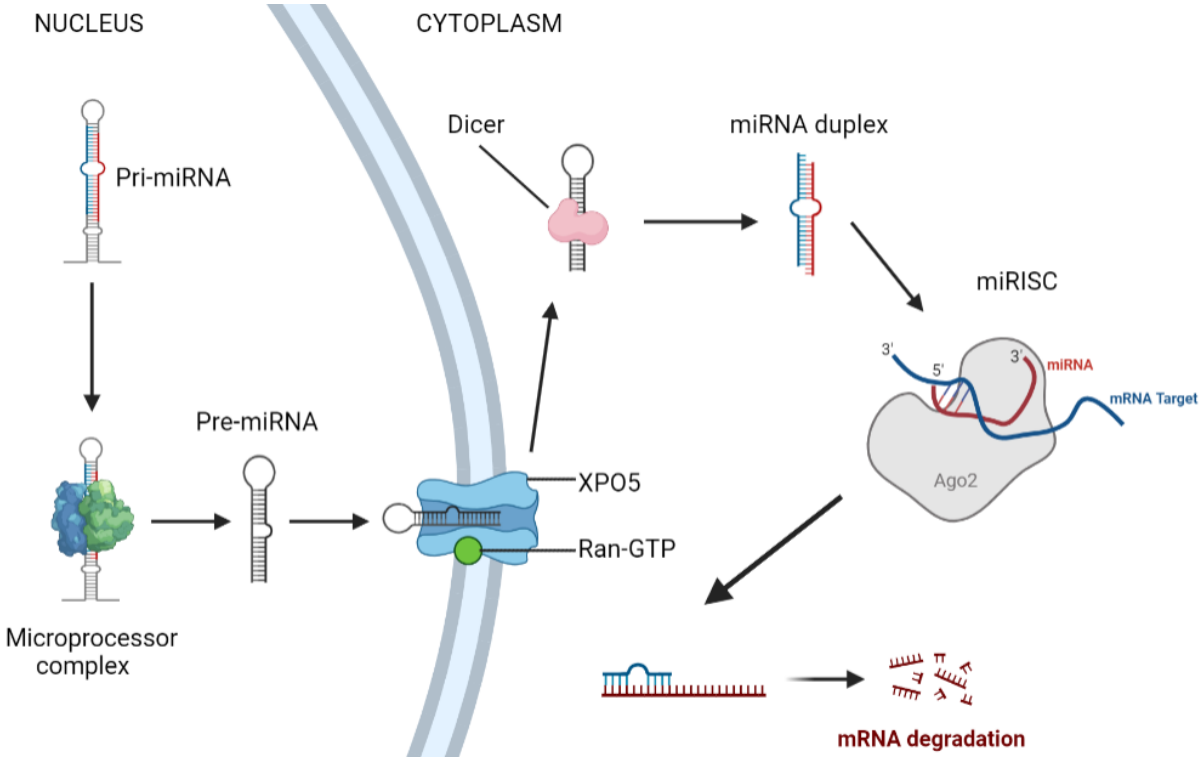

Figure 1.3 The biogenesis of microRNAs in the nucleus and their targeting of mRNAs in the cytoplasm. The biogenesis of miRNAs involves multiple processing and transportation steps. The first transcribed miRNA is the primary-miRNA (Pri-miRNA) which is processed by the microprocessor complex by removal of its characteristic hairpin. This produces the pre-miRNA which is exported to the cytoplasm by the exportin (XPO5)/RanGTP complex. The pre-miRNA is then processed to become a miRNA duplex and one strand of this duplex is loaded into an Argonaute (AGO) protein and then finally directs targeting to mRNA containing a specific seed sequence, which are then degraded to prevent protein translation. Created with BioRender.com.

1.5.2 MicroRNA Families

An important concept to understand when investigating the levels of specific miRNAs in a sample or when transfecting with commercially available anti-miRs (used to inhibit miRNAs) or pre-miRs (used to overexpress miRNA levels) is that different miRNA families exist and within these families there are miRNA "sisters" (Chipman and Pasquinelli, 2019). MiRNAs fall within the same family when they recognise the same 3' UTR seed sequence in mRNA, for example the miRNAs that are part of the miR-25 and miR-103 families differ in such a way and miRNA families are designated with a specific number. There are however overlaps that occur within each of these families where different miRNAs recognise different target mRNAs or have a bias for certain mRNAs and family members that exhibit this difference in binding are referred to as "sister" miRNAs. These miRNAs differ only by one or two nucleotides but letter suffixes such as "a" or "b" can be used to differentiate between them, for example the miR-30 family is made up of 6 family members (miR-30a, miR-30b, miR-30c-1, miR-30c-2, miR-30d, and miR-30e). Finally, as aforementioned, the specific strand loaded into the miRISC (3p or 5p) also governs the target specificity of each miRNA. It is therefore important that the specific miRNA being discussed is consistent throughout our investigations.

1.5.3 Intracellular and extracellular roles of microRNAs

A final level of regulation that will be discussed here is the localisation of miRNAs. MiRNAs can be localised on a subcellular level and in specific cell types or alternatively they can circulate and be found in circulating bodily fluids such as plasma, urine and saliva (Wang et al., 2018a). One example of a well-established cardiac specific miRNA is miR-208 (Malizia and Wang, 2011). It was found that around 50% of all miRNAs are cell type enriched and around 25% are broadly expressed (O'Brien et al., 2018). This finding points towards the importance of investigating the role that miRNAs play within the specific cell type of interest rather than using model cell lines that may not necessarily reflect endogenous miRNA levels or even miRNA activity (when we consider the basal transcription levels of target mRNAs). Similarly, another factor we should consider are the inter patient differences that exist between biological samples. For this reason, and indeed is the case in most *in vitro* experiments, the most accurate and translational findings would be achieved by investigating miRNA levels in primary human cells of the specific cell type of interest.

1.6 MicroRNA-21a-5p

Of all the identified microRNAs to date, miR-21a-5p (or miR-21) is one of the most widely researched in the field of human health and disease. It was also one of the first identified miRNAs, discovered in vertebrates and invertebrates by Lagos-Quintana et al. (2001) who recognised the impact of miRNAs on general post-transcriptional regulation. The human miR-

21 (denoted as hsa-miR-21-5p) is expressed on chromosome 17q23.2, which is downstream of the vacuole membrane protein-1 (VMP1) gene. The mature sequence of miR-21 is 22nts in length and has a sequence comprising: UAGCUUAUCAGACUGAUGUUGA (miRBase, 2022a). There are numerous cytokines that have been demonstrated to induce miR-21 transcription. Löffler et al. (2007) established that signal transducer and activator of transcription 3 (STAT3) is the major mediator of IL-6 signalling. IL-6 leads to an increase in miR-21 levels due to the presence of enhancers upstream from miR-21 (in the overlapping transmembrane protein 49 (TMEM49) gene) that contain two consensus STAT3 binding sites. Also interestingly, Davis et al. (2008) found that TGF-β and BMPs, induce an increase in the expression of mature miR-21 specifically, through post-transcriptional regulation. This regulation involves recruitment of TGF-β- and BMP-specific SMAD signal transducers to pri-miR-21 and lead to DROSHA-mediated processing into pre-miR-21. The net result of this is miR-21 mediated silencing of the target programmed cell death 4 (PDCD4) and induction of a contractile phenotype in human vascular SMCs (Davis et al. (2008)).

The research on miR-21 related to human health and disease has largely concerned cancer, however it also plays important roles in CVD and inflammation (which has overlaps with both). MiR-21 is also important in healthy early development and Ramachandra et al. (2008) found that miR-21 and STAT3 expression is increased during embryonic gene activation, suggesting miR-21 may be responsible for the targeted degradation of maternal mRNAs. Hayashi et al. (2011) have also suggested that miR-21 plays a role in early branching morphogenesis by modulating MMPs and degrading ECM through the targeting of the apoptosis-related factor, PDCD4 and endogenous MMP inhibitor, RECK. MiR-21 has been demonstrated extensively as an anti-apoptotic and pro-survival factor and Chan et al. (2005) found that human glioblastoma tumour tissues show elevated miR-21 and that knockdown of miR-21 led to increased apoptosis through activation of caspases. In fact, the role of miR-21 throughout cancer means that it is commonly referred to as an onco-miR and the fact that miR-21 degradation of PDCD4 leads to aromatase inhibitor resistance in breast cancer means that is an important therapeutic target (Chen et al., 2015). The role of miR-21 extends however beyond cancer and its targets can be important in other disease pathologies. Phosphatase and tensin homolog (PTEN) for example inhibits the phosphoinositide-3-kinase (PI3K) pathway and prevents Akt activation. MiR-21 mediated regulation of PTEN is observed in many cancers, however it is also known that PTEN normally suppresses expression of MMP2 and MMP9 via focal adhesion kinase (FAK). Transfection with pre-miR-21 has hence shown increased expression of these MMPs, which are important in ECM remodelling (Jazbutyte and Thum, 2010).

In the human heart, all cardiac cell types have high expression of miR-21, including vascular SMCs, ECs, CMs and CFs (Cheng and Zhang, 2010). As in cancer research, miR-21 has been thoroughly investigated in CVD and it has reproducibly been shown to confer a fibrotic phenotype. One way that miR-21 has demonstrated this is through regulation of the pivotal ERK-MAPK signalling pathway. Thum et al. (2008) reported that miR-21 levels are elevated in the early, intermediate, and late stages of the failing human heart. Importantly, they found that miR-21 mediated ERK-MAPK signalling in primary CFs by targeting sprouty homologue 1 (Spry1) and inhibition of miR-21 through an antagomir inhibited interstitial fibrosis and attenuated cardiac dysfunction in a pressure-overload-induced disease model in mice. Another investigation that has contextualised the onco-miR properties to CVD was performed by Cao et al. (2017) who found that miR-21 targets the tumour suppressor, cell adhesion molecule-1 (CADM1), in CFs. They showed that miR-21 enhances STAT3 expression, decreases CADM1 expression and ultimately results in cardiac fibrosis and increased CF proliferation. Conversely, knockdown of miR-21 with an inhibitor resulted in decreased fibrosis and suppressed CF proliferation. Interestingly, Yuan et al. (2017) found that miR-21, while being increased in cardiac fibrosis, is also a factor that potentiates the activities of the profibrotic cytokine, TGF-β. The authors found that miR-21 expression is increased in the infarct zone following LAD ligation, and TGF-β treatment increased the levels of miR-21 in CFs. It was shown that by overexpressing miR-21, the expression levels of type I collagen and α-SMA were increased, and that inhibition of miR-21 prevented this increase. Finally, they showed through luciferase reporter assays that miR-21 directly targets SMAD7 which is an inhibitor of TGF-β signalling, and so miR-21 releases the breaks on TGF-β signalling. The activities of miR-21 in CFs encapsulate the importance of viewing miRNAs as mediators of signalling pathways rather than isolated negative regulators of individual mRNAs and no more important is this than in the mediation of fibrotic signals that induce cardiac remodelling.

1.7 MicroRNA-214-3p

MiR-214-3p is a vertebrate specific miRNA that was first identified by Lim et al. (2003) and then later by Landgraf et al. (2007) after sequencing both mouse and human small RNA libraries respectively. MiR-214 was found to belong to a cluster, along with miR-199, in an intronic region located opposite the *Dynamin3* (dnm3) gene (Desvignes et al., 2014). The precise location of this region is at 1q24.3 and the distance between the regions encoding miR-199 and -214 means that the two are transcribed independently of each other and possess different seed sequences. The mature sequence of miR-214 is 22nt in length and consists of a sequence of ACAGCAGGCACAGACAGGCAGU (miRBase, 2022c). The regulatory activities of miR-214 have been implicated in a variety of organs and diseases, including but not limited to: cancer, osteoporosis, nephrology and CVD (Amin et al., 2021).

Although there are a range of publications investigating the role of miR-214 in CFs, like miR-21, the emphasis of existing research is on its role in cancer. In fact, its regulatory activity in melanoma has earned it the title of being a “melano-miR”, a miRNA that is influential in the progression of melanoma (Bar-Eli, 2011). Transcription of miR-214 can be regulated by the action of polycomb group (PcG) proteins which are epigenetic regulators and during differentiation, become disengaged from the miR-214 transcriptional unit and allow MyoD and myogenin recruitment to induce transcription (Juan et al., 2009). The transcription factor Twist-1, important during early development, has also been shown to induce the transcription of miR-214 (Lee et al., 2009). In cancer, Penna et al. (2015) commented on the fact that miR-214 is upregulated and down-regulated in different types of cancer and that this highlights the context of cell-specificity. This is the same in CVD, where depending on the disease model, we see miR-214 increased or decreased, and its role is not as definitive as miR-21a.

Just like miR-21, miR-214 also targets the important tumour suppressor enzyme PTEN (Liu et al., 2017). MiR-214 was found to be overexpressed in ovarian cancer and it was demonstrated that the miR-214 mediated degradation of PTEN resulted in upregulated phosphatidylinositol (3,4,5)-trisphosphate (PIP3), p-Akt and phosphorylated glycogen synthase kinase-3 (p-GSK-3β). The overall effect of this is induction of proliferation and inhibition of apoptosis. Zhang et al. (2019) also identified an effect on the PI3K/Akt/mTOR pathway, but in this case concerning the migration of triple negative breast cancer (TNBC) cells. It was found that with inhibition of miR-214, there was decreased viability, invasion, and migration (all behaviours relevant to CFs during cardiac remodelling), as well as increased expression of TIMP-2 and decreased expression MMP-2 (i.e., profibrotic). Finally, Cao et al. (2021) proposed a therapeutic role for miR-214 in the progression of osteoarthritis (OA) based on miR-214 regulation of ECM degradation. The authors found that miR-214 is downregulated in inflamed chondrocytes and that increased miR-214 decreases IKBKB expression and leads to dysfunction of NF-kB signalling. They also found that miR-214 partially inhibited IL-1β induced ECM degradation. The effect of this on ECM proteins was increased expression of COL2A1 and SOX9 but decreased expression of MMP3 and MMP13 with an overall protection against OA.

There are questions that remain regarding the role of miR-214 in CVD and in CFs specifically because there is no clear consensus as to whether miR-214 plays a protective or dysfunctional role. Of course, it is possible that miRNAs can play both roles or indeed that the targets they degrade can be helpful or harmful depending on the event they are responding to or the time since the initiating event. For example, one pattern of ECM regulation may be helpful in the acute phase of MI or harmful long after the MI where long-term chronic remodelling may be taking place. Firstly, Yang et al. (2019) found that a deficiency of miR-214 actually exacerbates cardiac fibrosis and that the presence of miR-214 plays a protective role. They found that miR-

214 levels were reduced in both TGF-β1 treated MyoFbs and in a transverse aortic constriction (TAC) induced mouse model of pressure overload. This protective role was at the levels of inhibiting proliferation and inhibiting the phenotypic switch to MyoFbs, two hallmarks of cardiac remodelling. Similarly, Dong et al. (2016) found that miR-214 plays a cardioprotective role by reversing Ang II mediated increases in collagen I and III, TGF-β1 and TIMP-1. MiR-214 was also found to increase the levels of MMP-1 that were otherwise reduced in CFs by Ang II treatment. The overall effect of miR-214 here was a protection against fibrosis. In contrast however, Sun et al. (2015) found that miR-214 mediated both neonatal rat CF proliferation and collagen synthesis in response to ISO and in fact that it was down-regulation of miR-214 that inhibited proliferation. They proposed that this activity by miR-214 is caused by inhibition of the mitochondrial fusion protein, MFN2, and activation of ERK1/2 MAPK signalling. In summary, miR-214 represents a miRNA implicated in the regulation of important genes relevant to CF behaviours in pathological remodelling, however the existing literature is not clear on whether miR-214 plays a protective or harmful role.

1.8 MicroRNA-224-5p

MiR-224-5p is a 25nt mature miRNA that is encoded on the X chromosome. The sequence of this miRNA is UCAAGUCACUAGUGGUUCCGUUUAG (miRBase, 2022d). The strongest mRNA target of miR-224 according to Wang (2022) is cyclin-dependent kinase 8 (CDK8) which is a serine-threonine kinase that is important for cell cycle progression and a transcriptional regulator. This regulation is a good example of the wide-reaching effects of miRNAs because in many cases they regulate transcriptional regulators which subsequently has downstream effects on the gene expression of many targets. Therefore, miRNAs work not only by inhibiting individual targets, but by inhibiting entire networks of genes.

MiR-224 is of particular interest in the disease of colorectal cancer (CRC) and specifically in the role it plays in metastasis of the disease (Ling et al., 2016). The first indication of its role was that miR-224 expression levels show correlation with tumour burden in CRC and that patients with higher expression of miR-224 showed shorter survival and shorter metastasis-free survival. Interestingly, this research found that SMAD4 protein expression was inversely correlated with miR-224, and miR-224 showed direct targeting of SMAD4 in a luciferase reporter assay. SMAD4 is a transcription factor which when active potentiates the effects of TGFβ stimulation as a tumour suppressor. Loss of SMAD4 however, seen in overexpression of miR-224, switches this TGFβ signalling to tumorigenic and metastatic. The overall effect of miR-224 overexpression was increased CRC motility. Like the activity of miR-21a and -214, there are translatable findings on the activity of miRNAs in cancer, where motility of CFs and MyoFbs is an occurrence found in migration of these cells to the infarct zone following MI.

Similarly, the inhibition of SMAD4 by miR-224 was also found to be important for the induction of proliferation in a CRC cell line (Zhou et al., 2017). SMAD4 therefore is an important miR-224 target for the control of behaviours relevant to cardiac remodelling.

There is a lack of published research concerning the role of miR-224 in CFs. There is a single report that studied miR-224 expression levels in rat CFs and found that Ang II treatment increased the expression levels of miR-224, but not miR-21 (Ning and Jiang (2013)). MiR-224 represents a miRNA that is implicated in the regulation of an important downstream mediator of TGFβ signalling (SMAD4) which itself is an important cytokine in cardiac dysfunction. There is no research however on the role of miR-224 in human CFs. There is an opportunity to understand how miR-224 might regulate human CFs and could be a potential therapeutic target in cardiac remodelling.

1.9 MicroRNA-30d-5p

MiR-30d-5p is a member of the miR-30d family which are an important family in the regulation of human development and disease (Mao et al., 2018). The miR-30d family is made up of five members, with six mature miRNAs which are; miR-30a, -30b, -30c-1, -30c-2, -30d and -30e. MiR-30d itself is located on chromosomal region 8q24 (Lin et al., 2017) and the mature sequence is composed of 22nt with the sequence: CUUUCAGUCAGAUGUUUGCUGC (miRBase, 2022b). MiR-30d differs from the three other miRNAs investigated in this project (miR-21a, -214 and -224) because its expression levels were decreased in the ISO infusion mouse model (Bageghni et al., 2018). This pattern of miR-30d expression levels being reduced in disease is something that occurs consistently in various pathologies. In fact, the importance of miR-30d in cancer especially is reflected in the fact that miR-30d is a reliable diagnostic and prognostic biomarker (Zhao et al., 2022). This role as a biomarker was explored by Xiao et al. (2017) who followed up 95 patients, diagnosed with acute HF for 1 year. It was found that those patients that died in this year had a significantly lower level of serum miR-30d. Similarly, Melman et al. (2015) found that the baseline plasma levels of miR-30d are associated with response to cardiac resynchronisation therapy (CRT) in patients with HF with dyssynchrony. The mechanism here was a protection against TNF signalling.

In pulmonary fibrosis, there is also differentiation of fibroblasts into a MyoFb phenotype. It was found by Zhao et al. (2018) that miR-30d expression levels were reduced in pulmonary fibrosis tissues. However, upon overexpression of miR-30d, primary normal human lung fibroblast (NHLF) proliferation resulting from TGFβ-1 signalling was attenuated. MiR-30d overexpression also prevented an increase in the protein expression of α-SMA and collagen I. It was demonstrated that miR-30d prevents the effect of TGFβ-1 signalling in NHLFs by binding to and inhibiting expression of JAG1 which subsequently inhibited activation of

JAG1/Notch signalling. This regulation of MyoFb markers is clearly translatable and important when looking at the role of miR-30d in the MyoFb transition in cardiac remodelling, considering that both α-SMA and collagen I are similarly upregulated here. Another important behaviour for cardiac remodelling that has been researched in cancer for miR-30d is motility. MiR-30d, in combination with the entire miR-30 family, was found to suppress breast cancer metastasis to the bone (Croset et al., 2018). This suppression is mediated through the inhibition of several pathways. Of note, there was inhibition of IL8 and IL11 expression (as well as twinfilin1, an upstream regulator of IL11). There was also inhibition of the integrins ITGA5 and ITGB3 which are important molecules for adhesion and invasion.

Until recently, research on miR-30d in CVD was lacking, however Li et al. (2021) published a novel and impactful investigation into the role that miR-30d plays in the regulation of cardiac remodelling by both intracellular and paracrine signalling. This work had been motivated by the earlier identification of miR-30d as a biomarker in HF patients by Xiao et al. (2017). First, it was found that overexpression of miR-30d was protective against cardiac remodelling in a rodent model of MI, defined by improved ventricular function, significantly lower fibrosis and suppressed α-SMA upregulation compared to WT mice. MiR-30d overexpression also protected CMs against apoptosis. Through RNA sequencing of miR-30d inhibition and overexpression in neonatal rat ventricular myocytes (NRVM), it was found that miR-30d regulated the expression of a range of focal adhesion genes (ITGA5, ITGA6, ITGAV, ITBL1, and ITGB3) and the MAPK signalling gene, MAP4K4. It was concluded, through luciferase reporter assays and investigating extracellular vesicle (EV) release, that miR-30d acts intracellularly on CMs to inhibit MAP4K4 expression to suppress apoptosis and is released in EVs from CMs to act by paracrine signalling on CFs to inhibit ITGA5 and subsequently prevent fibrosis and MyoFb activation. MiR-30d has therefore been found as a regulator of the two arms of cardiac remodelling, both protection of CMs from cell death and suppression of fibrosis. It should be noted however that as illuminating as this research is, there is still a lack of research on the role of miR-30d in human CFs. The current project therefore addresses a knowledge gap by investigating how miR-30d acts in human CFs.

1.10 Summary

CFs are a primary nodal regulator of cardiac remodelling which can be a pathological process following cardiac injury. The two main hallmarks of cardiac remodelling are increased fibrosis and myocyte hypertrophy. CF are drivers of both processes. Cardiac injury through events such as MI leads to activation of CF and induces a fibroblast-to-MyoFb transition to the MyoFB phenotype. This phenotype is highly proliferative and highly matrix synthetic. Through the excessive deposition of ECM proteins such as collagens and contractile proteins such as

αSMA, CFs cause myocardial fibrosis. This fibrosis leads to stiffening of the myocardium with resultant contractile impairment and can also impede electrical conductance. Activated CF also synthesise and release the proinflammatory cytokine, IL-6. IL-6 can then act by paracrine signalling on CMs to induce hypertrophy. The long-term consequence of this stimulation is increased thickening of the left ventricle, known as left ventricular remodelling, which ultimately reduces cardiac output. P38 MAPK is an important signalling node in the response of CF to DAMPs and governs the response of this cell-type during cardiac remodelling. There are four microRNAs that were identified as being of interest in our previous study following ISO infusion in fibroblast-specific p38 KO mice, namely miR-21a-5p, -214-3p, -224-5p and -30d-5p. MiRNAs are epigenetic regulators important in the modulation of CF behaviour and miRNAs represent a novel and exciting therapeutic target in this disease. By understanding more about the mechanisms of action of these 4 microRNAs in human CF, it is hoped that novel therapeutic targets can be identified to reduce the impact of CVD.

1.11 Aims and objectives

Overall aim

The overall aim of this project was to understand what role miR-21, -214, -224 and -30d each play in the regulation of CF gene expression, protein expression and behaviour relevant to cardiac remodelling, in cultured human CFs.

Hypothesis

MiR-21, -214, -224 and -30d play important regulatory roles in human CFs of relevance to pathological cardiac remodelling.

Objectives

1. Investigate the expression of miR-21a, 214, 224 and 30d in mouse models of cardiac dysfunction (Chapter 3).
2. Investigate the expression of each miRNA in human CFs.
3. Modulate the activity of these miRNAs and to investigate the effect on gene and protein expression of targets relevant to cardiac remodelling (Chapter 4).
4. Perform proteomics analysis of human CF protein expression following overexpression of miR-214 and miR-30d (Chapter 5).
5. Validate findings from bioinformatics analysis by investigating gene and protein expression and functional assays (Chapter 5).

Chapter 2 Materials and Methods

2.1 Chemicals and Reagents

Item	Catalogue number	Manufacturer
Dulbecco's Modified Eagle Medium	21969035	Thermo Fisher Scientific
Phosphate Buffered Saline	D8537	Sigma Aldrich
Foetal Bovine Serum		BioSera
Trypsin-EDTA (0.25%)	25200056	Thermo Fisher Scientific
Corning T-75 Flasks	430641U	Corning
Corning T-25 Flasks	430639	Corning
6-Well Tissue Culture Plates	10578911	Thermo Fisher Scientific
12-Well Tissue Culture Plates	10253041	Thermo Fisher Scientific
24-Well Tissue Culture Plates	10380932	Thermo Fisher Scientific
96-Well Tissue Culture Plates	10695951	Thermo Fisher Scientific
Trypan Blue Stain	15250061	Thermo Fisher Scientific
Collagenase Type II Solution	LS004176	Worthington Biochemicals
L-Glutamine (200mM)	25030024	Thermo Fisher Scientific
Penicillin-Streptomycin	15070063	Thermo Fisher Scientific
Aurum™ Total RNA Mini Kit	7326820	Bio-Rad Laboratories, Inc.
Molecular Biology Grade Ethanol	16685992	Thermo Fisher Scientific
B-Mercaptoethanol	21985023	Thermo Fisher Scientific
TaqMan™ MicroRNA Reverse Transcription Kit	4366596	Thermo Fisher Scientific
TaqMan™ Universal Master Mix II, no UNG	4440043	Thermo Fisher Scientific
Reverse Transcription System	A3500	Promega Corporation
TaqMan™ Gene Expression Master Mix	4369016	Thermo Fisher Scientific
Opti-MEM™ I Reduced Serum Medium	31985070	Thermo Fisher Scientific
Lipofectamine™ 2000 Transfection Reagent	11668019	Thermo Fisher Scientific
DAPI (4',6-Diamidino-2-Phenylindole, Dihydrochloride)	D1306	Thermo Fisher Scientific
Paraformaldehyde Solution (4% in PBS)	15670799	Thermo Fisher Scientific

Bovine Serum Albumin	9048-46-8	Sigma Aldrich
Collagen I, Rat Tail	A1048301	Thermo Fisher Scientific
10X Dulbecco's Modified Eagle's Medium - low glucose	D5523-10X1L	Sigma Aldrich
Human IL-6 DuoSet ELISA	DY206	R&D Systems
DuoSet® Ancillary Reagent Kit 2	DY008	R&D Systems
Pierce™ BCA Protein Assay Kit	23225	Thermo Fisher Scientific
RIPA Buffer (10X)	9806	Cell Signalling Technology
Phosphatase Inhibitor Cocktail 2	P5726	Sigma Aldrich
Phosphatase Inhibitor Cocktail 3	P0044	Sigma Aldrich
Laemmli 4X sample buffer	1610747	Bio-Rad Laboratories, Inc.
NUPAGE 10% Gels	NP0301BOX	Thermo Fisher Scientific
DTNB	22582	Thermo Fisher Scientific
Citrate Synthase Assay Kit	CS0720	Sigma Aldrich
Poly-D-lysine, black/clear bottom plate	152037	Thermo Fisher Scientific
Pluronic® F-127	P2443	Sigma Aldrich
Probenecid	P8761-100G	SLS
YODA-1	Prepared in house	School of Chemistry, University of Leeds
DMSO	D8418	Sigma Aldrich
ATP	R0441	Thermo Fisher Scientific

Table 2.1. List of materials used throughout the experiments performed in this project. The generic materials used in this project are listed here along with the specific catalogue numbers and manufacturers of each.

2.2. Human Cardiac Fibroblast Culture

Human CFs were obtained from liquid nitrogen banks or original cultures were established as described previously (Turner et al., 2003). Biopsies of human right atrial appendage were obtained from patients (without left ventricular dysfunction) undergoing elective coronary artery bypass grafting at the Leeds General Infirmary following local ethical committee approval and informed patient consent. The study reference for cells taken from liquid nitrogen was Ref 01/040 (K. Porter) and for cells derived from fresh tissue was Ref 17/WA/0314 (A. Smith). Heart tissue was minced and digested by incubation with 20mg of 740U/ml collagenase type II solution (Worthington Biochemical Corporation, Lakewood, NJ, USA)

dissolved in 10mL of Dulbecco's modified Eagle medium (DMEM) containing 0.05% bovine serum albumin (BSA) for 2 hours at 37 °C. Cells were pelleted by centrifugation at a temperature of 4°C and speed of 600xg for 6 minutes and the media was discarded. The pellet was then agitated and washed with 50mL of DMEM (containing 0.05% BSA) and then re-centrifuged as previously described. The media was again discarded, the pellet agitated and resuspended in 10mL of full growth medium (FGM); DMEM supplemented with 10% FCS, 1% L-Glutamine and 1% Pen/Strep). The cell suspension was then dispensed with 5mL in each of two T25 tissue culture flasks for 30 minutes to allow fibroblasts to adhere. After incubation, non-adherent cells were removed by discarding the media within each flask and this was replaced with a further 5mL of FGM and fibroblasts were cultured to confluence in a humidified atmosphere of 5% CO2 in air at 37 °C, and subsequently passaged by trypsinisation (using Trypsin-EDTA 0.25%). For previously frozen cells, cells were brought up from liquid nitrogen by placing in water at ~37 °C to thaw and then dispensing the cells in T75 flasks containing 10mL of pre-warmed (37 °C) FGM and then incubating overnight. Following incubation, media was removed for the purpose of removing DMSO and was replaced with fresh pre-warmed FGM. Experiments were performed on human cardiac fibroblasts from passages 2-5. Experiments that involved treating cells with reagents and stimuli involved culturing cells in T75 flasks until ~80% confluent, trypsinising and counting and then plating out for overnight incubation. Cells were then serum starved for 24 hours by culturing in SFM in order to quiesce and then treated with appropriate stimuli, diluted in SFM.

2.3. RNA Isolation

RNA for both miRNA RT-PCR and mRNA RT-PCR was isolated from human CFs by using the Aurum™ Total RNA Mini Kit (Bio-Rad Laboratories, Inc., Hercules, California, USA) which is a spin-based RNA elution method. The method was performed as per the manufacturer's instructions and for all RNA work, the environment was cleaned prior using 70% ethanol and RNase Away. The first step of this method involved lysing cells by agitating and resuspending pellets using 350µL of cell lysis buffer (containing β-mercaptoethanol) and 350µL of 70% molecular grade ethanol per sample and then transferring the total ~700µL homogenate to a spin column basket within a 2mL capless tube. The spin column was then centrifuged at 13,000xG for 30 seconds and the waste was discarded. 700µL of low stringency wash solution was then added to each spin column and re-centrifuged and the waste discarded. Each spin column matrix was then incubated with 80µL of DNase1 (prepared by combining 5µL of DNase1 with 75µL of DNase1 dilution solution) for 15 minutes at room temperature. The samples were recentrifuged and waste discarded before washing with 700µL of high stringency wash solution and the waste discarded. The samples were then washed with 700µL of low stringency wash solution and recentrifuged for 1 minute, waste discarded and

recentrifuged for a further 2 minutes. The spin columns were then transferred to 1.5mL Eppendorf tubes and the spin column matrix was incubated for 1 minute at room temperature with 80µL of RNA elution solution (pre-warmed to 70°C). The sample was then recentrifuged for 2 minutes to elute the RNA in each Eppendorf to produce a final product of DNA free, total RNA which was stored at -80°C.

2.4. RT-PCR Primers

Primer	Catalogue number
miR-21a-5p (mouse and human)	4427975 (000397)
miR-214-3p (mouse and human)	4427975 (002306)
miR-224-5p (mouse)	4427975 (002553)
miR-224-5p (human)	4427975 (000599)
miR-30d-5p (mouse and human)	4427975 (000420)
U6 (mouse and human)	4427975 (001973)
GAPDH	Hs99999905_m1
IL6	Hs00174131_m1
TNC	Hs01115665_m1
COL1A1	Hs00164004_m1
ACTA2	Hs00426835_g1
MMP2	Hs00234422_m1
MMP3	Hs00233962_m1
TGFB1	Hs00998133_m1
TGFB3	Hs01086000_m1
IL6R	Hs01075666_m1
IL11	Hs01055413_g1
IL11RA	Hs00234415_m1
AGTR1	Hs00258938_m1
EDN1	Hs00174961_m1
ITGA5	Hs01547673_m1

Table 2.2. RT-PCR Primers used in RT-PCR analysis in this study. Each of the specific primer targets (both miR-RT-PCR and mRNA RT-PCR) are listed here along with the generic catalogue numbers and the specific assay IDs for each of them.

2.5. MiRNA RT-PCR

2.5.1. MiRNA cDNA synthesis

For miRNA RT-PCR, cDNA was synthesised by using the TaqMan™ MicroRNA Reverse Transcription Kit (Thermo Fisher Scientific, Waltham, MA, USA) along with a TaqMan™ MicroRNA Assay which contains specific miRNA RT primers (dependent upon the specific miRNA of interest, as well as U6 snRNA as a housekeeping control). This method involves creating a 5.4µL mastermix per sample containing nuclease free water, 10X RT buffer, dNTP mix with dTTP, RNase inhibitor and MultiScribe™ RT enzyme at volumes as described in Table 3. Mastermix was aliquoted so that for each specific sample and primer of interest, 5.4µL was aliquoted per 0.2mL PCR tube. To this tube, 1µL of RNA sample and 1.6µL of miRNA RT primer was added to a final volume of 8µL. The reaction mixture was centrifuged to spin down the reagents and then incubated on ice for 5 minutes. For the final step, reaction tubes were then incubated in a Bio-Rad T100 PCR Thermal Cycler (Bio-Rad Laboratories, Inc., Hercules, California, USA) using a pre-set miRNA RT reaction process. The reaction process involved 16°C for 30 minutes, 42°C for 30 minutes, 85°C for 5 minutes and 4°C holding. cDNA samples were immediately processed for RT-PCR analysis.

Reagent	**Amount per sample (µL)**	**Amount for 6 samples (µL)**
dNTP mix w/dTTP (100M total)	0.08	0.48
Multiscribe RT enzyme (50U/µL)	0.533	3.2
10X RT buffer	0.8	4.8
RNase inhibitor (20U/µL)	0.1013	0.61
Nuclease free water	3.886	23.32

Table 2.3. Volumes required to produce RT reaction mixtures for miRNA RT-PCR. The specific volumes required to make a 5.4µL miRNA RT reaction mixture per sample are described and the amount for 6 samples described as an example.

2.5.2. MiRNA RT-PCR

For miRNA RT-PCR, a mastermix of 18µL per well was prepared containing 7.25µL nuclease free water, 10µL TaqMan™ Universal Master Mix II (no UNG) and 0.75µL specific TaqMan™ MicroRNA Assay RT primers (depending on the miRNA of interest, as well as U6 snRNA as a housekeeping control) per sample. 18µL of mastermix was then aliquoted in each relevant well of a 96 well plate so that there were duplicate wells per specific sample and miRNA of interest. To each of these wells, 2µL of miRNA cDNA (synthesised as previously described) was dispensed into the relevant duplicate wells. A plate seal was then attached to the plate, and it was pulse centrifuged for 30 seconds to spin down the reagents. The Design and Analysis Software v1.5.2, QuantStudio 3 and 5 systems (Thermo Fisher Scientific, Waltham, MA, USA) was used to prepare the plate template. The comparative CT experiment was selected and set to 50 cycles of PCR. The run was performed using the QuantStudio™ 3 Real-Time PCR System (Thermo Fisher Scientific, Waltham, MA, USA). PCR was performed as per a template protocol that involved a denaturation step at 95˚C for 1 minute and then 50 cycles of denaturation (95˚C), annealing and extension (60˚C).

2.6. MRNA RT-PCR

2.6.1. MRNA cDNA synthesis

mRNA cDNA synthesis was performed using the Reverse Transcription System (Promega Corporation, Madison, WI, USA). First, RNA samples to synthesise cDNA from had 5µL of RNA incubated for 10 minutes at 70°C prior to cDNA synthesis. This method involved creating an 18µL mastermix per sample that was composed of and added in the order of; nuclease free water, MgCl2, RT 10X buffer, dNTPs, Recombinant RNasin® Ribonuclease Inhibitor, AMV Reverse Transcriptase (HC) and lastly, Random Primers, in volumes as described in Table 2.4. 18µL of mastermix was aliquoted into a 0.2mL PCR tube as well as 2µL of pre-warmed RNA. The 20µL reaction mixtures were incubated in a Bio-Rad T100 PCR Thermal Cycler (Bio-Rad Laboratories, Inc., Hercules, California, USA) using a pre-set RT reaction process. The reaction process involved 25°C for 10 minutes, 42°C for 15 minutes, 95°C for 5 minutes and 4°C for holding.

Reagent	Amount per sample (µL)	Amount for 6 samples (µL)
Nuclease free water	7.9	47.4
$MgCl_2$	4	24
Reverse Transcription 10X Buffer	2	12
dNTP Mix	2	12
Recombinant RNasin® Ribonuclease Inhibitor	0.5	3
AMV Reverse Transcriptase (HC)	0.6	3.6
Random Primers	1	6

Table 2.4. Volumes required to produce RT reaction mixtures for mRNA RT-PCR. The specific volumes required to make an 18µL mRNA RT reaction mixture per sample are described and the amount for 6 samples described as an example.

2.6.2. mRNA RT-PCR

For mRNA RT-PCR, a mastermix of 18µL per well was prepared containing 7.5µL of nuclease free water, 10µL of TaqMan™ Gene Expression Master Mix and 0.5µL of specific TaqMan™ Real-Time PCR Assay primers (depending on the mRNA of interest, as well as GAPDH as a housekeeping control). 18µL of mastermix was then aliquoted in each relevant well of a 96 well plate so that there were duplicate wells per specific sample and mRNA of interest. To each of these wells, 2µL of mRNA cDNA (synthesised as previously described) was dispensed into the relevant duplicate wells. A plate seal was then attached to the plate, and it was pulse centrifuged for 30 seconds to spin down the reagents. The Design and Analysis Software v1.5.2, QuantStudio 3 and 5 systems (Thermo Fisher Scientific, Waltham, MA, USA) was used to prepare the plate template. The comparative CT experiment was selected and set to 50 cycles of PCR. The run was performed using the QuantStudio™ 3 Real-Time PCR System (Thermo Fisher Scientific, Waltham, MA, USA). PCR was performed as per a template protocol that involved a denaturation step at 95˚C for 1 minute and then 50 cycles of denaturation (95˚C), annealing and extension (60˚C).

2.7. RT-PCR Data Analysis

The experiment type for all RT-PCR runs performed by the QuantStudio™ 3 Real-Time PCR System was the comparative C_T ($\Delta\Delta C_T$) method. The amplification plot of these experiments

generates a ΔRn value for each sample and gene of interest at each specific cycle number being measured. The Rn is calculated by dividing the fluorescence of the reporter dye by the fluorescence of Rox which is the passive reference dye in our RT-PCR experiments. The analysis settings were changed post-run so that the cycle threshold (C_T) value for each well was calculated at a threshold of 0.1 ΔRn, as depicted in Figure 2.1. The data were then exported to an Excel file and the C_T value for each replicate was checked for each sample to ensure that values were within at least one whole cycle of each other. The ΔC_T mean value (which is the difference between the C_T value for the gene of interest and the value for the housekeeping control of U6 or GAPDH for any given sample) was then used to calculate the percentage expression of each gene or miRNA relative to the housekeeping control by calculating the 2^-ΔC_T value and multiplying by 100 to find the specific percentage change.

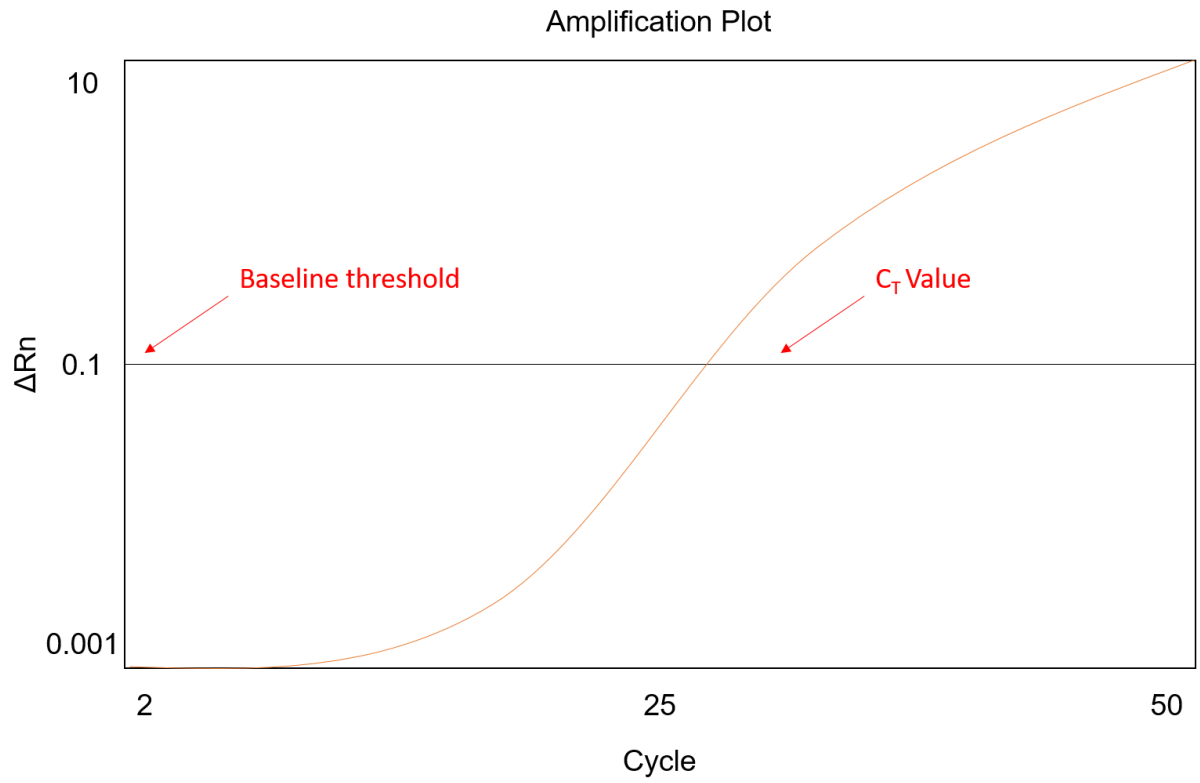

Figure 2.1. Graphical display of the amplification curve generated during RT-PCR, the baseline threshold, and the cycle threshold (C_T). Usually, the quencher dye prevents light emission from the reporter dye when the probe is intact however during amplification, the quencher and reporter dyes are released and so light is emitted as they are no longer in proximity. The C_T value is the PCR cycle number at which point the baseline threshold is met (when amplification is in the exponential phase). The C_T value can be used to determine the relative expression of a specific gene or microRNA, relative to a housekeeping control.

2.8. Transfection of Cultured Human Cardiac Fibroblasts

Human CFs were grown to ~80% confluence in T75 flasks and then trypsinised, counted and plated out in FGM and were seeded into wells of a 6-well plate at a density of 70,000 cells per well in 2 mL of FGM and incubated for 24 hours at 37˚C. Transfection reagents were prepared according to manufacturer's instructions and depending on whether the molecule to be transfected was miRNA (pre- or anti-miR) (Table 2.5) or siRNA (Table 2.6). Stocks of transfection reagents were prepared to allow 2mL of the necessary reagents per well and volumes and concentrations are described in Tables 2.5 and 2.6. For each incubation performed, the contents of tube 1 were incubated for 5 minutes at room temperature before addition to the contents of tube 2 for a further incubation of 20 minutes at room temperature and finally addition to tube 3. After incubation with transfection reagents, cells were incubated for a range of times (dependent upon manufacturer's instructions; typically, 6 hours to 24 hours) and then media was replaced with FGM. Cells were incubated for an appropriate period of several days (see individual experiments for specific time) before performing functional assays or isolating protein or RNA.

Transfection volumes for pre/anti-miRs in 6-well plates					
Transfection condition	**Reagent**				
	Tube 1		**Tube 2**		**Tube 3**
Pre-miR (60nM)	6µL Pre-miR (10µM)	500µL Optimem	5µL Lipofectamine	500µL Optimem	1mL 0.4% FCS DMEM
Anti-miR (200nM)	20µL Anti-miR (10µM)	500µL Optimem	5µL Lipofectamine	500µL Optimem	1mL 0.4% FCS DMEM

Table 2.5. Transfection volumes for transfecting human CFs with pre- or anti-miRs. Pre-miRs were transfected at a final concentration of 30nM whereas anti-miRs were transfected at a final concentration of 100nM. Lipofectamine 2000 was used as lipid mediated transfection agent at a concentration of 1%. The final volume for each well was 2mL, made up with 1mL of 0.4% FCS DMEM.

Transfection volumes for siRNA in 6-well plates					
Transfection condition	**Reagent**				
	Tube 1		**Tube 2**		**Tube 3**
siRNA (20nM)	8µL siRNA (5µM)	192µL Optimem	2µL Lipofectamine	198µL Optimem	1600µL SFM DMEM (antibiotic free)

Table 2.6. Transfection volumes for transfecting human CFs with siRNA. SiRNA were transfected at a final concentration of 20nM. The final volume for each well was 2mL, made up with 1.6mL of SFM DMEM.

Primer	Catalogue number	Manufacturer
ON-TARGETplus Non-targeting Control Pool	D-001810-10-05	Horizon Discovery
ON-TARGETplus siRNA MFN2 – SMARTPool	L-012961-00-0005	Horizon Discovery
hsa-pre-miR-21-5p	AM17100; PM10206	Thermo Fisher Scientific
hsa-pre-miR-124-3p	AM17100; PM12124	Thermo Fisher Scientific
hsa-pre-miR-224-5p	AM17100; PM11010	Thermo Fisher Scientific
hsa-pre-miR-30d-5p	AM17100; PM10756	Thermo Fisher Scientific
hsa-anti-miR-21-5p	AM17000; AM10206	Thermo Fisher Scientific
hsa-anti-miR-124-3p	AM17000; AM12124	Thermo Fisher Scientific
hsa-anti-miR-224-5p	AM17000; AM11010	Thermo Fisher Scientific
hsa-anti-miR-30d-5p	AM17000; AM10756	Thermo Fisher Scientific

Table 2.7 Synthetic siRNAs, pre-miRs and anti-miRs transfected into human cardiac fibroblasts. Listed here are the full names for and the catalogue numbers for siRNAs, pre-miRs and anti-miRs that were transfected into human CFs.

2.9. Proliferation Assay

Human CFs were plated out at a density of 10,000 cells/mL in 1mL FGM per well in 24 well plates and incubated overnight. The following day, each well was rinsed with 1mL PBS and incubated overnight with 1mL SFM. 48 hours later, day 0 counts were performed by trypsinising wells in triplicate and then counting using a haemocytometer to calculate the total number of cells per well (see Figure 2.2). The remaining wells were supplemented with 1mL of DMEM containing predefined concentrations of FCS and then incubated for a further 48 hours. Counts were then taken on day 2 and remaining wells were supplemented again with the same method being performed to count cells on days 4 or 7, depending on the experiment being performed. Counts were averaged between triplicate wells and mean cell counts were plotted versus time.

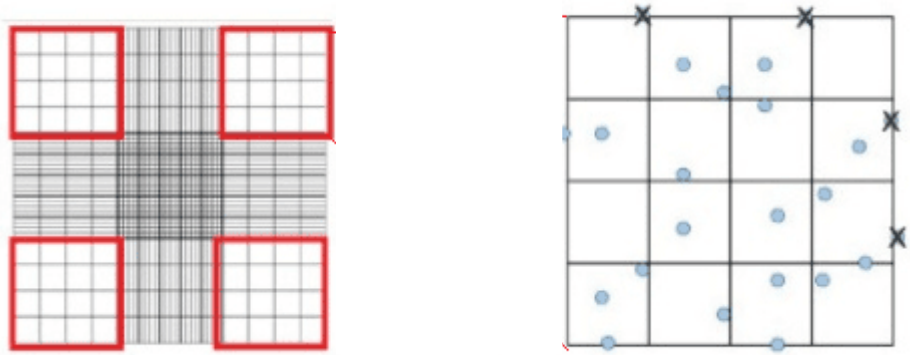

Figure 2.2. A haemocytometer grid containing 9 squares and an individual square zoomed in to show which cells should be counted. A haemocytometer was used to perform cell counts, where each individual square contains a total volume of 100nL of cell suspension. To calculate the total number of cells in the original 1mL suspension, 50µL of cell suspension was mixed with 50µL of trypan blue. Counts were performed considering cells within the grid and only cells bordering two pre-determined sides of the grid. A minimum of 3 grids were counted and the mean was calculated. The mean figure was then multiplied by two (to factor in the 1 in 2 dilution with trypan blue) and then multiplied by 10,000 (to factor in the difference between 100nL and 1mL).

2.10. ELISA for Detection of Human IL-6

Conditioned media was centrifuged at 600xG for 15 minutes at 4°C and the supernatant stored at -80°C. A Human IL-6 DuoSet ELISA kit and DuoSet ELISA Ancillary Reagent Kit 2 (R&D Systems, Minneapolis, USA) were used to measure IL-6 concentrations. Manufacturer's instructions were followed. Plates were incubated overnight with 100µL of capture antibody at room temperature. The following day, wells were aspirated and washed with 400µL wash buffer (three times) and blocked for 1 hour at room temperature using 300µL of reagent diluent. The wash steps were repeated as previously described before the plate was ready for sample addition. Standards were made up by diluting 3µL of stock standard with 997µL of reagent diluent and performing 1:2 serial dilutions to produce standards of 600, 300, 150, 75, 37.5, 18.8 and 9.38 pg/mL. Duplicate wells of 100µL of standards and samples (diluted to 1:50 with reagent diluent) were added and incubated for 2 hours at room temperature. Washing was re-performed and 100µL of detection antibody was added and incubated at room temperature for a further 2 hours. The wash was performed again and 100µL of Streptavidin-HRP was then added to each well and incubated for 20 minutes at room temperature and wrapped in foil. The wash step was performed again and 100µL of substrate solution was added (1:1 mix of colour reagent A and B) to each well. The plate was incubated at 20 minutes at room temperature and wrapped in foil before 50µL of stop solution was added to each well and plates were agitated to ensure thorough mixing. The optical density of each well was then measured at 450nm with wavelength correction at 540nm using a PowerWave HT Microplate Spectrophotometer (Agilent Technologies, Santa Clara, CA, USA). Manufacturer's IL-6 standards were used to generate a standard curve with an assay range of 9.4 - 600 pg/mL which was then used to calculate the IL-6 concentration in each sample (see Figure 2.3).

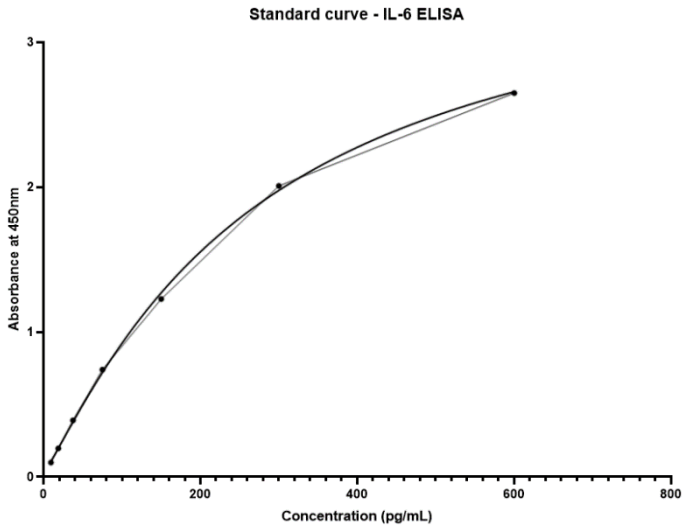

Figure 2.3. Standard curve generated from IL-6 ELISA standards supplied in the DY206-05 human IL-6 ELISA kit. A seven-point standard curve was prepared by performing 2-fold serial dilutions, starting with a high standard of 600 pg/mL and then covering 300, 150, 75, 37.5, 18.8 and 9.38 pg/mL. The standard curve was used to calculate the concentration of IL-6 within our samples of conditioned media, considering the dilution factor of the original samples (1:50).

2.11. ELISA for Detection of Human MMP-2

Conditioned media was centrifuged at 600xG for 15 minutes at 4°C and the supernatant stored at -80°C. A Human MMP-2 DuoSet ELISA kit and DuoSet ELISA Ancillary Reagent Kit 2 (R&D Systems, Minneapolis, USA) were used to measure MMP-2 concentrations. Manufacturer's instructions were followed. Plates were incubated overnight with 100µL of capture antibody at room temperature. The following day, wells were aspirated and washed with 400µL wash buffer (three times) and blocked for 1 hour at room temperature using 300µL of reagent diluent. The wash steps were repeated as previously described before the plate was ready for sample addition. Standards were made up by diluting 3µL of stock standard with 997µL of reagent diluent and performing 1:2 serial dilutions to produce standards of 20, 10, 5, 2.5, 1.25, and 0.625 ng/mL. Duplicate wells of 100µL of standards and samples (diluted to 1:2 with reagent diluent) were added and incubated for 2 hours at room temperature. Washing was re-performed and 100µL of detection antibody was added and incubated at room temperature for a further 2 hours. The wash was performed again and 100µL of Streptavidin-HRP was then added to each well and incubated for 20 minutes at room temperature and wrapped in foil. The wash step was performed again and 100µL of substrate solution was added (1:1 mix of colour reagent A and B) to each well. The plate was incubated at 20 minutes at room temperature and wrapped in foil before 50µL of stop solution was added to each well and plates were agitated to ensure thorough mixing. The optical density of each well was then measured at 450nm with wavelength correction at 540nm using a PowerWave HT Microplate Spectrophotometer (Agilent Technologies, Santa Clara, CA, USA). Manufacturer's MMP-2 standards were used to generate a standard curve with an assay range of 0.625 - 20 ng/mL which was then used to calculate the MMP-2 concentration in each sample.

2.12. BCA Protein Assay

A BCA assay was performed on all protein lysates in order to determine the concentration and total amount of protein in each sample before performing any downstream assays. The BCA assay was performed using the Pierce™ BCA Protein Assay Kit (Thermo Fisher Scientific, Waltham, MA, USA) which is a colourimetric assay with a linear working range for BSA of 20 to 2000 µg/mL. 8µL of each sample was diluted in 56µL of deionised water to perform a 1 in 8 dilution. Standards were made up from a 2000 µg/mL stock. A six-point standard curve was prepared, starting with a high standard of 1,000 µg/mL, and then covering 500, 250, 125, 62.5 and 31.2 µg/mL. 25µL of standards and samples were added to a 96 well-plate, in duplicate. Sufficient BCA working reagent was prepared to allow for 200µL of reagent per well by combining 50 parts BCA Reagent A with 1 part BCA Reagent B. 200µL was dispensed per well and the plate was sealed, wrapped in foil to protect from light and incubated at 37°C for

30 minutes. The absorbance was then measured at 562nm using a PowerWave HT Microplate Spectrophotometer (Agilent Technologies, Santa Clara, CA, USA) and a standard curve was generated, from which protein concentrations were calculated (see Figure 2.4).

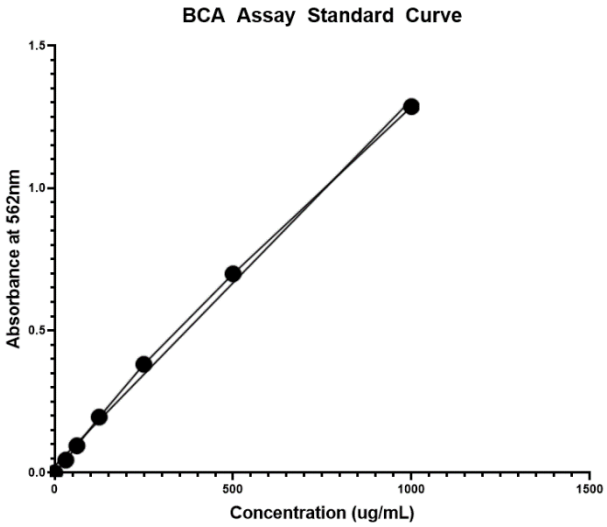

Figure 2.4. A BCA assay standard curve generated using known concentrations of Bovine Serum Albumin (BSA) and absorbance read at 562nm. A six-point standard curve was prepared, starting with a high standard of 1,000 µg/mL, and then covering 500, 250, 125, 62.5 and 31.2 µg/mL of BSA. The curve was used to calculate the unknown protein concentrations of samples, considering the dilution factor of the original samples (1:8).

2.13. Western Blotting

2.13.1. Sample preparation

Protein lysates were obtained by incubating with 1X RIPA lysis buffer (containing 1% of phosphatase inhibitor (PPI) cocktail 2 and 1% PPI cocktail 3) and scraping each well to obtain a cell lysate mixture. Lysates were centrifuged at 14,000 xG at 4°C and the supernatant was obtained. A BCA assay was performed to determine the protein concentration in each sample by using 8µL of lysate in a 1:8 dilution (see Section 2.12). Samples and a molecular weight ladder (covering 10-180 kDa) to load on gels were prepared by combining 7.5µL Laemmli 4X sample buffer, 2µL β-mercaptoethanol and ddH_2O and protein lysate in volumes determined by the BCA assay, to a final volume of 30µL and protein amount of 9µg. Samples were then boiled for 4 minutes and stored at -20°C.

2.13.2. SDS-PAGE and western blotting

Western Blot tank gel apparatus was assembled and precast gels (Bio-Rad Laboratories, Inc., Hercules, California, USA) were used. 30µL of sample was loaded per well and ran at 150 V for ~45 minutes or until the dye reached the bottom of the gels. Gel transfer was performed by assembling a blotting cassette sandwich containing foam insert, pre-wet filter paper, pre-wet PVDF membrane, gel, pre-wet filter paper and foam insert. Blotting apparatus was run at 40 V overnight at 4°C. After transfer, PVDF membranes were dried at room temperature and then re-wet in methanol, water and TBST. PVDF membranes were then blocked-in blocking solution (5% dried milk powder in TBST) and then incubated with primary antibody (Table 2.8) in blocking solution for 3 hours at room temperature (RT). The membrane was then washed and incubated with secondary antibody in blocking solution for 1 hour at RT. After further washing, membranes were incubated for 2 minutes with Super-Signal ECL solution and imaged to observe bands using an IBright FL1500 Imaging System (Thermo Fisher Scientific, Waltham, MA, USA).

2.14. TMT Proteomics

2.14.1. Sample preparation and analysis

Protein expression was measured by tandem mass tagging (TMT) in protein lysates isolated from human CFs following pre-miR-negative control, -214 and -30d transfection. Human CFs were seeded at a density of 35,000 cells/mL in 2mL of FGM per well of a 6 well plate. They were transfected for 5 hours with 30nM pre-miR or 100nM anti-miR and incubated for a further 72 hours in FGM. The cells were then washed twice with 1mL of cold PBS. Cells were treated on ice with 100uL of ice-cold RIPA buffer (containing 1% of each of phosphatase inhibitor II and III cocktails) for 5 minutes. Cells were then scraped, and the RIPA buffer and cell lysis

mixture was transferred to the subsequent well. Once this had been performed for 3 wells in total, the final mixture was transferred to an Eppendorf tube and sonicated for 30 seconds in ice cold water. The mixture was then centrifuged at 14,000xG for 15 minutes and the supernatant was stored at -80°C. A BCA assay was performed to ensure the protein concentration was at least >100µg/mL. Samples were shipped to the University of Bristol Proteomics Facility on dry ice where they underwent TMT analysis. Experimentation performed at the University of Bristol Proteomics Facility involved samples for TMT analysis being labelled within the facility and then fractionated and analysed by nano-LC MSMS using the SPS-MS3 approach on a Orbitrap Fusion Tribid mass spectrometer. Samples were digested and analysed and labelled using TMT reagents which are amine-specific isobaric tags. RP chromatography was performed to fractionate the samples and then each fraction was analysed by acidic RP nano-LC MSMS. Two 10-plex experiments were performed each containing 9 samples plus a common pooled reference sample (which contained an aliquot of each sample, acting as an internal reference) whereby tagged peptides were used to track protein expression.

An initial data analysis was also performed at University of Bristol Proteomics Facility whereby Proteome Discover software was used to generate an Excel report listing the proteins identified and showing how levels of those proteins change between the conditions under comparison as well as the generation of volcano plots and principal component analysis. Subsequent analysis was then performed at the University of Leeds to filter the data prior to pathway analysis, as described in Figure 2.5. In total, 8793 proteins were investigated. Firstly, non-human proteins were eliminated, of which there were 99 (made up of bovine, trypsin and BSA derived proteins which are commonly found in FCS and trypsin-EDTA used for cell trypsinisation), leaving 8,694 proteins. Then any contaminants were eliminated, of which there were 49 (made up largely of keratin proteins), leaving 8645 proteins. Proteins were then eliminated based on whether they passed or failed the false discovery rate (FDR) which is a statistical value that estimates the number of false positive identifications among a peptide identification sequence. For pre-miR-214 transfected samples, 5,279 proteins failed the FDR, leaving 3,365 proteins. For pre-miR-30d transfected samples, this figure was 6,127, leaving 2,517 proteins. These remaining proteins for each transfection were then filtered into lists based on the most significantly changed proteins – this involved analysing the top 500, 250, 100 and 50 significantly changed proteins (measured by P value) for each of pre-miR-214 and -30d transfected samples. Proteins were then filtered based on the most changed proteins (either decreased or increased) based on the log2 fold change results from the original analysis.

Antibody	Catalogue number	Manufacturer
Beta-actin (Mouse Anti Human)	MCA5775GA	Bio-Rad
Mitofusin 2 (Rabbit Anti Human)	12186-1-AP	Proteintech
Pan-LOX (Rabbit Anti Human)	PA116989	Thermo Fisher Scientific

Table 2.8 Antibodies used in Western Blot analysis of protein expression. A list of the antibodies used in the analysis of protein expression in human CFs.

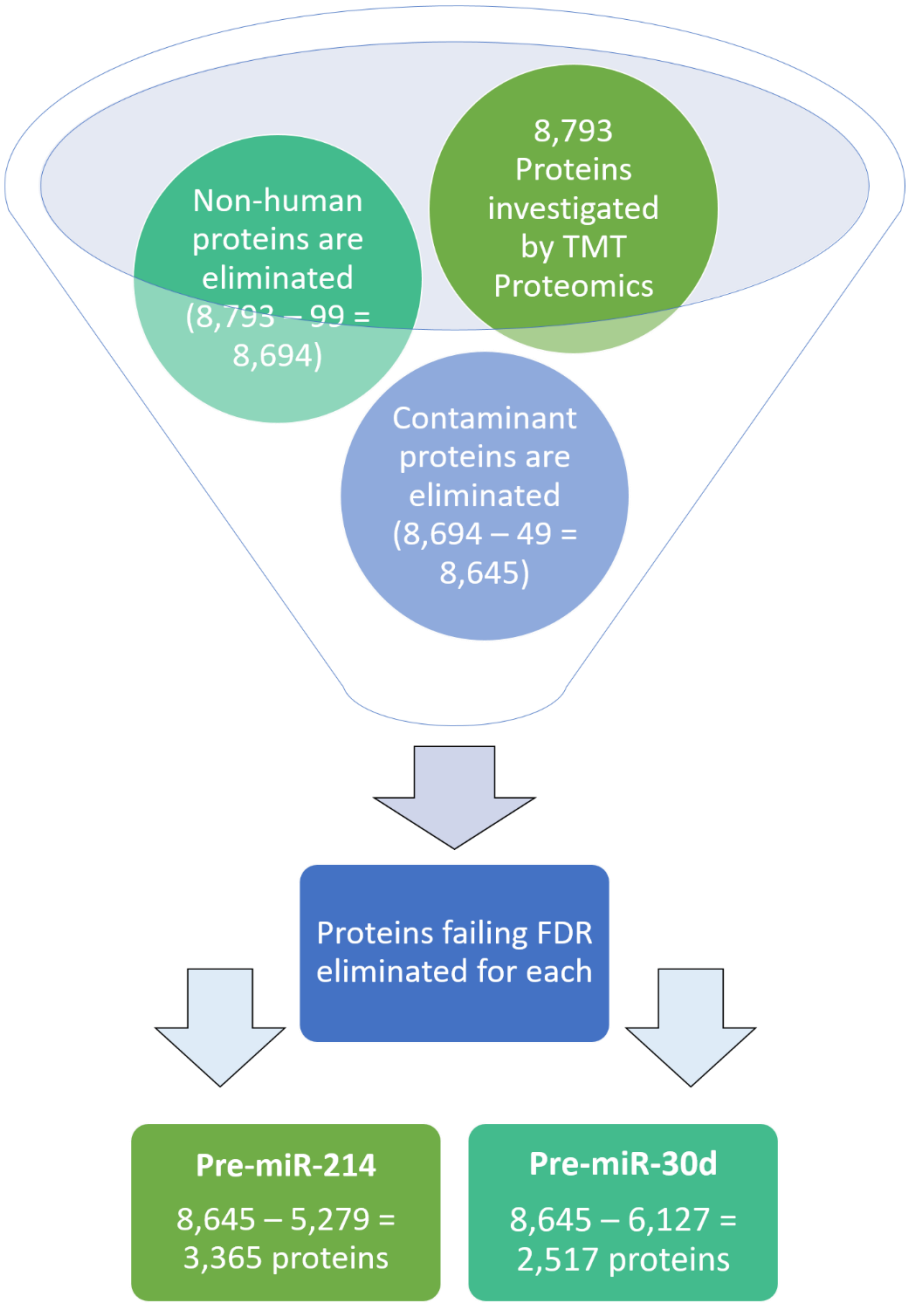

Figure 2.5. A graphical representation of the filtering process taken for proteins investigated by TMT Proteomics. 8,793 proteins were initially investigated by TMT Proteomics, but this number was filtered to 3,365 proteins for pre-miR-214 transfection and 2,517 proteins for pre-miR-30d transfection after filtering steps to eliminate proteins that were either non-human, contaminants or failed the false discovery rate (FDR) test.

2.14.2. Ingenuity Pathway Analysis, STRING and Bioinformatics Analyses

Filtering was applied to the TMT proteomics dataset as described in Section 2.14.1 and further bioinformatics analyses was performed on this dataset using a range of tools. Ingenuity pathway analysis (IPA) (Quiagen, Germany) is a licensed tool that was used to generate predictions based upon the proteins changed by each of the miRNA overexpression and the actual log2 fold changes (either up or down) of each protein. The specific predictions of IPA that were of most interest included canonical pathways, upstream analysis and diseases and functions. Each of the canonical pathways were investigated based on the significance value of the pathway (which indicated the strength of the prediction), the specific targets from the protein list that were implicated in the pathway and the location of each of these proteins in the pathway based on a graphical description generated within IPA. Other free to use online bioinformatics prediction tools were also used to analyse the dataset, including STRING which makes predictions on shared networks between the proteins in the dataset. The limit on the number of proteins analysed in STRING is 2,000 proteins and so the dataset was further refined to analyse the top 2,000 proteins changed based on statistical significance, the top 2,000 most increased or decreased proteins and a combination of both. Other free to use tools included WebGestalt and a literature analysis of research conducted on the specific miRNAs and the canonical pathways predicted as significant by IPA.

2.15. Citrate Synthase Assay

Human CFs were transfected for 6 hours, and protein lysates were obtained after 48 hours using RIPA lysis buffer. The citrate synthase assay was then performed as a measure of mitochondrial function. 1mM of 5', 5'-Dithiobis 2-nitrobenzoic acid (DTNB) was made up fresh by dissolving 2mg DTNB in 5mL 1M Tris-HCl buffer (pH to 8.1) and 10mM oxaloacetate (OAA) was made up fresh by dissolving 6.6mg OAA in 4.5mL ddH_2O and 0.5mL 1M Tris Hcl buffer (pH 8.1). In a 96 well plate, a working solution was prepared so that blank wells contain 200µL (made up of 175.5µL dH_2O, 19.5µL DTNB and 5µL acetyl-CoA) and experimental wells contain 199µL of working solution plus 1µL of sample or citrate synthase standard where each sample or standard was plated in triplicate. The spectrophotometer was set to 37°C and the wavelength to 412nm. The plate was loaded and allowed to equilibrate to temperature for 5 minutes. 5µL of OAA was then added to each of the experimental wells only. Reading was performed at 412nm for 5 minutes and only ¼ of a plate was read at a time.

2.16. Flex Station Measurement of Piezo1 Activity Assay

Human CFs were transfected for 6 hours and then trypsinised from 24 well cell culture plates after 48 hours and plated at a density of 12,000 cells/mL in 1mL FGM in each well of a 96 well poly-D-lysine, black/clear bottom plate and incubated overnight at 37°C. Cells were checked

under a light microscope to ensure they were in a confluent monolayer. Fura2-AM was made up in salt buffered saline (SBS) (containing probenecid at a concentration of 12.5mM) by adding 1:1000 dilution of 10% pluronic acid and 1:500 dilution of 1mM Fura2-AM stock to a final concentration of 2µM which was then protected from light. Growth media was removed from each well and 50µL of Fura2-AM mix was added before incubating the plate, wrapped in foil, at 37°C for 1 hour. After the incubation, the Fura2-AM mix was removed and 100µL of SBS (containing probenecid) was added to each well and then incubated for 30 minutes, wrapped in foil, at RT. During the 30-minute incubation, recording buffer was made up by adding a 1:1000 dilution of 10% pluronic acid to 1:1000 dilution of DMSO and SBS (containing pluronic acid) so there was 60µL per well. During the incubation, compound plates were prepared in a U bottom 96 well plate. Compound plates were designed so that triplicate wells of each condition would be treated with 60µL of YODA1 or DMSO (both to a final concentration of 5µM) and both would be treated subsequently with 60µL ATP (to a final concentration of 5µM), each made up in SBS (containing probenecid). After incubation, the 100µL SBS was removed and 60µL recording buffer was added. Plates were read at an excitation wavelength of 340nm and 380nm for a total run time of 7 minutes and intervals of 5 seconds and ATP compound transfer at 300 seconds. After the run, data were exported and analysed using Excel. Data analysis involved dividing the results at 340nm by the result at 380nm for the same time point and then subtracting the baseline (the average result for the initial 30 seconds of each run) from each result. These final values were plotted against the length of time (in seconds).

2.17. Statistical Analyses

GraphPad Prism 8 (San Diego, CA, USA) was used for data analysis and presentation. Averaged data are presented as mean ± SEM, where “n” represents the number of independent experiments on cells from different patients (i.e., biological replicates). For comparisons between two sets of normalised data (e.g., RT-PCR), values were transformed (Y=Log(Y)). Unpaired t tests were performed to calculate a two tailed P value when comparing data deriving from different biological samples and paired t tests were performed for data belonging to the same patients. A two-way ANOVA was performed to measure significance across two different variables and was followed by a Tukey post-hoc test. When there were large differences in the values obtained between different groups on the same graph, data was plotted on a Log10 scale. $P<0.05$ was considered statistically significant *$P<0.05$, **$P<0.01$ and ***$P<0.001$. No significant difference is indicated by NS ($P>0.05$).

Chapter 3 Expression levels and regulatory activity of miR-21a, -214, -224 and -30d in the murine heart, and in murine and human cardiac fibroblasts

3.1 Introduction

Adverse cardiac remodelling involves both increased fibrosis and increased hypertrophy. CFs have been demonstrated as pivotal in both processes, driving fibrosis through the secretion of extracellular matrix (ECM) related proteins and mediating hypertrophy through the secretion of paracrine signalling molecules, including the cytokine interleukin-6 (IL-6). Our group has been studying the role of the p38 MAPK signalling pathway in the regulation of CF responses to inflammatory stimuli and cardiac injury. p38 MAPK has been demonstrated as a pivotal signalling molecule in the response to inflammatory stimuli and cardiac injury, resulting in CF activation. Following activation CFs then exhibit behaviours that ultimately lead to pathological cardiac remodelling such as fibrosis and induction of cardiomyocyte hypertrophy (Turner and Blythe, 2019).

Specifically, our group has investigated human CFs *in vitro* and found that the subtype of p38 MAPK that is primarily expressed in human CFs is p38α and this subtype is integral to CF behaviour in cardiac remodelling, including the expression and secretion of IL-6 (Sinfield et al., 2013). Following on from this work, our group performed an investigation producing a loxP-directed deletion of *p38α MAPK* in fibroblasts in mice (Fb-p38α KO). A cardiac injury model was then performed in Fb-p38α KO and wild type (WT) mice by infusing with the β-adrenergic receptor agonist, isoproterenol (ISO), as a model of HF, as published by Bageghni et al., (2018). This model was conducted by injecting mice (at 3 weeks of age) with tamoxifen to induce Cre activity and facilitate loxP-directed deletion of fibroblast specific p38α (Fb-p38α). Then, at 10-12 weeks of age, ISO or saline was infused for 14 days in control or Fb-p38α KO mice before removal of osmotic mini-pumps. Cardiac function was analysed after 3 weeks at which point RNA was extracted. It was demonstrated that the activity of p38α MAPK is pivotal for cardiac hypertrophy and the release of IL-6 and that Fb-p38α KO were protected against cardiac dysfunction in comparison to WT mice (Bageghni et al., 2018). Targeting p38α MAPK with therapeutics has however shown mixed success in the clinic and inhibition of p38α/β did not improve outcomes after 6 months post-MI and so there is great importance in the discovery of other therapeutic targets involved in the regulation of CF behaviour to treat adverse cardiac remodelling (O'Donoghue et al., 2016).

CFs, alike other cell-types, express cell specific and generic miRNAs which govern post-transcriptional regulation through the binding to (either perfect or imperfect) target mRNAs to facilitate inhibition of translation (Humphreys et al., 2005). Hearts from these Fb-p38α KO mice and WT mice were isolated and miRNA levels were assessed by performing an 84-target

miRNA microarray (Bageghni et al., 2018). In this microarray, 14 miRNAs were modulated, with 12 being increased and 2 being decreased following ISO treatment. The group identified five miRNAs that were significantly regulated by ISO in control mice but not in Fb-p38α KO mice, which were miR-21a, -214, -224, -208b, and -30d (Figure 3.1). It was found by Bageghni et al., (2018) that miR-21a-5p, -214-3p and -224-5p levels were increased, and miR-30d-5p levels were decreased, 3 weeks post-ISO infusion compared to saline infusion (Figure 3.1). The levels of these miRNAs were modulated significantly for miR-214, -224 and -30d and was near significance ($P = 0.09$) for miR-21 and they showed no significant difference when comparing the levels in saline infused mice compared to ISO infused fibroblast specific p38α (Fb-p38α) KO mice for all four miRNAs (Figure 3.1). The dependence of these miRNAs on p38α MAPK activity suggests they are important for the cardioprotective effect of fibroblast-specific p38α KO. The miR-208b is expressed specifically in cardiac and skeletal muscle (and is encoded by an intron of the β-MHC gene) and so was not included in our investigation in CFs.

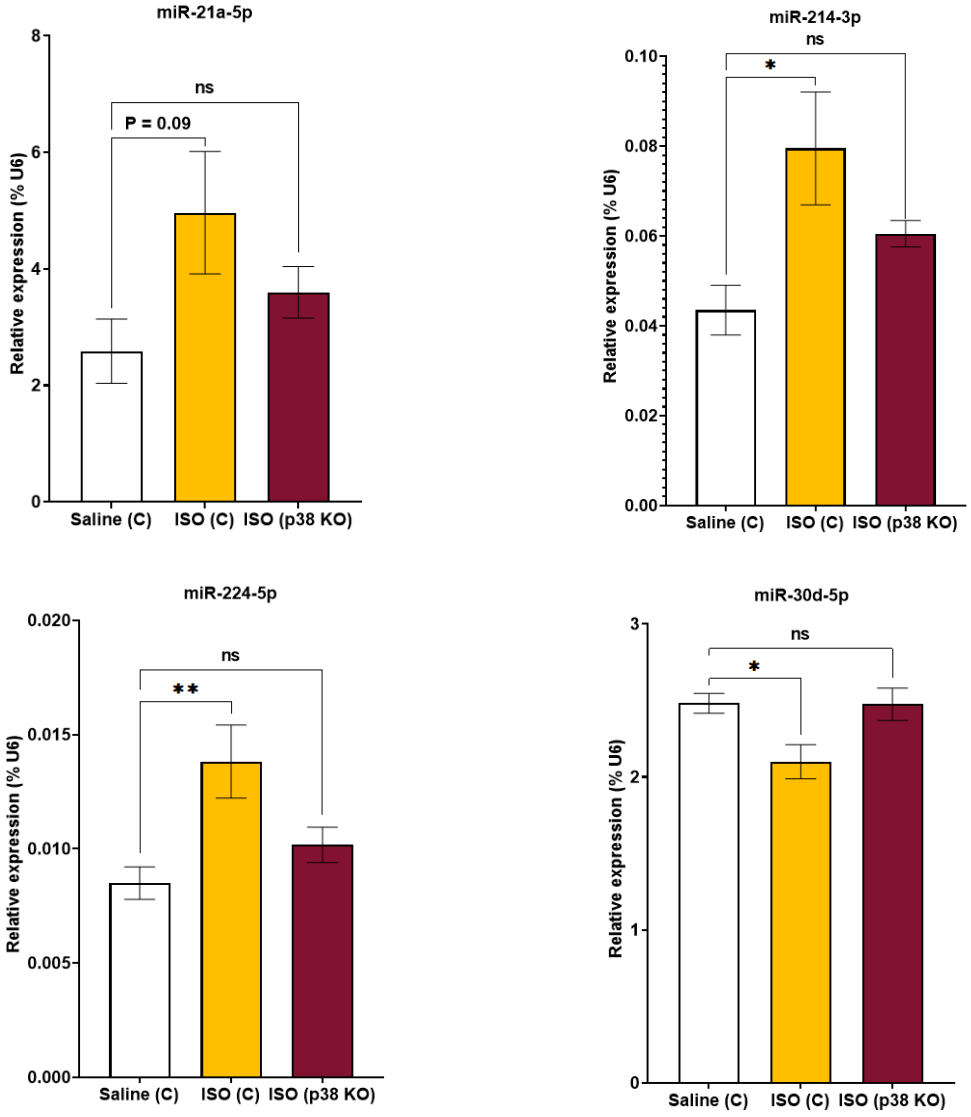

Figure 3.1. MiRNA levels in whole heart 3 weeks post-isoproterenol infusion in control and fibroblast-specific p38 MAPK KO mice. Isoproterenol (ISO) infusion was performed to induce chronic β-adrenergic receptor stimulation in WT mice or mice with a loxP-directed deletion of fibroblast specific p38α (Fb-p38α). Saline infusion was performed in WT mice as a control. MiRNA levels were calculated by performing an 84-target SYBR Green miRNA array and normalising levels relative to a range of controls including: SNORDs 61, 68, 72, 95 and 96A and U6. Horizontal bars indicate the mean value and error bars represent SEM. Group sizes; n=4. Ordinary one-way ANOVA, with a Šidák multiple comparisons test, performed on log transformed data (Y=Log(Y)). *P<0.05 and **P<0.01. ns=not significant. Original data published in FASEB Journal (Bageghni et al., 2018).

It is important to investigate and discover the expression levels of each of these miRNAs in a range of murine models of cardiac remodelling, including MI and chronic hypertensive models (Bageghni et al., 2018). Similarly, it is important for translatability to investigate the level of these miRNAs in human CFs and to understand how the stimulation of CFs *in vitro* with relevant stimuli, and the inhibition of p38, may modulate the expression levels of all four miRNAs.

3.2 Aims

The main aims of this chapter were:

- To investigate the expression levels of miR-21a, -214, -224 and -30d in the murine heart, and whether their expression changes with cardiac dysfunction (HF, MI or chronic hypertension models);
- To measure the basal miRNA expression levels in unstimulated cultured murine and human CFs;
- To measure the miRNA levels in human CFs after stimulation with cardiac dysfunction relevant stimuli;
- To measure the miRNA levels in human CFs after pharmacological inhibition with a p38 inhibitor.

3.3 Methods

3.3.1 Generic methods

Human CFs were cultured from right atrial appendage (RAA) biopsies as described in Section 2.2. Mouse CFs were cultured using a similar collagenase digestion technique, as described in Mylonas et al., (2017). RNA was isolated as described in Section 2.3 and miRNA levels were quantified by qRT-PCR as described in Section 2.5. All animal procedures were carried out in accordance with the Animal Scientific Procedures Act (United Kingdom) 1986 under United Kingdom Home Office authorisation, following review and approval by the University of Leeds Animal Welfare and Ethical Review Committee.

3.3.2 Mouse model of MI (LAD coronary artery ligation)

Experimental MI was performed in mice by permanently ligating the left anterior descending (LAD) coronary artery (Bageghni et al., 2019). This was ligated at the edge of the left atrium using 8-0 prolene suture, and occlusion was confirmed by observing the pallor of the anterior LV wall. Sham-operated animals underwent a similar surgical procedure without tying the ligature. RNA was purified from snap-frozen heart tissue 3 days and 4 weeks after LAD ligation. Mice from which RNA was extracted at 3 days post-LAD were Cre-negative controls

from a cardiomyocyte-specific *IL-1α* KO (MIL1AKO) mouse line (Bageghni et al 2019). Mice from which RNA was extracted at 4 weeks were from Cre-negative controls for a fibroblast-specific *IL-1R1 KO* (FIL1R1KO) mouse line that had been injected with tamoxifen for 5 days, at 12 days old before performing LAD ligation at 10-12 weeks old (Bageghni et al., 2019). Surgical techniques were performed by Dr Mark Drinkhill, and RNA extraction performed by Dr Sumia Bageghni and Dr Karen Hemmings.

3.3.3 Mouse model of hypertensive remodelling (chronic Ang II infusion)

A model of chronic hypertension was performed in mice using the vasoconstrictive peptide Ang II. Alzet mini-pumps delivered Ang II (1,000 ng/kg/min) or saline as a control to 12-week-old mice for 4 weeks. Echocardiography and morphometric analysis revealed overt cardiac hypertrophy in mice receiving Ang II compared with saline, without a reduction in ejection fraction i.e., compensated cardiac hypertrophy (unpublished data). Heart tissue was then collected, and RNA extraction was performed. Surgical techniques, morphometric and echocardiographic analysis, and RNA extraction were performed by Dr Leander Stewart.

3.3.4 Murine whole heart cell fractionation

Cardiac cell fractionation was performed by magnetic antibody cell separation (MACS) as described by Bageghni et al., (2018). Mouse hearts were digested with collagenase and then filtered through a 30-μm MACS SmartStrainer (Miltenyi Biotec, Bergisch Gladbach, Germany) to remove CMs. Non-myocytes were separated into 2 fractions: non-fibroblasts (endothelial cells and leukocytes) and fibroblasts with a Cardiac Fibroblast MACS Separation Kit (Miltenyi Biotec). RNA was extracted from cell fractions, and quantitative RT-PCR was used to quantify mRNA for cell type-specific marker genes which included *Myh6* (cardiomyocyte marker); *Pecam1* (endothelial cell marker); *Ddr2, Pdgfra, Col1a1*, and *Col1a2* (fibroblast markers) (Bageghni et al 2019). Gene expression levels were compared with those obtained from a single sample of collagenase-digested whole heart. MACS separation, RNA extraction and miRNA RT-PCR were performed by Dr Sumia Bageghni and Dr Karen Hemmings.

3.3.5 Stimuli and p38 inhibitor treatment of human CFs

Human CFs were treated in vitro with a range of growth factors or cytokines as stimuli or a p38 inhibitor (SB203580) to assess the effect on miRNA expression. Cells were plated at a density of 30,000 cells/mL in 1mL of FGM overnight. They were then washed with 1mL PBS and incubated with 1mL SFM for 24 hours to quiesce. Cells were treated with 10nM Ang II, 10μM ISO, 10ng/mL TNFα, 1ng/mL TGFβ, 10ng/mL IL1α, 10μM SB203580 or 10μM DMSO (control) in 1mL SFM or 0.4% FCS for 6 hours or 24 hours. At each time point, cell pellets were obtained, and RNA isolation was performed (as described in Section 2.3) before

subsequent miR-RT-PCR (Section 2.5). Data are expressed relative to the U6 housekeeping gene mRNA expression with the cycle threshold ($2^{-\Delta Ct}$) method.

3.4 Results

3.4.1 Measuring miRNA levels in murine models of cardiac dysfunction

Building on the results from the ISO-HF model, the second model of cardiac dysfunction that was used to measure any effect on miRNA expression levels was left anterior descending (LAD) coronary artery ligation which is a permanent occlusion model of MI. MiRNA levels were first measured at 3 days post-MI and it was found that the levels of miR-21 and -214 were both significantly higher (2.5-fold and 2.7-fold higher respectively) in MI mice compared to sham mice (Figure 3.2). MiR-224 and -30d showed no change in expression levels at the 3-day time point (Figure 3.2). At 4 weeks post-MI however, a different expression pattern was evident whereby miR-21, -214 and -224 levels were similar in the MI and sham groups, but miR-30d showed significantly lower expression levels in the MI mice (a decrease of 90.5%) (Figure 3.3). It was noticeable that basal miRNA levels were different (relative to U6) between the 3-day and 4-week samples, possibly reflecting that the samples had been obtained on different occasions from different control mouse populations.

The third and final murine model of cardiac dysfunction from which miRNA levels were measured was that of an angiotensin II (Ang II) infusion model to mimic chronic hypertension and compensated hypertrophy. MiRNA levels were measured at 4-weeks post infusion of Ang II or saline. Like the LAD model of MI, in this model it was found that whereas miR-21, -214 and -224 remained similar between both groups, miR-30d had significantly lower expression in the Ang II infusion group compared to saline infusion (a decrease of 48.3%) (Figure 3.4).

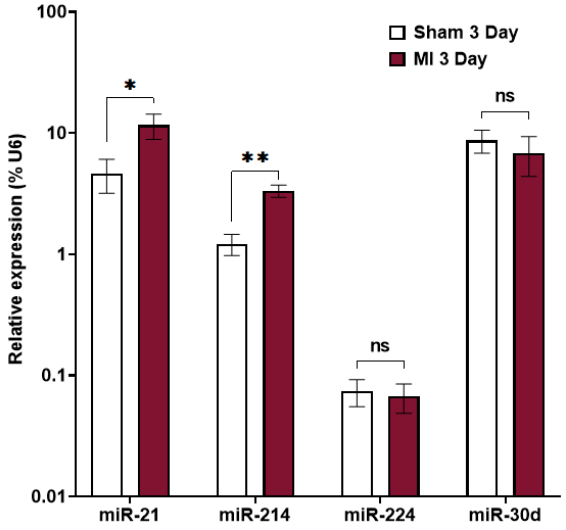

Figure 3.2. MiRNA levels in whole heart murine RNA extracted at 3 days post-MI. Left anterior descending (LAD) coronary artery ligation or a sham procedure was performed on mice and RNA was extracted from hearts after 3 days. MiRNA levels were calculated by performing qRT-PCR and normalising levels relative to the housekeeping control, U6. Note the Log10 scale. Horizontal bars indicate the mean value and error bars represent SEM. Group sizes; n=5 for sham and n=4 for MI. Two tailed, parametric, unpaired t test performed on log transformed data (Y=Log(Y)). **P<0.01 and *P<0.05. ns=not significant.

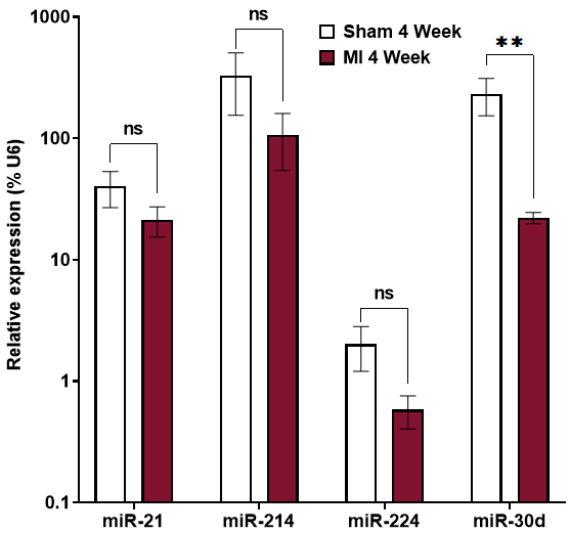

Figure 3.3. MiRNA levels in whole heart murine RNA extracted at 4 weeks post-MI. Left anterior descending (LAD) coronary artery ligation or a sham procedure was performed on mice and RNA was extracted from hearts after 4 weeks. MiRNA levels were calculated by performing qRT-PCR and normalising levels relative to the housekeeping control, U6. Note the Log10 scale. Horizontal bars indicate the mean value and error bars represent SEM. Group sizes; n=5 for sham and n=4 for MI. Two tailed, parametric, unpaired t test performed on log transformed data (Y=Log(Y)). **P<0.01. ns=not significant.

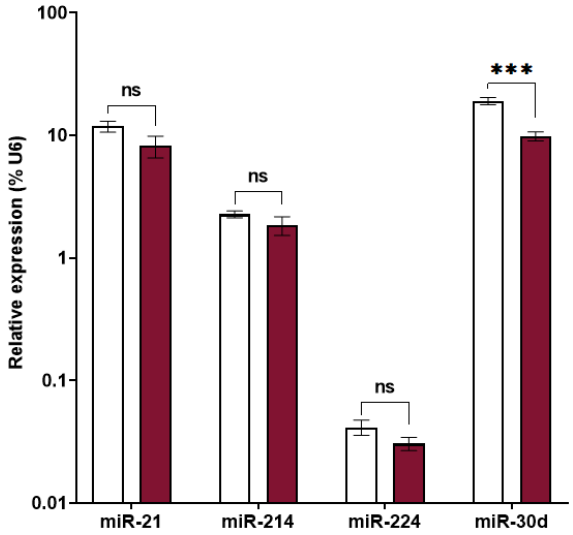

Figure 3.4. MiRNA levels murine whole heart at 4 weeks post-angiotensin II infusion. The vasoactive peptide Ang II was delivered in mice using mini pumps as a model of chronic hypertension. Heart tissue was collected, and RNA extraction performed. MiRNA levels were calculated by performing qRT-PCR and normalising levels relative to the housekeeping control, U6. Note the Log10 scale. Horizontal bars indicate the mean value and error bars represent SEM. Group sizes; n=4. Ordinary one-way ANOVA, with a Šidák multiple comparisons test, performed on log transformed data (Y=Log(Y)). ***P<0.001. ns=not significant.

3.4.2 Detection of microRNAs in murine and human cardiac fibroblasts

To validate that the miRNAs modulated in the ISO model could be observed in CFs, our group first performed qRT-PCR analysis to measure miRNA expression levels in cardiac cell fractions obtained from mouse heart using the MACS technique (Figure 3.5). It was observed that miR-21a, -214 and -224 were enriched in CFs compared to endothelial cells (EC), with significant differences for miR-214 and -224 and a trend for miR-21a (P=0.06). MiR-30d however appeared to show more similar levels across CFs, ECs, and the whole heart (Figure 3.5).

The expression levels of each miRNA were then analysed specifically in cultured murine CFs from 4 separate heart preparations under basal conditions to assess the expression pattern (Figure 3.6). This analysis found that miR-214 was expressed at the highest level, followed by -21a, -30d and then -224 (with miR-214 being expressed 6-fold higher than miR-21a, 25.5-fold higher than miR-30d and 140.7-fold higher than miR-224) (Figure 3.6).

Similarly, the expression levels were then analysed in cultured human CFs from 4 different donors under basal conditions to assess the translatability of the investigation into these specific miRNAs (Figure 3.7). The same expression pattern was observed as in murine CFs (Figure 3.6), where miR-214 showed the highest level of expression, followed by -21a, -30d and finally -224 (with miR-214 being expressed 2.4-fold higher than miR-21a, 37.4-fold higher than miR-30d and 109.4-fold higher than miR-224) (Figure 3.7).

In summary, the expression levels of the four miRNAs were found to be generally similar between freshly isolated murine CF, cultured murine CF and cultured human CF, with miR-214 being most highly expressed and miR-224 having the lowest expression, and miR-21 and miR-30d being somewhere in between.

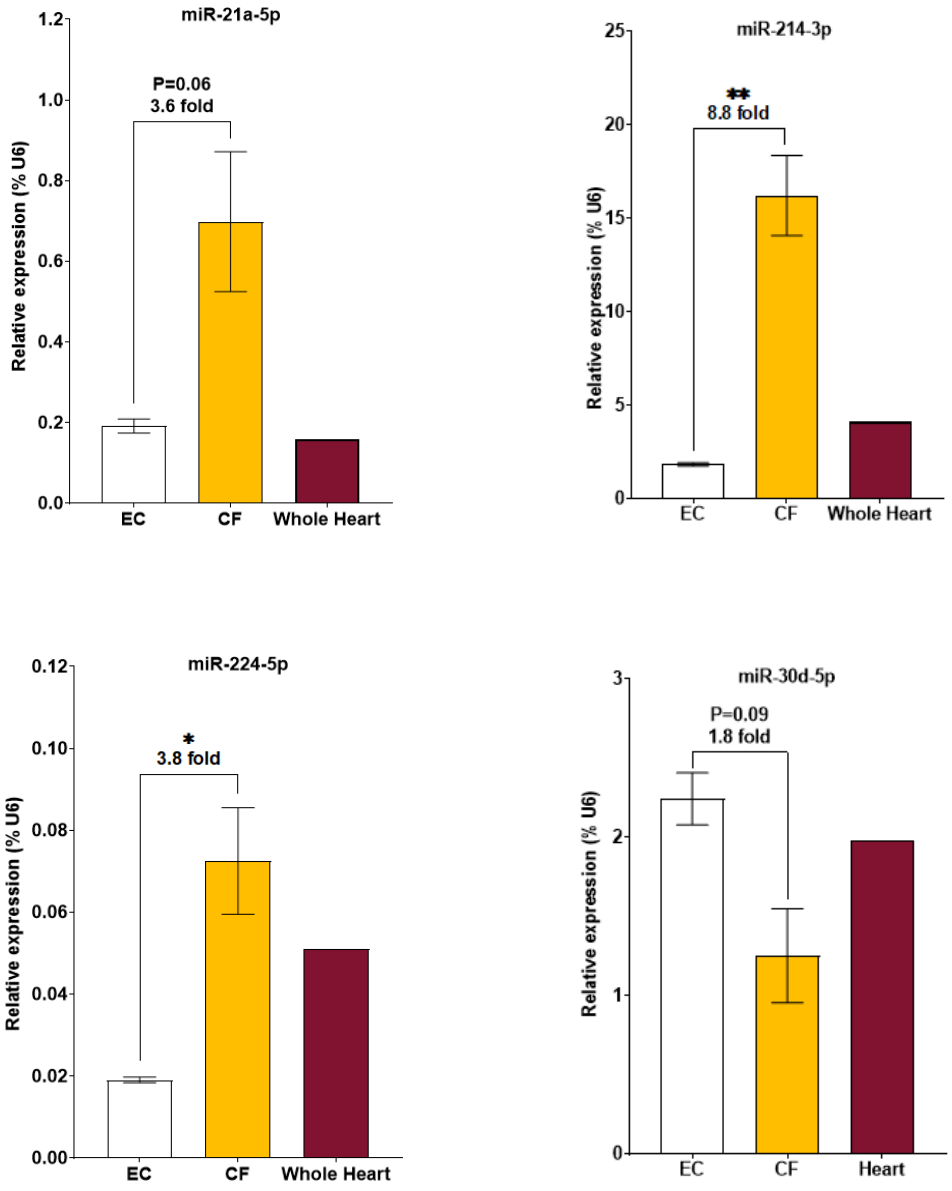

Figure 3.5. MiRNA levels in freshly isolated endothelial cells, cardiac fibroblasts, and murine whole heart. Non-myocytes from collagenase-digested murine hearts were separated into two fractions by magnetic antibody cell separation (MACS). EC = endothelial cells and leukocytes; CF = cardiac fibroblasts; and whole heart (all cardiac cell types, including cardiomyocytes). MiRNA levels were calculated by performing qRT-PCR and normalising levels relative to the housekeeping control, U6. Horizontal bars indicate the mean value and error bars represent SEM. Group sizes; n=3 for EC and CF and n=1 for whole heart. Two-tailed, ratio paired t test performed on non-transformed data and fold difference reported. *P<0.05 and **P<0.01. Unpublished data by Dr Sumia Bageghni.

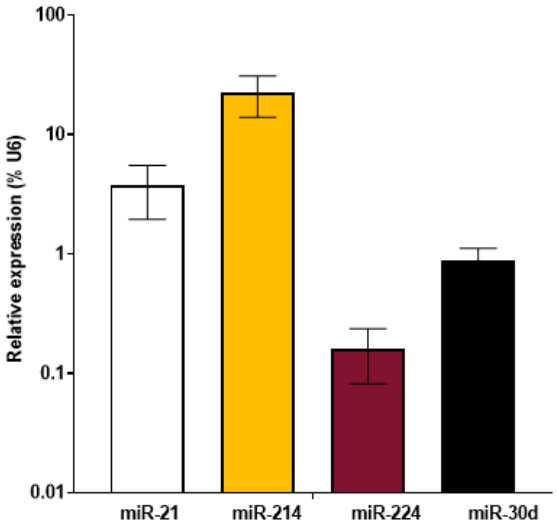

Figure 3.6. MiRNA levels in cultured murine cardiac fibroblasts. RNA was isolated from murine cardiac fibroblasts from 4 different hearts and miRNA levels were calculated by performing qRT-PCR and normalising levels to the housekeeping control, U6. Note the log10 scale. Horizontal bars indicate the mean value and error bars represent SEM. Group sizes; n=4.

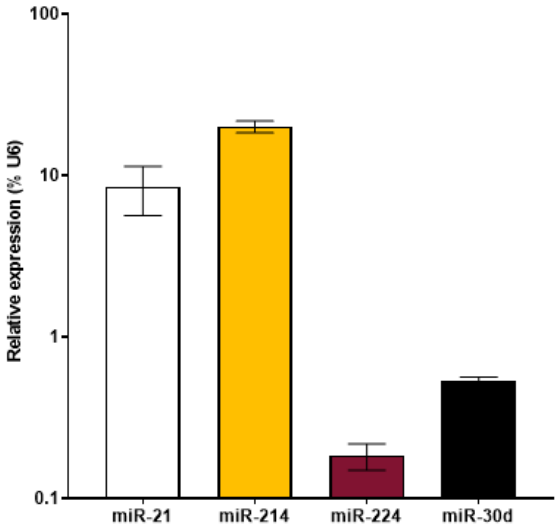

Figure 3.7. MiRNA levels in cultured human cardiac fibroblasts. RNA was isolated from human cardiac fibroblasts, derived from right atrial appendage tissue from 4 different donors, and miRNA levels were calculated by performing qRT-PCR and normalising levels to the housekeeping control, U6. Note the log10 scale. Horizontal bars indicate the mean value and error bars represent SEM. Group sizes; n=4.

3.4.3 MiRNA expression levels in human CFs under a range of stimuli and p38 inhibition

The expression levels of each miRNA were investigated in human CFs, *in vitro*, under the influence of a range of stimuli known to be influential in cardiac remodelling (Figures 3.8-3.11). First, the influence of cardiac dysfunction relevant stimuli was investigated, including TNFα, Ang II, ISO, IL1α, TGFβ and 10% FCS. These stimuli were chosen as they are known stimulators of CFs, inducers of cardiac remodelling and/or known to be released during cardiac dysfunction. Experiments were performed over a 6 h or 24 h period in either SFM or medium containing a low concentration of serum (0.4% FCS). Whereas for most stimuli treatments and serum concentrations (both SFM (panels A and B) or 0.4% FCS (panel C)), there was little effect on the expression levels of the miRNAs (Figures 3.8-3.11), there was an effect on the level of miR-21a after treatment with TNFα (Figure 3.8). It was found that at 24 hours post-TNFα treatment, the level of miR-21a was significantly lower (a decrease of 27.6%) compared to 24 hours post-SFM incubation (Figure 3.8B). There also appeared to be a trend of lower miR-224 levels when treated with IL1-α (made up in 0.4% FCS) for 24 hours with a decrease of 62.5% (P=0.0778) (Figure 3.10C). A trend for lower miR-30d levels was further observed when cells were treated with ISO (made up in SFM) for 6 hours with a decrease of 17.3% (P=0.0915) (Figure 3.11A).

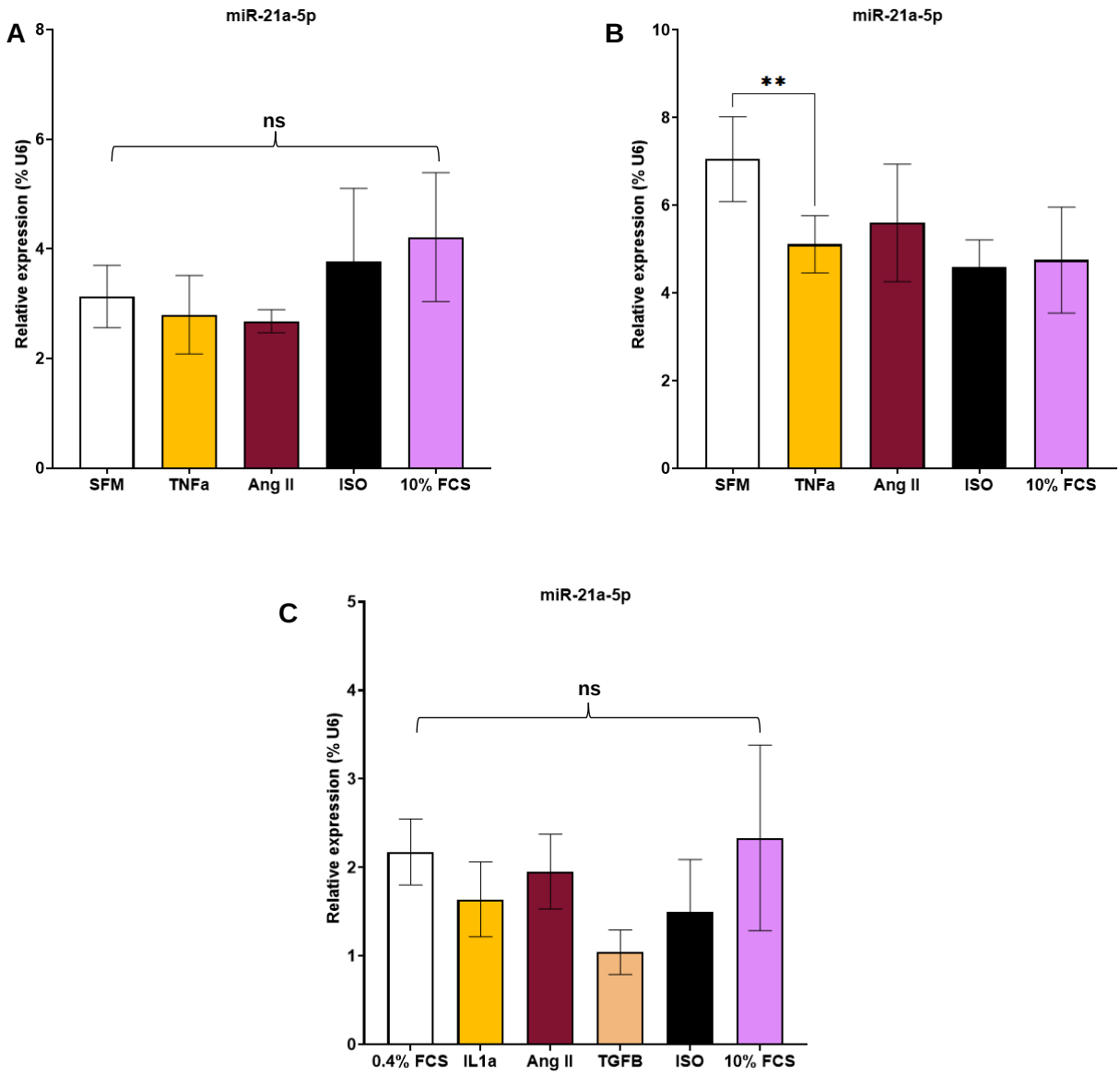

Figure 3.8. MiR-21a levels in human cardiac fibroblasts post-stimuli treatment. Human CFs were treated with stimuli including SFM, TNFα (1ng/mL), Ang II (10nM), ISO (10μM) (made up in SFM) and 10% FCS **(A** and **B)** and IL1α (10ng/mL), Ang II (10nM), TGFβ (1ng/mL), ISO (10μM) (made up in 0.4% FCS) and 10% FCS **(C)**. RNA was isolated at either 6 hours **(A)** or 24 hours post-treatment **(B** and **C)**. MiRNA levels were calculated by performing qRT-PCR and normalising levels to the housekeeping control, U6. Horizontal bars indicate the mean value and error bars represent SEM. Group sizes; n=3 (A) and n=4 (B). Ordinary one-way ANOVA, with a Šidák multiple comparisons test, performed on log transformed data (Y=Log(Y)). **P<0.01. ns=not significant.

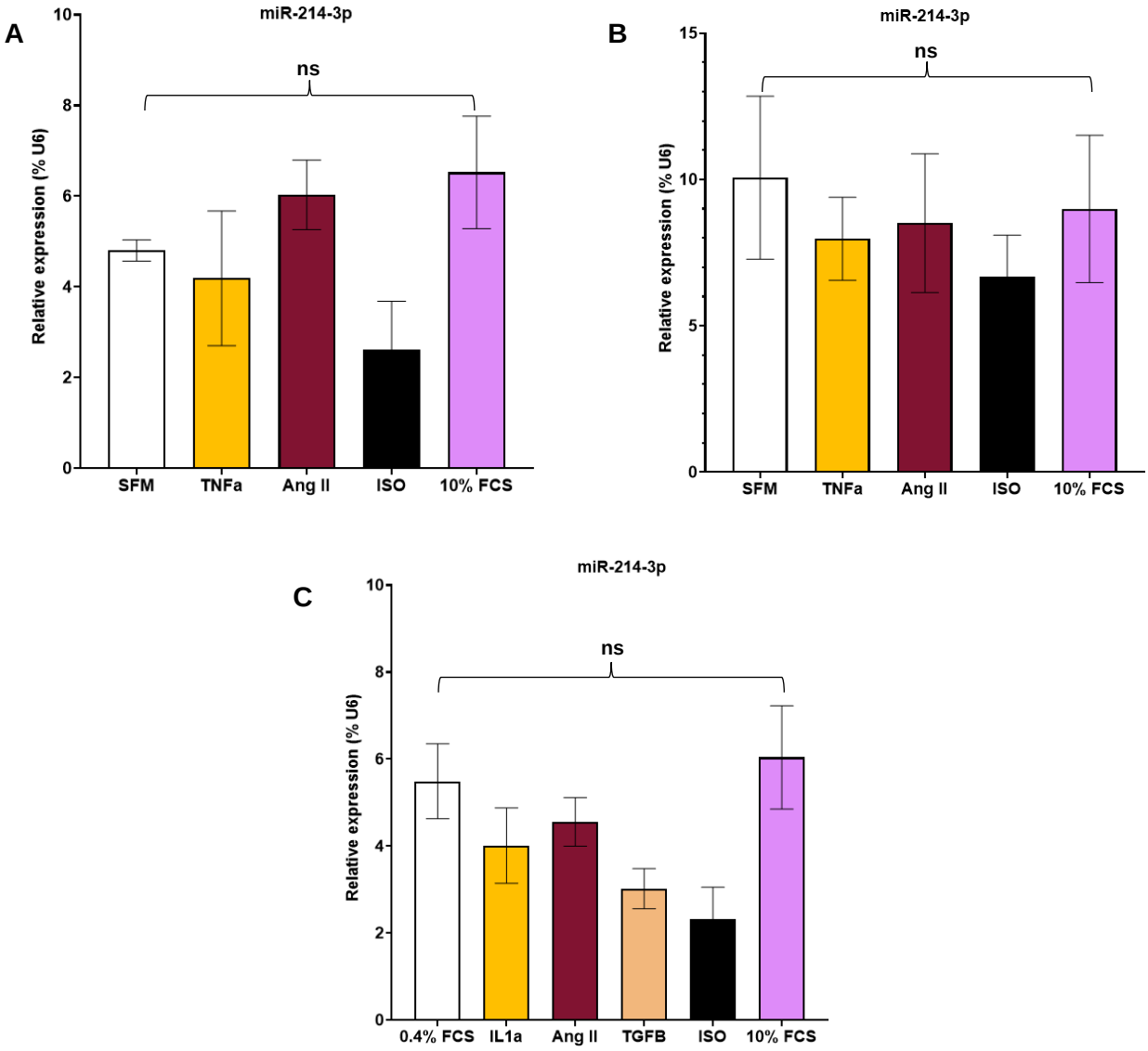

Figure 3.9. MiR-214 levels in human cardiac fibroblasts post-stimuli treatment. Human CFs were treated with stimuli including SFM, TNFα (1ng/mL), Ang II (10nM), ISO (10μM) (made up in SFM) and 10% FCS **(A** and **B)** and IL1α (10ng/mL), Ang II (10nM), TGFβ (1ng/mL), ISO (10μM) (made up in 0.4% FCS) and 10% FCS **(C)**. RNA was isolated at either 6 hours **(A)** or 24 hours post-treatment **(B** and **C)**. MiRNA levels were calculated by performing qRT-PCR and normalising levels to the housekeeping control, U6. Horizontal bars indicate the mean value and error bars represent SEM. Group sizes; n=3 (A) and n=4 (B). Ordinary one-way ANOVA, with a Šidák multiple comparisons test, performed on log transformed data (Y=Log(Y)). ns=not significant.

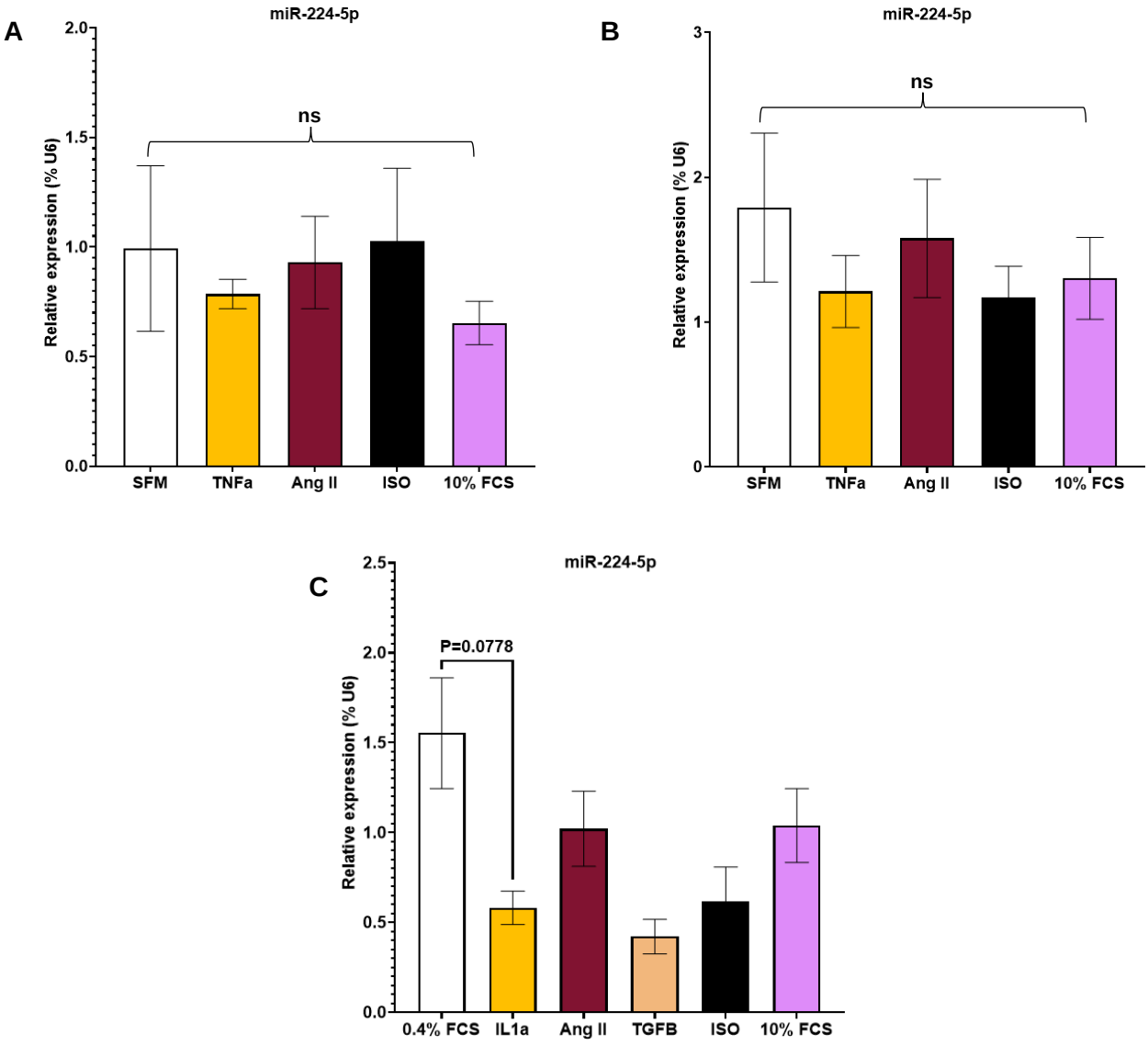

Figure 3.10. MiR-224 levels in human cardiac fibroblasts post-stimuli treatment. Human CFs were treated with stimuli including SFM, TNFα (1ng/mL), Ang II (10nM), ISO (10μM) (made up in SFM) and 10% FCS **(A** and **B)** and IL1α (10ng/mL), Ang II (10nM), TGFβ (1ng/mL), ISO (10μM) (made up in 0.4% FCS) and 10% FCS **(C)**. RNA was isolated at either 6 hours **(A)** or 24 hours post-treatment **(B** and **C)**. MiRNA levels were calculated by performing qRT-PCR and normalising levels to the housekeeping control, U6. Horizontal bars indicate the mean value and error bars represent SEM. Group sizes; n=3 (A) and n=4 (B). Ordinary one-way ANOVA, with a Šidák multiple comparisons test, performed on log transformed data (Y=Log(Y)). ns=not significant.

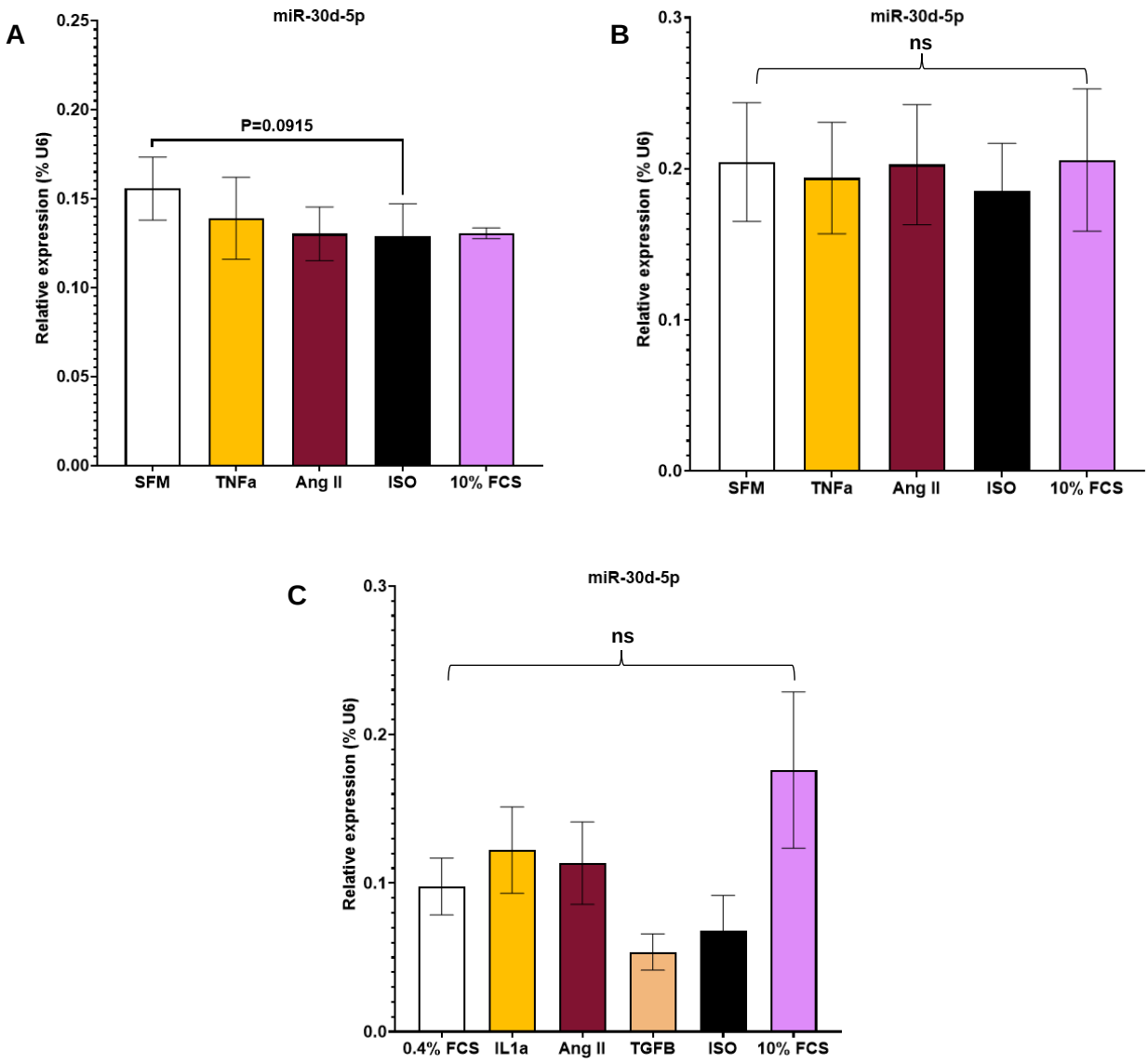

Figure 3.11. MiR-30d levels in human cardiac fibroblasts post-stimuli treatment. Human CFs were treated with stimuli including SFM, TNFα (1ng/mL), Ang II (10nM), ISO (10μM) (made up in SFM) and 10% FCS **(A and B)** and IL1α (10ng/mL), Ang II (10nM), TGFβ (1ng/mL), ISO (10μM) (made up in 0.4% FCS) and 10% FCS **(C)**. RNA was isolated at either 6 hours **(A)** or 24 hours post-treatment **(B and C)**. MiRNA levels were calculated by performing qRT-PCR and normalising levels to the housekeeping control, U6. Horizontal bars indicate the mean value and error bars represent SEM. Group sizes; n=3 **(A)** and n=4 **(B)**. Ordinary one-way ANOVA, with a Šidák multiple comparisons test, performed on log transformed data (Y=Log(Y)). ns=not significant.

Finally, the effect of p38 inhibition on miRNA levels in human CFs was investigated to further understand the dependence of these miRNA levels on p38 MAPK activity, as previously suggested in murine whole heart (Figure 3.1; Bageghni et al 2018). It was demonstrated that a trend exists where the levels of each miRNA were decreased in human CFs treated with p38 inhibitor SB203580 vs treated with DMSO (control) (at 24 hours post-treatment) and specifically, the levels of miR-224 were significantly decreased by 46.5% (Figure 3.12A). However, at 48 hours post-p38 inhibitor treatment, there was no effect on miRNA expression levels, indicating that the effect of p38 inhibition on miR-224 was short-lived (Figure 3.12B).

An important role of p38 MAPK is to respond to stress stimuli such as cytokines by inducing the transcription of genes and miRNAs which subsequently coordinate their own downstream regulation. Therefore, the pharmacological inhibition of p38 resulting in a significant decrease in miR-224 expression, is suggestive that miR-224 transcription can be induced by the activity of p38 MAPK. Similarly, the fact that miR-21a expression was lower upon treatment with TNFα, a cytokine that induces necrosis and apoptosis, suggests that miR-21 levels are decreased by TNFα activity, which may be important in inflammatory cardiac remodelling such as post-MI.

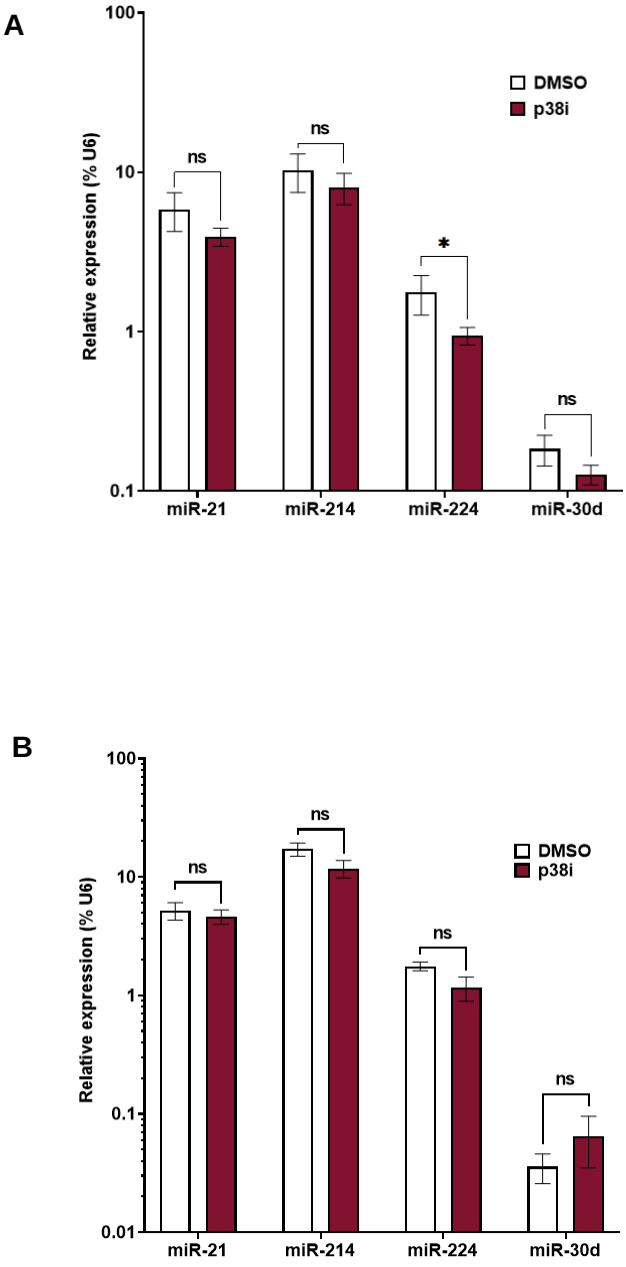

Figure 3.12 MiRNA levels in human cardiac fibroblasts at 24 hours and 48 hours post-p38 inhibitor or DMSO treatment. Human CFs were treated with 10µM SB203580 (p38 inhibitor) or DMSO (vehicle control) and RNA was isolated at 24 **(A)** or 48 hours **(B)** post-treatment. MiRNA levels were calculated by performing qRT-PCR and normalising levels to the housekeeping control, U6. Note the log10 scale. Horizontal bars indicate the mean value and error bars represent SEM. Group sizes; n=4. Paired t test performed on log transformed data (Y=Log(Y)). *P<0.05 and ns=not significant.

3.5 Discussion

The aim of this chapter was to identify alterations in expression levels of miR-21a-5p, -214-3p, -224-5p and -30d-5p in murine models of cardiac dysfunction, and to investigate expression levels and modulation of these miRNAs in mouse and human CFs.

We have shown for the first time that ISO-induced miR-21a overexpression in murine models is dependent upon the expression of p38 MAPK in fibroblasts (Figure 3.1). The post-transcriptional regulation of miR-21a is of particular interest in CVD and its aberrant expression has been detected in previous mouse models of cardiac dysfunction, although without elucidating the role of p38 MAPK. Increased expression of miR-21a was detected post-ISO infusion by both Thum et al. (2008) when looking at the left ventricular myocardium and Cao et al. (2017) when looking at rat CFs. In a model of MI, we found that miR-21a expression was increased in a mouse model at 3 days post-LAD ligation but was unchanged at 4 weeks post-ligation (Figure 3.2 and 3.3). This was also found by Yuan et al. (2017) who found that LAD ligation increased miR-21a in the border and infarct zones at 3 days but interestingly they also found miR-21a was increased at 7 and 14 days post-ligation in the remote, border and infarct zones and Yang et al. (2018) made a similar finding, with miR-21a elevated from day 1 to 7 but peaking at day 3 post-ligation. Dong et al. (2009) identified this same expression signature of elevated miR-21a levels in the early phase of AMI after performing a 341-miRNA expression signature array on RNA isolated from infarct, border, and non-infarct areas of rat left ventricles at 6 hours post-LAD ligation (miR-214 was also aberrantly expressed in this array). The group found that miR-21a was upregulated in the border but interestingly, downregulated in the infarct area. They then performed overexpression of miR-21 (by adenovirus-mediated miR-21 gene transfer) in an *in vivo* model of LAD ligation and found that MI size was decreased by 29% at 24 hours post-LAD ligation and that left ventricular dimension was reduced at 2 weeks post-LAD ligation. They demonstrated that the upregulation of miR-21 in the acute phase of MI protects against ischemia induced CM damage and apoptosis by targeting the programmed cell death 4 (PDCD4) and activator protein 1 (AP-1) pathway. In our model of hypertension, we did not find that Ang II infusion affected miR-21a expression at 4 weeks post-Ang II but in comparison, Watanabe et al. (2020) found an increase in miR-21a at 2 weeks post-Ang II infusion in mice and in the same paper, they also found in another model of hypertension that miR-21a was elevated at 4 weeks post-trans aortic constriction (TAC). Finally, miR-21a increase has also been found at 3 weeks post-TAC in a rat model where miR-21a was increased in rat ventricular fibroblasts specifically (Thum et al., 2008).

Of all the miRNAs studied in CVD and in patient samples, miR-21a is one of the most researched. MiR-21a is highly implicated in CVD as it has been shown to respond to and

mediate stress signalling pathways to inhibit CM apoptosis and also activating CFs to MyoFbs and increasing myocardial fibrosis (Dai et al., 2020). Differential expression of miR-21a is identifiable across a range of CVDs in clinical samples. In atrial fibrillation (AF), the left atria from patients with AF showed 2.5-fold higher miR-21a expression compared to patients with normal sinus rhythm and interestingly, miR-21a expression was positively correlated with atrial collagen content (Adam et al., 2012) and (Chen et al., 2021) found that plasma miR-21a was increased in AF patients and increasing levels of circulating miR-21a correlated with higher risk of AF and left atrial fibrosis. Regarding coronary artery disease, Kumar et al. (2020) found that miR-21a was increased 2.46-fold in acute coronary syndrome (ACS) and 1.9-fold in stable angina. This is even further supported by an interesting publication from Zile et al. (2011) which found that miR-21a showed differential expression at different times post-MI, with a decrease in plasma miR-21a at 2 days and increased at 5 days but back to normal levels at day 90. Finally, miR-21a has been suggested as a promising biomarker in HF, as Zhang et al. (2017) found that miR-21a was associated with HF and also at predicting rehospitalisation with HF and Ding et al. (2020) found that miR-21a could be used in combination with other miRNAs as a biomarker for HF.

We have shown that miR-21a expression is downregulated in human CFs after treatment with TNFα at 24 hours post-treatment, however it was unchanged after treatment with Ang II, ISO, IL1α, TGFβ and 10% FCS. TNFα is a proinflammatory cytokine that is elevated in patients suffering from HF and is associated with a decrease in survival (Dunlay et al., 2008). It is interesting to note that while TNFα is a driver of necrosis and apoptosis, miR-21a is associated with cell survival and proliferation and so have opposing effects on cells (Møller et al., 2019). Our finding that TNFα reduced miR-21 expression was also found by Zou et al. (2020) when investigating fibroblasts isolated from the hips of patients with ankylosing spondylitis. This group found that TNFα only reduced miR-21 expression at a concentration of 10ng/mL (the same concentration used in our investigation). Interestingly, they found that miR-21 levels were upregulated by a lower concentration of TNFα (0.1ng/mL). This suggests that the measurement of miRNA levels following TNFα treatment is concentration dependent. TNFα has also been investigated in the context of CMs by Palomer et al. (2015) also who used the AC16 cell line which is a proliferating human CM cell line although they found that miR-21 levels were unchanged following treatment with 100ng/mL of TNFα. An investigation by Ning and Jiang (2013) supported our findings by showing that Ang II treatment of rat CFs did not affect miR-21a expression but conversely, Lorenzen et al. (2015) did find that Ang II treatment increased miR-21a expression in mouse CFs. In contrast to our finding that TGFβ did not affect miR-21a expression, Yuan et al. (2017) found that TGF-β1 increased miR-21a expression levels in rat CFs in a dose-dependent manner and peaking at 48-hours of

treatment, whereas our treatment was performed for up to 24 hours and Cao et al. (2017) also found TGF-β1 increased miR-21 in CFs after 24 and 48 hours of treatment. Research on treatment of CFs with ISO *in vitro* is lacking, for comparison, but in CMs, Sayed et al. (2008) found that ISO treatment of cultured neonatal CMs led to increase in miR-21a expression.

The role of miR-214 in CVD is not clearly understood and the literature suggests that it could be either cardioprotective or pathological. There are two existing publications investigating the expression levels of miR-214 post-ISO infusion in rodents and both agree with the findings of the current investigation. Duan et al. (2015) found that miR-214 was increased by ~1.5-fold and ~2.5-fold in murine whole heart samples at both 2 weeks and 4 weeks post-ISO infusion and Sun et al. (2015) found miR-214 was increased by ~4.5-fold in rat myocardium at 7 days post-ISO infusion. This finding concurs with our own finding that miR-214 is increased in murine whole heart samples at 3 weeks post ISO infusion (Figure 3.1). MiR-214 expression was increased at 3 days post-LAD ligation but unchanged at 4 weeks post-ligation in the current investigation (Figure 3.2 and 3.3). This increase was similarly identified by Aurora et al. (2012) in the hearts of mice subjected to 45 minutes of ischemia and 1 or 7 days of reperfusion in a model of permanent or transient ligation of the LAD. Research on miR-214 levels following the TAC model of hypertension is not in agreement, as Lv et al. (2018) found a 2-fold increase in mouse left ventricle following TAC surgery for 4 weeks however Yang et al. (2016) found a ~50% decrease in mouse hearts at 6 weeks post-TAC. They found that by treating with adenovirus-expressing miR-214 (Ad-miR-214) for 4 days prior to AMI, these rats were protected against left ventricular remodelling and showed decreased cardiac cell apoptosis and decreased infarct size. It was found that these effects were mediated by miR-214 targeting the tumour suppressor, *Pten*, which encodes PTEN, an enzyme that usually acts by inhibiting proliferation and promoting apoptosis (Lu et al., 2016). There are also conflicting findings on the effect of Ang II infusion on miR-214 expression in mouse models. Tang et al. (2016) demonstrated a >50% reduction, but conversely Ding et al. (2021) reported a 4.88-fold increase and both involved 2 weeks of Ang II infusion.

First, Duan et al. (2015) found that miR-214 levels were upregulated in patients with chronic HF compared to healthy controls however in comparison, circulating miR-214 expression was found to be lower in patients with coronary artery disease (CAD) and a drop in miR-214 is suggested as a loss of protection. Yin et al. (2019) investigated the miR-214 levels in the serum of elderly patients categorised as either AMI, unstable angina (UA), or healthy patients. They found that miR-214 expression levels were significantly upregulated in AMI patients compared to UA and healthy patients. They also found that the expression levels of miR-214 were positively correlated with serological markers of AMI in AMI patients, including aspartate

aminotransferase (AST), lactate dehydrogenase (LDH), creatinine kinase-MB (CK-MB), cardiac troponin (cTnI).

We found that miR-214 expression was unchanged after treatment with ISO, Ang II, IL1α, TNFα, TGFβ and 10% FCS. In comparison, Sun et al. (2015) performed *in vitro* ISO treatment in rat CFs and found there was a dose and time-dependent increase of miR-214 in response to 1μM and 10μM ISO and increasing at 6 hours, peaking at 24 hours and dropping at 48 hours. We did not see any change in miR-214 and we also treated with 10μM ISO for 6 and 24 hours. Although we found no change in miR-214 after treatment with TGFβ, Yang et al. (2019) did find that miR-214 was decreased in mouse CFs after treatment with 10ng/mL TGF-β1 for 48 hours (to compare, we treated with 10ng/mL TGFβ for 24 hours). There is a lack of research on the treatment of isolated CFs with Ang II however in mouse ventricular myocytes, Tang et al. (2016) found that miR-214 was increased by Ang II treatment for 48 hours.

We demonstrated for the first time that ISO infusion increases the expression levels of miR-224 in mice (Figure 3.1). MiR-224, despite being of interest in the field of CVD, has not been extensively researched in *in vivo* models of HF. We did not however find any change in miR-224 following LAD ligation and similarly, there is no existing research investigating the expression of miR-224 in MI models. Finally, we did not find any change in miR-224 expression at 4 weeks post-Ang II infusion. There is however evidence of expression changes in a model of hypertension as Zheng et al. (2021) reported that miR-224 increased by ~2-fold after 28 days of TAC surgery.

In regard to miR-224 expression in clinical samples, it was found by James et al. (2022) that miR-224 was the most differentially expressed circulating miRNA (out of a panel of 190 miRNAs) in low coronary flow reserve (CFR) patients compared with high CFR patients. CFR is used as a measure of major adverse cardiac events (MACE) and patients who survive MI are at a high risk of developing MACE. The higher the CFR, the lower the risk of developing MACE and this research suggests that increased miR-224 is associated with poorer outcomes following MI.

It was found that miR-224 expression levels are decreased in response to IL1α treatment *in vitro*, although not statistically significant (P=0.0778) (Figure 3.10). IL-1 has been shown to regulate various processes in CFs specifically, leading to increased release of proinflammatory cytokines, cell migration and ECM degradation and decreased ECM synthesis and MyoFb differentiation (Turner, 2014). In existing literature, the measurement of miR-224 specifically, or miRNA profiling in general, has not been performed following IL-1α/β stimulation. Ning and Jiang (2013) Ang II increased miR-224. Jiang et al. (2013) made a

similar finding when they found that miR-224 was upregulated in adult rat CFs but again, this experiment was an *in vitro* treatment for 24 hours.

MiR-30d represents an exciting regulatory miRNA in response to ISO induced cardiac dysfunction as this miRNA (unlike the other three miRNAs investigated) is decreased following ISO infusion (Figure 3.1). Very recently, Li et al. (2022a) investigated miR-30d expression in *in vivo* models of both HF and hypertension. They found that miR-30d expression was decreased in hypertrophic hearts obtained from mice and rats after 2 weeks of ISO infusion as a model of HF. Interestingly, they found that overexpression of miR-30d in a transgenic rat model ameliorated cardiac hypertrophy and cardiac fibrosis from ISO infusion. We also found that miR-30d was unchanged in mice at 3 days post-LAD ligation but decreased at 4 weeks post-ligation in our *in vivo* model of MI. Interestingly, Li et al. (2021) found that transgenic miR-30d overexpression was protective against cardiac hypertrophy and cardiac fibrosis in an ischemic MI model in rats, at 3 weeks post-MI and it was demonstrated that this protection was via miR-30d targeting of *Map4k4* in CMs and *Itga5* in CFs. Also, Roca-Alonso et al. (2015) found that miR-30d was decreased in adult rat ventricular myocytes isolated from rats at 3 weeks post-doxorubicin and 4 weeks post-LAD ligation. We also demonstrated that miR-30d was decreased at 4 weeks post-Ang II infusion as a model of hypertension. The investigation by Li et al. (2022a) performed two models of hypertension in mice which were TAC and Ang II infusion. They found that miR-30d was consistently decreased in mice hearts and supported our findings by showing miR-30d was decreased at 4 weeks post-Ang II and 4 weeks post-TAC which again supports our findings.

The study performed by Li et al. (2022a) supports our findings for miR-30d expression at 4 weeks. Huo et al. (2019) comparatively, performed an *in vivo* Ang II model by infusing with Ang II for with the same amount of Ang II infused in our experiment (1000ng/kg/minute), however they treated for 7 days, and 14 days as opposed to 4 weeks. Small RNA sequencing was performed to measure miRNA expression levels and none of miR-21a, -214, -224 or -30d were found to be changed by this treatment. The fact they did not detect a change in miR-30d levels like we did could be because, this treatment was at too early a stage to detect miR-30d change. Morishima and Ono (2021) also performed an Ang II infusion and measured miR-30d expression at 6 hours and 2 weeks post-infusion. They found that miR-30d was significantly upregulated at 2 weeks in the atrium but not the ventricles. These findings are valuable as they suggest that miR-30d is only decreased at later time points post-MI, HF, and hypertension. This supports the argument that miR-30d levels are increased as a regulator of repair although as the levels of miR-30d decrease at the later stages (such as 4 weeks) and at this later time point, the anti-apoptotic and anti-fibrotic effects of miR-30d are lost.

The circulating levels of miR-30d have been suggested as a prognostic biomarker for survival in acute HF. Xiao et al. (2017) found that miR-30d was significantly lower in the serum from patients who died during a 1-year follow up with acute HF compared to those who survived and the authors suggest miR-30d as a predictive marker for 1-year all-cause mortality in acute HF patients. This is in support of findings made by Melman et al. (2015) who found that plasma miR-30d level was associated with protection against deleterious TNF signalling and was associated with response to cardiac resynchronisation therapy (CRT) in HF patients with dyssynchrony (HF_{DYS}).

We did not find any effect on miR-30d expression in human CFs following treatment with Ang II, ISO, IL1α, TNFα, TGFβ or 10% FCS. This is in opposition to finding from Li et al. (2022a) who found that miR-30d was decreased in primary neonatal rat CMs (NRCMs) after *in vitro* treatment with Ang II treatment or phenylephrine (PE) treatment for 48 hours. Similarly, Roca-Alonso et al. (2015) found that *in vitro* treatment of primary isolated adult rat ventricular cardiomyocytes (ARVCMs) with DOX (as an *in vitro* HF stimuli, similar to ISO) resulted in decreased expression of miR-30d.

We found that miR-21a, -214 and -224 are enriched in murine CFs compared to endothelial cells (ECs) but not miR-30d (Figure 3.5). Interesting to note is that there have been numerous studies that have demonstrated the capability of cells to secrete miRNAs in EVs which can then act by paracrine signalling on other cell types. In fact the publication by Li et al. (2021) showed that miR-30d expressed and secreted by CMs acts on CFs in a murine model of cardiac hypertrophy. The authors even went on to confirm our findings by measuring miR-30d expression levels in both neonatal rat ventricular myocytes (NRVMs) and neonatal rat cardiac fibroblasts (NRCFs) at baseline or 24 hours after acute ischemic stress. They found that NRVMs showed increased expression of miR-30d after ischemic stress and increased miR-30d packaged in EVs. In comparison, NRCFs showed significantly lower cellular pre–miR-30d, mature miR-30d and EV packaged miR-30d both at baseline and no increases after ischemic stress. Also, after culture with conditioned media derived from these NRVMs, miR-30d was found to target the integrin, *Itga5* in NRCFs, which is a transmembrane receptor capable of sensing changes in the ECM and decreases in *Itga5* resulted in decreased fibrosis.

We have validated that the expression levels of miR-21a, -214, 224 and -30d are detectable in murine CFs and in human CFs (Figure 3.6 and 3.7). The most interesting finding from these investigations was that the relative expression levels between each of the miRs was the same for that in murine CFs and in human CFs. We importantly found that miR-214 was most highly expressed, miR-21 was second most, miR-30d was third most and miR-224 was the least

expressed in both murine CFs and human CFs. This finding provides added translatability to our investigations in mouse models and in mouse CFs to clinical relevance for human CFs.

Our final investigation into the regulation of miRNAs in human CFs found that miR-224 expression is decreased upon inhibition of p38 MAPK (Figure 3.12). This pharmacological inhibition of p38 MAPK mirrors the finding in our ISO infusion model that miR-224 expression was decreased in fibroblast specific p38 MAPK KO mice compared to WT mice (Figure 3.1). The three other miRNAs investigated remained unchanged. Antoon et al. (2013) have already shown that p38 inhibition can influence miRNA expression, inducing a decrease in miR-21a, and leads to functional changes, to the extent of reversing epithelial to mesenchymal transition (EMT). As we hypothesised that miR-21a, -214, -224 and -30d play important roles in regulating CF behaviour in cardiac remodelling, and as fibroblast to myofibroblast transition (FMT) is an important step in CF to MyoFb activation, this poses a potential mechanism for p38 and miRNA regulation in this process. The miRNA profiling after p38 inhibition of a chemoresistant breast cancer cell line (MCF-7TN-R) found that only miR-214 out of our four miRNAs of interest was changed and the expression levels of this miRNA were reduced. As the literature concerning miRNA expression following p38 inhibition is sparse, the identification of p38 dependent binding sites in miRNA promoters or repressors should be considered. Whitmarsh (2010) compiled a list of p38 MAPK dependent transcription factors (TFs) and each of the stresses their activation is induced by. There are TFs that are activated by all the stresses that activate p38 MAPK, which are Jun, Fos, Myc, Egr-1 and Maff. The current investigation used the online tool TransmiR (https://www.cuilab.cn/transmir) to investigate the existence of TF binding sites in each miR. While each of the miRNAs comprise of binding sites for a variety of p38 MAPK dependent TFs, all four miRNAs comprise of a binding site for the TF, Jun. However, only miR-224 was directly decreased in CFs in this investigation and the fact that p38α MAPK KO in fibroblasts decreased expression of all four miRNAs may be simply associated with the extent of remodelling rather than being due to p38 itself.

This investigation found that the expression levels of miR-21a, -214, -224 and -30d were each affected by different *in vivo* models of cardiac dysfunction. In a model of HF, miR-21a, -214 and -224 were increased at 3 weeks post-ISO infusion whereas miR-30d was decreased. In a model of MI, miR-21a and -214 were increased at 3 days post-LAD ligation and -30d was decreased at 4 weeks post-ligation. In a final model, of hypertension, miR-30d was decreased at 4 weeks post-Ang II infusion. In *in vitro* experiments of human CFs, it was found that TNFα treatment decreased miR-21a expression and that there was a trend of decreased miR-224 after treatment with IL1α. It was also found that although miR-21a, -214, -224 and -30d expression levels returned to basal levels following ISO infusion in p38α MAPK KO mice, that treatment of human CFs with pharmacological inhibition of p38 MAPK decreased the

expression of miR-224 only. This chapter found that there are different expression signatures for each of the four miRNAs in response to different *in vivo* or *in vitro* triggers of cardiac dysfunction in whole heart and human CFs. Chapter 4 will investigate the effect of overexpressing or inhibiting each miRNA on gene expression, protein expression and regulation of human CF behaviour, relevant to cardiac remodelling.

Chapter 4 Investigating the influence of overexpressing and inhibiting miR-21a, -214, -224 and -30d on human cardiac fibroblasts

4.1 Introduction

In Chapter 3, it was established that both mouse and human CFs express miR-21a-5p, -214-3p, -224-5p and -30d-5p and that levels are modulated in models of cardiac dysfunction. This suggests that the miRNAs play a role in cardiac dysfunction/remodelling through modulation of CFs.

One of the cell-type specific hallmarks of cardiac remodelling is a phenotypic switch of CFs into a MyoFb state. During the proliferative phase of cardiac remodelling, MyoFbs adopt a highly proliferative state compared to CFs in the healthy human heart (Humeres and Frangogiannis, 2019). MiR-21a is relatively well researched in the field of both CVD and cardiac remodelling specifically. In this research, fibroblast proliferation has been covered extensively and the findings largely support that miR-21a mediates increased proliferation. The first research identifying the role of miR-21 in CFs was conducted by Thum et al. (2008) who demonstrated that miR-21 is capable of regulating ERK MAPK activation in CFs via the inhibition of *Spry1*. The implication of this miR-21/ERK MAPK signalling cascade is that miR-21 induces fibroblast survival and growth factor secretion that ultimately results in cardiac fibrosis and dysfunction. The importance of miR-21 in CFs was then demonstrated shortly thereafter when Roy et al. (2009) found that miR-21 regulates *Mmp2*, which has already been described as important for cardiac remodelling, via the inhibition of *Pten*. Cao et al. (2017) more recently demonstrated that miR-21a targeted the mRNA for the tumour suppressor cell adhesion molecule-1 (CADM1) and thus inhibited its expression. The subsequent downstream effect of this targeting resulted in enhanced expression of Signal transducer and activator of transcription 3 (STAT3) and knockdown of miR-21a resulted in decreased CF proliferation. Similarly, Zhou et al. (2018) found that TGF-β1 treatment resulted in an increase in the expression of miR-21a, a decrease in the notch signalling activation protein, Jagged1 (JAG1), and pivotally, an increase in CF proliferation. Interestingly, inhibition of miR-21a was found to increase *Jag1* levels and decrease CF proliferation in rat CFs.

A role for miR-214 in CF proliferation has also been reported by Sun et al. (2015) who demonstrated that ISO treatment increased both CF proliferation and miR-214 expression, suggesting that miR-214 acts mechanistically through inhibiting translation of the mitochondrial fusion protein, Mitofusin 2 (MFN2), to regulate ERK1/2 MAPK signalling and promote CF proliferation. Less is known about miR-224 and its role in regulating CF proliferation, however Ning and Jiang (2013) suggested that miR-224 may induce CF proliferation as it is upregulated in tumours and induces proliferation in this setting, as well as

being increased in CFs following Ang II treatment. Finally, miR-30d is not well understood in CFs however there has been demonstration that it inhibits proliferation in the pathology of cancer. Liang et al. (2021) reported that miR-30d inhibited proliferation and autophagy in renal cell carcinoma by targeting the mRNA for autophagy protein 5 (ATG5) and so it is possible that miR-30d plays a similar role in human CFs.

Another important factor to consider for the regulation of these miRNAs in the context of cardiac remodelling is the expression of relevant genes. This is particularly important for two reasons. Firstly, gene expression changes may not necessarily result in phenotypic changes that can be measured by limited behavioural assays, and secondly because miRNAs act through the inhibition of protein translation through binding to mRNA and any direct binding and degradation of target mRNAs could be demonstrated through this assay. Because miRNAs also act by degrading mRNA, RT-PCR is useful to determine if miRNA effects are at the level of mRNA degradation or inhibition of protein translation. The MyoFb phenotype also demonstrates highly matrix-synthetic behaviours and as previously discussed, important proteins in the regulation of the ECM include the MMPs MMP-2, MMP-3 and MMP-9 (Page-McCaw et al., 2007) as well as tenascin C (TNC) which has been researched as a potential biomarker for myocarditis (Imanaka-Yoshida et al., 2020). Similarly, there are also increases in the levels of the contractile protein α-SMA and collagens such as collagen type I (Shinde et al., 2017). The mRNA levels of these genes were therefore investigated following pre- and anti-miR transfection.

IL-6 is an important signalling molecule in cardiac remodelling and has been demonstrated as a paracrine signalling molecule, released by CFs, and acting on CMs to induce cardiac hypertrophy (Bageghni et al., 2018). Interleukin-11 (IL-11), an IL-6 family member, is similarly another important signalling molecule in cardiovascular disease and cardiovascular fibrosis specifically (Schafer et al., 2017). In fact, it was demonstrated that upregulation of IL-11 occurs following exposure to TGFβ1 (a cytokine secreted by immune cells after cardiac injury and a stimulator of CFs). What is also important to note is that IL-11 and its receptor, IL11RA, are specifically expressed in fibroblasts and genetic deletion of *Il11ra1* was found to protect against disease (with reduced ERK signalling) (Schafer et al., 2017). Due to the importance of these cytokines and their subsequent response through binding to their specific receptors, the mRNA levels of IL-6, IL6R, IL-11 and IL11RA were included in this investigation.

CFs respond to stimuli of cardiac dysfunction, including triggers like hypertension and cytokines, by synthesising ECM proteins that mediate cardiac remodelling. Measuring mRNA levels for these ECM components is not sufficient and so the levels of IL-6 and MMP-2 protein

expression was measured in conditioned media to investigate the influence of each miRNA on their expression.

Transfections were performed with pre-miRNAs to overexpress miRNA or anti-miRNAs to inhibit miRNAs to determine their regulatory roles. After validating successful transfections, this investigation sought to understand what influence these miRNAs have on human CF activity relevant to the cardiac remodelling process.

4.2 Aims

The main aims of this chapter were:

- To validate the successful transfection of human CFs with pre-miRs and anti-miRs and measure the change in miRNA levels;
- To determine the effect of specific miRNA overexpression on human CF proliferation rates;
- To evaluate the pre- and anti-miR mediated change in mRNA expression levels of genes important to cardiac remodelling;
- To measure the concentration of important cardiac remodelling proteins, in conditioned media, following miRNA overexpression and inhibition.

4.3 Methods

4.3.1 Generic methods

Human CFs were isolated from RAA biopsies as described in Section 2.2. Human CFs were transfected with pre-miRNA and anti-miRNA as described in Section 2.8. Proliferation assays were performed following transfection, according to the method described in Section 2.8. RNA was isolated as described in Section 2.3 and miRNA and mRNA levels were quantified by qRT-PCR as described in Sections 2.5 and 2.6 respectively. IL-6 and MMP-2 ELISAs were performed as described in Sections 2.10 and 2.11 respectively.

4.3.2 Fluorescence Microscopy

Human CFs were grown to ~80% confluence in FGM, trypsinised and then diluted to 40,000 cells in 8 mL FGM (5,000 cells/mL). Glass coverslips were sterilised and then one was placed per well for 8 wells of a 24-well plate. Using a 5mL stripette and mixing the cell solution each time, 1 mL of the 5,000 cell/mL solution was dispensed into 8 wells. The cell solution was dispensed so that all the solution remained above the coverslip. The plate was then gently agitated and incubated for 24 hours to allow cells to attach. After incubation the media was removed from each well and washed once with 1 mL PBS. Each well was then transfected with the Cy™3 Dye-Labeled Pre-miR™ Negative Control (30nM) according to the transfection

protocol previously stated in Section 2.8. At 48 hours post-transfection, growth media was removed and 1mL of 4% PFA (diluted in PBS) was added to fix the transfected cells to the coverslip. The coverslips were then viewed under a Zeiss Axio Observer microscope in order to view the fluorescently conjugated pre-miR negative control and calculate transfection efficiency. Transfection efficiency was calculated by studying five different fields of view, from three triplicate wells and counting the number of wells stained with DAPI and/or pre-miR-NC. The number of cells stained for fluorescent pre-miR were then calculated as a proportion of the total number of viable cells stained with DAPI ((number of cells stained with negative control / number of cells stained with DAPI) * 100 = transfection efficiency %).

4.4 Results

4.4.1 Confirming high transfection efficiency of human cardiac fibroblasts

The transfection efficiency of human CFs was assessed by measuring the successful transfection of human CFs in culture with a Cy™3 Dye-Labeled Pre-miR™ Negative Control. The total number of live cells stained with DAPI and the number of cells incorporating the pre-miR negative control were observed by fluorescence microscopy. All cells were found to contain punctate fluorescent labelling, so the transfection efficiency was effectively 100%. Figure 4.1 shows multiple human CFs with DAPI stained nuclei (blue) and each cell containing Cy3-labelled pre-miR negative control (red) at 20X magnification (Fig. 4.1A) and specifically focused on one cell at 40X magnification (Fig. 4.1B).

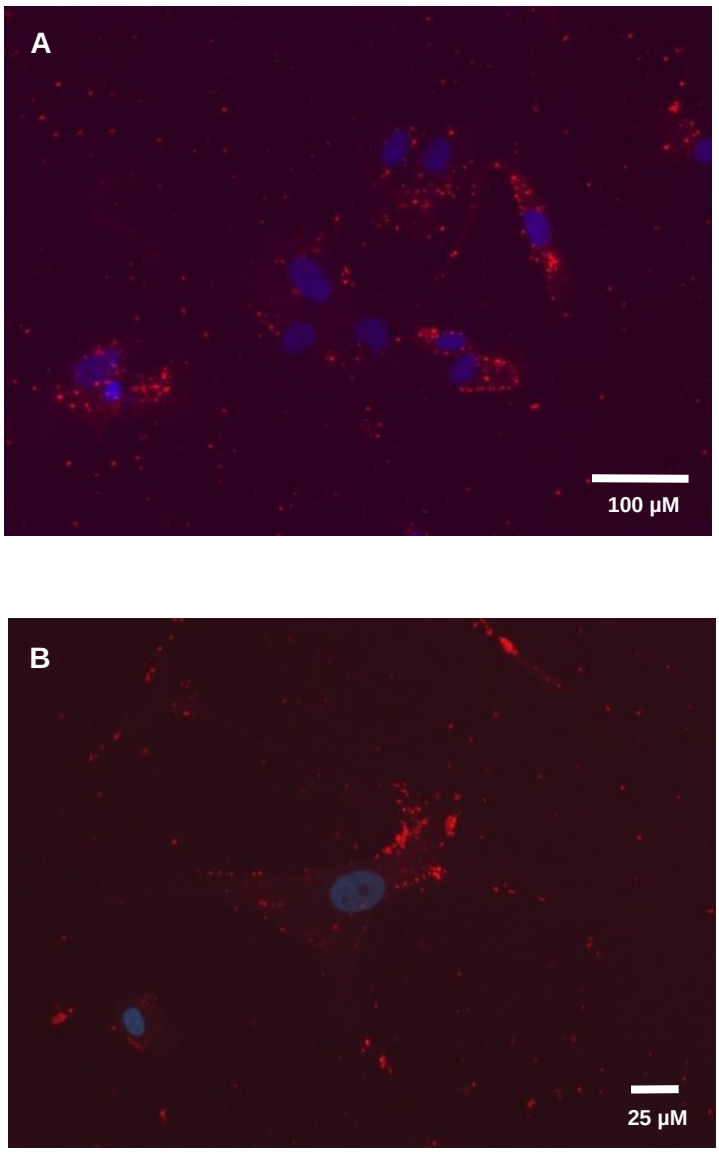

Figure 4.1 Transfection efficiency of human cardiac fibroblasts transfected with Cy3™ dye-labelled pre-miR negative control. Human cardiac fibroblasts were transfected with 30nM Cy3™ dye-labelled pre-miR negative control (red) and stained with DAPI (blue) to assess the transfection efficiency of human CFs with miRNA mimics. Image viewed at 20X magnification **(A)** and 40X magnification **(B)**.

4.4.2 MiRNA expression levels in human cardiac fibroblasts following pre-miR transfection

The expression levels of each miRNA were investigated in human CFs post-transfection with specific pre-miRs or anti-miRs to validate whether miRNA expression levels and/or activity could be successfully modulated ahead of downstream investigations. The pre-miRs and anti-miRNAs transfected were pre/anti-miR-NC (negative control), -21a-5p, -214-3p, -224-5p and -30d-5p. Expression levels of all 4 miRNAs were measured at 24 hours and 48 hours post-transfection with pre-miRs.

Transfection with pre-miR-21a resulted in significantly higher levels of miR-21a (560- and 700-fold higher at 24 hours and 48 hours post-transfection respectively) as expected, but also led to an increase in miR-214 levels (40- and 50-fold higher at 24 hours and 48 hours post-transfection respectively) compared to pre-miR-NC (Figure 4.2). MiR-224 and 30d levels were unaffected by pre-miR-21a transfection (Figure 4.2).

Transfection with pre-miR-214 resulted in significantly higher levels of miR-214 (3,880 and 4,290-fold higher at 24 hours and 48 hours respectively) compared to pre-miR-NC, without affecting levels of other miRNAs (Figure 4.3).

Transfection with pre-miR-224 resulted in significantly higher levels of miR-224 (4,430 and 12,960-fold higher at 24 hours and 48 hours respectively) and led to elevation of miR-30d (40-fold higher at 24 hours and 48 hours) compared to pre-miR-NC (Figure 4.2). Mir-21a and 214 levels were unaffected by pre-miR-224 transfection (Figure 4.4).

Finally, transfection with pre-miR-30d resulted in significantly higher levels of miR-30d (9,360 and 11,320-fold higher at 24 hours and 48 hours respectively) compared to pre-miR-NC, without affecting levels of the other miRNAs (Figure 4.5).

To summarise, these findings demonstrate that each miRNA could be successfully overexpressed by transfecting with specific pre-miRs. It was also found that overexpression of each miRNA is maintained at 48 hours and these expression levels are higher than those seen at 24 hours. However, it is important to remember when discussing the effect of specific miRNA overexpression on mRNA and protein levels, that treatment with specific miRNAs has resulted in elevation of “off-target” miRNAs in some cases (pre-miR-21a elevating miR-214 and pre-miR-224 elevating miR-30d).

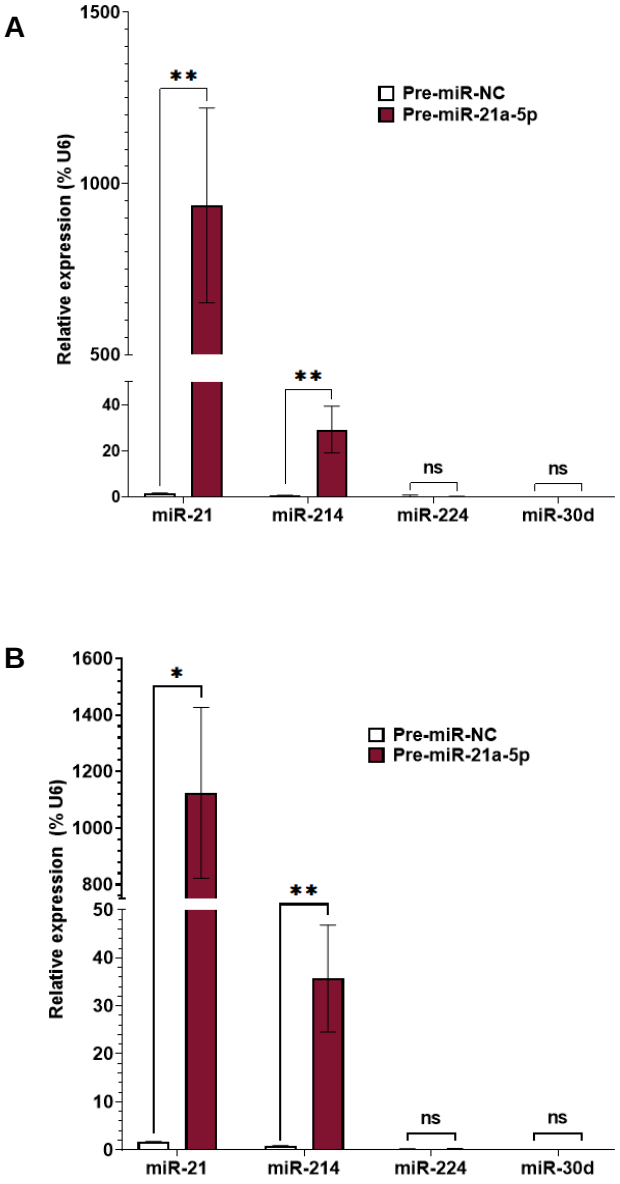

Figure 4.2 MiRNA levels in human cardiac fibroblasts following transfection with pre-miR-21a. Human CFs were transfected with 30nM pre-miR-NC or pre-miR-21a and RNA was isolated at 24 **(A)** or 48 **(B)** hours post-transfection. MiRNA levels were calculated by performing qRT-PCR and normalising levels relative to the housekeeping control, U6. Horizontal bars indicate the mean value and error bars represent SEM. Group sizes; n=3. One-way repeated measures ANOVA, with a Šidák multiple comparisons test, performed on log transformed data (Y=Log(Y)). *P<0.05 and **P<0.01. ns=not significant.

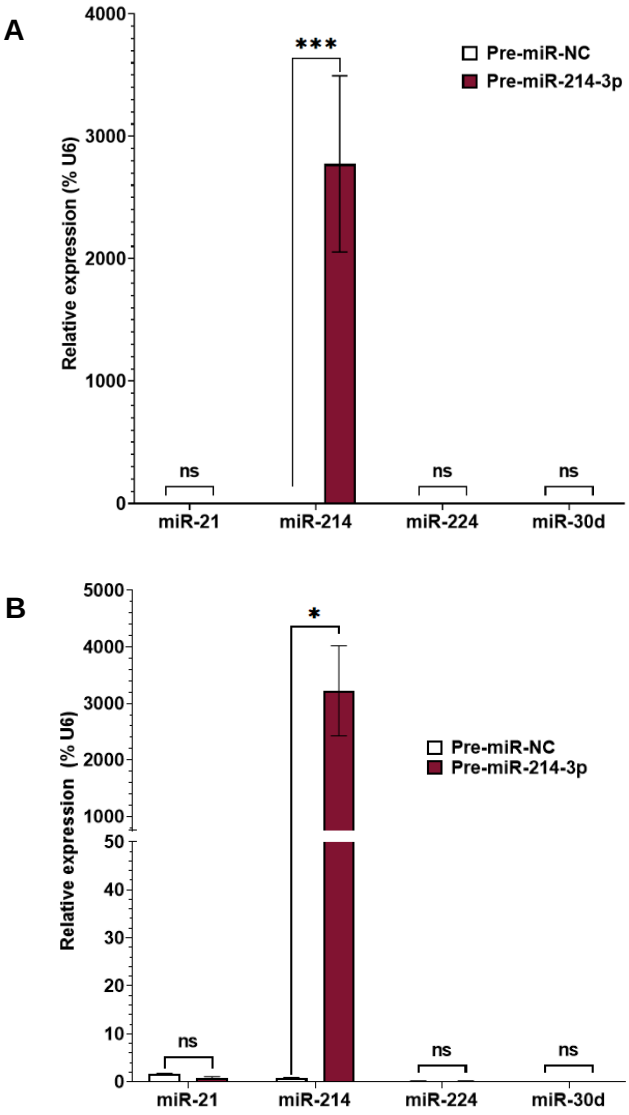

Figure 4.3 MiRNA levels in human cardiac fibroblasts following transfection with pre-miR-214. Human CFs were transfected with 30nM pre-miR-NC or pre-miR-214-3p and RNA was isolated at 24 (A) or 48 (B) hours post-transfection. MiRNA levels were calculated by performing qRT-PCR and normalising levels relative to the housekeeping control, U6. Horizontal bars indicate the mean value and error bars represent SEM. Group sizes; n=3. One-way repeated measures ANOVA, with a Šidák multiple comparisons test, performed on log transformed data (Y=Log(Y)). *P<0.05 and ***P<0.001. ns=not significant.

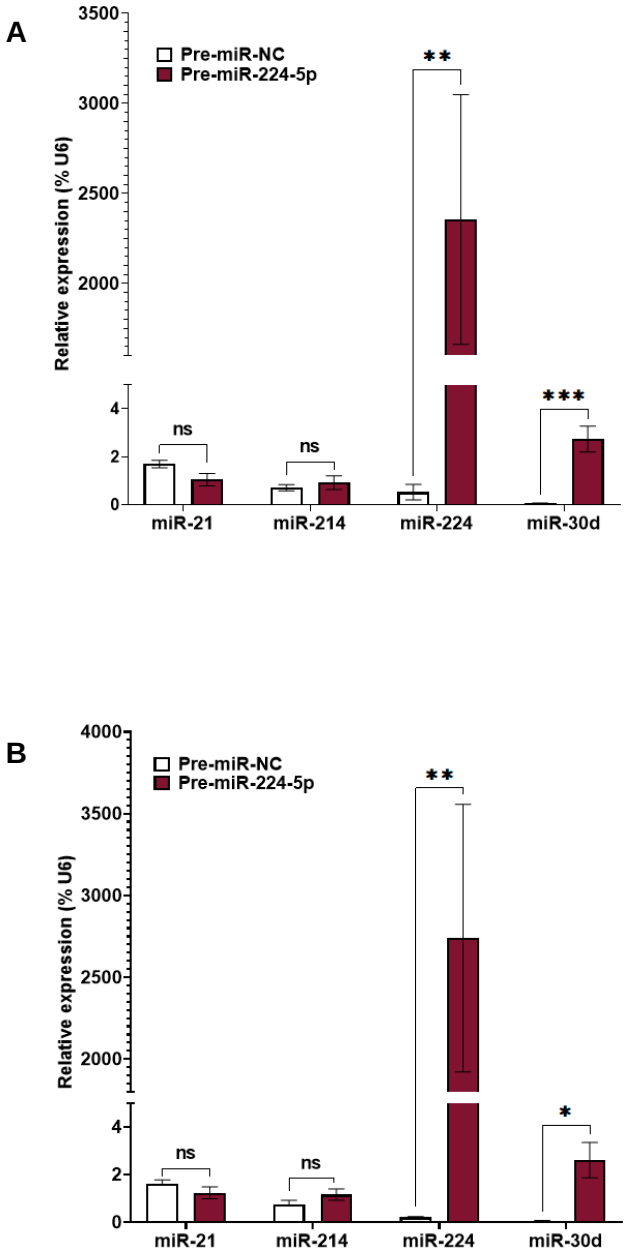

Figure 4.4 MiRNA levels in human cardiac fibroblasts at following transfection with pre-miR-224. Human CFs were transfected with 30nM pre-miR-NC or pre-miR-224-5p and RNA was isolated at 24 (A) or 48 (B) hours post-transfection. MiRNA levels were calculated by performing qRT-PCR and normalising levels relative to the housekeeping control, U6. Horizontal bars indicate the mean value and error bars represent SEM. Group sizes; n=3. One-way repeated measures ANOVA, with a Šidák multiple comparisons test, performed on log transformed data (Y=Log(Y)). *P<0.05, **P<0.01 and ***P<0.001. ns=not significant.

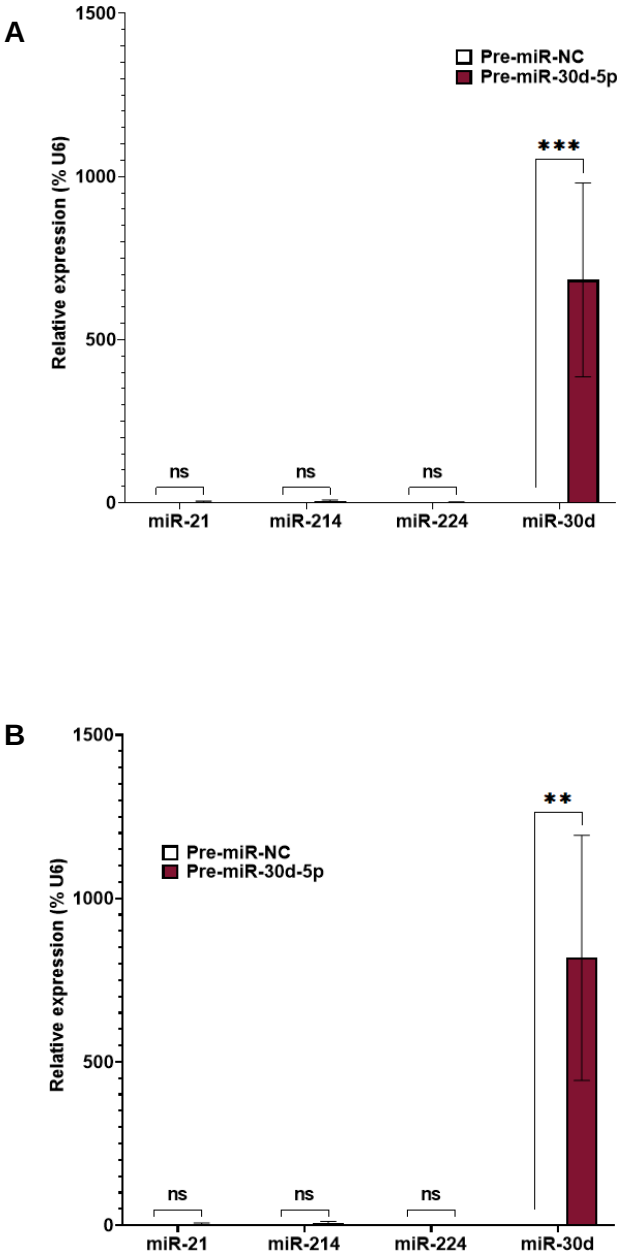

Figure 4.5 MiRNA levels in human cardiac fibroblasts at following transfection with pre-miR-30d. Human CFs were transfected with 30nM pre-miR-NC or pre-miR-30d-5p and RNA was isolated at 24 (A) or 48 (B) hours post-transfection. MiRNA levels were calculated by performing qRT-PCR and normalising levels relative to the housekeeping control, U6. Horizontal bars indicate the mean value and error bars represent SEM. Group sizes; n=3. One-way repeated measures ANOVA, with a Šidák multiple comparisons test, performed on log transformed data (Y=Log(Y)). **P<0.01 and ***P<0.001. ns=not significant.

4.4.3 MiRNA expression levels in human cardiac fibroblasts following anti-miR transfection

Anti-miRs function by binding to endogenous miRNAs to prevent them from targeting mRNA. Therefore, anti-miRs do not always reduce miRNA levels; however their binding may prevent reverse transcription of the specific miRNAs and this may be recognised as a decrease by qRT-PCR. MiRNA expression levels were measured at 48 hours post-transfection with anti-miRs (Fig 4.6-4.9). Transfection with anti-miR-21a showed an apparent 4-fold increase in miR-21 expression, although this was not close to significance (P=0.3) (Figure 4.6). Transfection with anti-miR-214 resulted in significantly lower levels of miR-214 (98.4% lower) and did not affect any other miRNAs (Figure 4.7). Transfection with anti-miR-224 did not reduce miR-224 levels, but did result in significantly lower levels of miR-30d (48.2% lower) compared to anti-miR-NC (Figure 4.8). Finally, transfection with anti-miR-30d resulted in significantly lower levels of miR-30d (98.3% lower), but also miR-21a (47% lower) and miR-214-3p (47% lower) compared to anti-miR-NC (Figure 4.9).

To summarise, the transfection of CFs with anti-miRs produced variable results, as opposed to the consistent overexpression of miRNAs observed with pre-miR transfection (Figures 4.2-4.5). The decrease in the levels of miR-214 and miR-30d following anti-miR-214 and anti-miR-30d transfection respectively, were the only anti-miR transfections to result in a decrease in the levels of its relevant mature miRNA (Figure 4.7 and Figure 4.9). Interestingly, the anti-miR-224 mediated decrease in miR-30d (Figure 4.8) is the reverse of what was observed with transfection of pre-miR-224 where miR-30d was increased (Figure 4.4). This could suggest that either pre-miR or anti-miR-224 are able to influence the expression levels of miR-30d directly or through their modulation of the levels of miR-224. The findings here show that miR-214 and miR-30d expression levels were lower following anti-miR transfection, however, the fact that lower expression levels are not seen for miR-21a and miR-224 does not necessarily suggest that the anti-miRs are not inhibiting these miRNAs, as this binding does not specifically prevent transcription or degrade miRNAs.

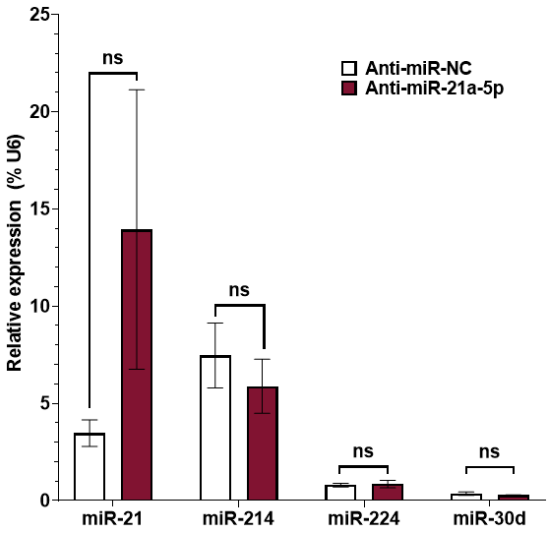

Figure 4.6 MiRNA levels in human cardiac fibroblasts after transfection with anti-miR-21a. Human CFs were transfected with 100nM anti-miR-NC or anti-miR-21a-5p and RNA was isolated at 48 hours post-transfection. MiRNA levels were calculated by performing qRT-PCR and normalising levels relative to the housekeeping control, U6. Horizontal bars indicate the mean value and error bars represent SEM. Group sizes; n=3. One-way repeated measures ANOVA, with a Šidák multiple comparisons test, performed on log transformed data (Y=Log(Y)). ns=not significant.

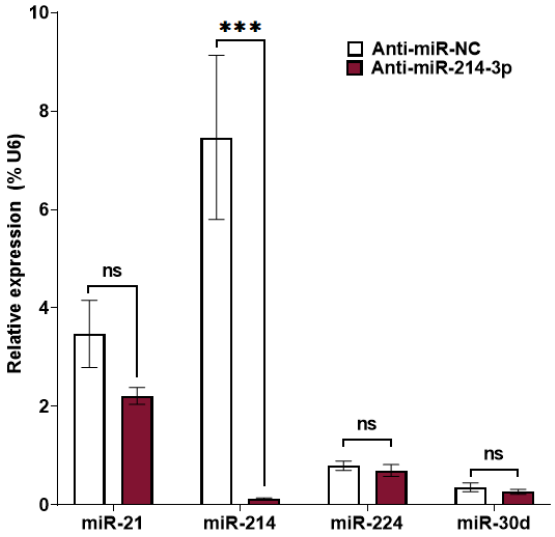

Figure 4.7 MiRNA levels in human cardiac fibroblasts following transfection with anti-miR-214. Human (CFs) were transfected with 100nM anti-miR-NC or anti-miR-214-3p and RNA was isolated at 48 hours post-transfection. MiRNA levels were calculated by performing qRT-PCR and normalising levels relative to the housekeeping control, U6. Horizontal bars indicate the mean value and error bars represent SEM. Group sizes; n=3. One-way repeated measures ANOVA, with a Šidák multiple comparisons test, performed on log transformed data (Y=Log(Y)). ***P<0.001. ns=not significant.

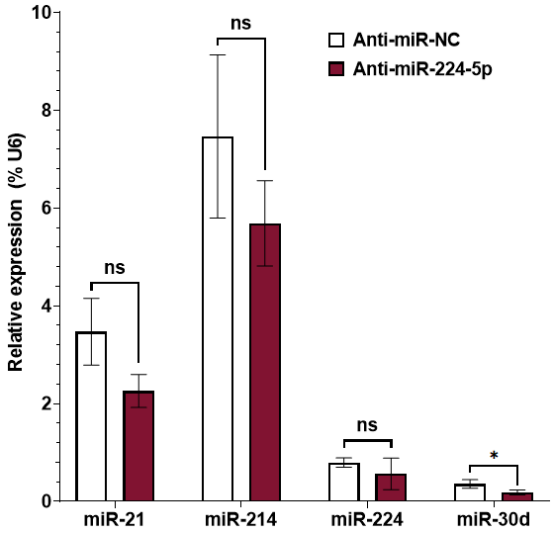

Figure 4.8 MiRNA levels in human cardiac fibroblasts following transfection with anti-miR-224. Human (CFs) were transfected with 100nM anti-miR-NC or anti-miR-224-5p and RNA was isolated at 48 hours post-transfection. MiRNA levels were calculated by performing qRT-PCR and normalising levels relative to the housekeeping control, U6. Horizontal bars indicate the mean value and error bars represent SEM. Group sizes; n=3. One-way repeated measures ANOVA, with a Šidák multiple comparisons test, performed on log transformed data (Y=Log(Y)). *P<0.05. ns=not significant.

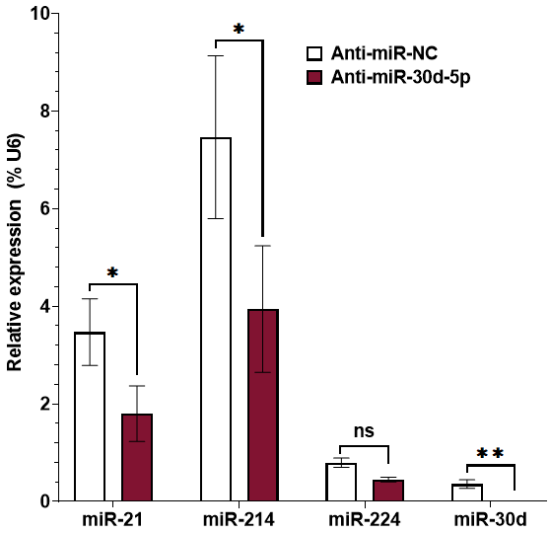

Figure 4.9 MiRNA levels in human cardiac fibroblasts following transfection with anti-miR-30d. Human (CFs) were transfected with 100nM anti-miR-NC or anti-miR-30d-5p and RNA was isolated at 48 hours post-transfection. MiRNA levels were calculated by performing qRT-PCR and normalising levels relative to the housekeeping control, U6. Horizontal bars indicate the mean value and error bars represent SEM. Group sizes; n=3. One-way repeated measures ANOVA, with a Šidák multiple comparisons test, performed on log transformed data (Y=Log(Y)). *P<0.05 and **P<0.01. ns=not significant.

4.4.4 Investigating the effect of miRNA modulation on human CF proliferation

As has been previously described in this investigation, CF proliferation and changes in the rate of proliferation are directly influential in the development of cardiac remodelling. CFs are regulators of ECM remodelling and inducers of CM hypertrophy and so increases in proliferation will have an impact on each of these processes. One of the investigations into the role of these miRNAs in CFs during cardiac remodelling therefore sought to investigate the effect of overexpression through pre-miR transfection on cell counts after 7 days of culture. The presence of growth factors in FCS has been demonstrated as essential for CF survival and growth and so transfected CFs were grown in both SFM as a control and 2.5% FCS as a way to measure the influence of the miRNAs and increase the potential to uncover both pro- and anti-proliferative effects of the miRNAs. The number of cells cultured in 2.5% FCS was 62% higher than those culture in SFM at day 7 for pre-miR-NC transfection ($P=0.06$), demonstrating the mitogenic effect of the serum (Figure 4.10-4.13). It was found that transfection with pre-miR-21a, -214, -224 or -30d did not lead to a significant change in the proliferation rate over a 7-day period in either SFM or 2.5% FCS. The number of cells at day 7 for pre-miR-NC transfected CFs (cultured in 2.5% FCS) was 153% relative to day 0. The number of cells at day 7 (relative to day 0) for pre-miR-30d transfection, in comparison, was 81% (Figure 4.13). Although it was not statistically significant, there appeared to be a trend of decreased proliferation over the 7-day period from pre-miR-30d transfection.

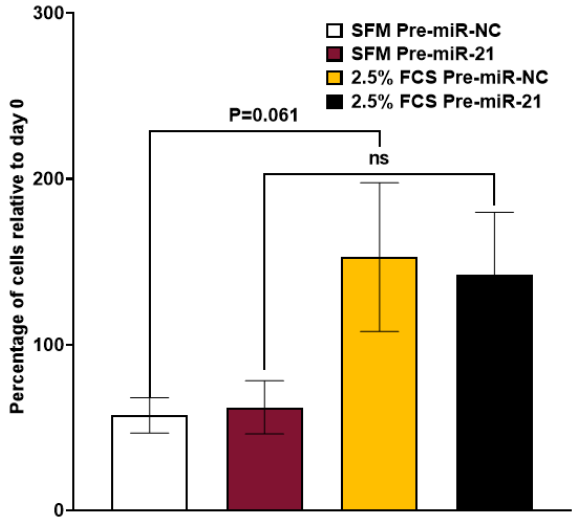

Figure 4.10 The effect of pre-miR-21a transfection on human cardiac fibroblast proliferation. Human CFs were transfected with 30nM pre-miR-NC or -21a-5p and incubated in either serum free media (SFM) or 2.5% foetal calf serum (FCS). Cell counts were performed on day 0 and day 7 post-transfection, with media changes performed on days 2 and 4. Cell counts were performed from triplicate wells using a haemocytometer and then averaged. Horizontal bars indicate the mean value and error bars represent SEM. Group sizes; n=4. One-way repeated measures ANOVA, with a Šidák multiple comparisons test, performed on log transformed data (Y=Log(Y)). ns=not significant.

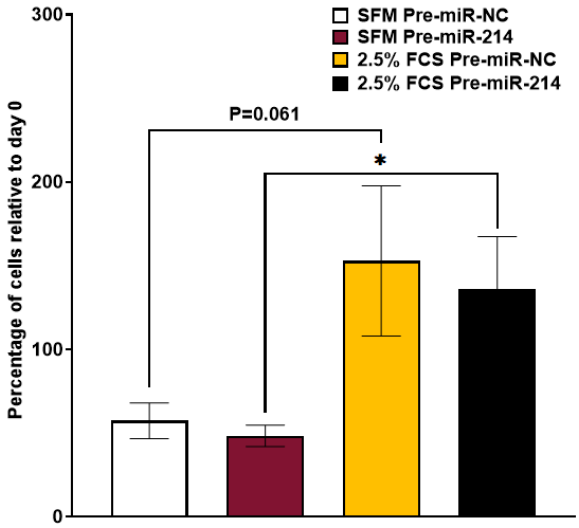

Figure 4.11 The effect of pre-miR-214 transfection on human cardiac fibroblast proliferation. Human CFs were transfected with 30nM pre-miR-NC or -214-3p and incubated in either serum free media (SFM) or 2.5% foetal calf serum (FCS). Cell counts were performed on day 0 and day 7 post-transfection, with media changes performed on days 2 and 4. Cell counts were performed from triplicate wells using a haemocytometer and then averaged. Horizontal bars indicate the mean value and error bars represent SEM. Group sizes; n=4. One-way repeated measures ANOVA, with a Šidák multiple comparisons test, performed on log transformed data (Y=Log(Y)). ns=not significant.

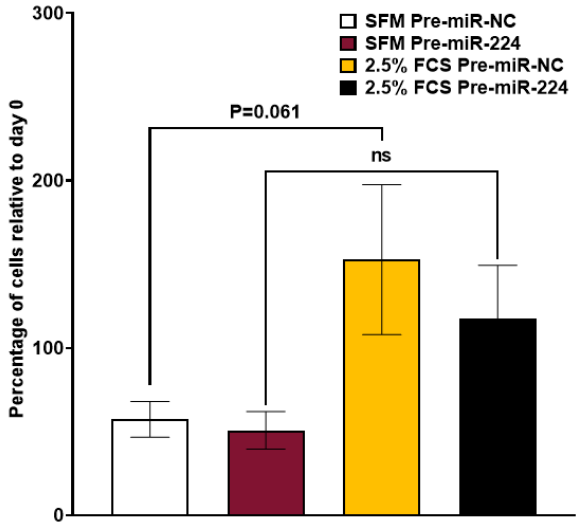

Figure 4.12 The effect of pre-miR-224 transfection on human cardiac fibroblast proliferation. Human CFs were transfected with 30nM pre-miR-NC or -224-5p and incubated in either serum free media (SFM) or 2.5% foetal calf serum (FCS). Cell counts were performed on day 0 and day 7 post-transfection, with media changes performed on days 2 and 4. Cell counts were performed from triplicate wells using a haemocytometer and then averaged. Horizontal bars indicate the mean value and error bars represent SEM. Group sizes; n=4. One-way repeated measures ANOVA, with a Šidák multiple comparisons test, performed on log transformed data (Y=Log(Y)). ns=not significant.

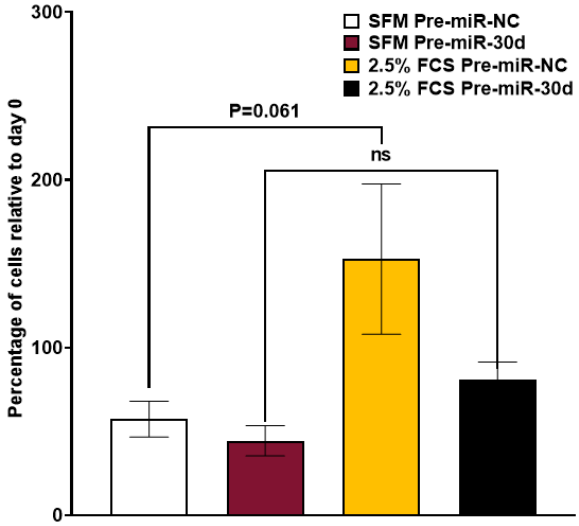

Figure 4.13 The effect of transfection with pre-miR-30d on human cardiac fibroblast proliferation. Human CFs were transfected with 30nM pre-miR-NC or -30d-5p and incubated in either serum free media (SFM) or 2.5% foetal calf serum (FCS). Cell counts were performed on day 0 and day 7 post-transfection, with media changes performed on days 2 and 4. Cell counts were performed from triplicate wells using a haemocytometer and then averaged. Horizontal bars indicate the mean value and error bars represent SEM. Group sizes; n=4. One-way repeated measures ANOVA, with a Šidák multiple comparisons test, performed on log transformed data (Y=Log(Y)). ns=not significant.

4.4.5 Measuring the change in expression of cardiac remodelling relevant genes following pre-miR and anti-miR transfection

	Pre-miR-21	Pre-miR-214	Pre-miR-224	Pre-miR-30d	Anti-miR-21	Anti-miR-214	Anti-miR-224	Anti-miR-30d
MMP2				v				
MMP3			v					
TNC		^						
TGFB1								
TGFB3								
IL6	v	v	v					
IL6R	v							
IL11	^							
ILL1RA								
ACTA2								v
COL1A1		v						
AGTR1						^		
EDN1					^			
ITGA5			^	v				

Table 4.1 The direction of cardiac remodelling relevant gene expression change at 48 hours post-transfection. Each cardiac remodelling relevant gene investigated is listed with whether it was increased or decreased at 48 hours post-pre-miR or -anti-miR transfection.

It is important that ECM proteins are investigated as the dysregulation in their turnover is a hallmark of cardiac remodelling (Bonnans et al., 2014). Similarly, it has been demonstrated that miRNAs can mediate post-transcriptional regulation of specific ECM genes (Piperigkou and Karamanos, 2019). The first panel of mRNA expression that was investigated, following pre-miR or anti-miR transfection, was that of the ECM-related proteins, including: MMP-2, MMP-3 and TNC (Figure 4.14). MMP-2 mRNA levels first of all were significantly lower following the overexpression of miR-30d (45% decrease). MMP-3 mRNA levels on the other hand were significantly lower following pre-miR-224-5p transfection (88% decrease). This suggests that miR-224 also plays an inhibitory role in the expression of MMP-3. Since miR-224 and miR-30d each decrease the levels of MMP-3 and MMP-2 respectively, this could be linked to the off-target effects of pre-miR-224 mediating an increase in miR-30d and anti-miR-224 mediating a decrease in miR-30d, observed in Figure 4.4 and 4.8.

Conversely, the levels of TNC mRNA were significantly higher following miR-214 transfection (4.5-fold increase) (Figure 4.14). This is a large increase in the expression levels of TNC, an ECM protein which has been suggested as an inducer of left ventricular remodelling post-MI (by macrophage polarisation) (Kimura et al., 2019). This could indicate that miR-214 acts in an opposing way to miR-224 and miR-30d in regulation of the ECM. In contrast to the effects of pre-miR transfection, there was no effect of anti-miR transfection on mRNA expression levels of MMP2, MMP3 or TNC (Figure 4.15).

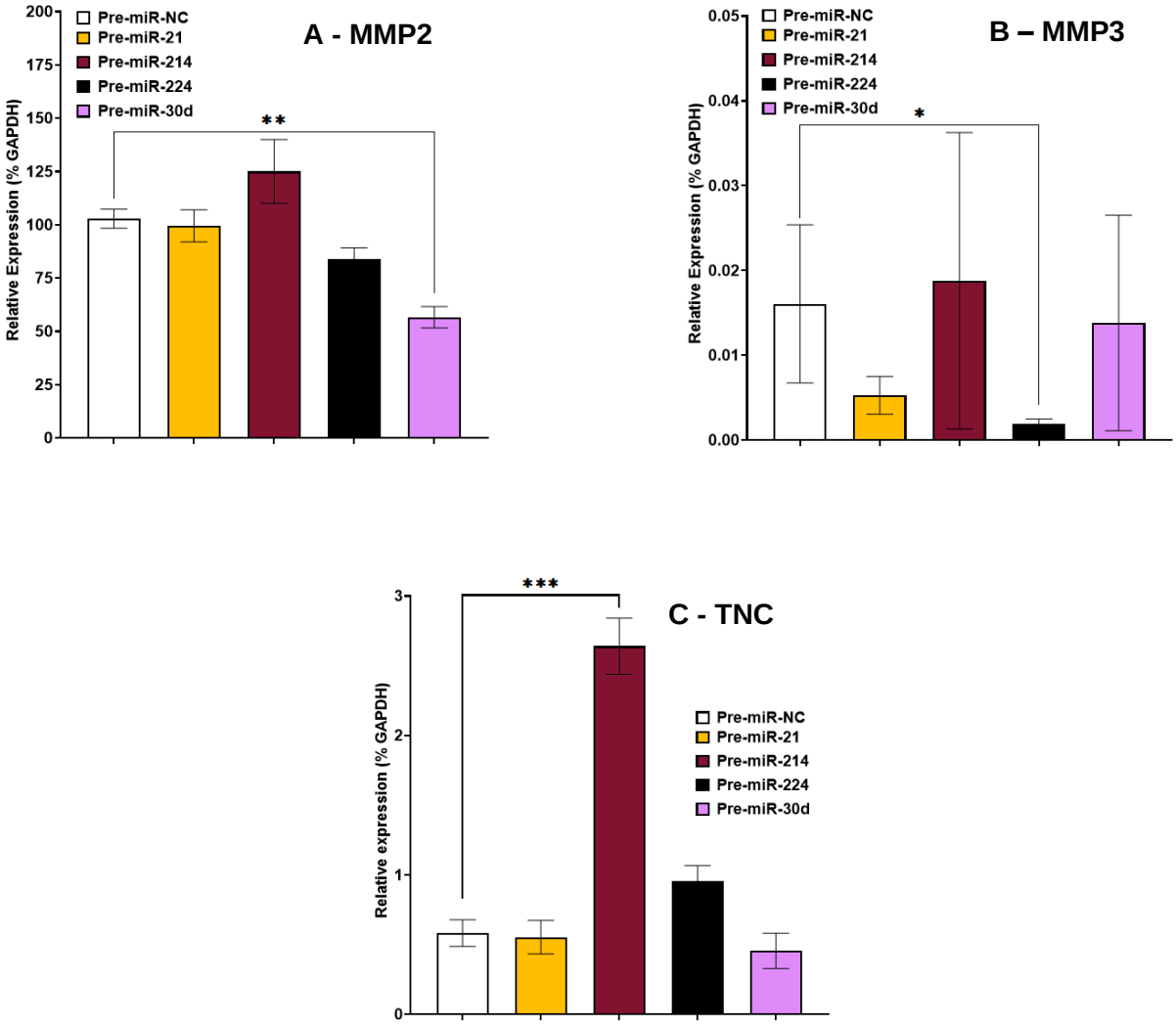

Figure 4.14 Expression levels of ECM genes in human cardiac fibroblasts at 48-hours post-transfection with pre-miRs. Human CFs were transfected for 6 hours with 30nM pre-miR-NC, -21a-5p, -214-3p, -224-5p or -30d-5p and RNA was isolated at 48 hours post-transfection. Gene expression levels of MMP2 **(A)**, MMP3 **(B)** and TNC **(C)** were calculated by performing qRT-PCR and normalising levels relative to the housekeeping control, GAPDH. Horizontal bars indicate the mean value and error bars represent SEM. Group sizes; n=4. One-way repeated measures ANOVA, with a Šidák multiple comparisons test, performed on log transformed data (Y=Log(Y)).*P<0.05 and ***P<0.001. ns=not significant.

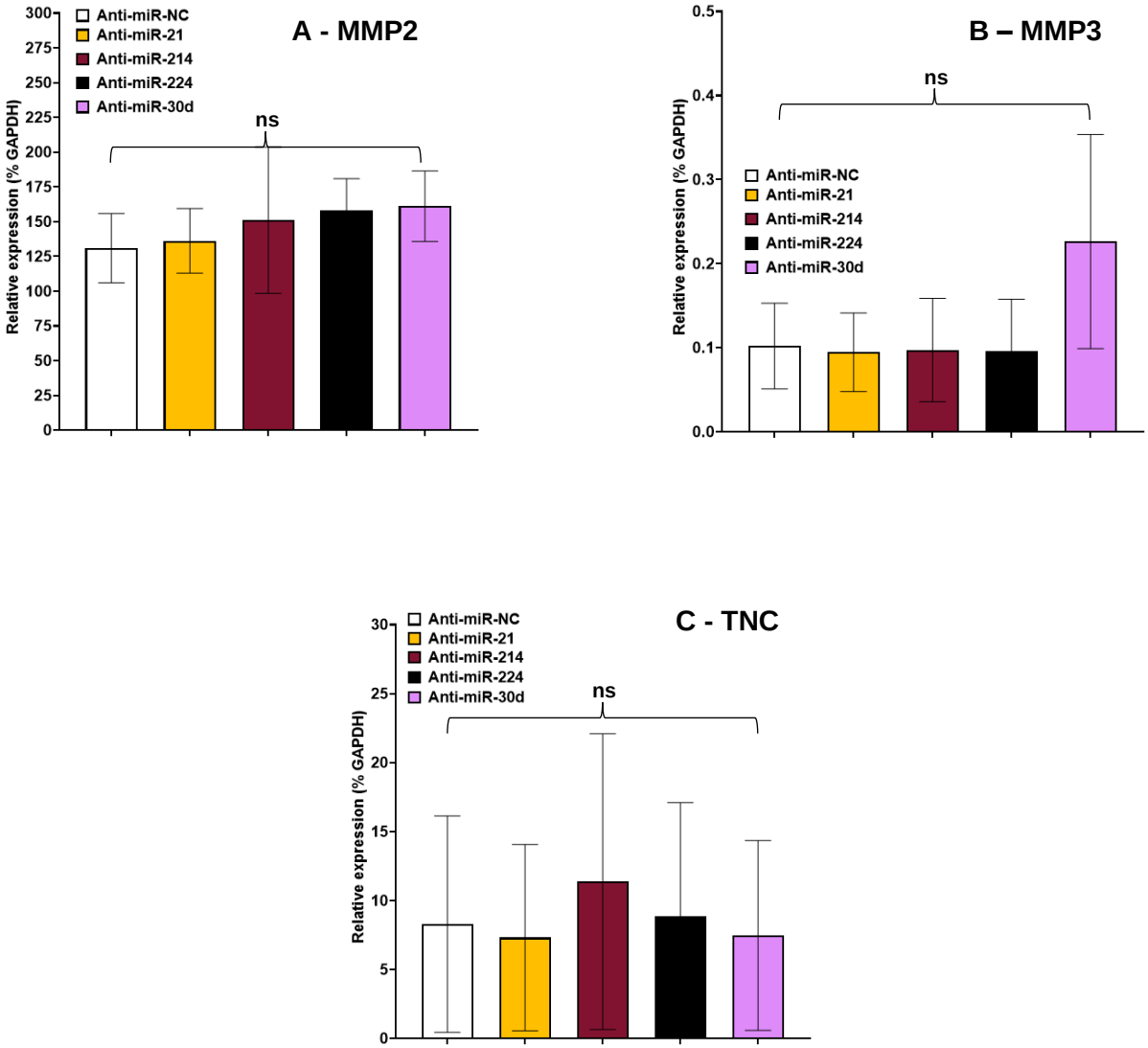

Figure 4.15 Expression levels of ECM genes in human cardiac fibroblasts at 48-hours post-transfection with anti-miRs. Human CFs were transfected for 6 hours with 100nM anti-miR-NC, -21a-5p, -214-3p, -224-5p or -30d-5p and RNA was isolated at 48 hours post-transfection. Gene expression levels of MMP2 **(A)**, MMP3 **(B)** and TNC **(C)** were calculated by performing qRT-PCR and normalising levels relative to the housekeeping control, GAPDH. Horizontal bars indicate the mean value and error bars represent SEM. Group sizes; n=3. One-way repeated measures ANOVA, with a Šidák multiple comparisons test, performed on log transformed data (Y=Log(Y)). ns=not significant.

The second panel included measuring mRNA levels for two of the members of the TGFβ family; TGFβ1 and TGFβ3. These proteins are multifunctional cytokines that have been studied extensively in CVD. TGF-β is a stimulator of FMT and leads to expansion of the MyoFb population (increasing the synthesis of α-SMA), as well as acting in a pro-fibrotic manner to increase expression of ECM proteins (Nagpal et al., 2016). Furthermore, TGFβ stimulates a signalling cascade that leads to SMAD molecule translocation to the nucleus, leading to their initiation of miRNA transcription (Saadat et al., 2020). It was therefore important to include these cytokines in the panel to investigate their effect on human CFs *in vitro*. What should be noted is that large SEMs exist for the measurement of TGFB1 and TGFB3 which may mask any real findings.

Transfection with pre-miR-21a suggested a trend of higher levels of TGFB3 mRNA expression (1.6-fold higher) although this was not quite statistically significant, with a P value of 0.0539 (Figure 4.16). Overexpression of the miRNAs, miR-214, -224 and -30d showed no change in the levels of either TGFB1 or TGFB3 at the time point studied (48 h). It appears therefore that none of the miRNAs influence TGFβ transcription. Similar to transfection with pre-miRs, transfection with anti-miRs for each of the miRNAs had no effect on the expression levels of TGFB1 or TGFB3 (Figure 4.17).

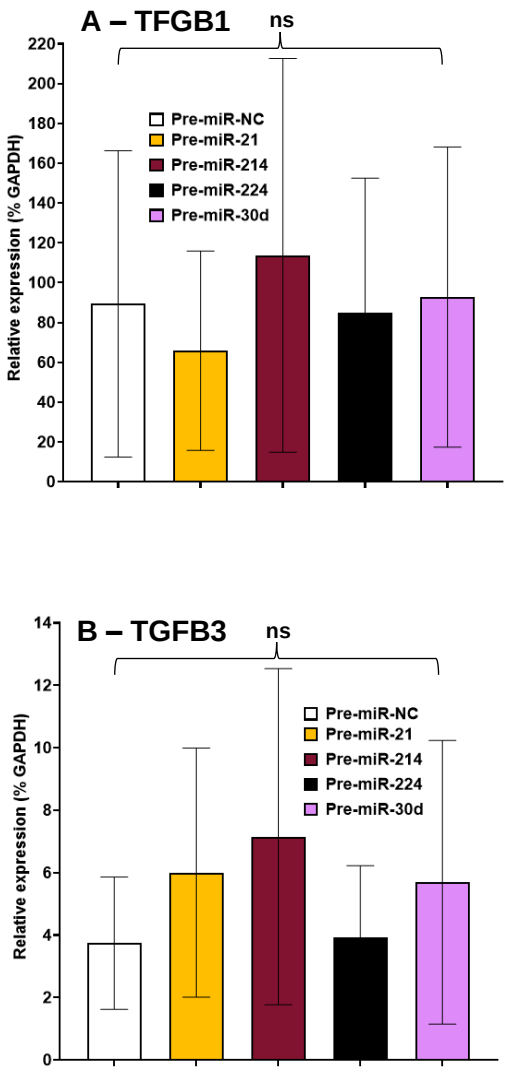

Figure 4.16 Expression levels of TGF-β genes in human cardiac fibroblasts at 48-hours post-transfection with pre-miRNA. Human CFs were transfected for 6 hours with 30nM pre-miR-NC, -21a-5p, -214-3p, -224-5p or -30d-5p and RNA was isolated at 48 hours post-transfection. Gene expression levels of TGFB1 **(A)** and TGFB3 **(B)** were calculated by performing qRT-PCR and normalising levels relative to the housekeeping control, GAPDH. Horizontal bars indicate the mean value and error bars represent SEM. Group sizes; n=4. One-way repeated measures ANOVA, with a Šidák multiple comparisons test, performed on log transformed data (Y=Log(Y)). ns=not significant.

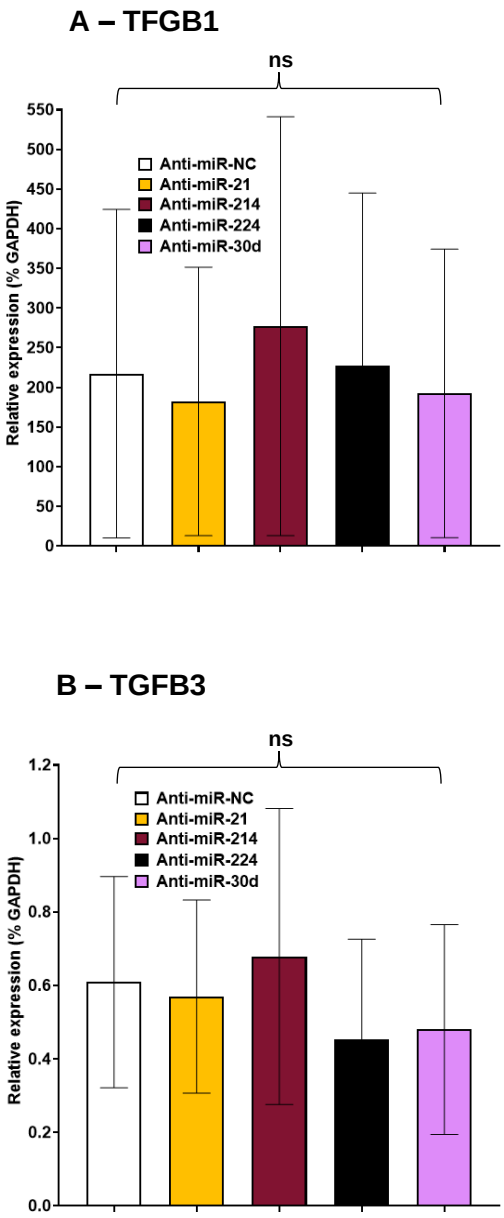

Figure 4.17 Expression levels of TGF-β genes in human cardiac fibroblasts at 48-hours post-transfection with anti-miRNA. Human CFs were transfected for 6 hours with 100nM anti-miR-NC, -21a-5p, -214-3p, -224-5p or -30d-5p and RNA was isolated at 48 hours post-transfection. Gene expression levels of TGFB1 **(A)** and TGFB3 **(B)** were calculated by performing qRT-PCR and normalising levels relative to the housekeeping control, GAPDH. Horizontal bars indicate the mean value and error bars represent SEM. Group sizes; n=3. One-way repeated measures ANOVA, with a Šidák multiple comparisons test, performed on log transformed data (Y=Log(Y)). ns=not significant.

The third panel included the interleukin 6 family members, IL6 and IL11 and each of their receptors, IL6R and IL11RA. As discussed, IL-6 has been demonstrated as a paracrine signalling molecule, being synthesised and released by CFs, to act on CMs to induce hypertrophy, in pathological cardiac remodelling (Bageghni et al., 2018). IL-11 has been shown to be increased following TGFβ1 stimulation and induce IL-11 dependent pro fibrotic protein expression (Widjaja et al., 2021).

Pre-miR-21a transfected CFs showed significantly lower levels of IL6 and IL6R mRNA (54% and 35% lower respectively) and significantly higher levels of IL11 mRNA (2.4-fold higher). Both pre-miR-214 and pre-miR-224 transfected CFs showed significantly lower levels of IL6 mRNA (30% and 70% lower respectively) (Figure 4.18). There was no effect of anti-miR transfection on each of the interleukins or their receptors however there was a strong trend of lower levels of IL11 mRNA after anti-miR-30d-5p transfection (P=0.0539) (Figure 4.19).

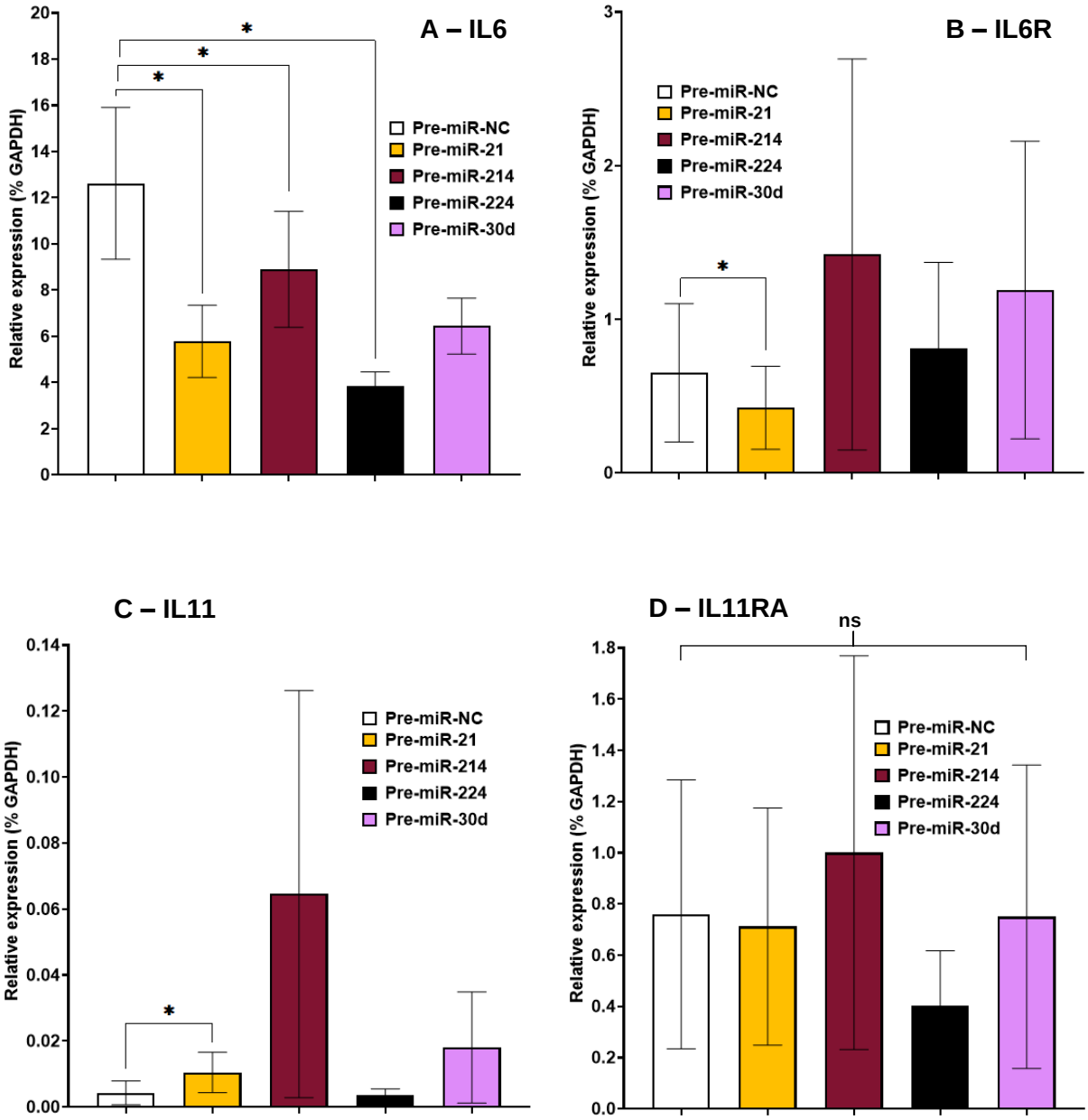

Figure 4.18 Expression levels of interleukin and interleukin receptor genes in human cardiac fibroblasts at 48-hours post-transfection with pre-miRNA. Human CFs were transfected for 6 hours with 30nM pre-miR-NC, -21a-5p, -214-3p, -224-5p or -30d-5p and RNA was isolated at 48 hours post-transfection. Gene expression levels of IL6 **(A)**, IL6R **(B)**, IL11 **(C)** and IL11RA **(D)** were calculated by performing qRT-PCR and normalising levels relative to the housekeeping control, GAPDH. Horizontal bars indicate the mean value and error bars represent SEM. Group sizes; n=4. One-way repeated measures ANOVA, with a Šidák multiple comparisons test, performed on log transformed data (Y=Log(Y)). *P<0.05. ns=not significant.

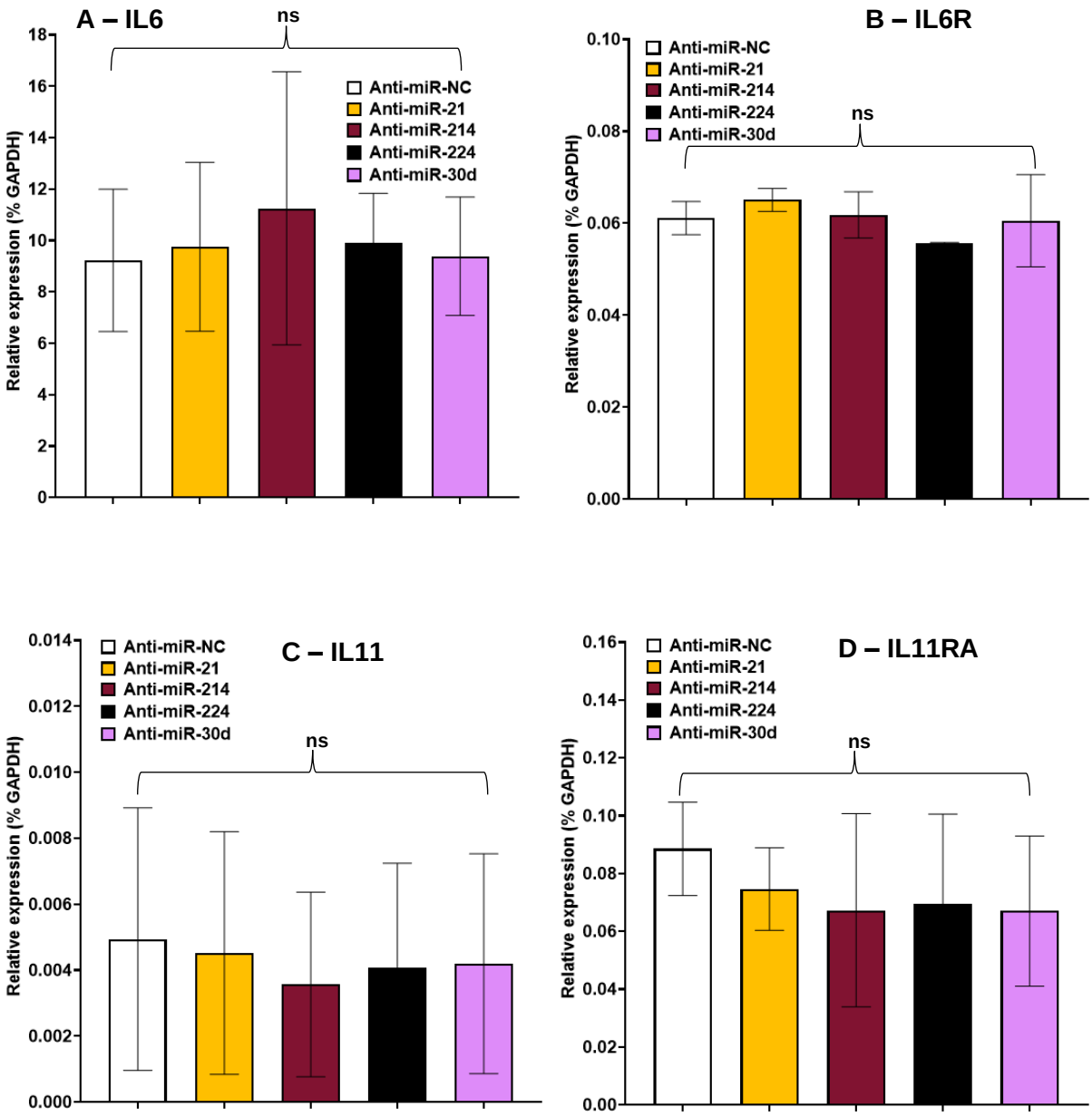

Figure 4.19 Expression levels of interleukin and interleukin receptor genes in human cardiac fibroblasts at 48-hours post-transfection with anti-miRNA. Human CFs were transfected for 6 hours with 100nM anti-miR-NC, -21a-5p, -214-3p, -224-5p or -30d-5p and RNA was isolated at 48 hours post-transfection. Gene expression levels of IL6 **(A)**, IL6R **(B)**, IL11 **(C)** and IL11RA **(D)** were calculated by performing qRT-PCR and normalising levels relative to the housekeeping control, GAPDH. Horizontal bars indicate the mean value and error bars represent SEM. Group sizes; n=3. One-way repeated measures ANOVA, with a Šidák multiple comparisons test, performed on log transformed data (Y=Log(Y)). ns=not significant.

The next panel looked at the MyoFb markers, ACTA2 and COL1A1. These MyoFb markers have been included to understand what role each of the four miRNAs may play in inducing the phenotypic switch to this fibrotic phenotype (FMT transition). ACTA2 specifically, is an important measure of this and is one of the hallmarks of the MyoFb, where increased expression levels are observed with both activation of CFs and expansion of CFs into this phenotype (Daseke et al., 2020). Transfection of CFs with pre-miR-214 resulted in significantly lower levels of COL1A1 mRNA (36% lower) without modulating ACTA2 mRNA (Figure 4.20). None of the other pre-miRs affected ACTA2 or COL1A1 mRNA levels (Figure 4.20).

When CFs were transfected with anti-miR-30d, to inhibit endogenous miR-30d, the mRNA expression levels of ACTA2 were significantly lower with a decrease of 12% however it could be questioned whether this decrease is biologically significant (Figure 4.21). This is particularly interesting because existing research on miR-30d suggests that it is decreased in models of CVD, in agreement with the ISO infusion model performed by our group (Figure 3.1). Inhibition of miR-30d leading to a decrease in ACTA2 levels may indicate that endogenous miR-30d prevents ACTA2 levels from being down-regulated. This could be specific to endogenous levels however and miR-30d may play a role in maintaining a healthy level of CF activation.

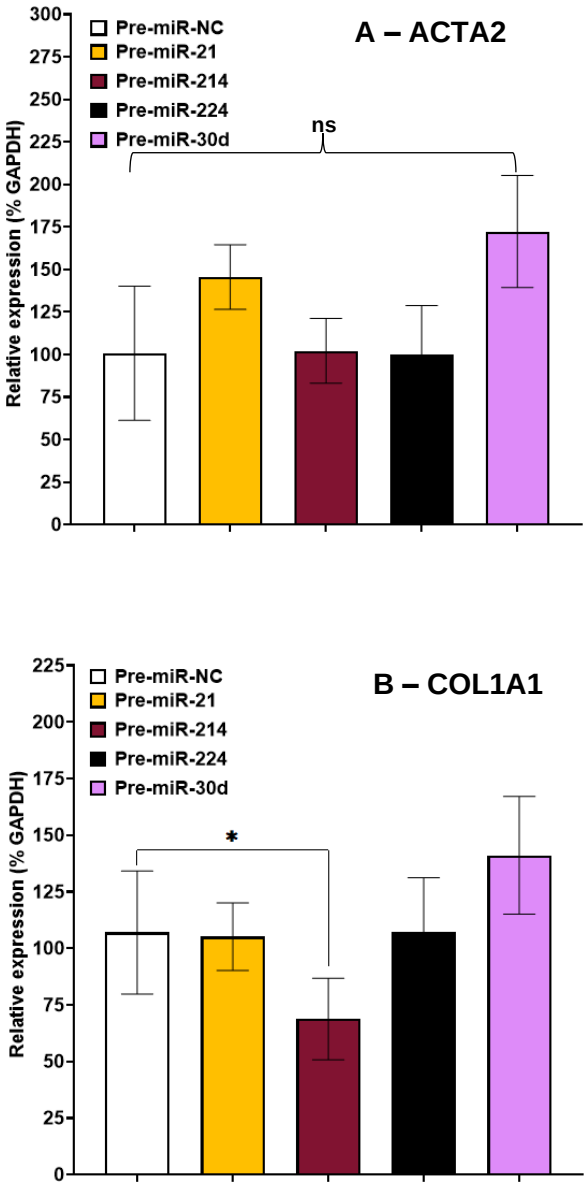

Figure 4.20 Expression levels of myofibroblast marker genes in human cardiac fibroblasts at 48-hours post-transfection with pre-miRNA. Human CFs were transfected for 6 hours with 30nM pre-miR-NC, -21a-5p, -214-3p, -224-5p or -30d-5p and RNA was isolated at 48 hours post-transfection. Gene expression levels of ACTA2 **(A)** and COL1A1 **(B)** were calculated by performing qRT-PCR and normalising levels relative to the housekeeping control, GAPDH. Horizontal bars indicate the mean value and error bars represent SEM. Group sizes; n=4. One-way repeated measures ANOVA, with a Šidák multiple comparisons test, performed on log transformed data (Y=Log(Y)). *P<0.05. ns=not significant.

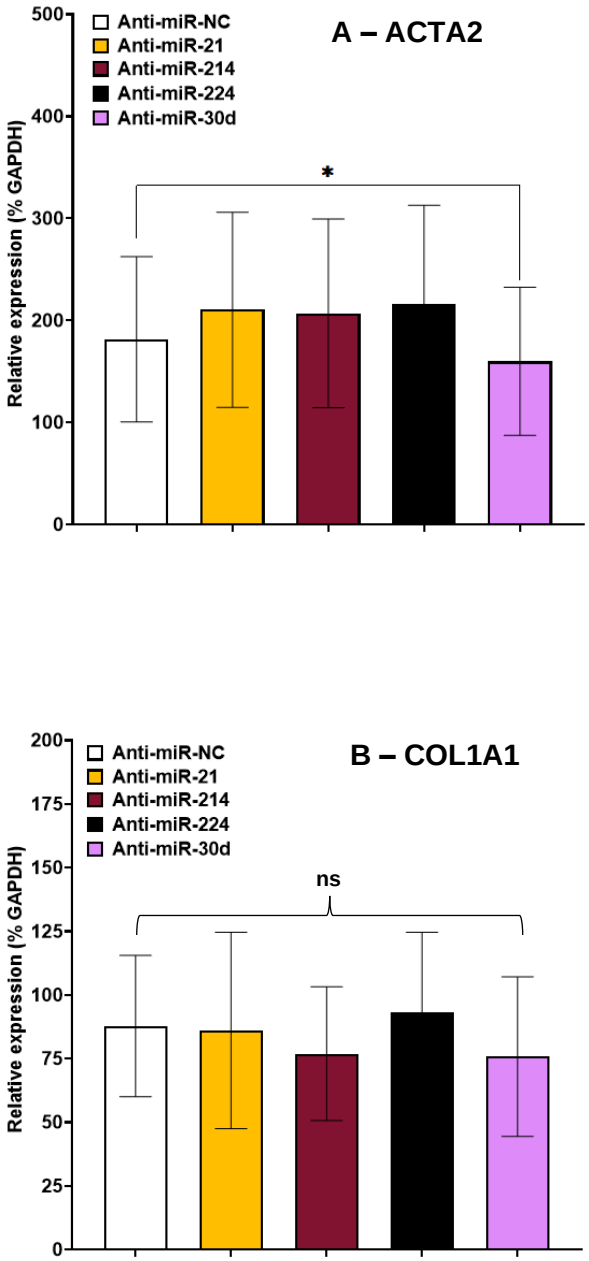

Figure 4.21 Expression levels of myofibroblast marker genes in human cardiac fibroblasts at 48-hours post-transfection with anti-miRNA. Human CFs were transfected for 6 hours with 100nM anti-miR-NC, -21a-5p, -214-3p, -224-5p or -30d-5p and RNA was isolated at 48 hours post-transfection. Gene expression levels of ACTA2 **(A)** and COL1A1 **(B)** were calculated by performing qRT-PCR and normalising levels relative to the housekeeping control, GAPDH. Horizontal bars indicate the mean value and error bars represent SEM. Group sizes; n=3. One-way repeated measures ANOVA, with a Šidák multiple comparisons test, performed on log transformed data (Y=Log(Y)). *P<0.05. ns=not significant.

Finally, other important genes relevant to cardiac remodelling were investigated including; angiotensin II receptor type-1 (AGTR1), endothelin 1 (EDN1) and integrin alpha 5 (ITGA5). ITGA5 was specifically studied due to existing research by Li et al. (2021) demonstrating that miR-30d acts on ITGA5 in CFs to inhibit proliferation, and therefore was included in part as a positive control.

It was discovered that transfection with pre-miR-224 resulted in significantly higher levels of mRNA for ITGA5 (1.6-fold higher). Pre-miR-30d transfection conversely showed significantly lower levels of ITGA5 mRNA (44% lower) as expected (Figure 4.22). Treatment with the inhibitory anti-miR-21a resulted in significantly higher levels of EDN1 mRNA (1.1-fold higher). Finally, transfection with anti-miR-214 resulted in significantly higher levels of AGTR1 mRNA (1.1-fold higher) (Figure 4.23). In comparison, there were no pre-miR transfections that changed mRNA expression levels of either AGTR1 or EDN1. Similarly, no anti-miR transfections affected the levels of ITGA5 mRNA, despite seeing that pre-miR-224 and -30d changed their levels (Figure 4.23).

To summarise, many differences were identified across all panels of gene expression explored for each of the four miRNAs overexpression and inhibitions. First, miR-21a overexpression resulted in lower mRNA levels of both IL6 and its receptor, IL6R, which would suggest that it could inhibit all elements of the IL6 signalling cascade (Figure 4.18). Interestingly, miR-21a overexpression increased the levels of IL11 mRNA. Inhibition of miR-21a on the other hand, resulted in higher levels of EDN1 mRNA (Figure 4.23).

MiR-214 overexpression reduced levels of IL-6 mRNA, similar to miR-21a overexpression (Figure 4.18). Inhibition of miR-214 also yielded increased levels of AGTR1 mRNA, perhaps suggesting that miR-214 could mediate the degradation of the AGTR1 mRNA at endogenous levels (Figure 4.23). MiR-214 overexpression reduced COL1A1 and increased TNC (4.5-fold higher), without modulating ACTA2 mRNA. This means it did not affect MyoFb differentiation markers specifically but more so influencing the production of specific matrix molecules (Figure 4.14 and 4.20).

MiR-224 overexpression, the same as with miR-21a and -214, resulted in lower levels of IL6 mRNA (Figure 4.18). MiR-224 overexpression also led to decreased mRNA levels of the matrix protease MMP3 (Figure 4.14). Overexpression of miR-224 also resulted in higher levels of ITGA5 mRNA (Figure 4.22). Finally, miR-30d overexpression resulted in lower levels of MMP2 mRNA (Figure 4.14).

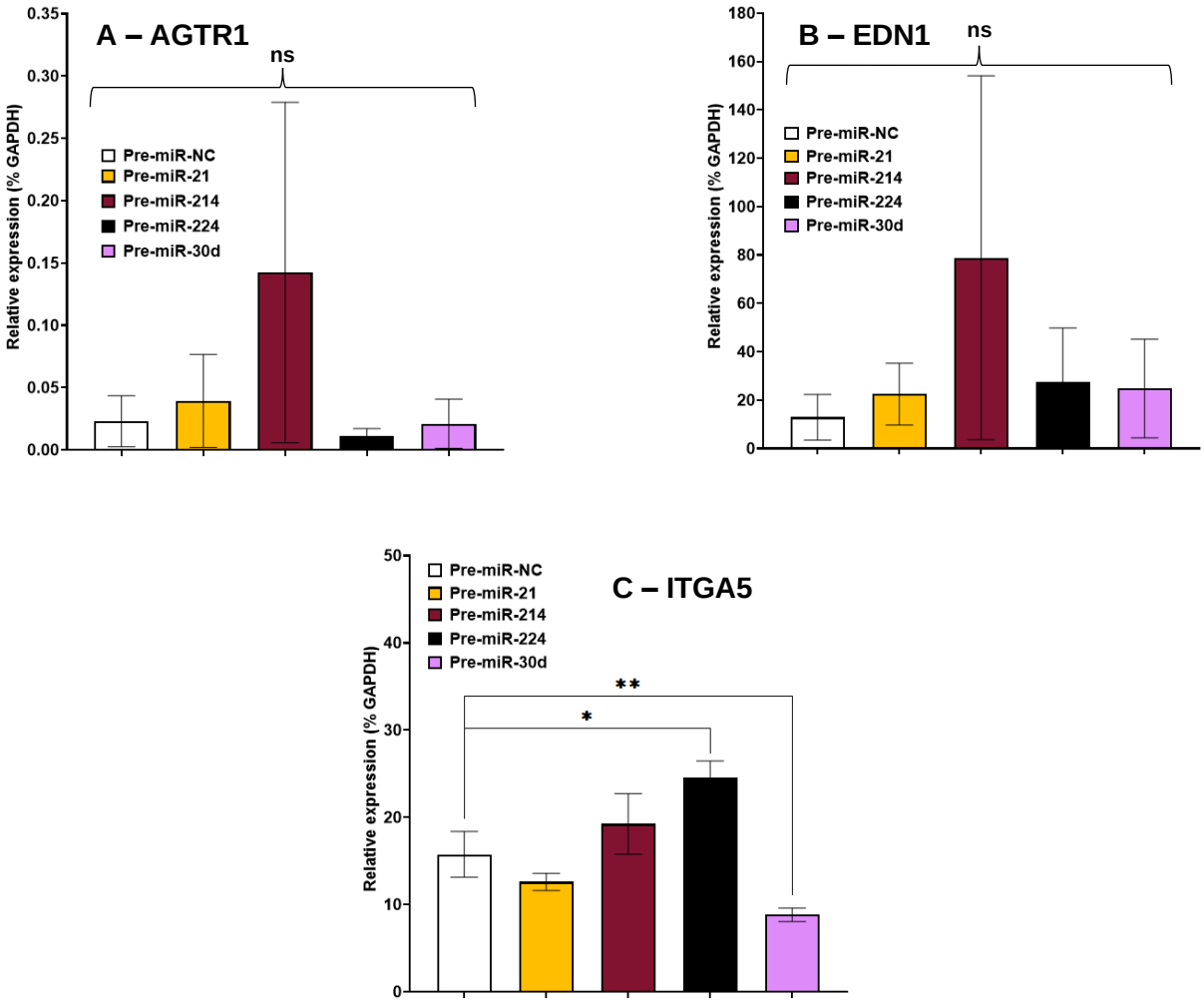

Figure 4.22 Expression levels of relevant cardiac remodelling genes in human cardiac fibroblasts at 48-hours post-transfection with pre-miRNA. Human CFs were transfected for 6 hours with 30nM pre-miR-NC, -21a-5p, -214-3p, -224-5p or -30d-5p and RNA was isolated at 48 hours post-transfection. Gene expression levels of AGTR1 **(A)**, EDN1 **(B)** and ITGA5 **(C)** were calculated by performing qRT-PCR and normalising levels relative to the housekeeping control, GAPDH. Horizontal bars indicate the mean value and error bars represent SEM. Group sizes; n=4. One-way repeated measures ANOVA, with a Šidák multiple comparisons test, performed on log transformed data (Y=Log(Y)). *P<0.05 and **P<0.01. ns=not significant.

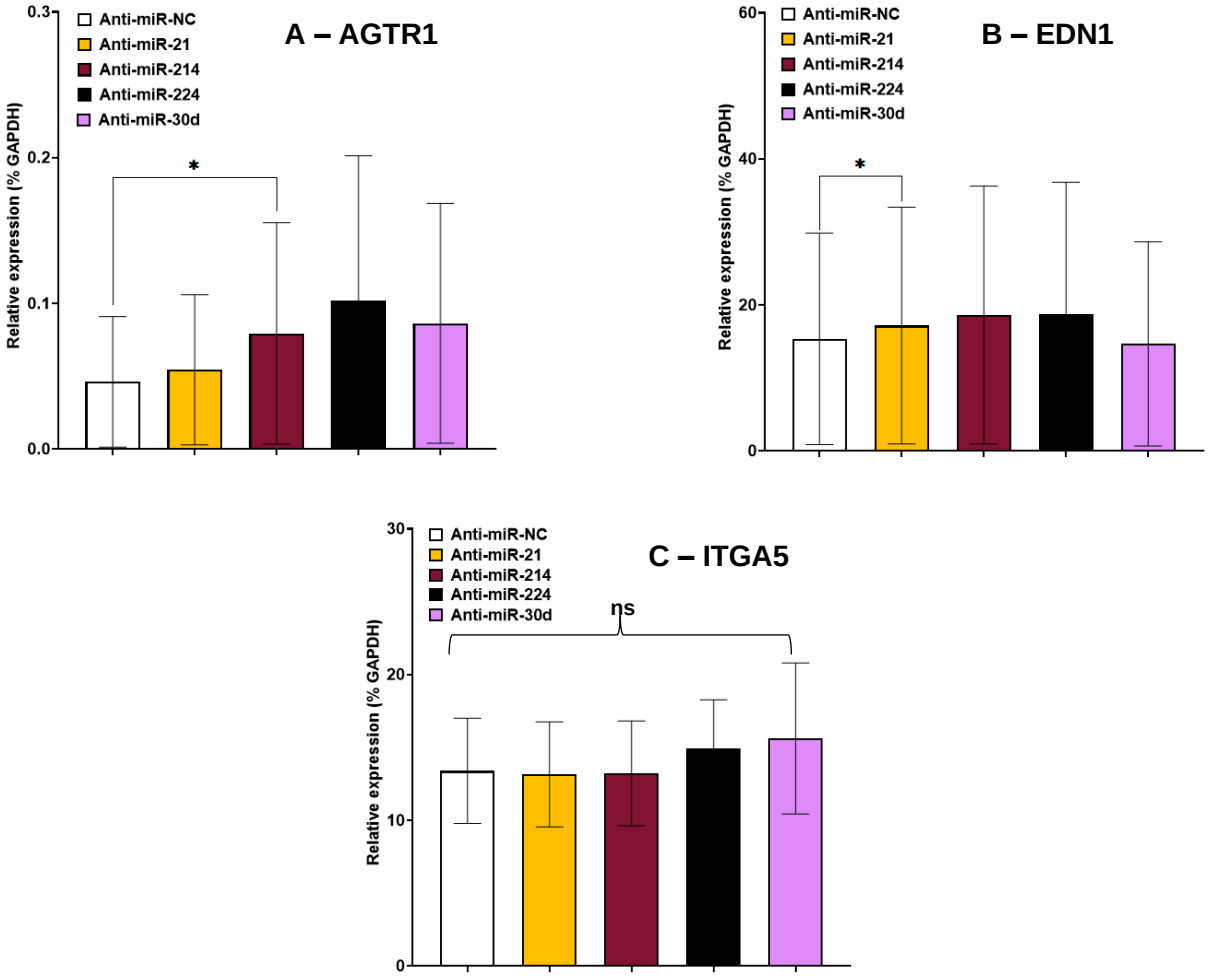

Figure 4.23 Expression levels of relevant cardiac remodelling genes in human cardiac fibroblasts at 48-hours post-transfection with anti-miRNA. Human CFs were transfected for 6 hours with 100nM anti-miR-NC, -21a-5p, -214-3p, -224-5p or -30d-5p and RNA was isolated at 48 hours post-transfection. Gene expression levels of AGTR1 **(A)**, EDN1 **(B)** and ITGA5 **(C)** were calculated by performing qRT-PCR and normalising levels relative to the housekeeping control, GAPDH.. Horizontal bars indicate the mean value and error bars represent SEM. Group sizes; n=3. One-way repeated measures ANOVA, with a Šidák multiple comparisons test, performed on log transformed data (Y=Log(Y)). *P<0.05. ns=not significant.

4.4.6 The effect of pre-miR and anti-miR transfection on IL-6 secretion in human cardiac fibroblasts

As well as measuring the effect of pre-miR or anti-miR transfection on the expression levels of IL6 mRNA, the concentration of IL-6 protein in the conditioned media of transfected CFs was also measured 72 h after transfection. Experiments were performed in 10% FCS DMEM, the same serum conditions as for CFs transfected for RNA isolations and qRT-PCR analysis. Despite the RT-PCR gene expression data revealing decreases in IL6 mRNA levels in response to pre-miRs 21, 214 and 224 (Figure 4.18), there was no significant difference in the conditioned media IL-6 concentrations obtained from CFs transfected with any of the specific pre-miRs compared to pre-miR-NC transfection (Figure 4.24). Similarly, there were no significant differences observed when CFs were transfected with anti-miRs (Figure 4.25), in agreement with the RT-PCR data (Figure 4.19). Although there was an apparent increase in the concentration of IL-6 in anti-miR-21a transfected CFs (44.9 ng/mL) compared to anti-miR-NC transfection (15.9 ng/mL) with a fold difference of 2.8, this had a P value of 0.8964 indicating it is not a real difference and the apparent increase was skewed by an outlier where one patient showed particularly high levels of IL-6.

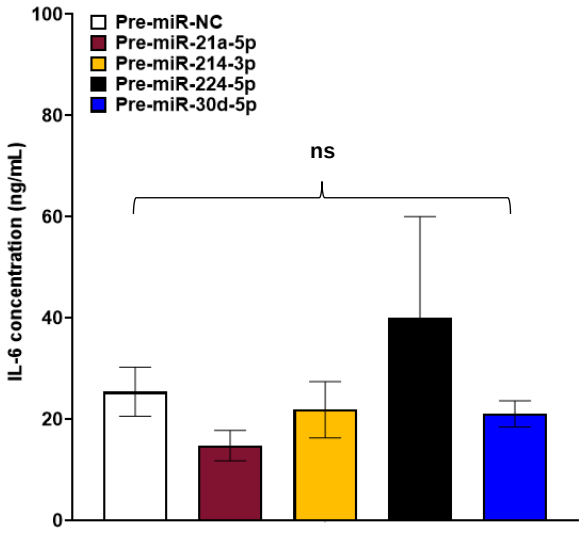

Figure 4.24 Interleukin-6 concentration in conditioned media taken from human cardiac fibroblasts at 72-hours post-transfection with pre-miRNAs. Human cardiac fibroblasts (CFs) were transfected for 6 hours with 30nM pre-miR-NC, -21a-5p, -214-3p, -224-5p or -30d-5p and conditioned media was taken at 72 hours post-transfection. IL-6 concentration was calculated by performing a human IL-6 specific ELISA and performing four parameter logistic regression (4PL) from IL-6 standards. Horizontal bars indicate the mean value and error bars represent SEM. Group sizes; n=3. One-way repeated measures ANOVA, with a Šidák multiple comparisons test, performed on log transformed data (Y=Log(Y)). ns=not significant.

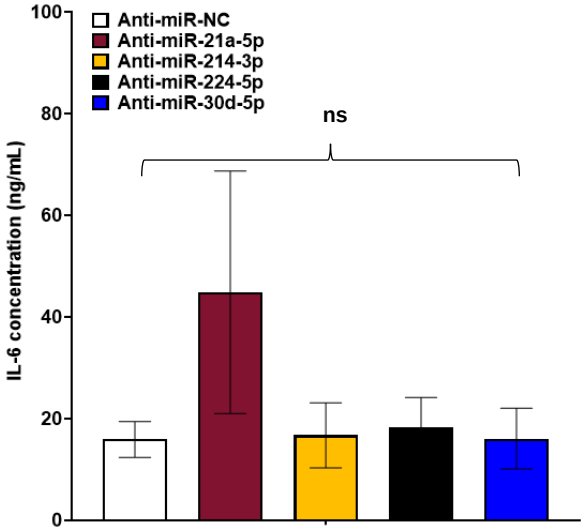

Figure 4.25 Interleukin-6 concentration in conditioned media taken from human cardiac fibroblasts at 72-hours post-transfection with anti-miRNAs. Human CFs were transfected with 100nM anti-miR-NC, -21a-5p, -214-3p, -224-5p or -30d-5p and conditioned media was taken at 72 hours post-transfection. IL6 concentration was calculated by performing a human IL-6 specific ELISA and performing four parameter logistic regression (4PL) from IL-6 standards. Horizontal bars indicate the mean value and error bars represent SEM. Group sizes; n=3. One-way repeated measures ANOVA, with a Šidák multiple comparisons test, performed on log transformed data (Y=Log(Y)). ns=not significant.

4.4.7 The effect of pre-miR and anti-miR transfection on MMP-2 secretion in human cardiac fibroblasts

MMP-2, similar to IL-6, is a secreted protein and so the expression levels in conditioned media obtained from human CFs was measured. The only miRNA transfection to have an affect on MMP-2 expression was pre-miR-214. Overexpression of miR-214 resulted in a signficantly higher concentration of MMP-2 (1.3 fold higher) (Figure 4.26). In comparison, there was no anti-miR transfection that had an effect on MMP-2 either on the mRNA level (Figure 4.15) or the protein level (Figure 4.27).

ELISAs for IL6 and MMP2 have allowed an investigation into the levels of secreted proteins present in the conditioned media which otherwise may not be identified from other methods for protein analyses (such as Western Blot or TMT proteomics; see Chapter 5). When comparing any changes observed for IL-6 at the mRNA or protein level, it was found that overexpression of miR-21a, -214 and -224 showed lower levels of IL6 mRNA (Figure 4.18) however there was no change observed in IL-6 protein expression (Figure 4.24). These results demonstrate that the decreased expression of IL6 mRNA does not manifest as changes in protein secretion. In terms of MMP2, miR-30d overexpression led to significantly lower levels of MMP2 mRNA (45% lower) (Figure 4.14). MMP-2 protein expression on the other hand, was significantly increased following miR-214 overexpression.

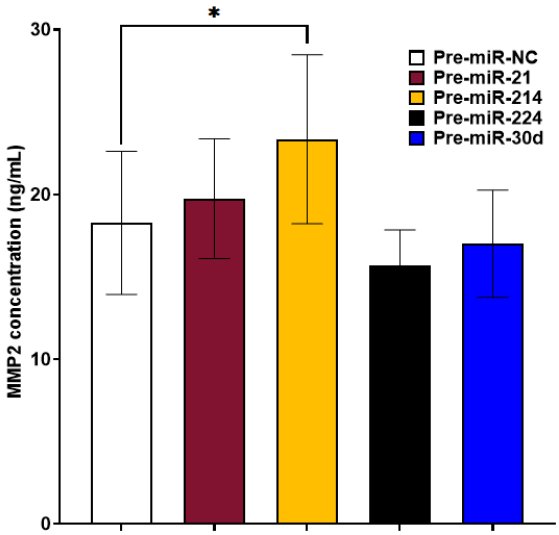

Figure 4.26 MMP-2 concentration in conditioned media obtained from human cardiac fibroblasts following pre-miR transfection. Human (CFs) were transfected with 30nM pre-miR-NC, -21a-5p, -214-3p, -224-5p or -30d-5p and conditioned media was taken at 72 hours post-transfection. MMP-2 concentration was calculated by performing a human MMP-2 specific ELISA and performing four parameter logistic regression (4PL) from MMP-2 standards. Horizontal bars indicate the mean value and error bars represent SEM. Group sizes; n=3. One-way repeated measures ANOVA, with a Šidák multiple comparisons test, performed on log transformed data (Y=Log(Y)). *P<0.05.

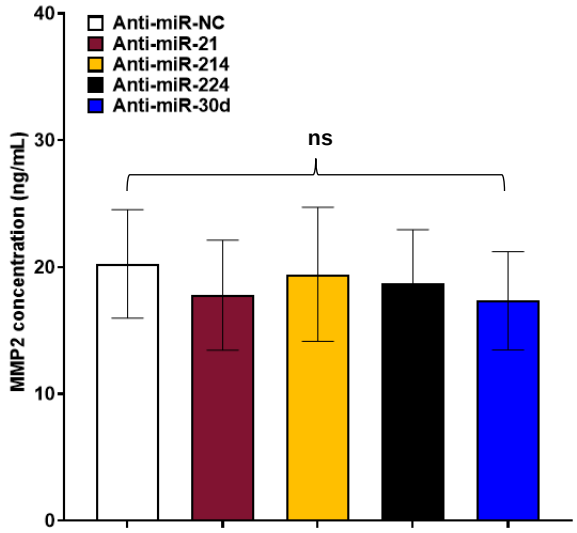

Figure 4.27 MMP-2 concentration in conditioned media obtained from human cardiac fibroblasts following anti-miR transfection. Human (CFs) were transfected with 100nM anti-miR-NC, -21a-5p, -214-3p, -224-5p or -30d-5p and conditioned media was taken at 72 hours post-transfection. MMP-2 concentration was calculated by performing a human MMP-2 specific ELISA and performing four parameter logistic regression (4PL) from MMP-2 standards. Horizontal bars indicate the mean value and error bars represent SEM. Group sizes; n=3. One-way repeated measures ANOVA, with a Šidák multiple comparisons test, performed on log transformed data (Y=Log(Y)). ns=not significant.

4.5 Discussion

The aim of this chapter was to validate the successful transfection of human cardiac fibroblasts with pre-miRs and anti-miRs for miR-21a, -214, -224 and -30d and to investigate the effect of this transfection on human CF proliferation and the expression of genes and proteins relevant to cardiac remodelling.

Human CFs were successfully transfected with pre-miRNAs, leading to large increases in each miRNA compared to basal levels. The increases of each miRNA ranged between 700-fold and 12,960-fold higher at 48 hours post-transfection. The intention of these increases is to make the downstream effects of these miRNAs easily detectable. However, it is important to consider the difference between the increases measured in the current investigation and those seen in models of cardiac dysfunction, either *in vitro* or *in vivo*. In our own investigation, ISO infusion increased the levels of miR-21a, -214 and -224 by 1.9-fold, 1.8-fold and 1.6-fold respectively (Figure 3.1) and LAD ligation increased the levels of miR-21a and -214 by 2.5-fold and 2.7-fold (Figure 3.2). These magnitudes of fold change have been demonstrated by other groups, for example Cheng et al. (2007) found miR-21a and -214 were increased 4-fold and 3-fold respectively at 7 days post-trans aortic banding (TAB) and van Rooij et al. (2006) found miR-21a and -214 were increased 8.5-fold and 7-fold at 21 days post-TAB. A similar increase was reported by Sayed et al. (2007) who found that miR-21a and -214 were increased by 2-fold and 2.5-fold respectively at 7 days post-TAC. The effect of cardiac dysfunction models has not been as extensively researched for miR-224 or -30d. However, Zheng et al. (2021) found miR-224 was increased by ~2-fold after 28 days of TAC surgery and Ning and Jiang (2013) showed that miR-224 was increased by around 1.7-fold after *in vitro* treatment of adult rat CFs with Ang II. It is apparent therefore that the increases mediated by transfection of pre-miRs are supra-physiological but nevertheless provide important information for detecting subtle and large changes in mRNA and protein expression.

It was found in exceptional cases that pre-miRNA and anti-miRNA transfections resulted in off-target changes in miRNA expression. Specifically, pre-miR-21a-5p transfection increased miR-21a (560-fold and 700-fold higher at 24 hours and 48 hours respectively) and miR-214 levels (40-fold and 50-fold higher at 24 hours and 48 hours). Also, pre-miR-224-5p transfection increased miR-224 (4,430 and 12,960-fold higher at 24 hours and 48 hours) and miR-30d (40-fold higher at 24 hours and 48 hours). Similarly, transfection with anti-miR-224-5p led to a decrease in expression of miR-30d, meaning miR-30d levels were regulated by both miR-224 transfections. Finally, anti-miR-30d-5p transfection led to a decrease in miR-21a, -214 and -30d. The capability of miRNAs to regulate the expression of other miRNAs has been

demonstrated and is a process known as miRNA:miRNA interaction (Lai et al., 2004). These interactions take the shape of miRNA duplexes where one miRNA binds to a miRNA that shares complementarity and prevents it from being loaded into the RISC and is therefore unable to target mRNA. In our case however, miRNA overexpressions were causing the overexpression of other miRNAs. This type of network has been demonstrated by Borzi et al. (2017) who found that miR-660-5p overexpression resulted in increased expression of miR-486-5p. This network involved miR-660-5p silencing Mouse Double Minute 2 (MDM2) and then stimulating p53 to increase miR-486-5p in the lung cancer cell line, A549. Our pre-miRNAs may therefore modulate the regulators of other miRNAs, such as promoters or repressors. Such a network has not been demonstrated for our miRNAs in existing literature and so this could be a novel finding from the present investigation. We used the miRNA/transcription factor (TF) prediction tool transmiR (https://www.cuilab.cn/transmir) to identify that hypoxia-inducible factor 1-alpha (HIF1A) upregulates miR-214 expression. Overexpression of miR-21a has been demonstrated to increase HIF1A levels and this could be a way in which off-target effects are observed (Liu et al., 2014). It is important to consider whether the detected effects from pre-miR transfection are attributable to that specific miRNA or the off-target miRNA that is also changed.

We found that pre-miR transfection led to higher expression levels at 48 hours compared to 24 hours. Therefore we investigated the effect of transfections on gene expression at 48 hours post-transfection. This decision is supported by numerous publications that involve measurement of mRNA targets at 48 hours post-transfection (Bertero et al., 2012) (Armada et al., 2019) (Jafari et al., 2021). In contrast, we investigated the effect on IL-6 and MMP-2 secretion at 72 hours post-transfection. This was because protein translation takes place following transcription and it was rationalised that any changes in protein expression would occur after post-transcriptional regulation was at its highest activity. Again, this time point for the investigation of pre-miR transfection on protein expression in harvested conditioned media has been chosen by numerous other research groups (Turchinovich et al., 2011) (van Balkom et al., 2013) (Almeida et al., 2016) (Wang et al., 2016).

We found that pre-miR-21a transfection reduced the expression of *IL6* and *IL6R* mRNA and increased expression of *IL11* mRNA. All other panels of genes including ECM and MyoFb markers were unchanged. This suggests miR-21a primarily regulates cytokines of the IL-6 family in human CFs. Our finding is supported by multiple groups that demonstrate miR-21a targeting of *IL6* as an important response to DAMPs. Liu et al. (2021) found that miR-21a expression negatively correlated with *IL6* mRNA and that miR-21a mimic treatment was able to reverse an increase in *IL6* caused by lipopolysaccharide (LPS). Furthermore, Yang et al.

(2018) found that miR-21a mimics decreased *IL6* in response to the DAMPs, high mobility group protein B1 (HMGB1) and heat shock protein 60 (HSP60) that were released in an MI model. The direct targeting of *IL6R* by miR-21a was identified by Wang et al. (2018b) through a luciferase reporter assay and they demonstrated this degradation suppressed cell proliferation, migration and invasion. We used the miRNA to mRNA prediction database, mirdb (mirdb.org), to identify a seed sequence of "ATAAGCTA" in the *IL6R* 3' UTR. No seed sequence exists in the *IL6* 3' UTR however which suggests there is an indirect regulation for this mRNA. These findings are in contradiction to those made by Mirna et al. (2022).

Our investigation is the first to confirm overexpression of miR-21a overexpression increases the levels of *IL11* mRNA. IL-11 has been shown to induce fibrosis in CVD and its inhibition has been suggested as a therapeutic strategy (Schafer et al., 2017). This increase could be due to miR-21a regulating the expression of a TF that suppresses *IL11* expression. In fact, it was found by Shin et al. (2012) that there are two binding sites for the TF, activator protein 1 (AP-1) upstream of *IL11* and Zhou et al. (2011) found that overexpression of miR-21a can increase the expression of AP-1, suggesting that a miR-21a/AP-1/IL-11 signalling axis could exist. The reason why miR-21a decreased mRNA expression of *IL6 and IL6R,* while increasing *IL11* in human CFs could be because immune cells predominantly express *IL6* whereas fibroblasts predominantly express *IL11* (Cook and Schafer, 2020).

Overexpression of miR-214 was similarly found to decrease expression of *IL6* mRNA. There is little literature reporting on miR-214 and *IL6* and of that literature, results are conflicting. He et al. (2020) demonstrated that inflammatory smooth muscle cells stimulated with TNFα produced an increase in *IL6* however this increase was ameliorated by transfection with miR-214 mimic. A similar finding was reported by Xu et al. (2022) who found that miR-214 mimic ameliorated an increase in *IL6* induced by LPS in the HD11 cell line. Conversely, Polytarchou et al. (2015) demonstrated a pre-miR-214 induced ~4-fold increase of *IL6* in a colonic epithelial cell line. These differing results could suggest cell type specific differences in the way that miRNAs regulate gene expression.

We have shown for the first time that overexpression of miR-214 increases the expression of the matricellular ECM protein, TNC. The increase induced by miR-214 is particularly large and is 4.5-fold higher than in the control transfection. TNC is upregulated in and secreted by fibroblasts in response to mechanical stress and wound healing (Zhao et al., 2017a). TNC is increased early in wound healing (Latijnhouwers et al., 1997) and this has been demonstrated in the border zone of rats, detected as early as 24 hours after LAD ligation, down-regulated at 7 days and near undetectable at 14 days (Imanaka-Yoshida et al., 2001). This is interesting

because in the current investigation, miR-214 expression was increased at 3 days post-LAD ligation and unchanged at 4 weeks and so this early increase in TNC could be induced by miR-214. Importantly for our investigation, there are several publications reporting on the role of TNC in CFs, with Maqbool et al. (2016) demonstrating that TNC upregulates the proinflammatory cytokine IL-6 and the ECM protein MMP-3, and Imanaka-Yoshida et al. (2001) suggested that TNC upregulation in MI may be important for the differentiation of interstitial resident fibroblasts into MyoFbs. Interestingly, miR-214 upregulation has been shown to induce differentiation of lung fibroblasts into MyoFbs in the context of pulmonary fibrosis (where it is referred to as a fibromiR) (Savary et al., 2014) and Cheng et al. (2022) demonstrated that overexpression of miR-214 reduced the infarct size in a ligation model of myocardial ischemia and reperfusion in rats. TNC upregulation has been identified as a response to ECM stiffness and in fact Miroshnikova et al. (2016) have demonstrated that miR-203 upregulated TNC by in turn upregulating HIF-1α which is interesting because Li et al. (2019) have shown that miR-214 itself can upregulate HIF-1α.

We have also shown that overexpression of miR-214 decreased the mRNA expression of *COL1A1*. As described in the introduction, *COL1A1* is one of the main components of the ECM and is a subtype of collagen that is expressed and secreted by CFs. Its expression is then upregulated after differentiation of CFs into the MyoFb phenotype which is highly matrix synthetic. Increased expression has been identified in mouse models of cardiac dysfunction, for example Zhu et al. (2016) showed *COL1A1* increased in fibrotic mouse myocardium after 2 weeks of Ang II infusion and Yang et al. (2020) showed increased *COL1A1* expression in rat heart tissue after 10 days of ISO infusion. The expression of *COL1A1* has been linked to HF in patients. This was demonstrated by Felkin et al. (2009) who found that *COL1A1* expression was higher in patients who didn't recover after treatment for dilatic cardiomyopathy, and Hua et al. (2020) found that *COL1A1* was increased in left ventricular heart tissue from HF patients and was associated with fibrosis. Based on these findings, COL1A1 has been suggested as a prognostic biomarker in HF. There are two publications that support our finding. First of all Zhu et al. (2016) found that transfection of an miR-214 mimic in mouse myofibroblasts decreased the expression of *COL1A1*, and Li et al. (2017) showed miR-214 targeted *COL4A1* as a mechanism to decrease *COL1A1* expression. In fact, our TMT proteomics results (discussed in Chapter 5) found that miR-214 overexpression decreased COL1A1 expression which demonstrates that this reduction in mRNA expression translates to protein expression. MiR-214 regulation of *COL1A1* expression therefore represents an interesting therapeutic target.

We demonstrated that miR-224 overexpression also resulted in a decrease in *IL6* mRNA. We found that miR-224, along with miR-21a and -214, all decreased *IL6* mRNA, but miR-30d did not. Interestingly, miR-21a, -214 and -224 were increased in our ISO infusion model but -30d was not, perhaps indicating a link between this HF model and the upregulation of miRNAs that regulate *IL6*. There are no publications demonstrating a role for miR-224 in regulating *IL6* expression. However, An et al. (2021) demonstrated that IL-6 can induce miR-224 expression and then miR-224 targets and decreases expression of *SMAD4* (a member of the TGF-β signalling pathway) which is interesting because inhibition of *SMAD4* by siRNA reduced IL-6 expression (Yamada et al., 2013). *SMAD4* has been validated as a target of miR-224 by numerous studies and so a potential regulatory axis could exist whereby miR-224 regulates *IL6* through a negative feedback loop (Yao et al., 2010) (Zhang et al., 2013) (Ma et al., 2018).

The present investigation is the first to show that miR-224 decreases the expression of *MMP3*, with a decrease of 88%. The MMP-3 protein (also known as stromelysin-1) is an enzyme that is secreted by CFs and acts by regulating ECM breakdown, specifically of collagen, fibronectin, laminins, proteoglycans, and vitronectin (Visse and Nagase, 2003). This activity means that MMP-3 is implicated in ECM turnover, and MMP-3 activity appears to be particularly important in the chronic phase of remodelling, as Samnegård et al. (2006) demonstrated MMP-3 serum concentration was significantly increased at 3 months post-MI but was low compared to time of admission and 48 hours post-admission. There was a particularly interesting finding by Philippe et al. (2012) that miR-19 directly targets *TLR2* which leads to a decrease in both *IL6* and *MMP3* mRNA in fibroblast-like synoviocytes and TLR2 has been shown to mediate inflammation by responding to the DAMP, HSP70, and inducing cardiac hypertrophy in response to pressure overload (Higashikuni et al., 2013). This is interesting because Li et al. (2020) validated *TLR2* as a direct target of miR-224 and in this same study also showed that *MMP9* expression was reduced via this targeting. This suggests that miR-224 could regulate the expression of both *IL6* and *MMP3* by directly targeting *TLR2* in a response to inflammatory stimuli released in response to cardiac injury.

We have demonstrated that miR-224 overexpression leads to an increase in mRNA expression of *ITGA5*. Integrins are transmembrane cell adhesion molecules that are the principle receptors required by cells for binding to the ECM and bridging this connection to the cytoskeleton (Schwartz, 2010). Integrins have been demonstrated as responders to multiple types of CVD, for example in cardiac hypertrophy (Brancaccio et al., 2006) and in hypertension (Heerkens et al., 2007). The importance of integrins in CFs in inducing cardiac remodelling has also been demonstrated as Hsueh et al. (1998). They found that activation of the integrins αvβ3 by fibronectin and β1 by collagen enhanced MAP kinase activity in rat CFs and that

integrin signalling propogated Ang II signalling to stimulate CF growth. Whereas a miR-224 increase in *ITGA5* has not been observed previously, Chen et al. (2013) did suggest that miR-224 decreased integrin alpha M (ITGAM) by investigating computationally predicted integrin α subunits-targeting miRNAs and we found using the tool miRdb that miR-224 is predicted to bind to ITGA6 and ITGA10. It could be that miR-224 regulates the epigenetics of integrins so that there is a bias towards expression of *ITGA5* and against *ITGAM*, *ITGA6* and *ITGA10* to favour binding of fibronectin (Schumacher et al., 2021).

Finally, as we discuss the effect of miR-30d overexpression, we can see that both *MMP2* and *ITGA5* mRNA were decreased by 45% and 44% respectively, and both of these genes encode for proteins important in the role of CFs and the ECM. Overexpression of MiR-30d has been shown to decrease MMP-2 protein expression in a Ewing's sarcoma (ES) cell line which resulted in suppression of invasion and migration (both behaviours which are exhibited by activated CFs in cardiac remodelling (Ye et al., 2018)) and transfection with a miR-30d mimic in a colorectal cancer (CRC) cell line decreased expression of MMP-2 as well as other Wnt signaling-associated proteins, including; β-catenin, cyclin D1, c-Myc and MMP9 (Yan et al., 2017). It was suggested that this effect on MMP-2 in CRC was due to miR-30d targeting liver receptor homologue-1 (LRH-1). MMP-2 is one of the most researched MMPs in CVD and its role in cardiac dysfunction has been demonstrated in mouse models, including ischemia and reperfusion injury in rats where MMP-2 peaked at 2-3 minutes after reperfusion and induced injury (which is preventable with MMP-2 inhibition) (Cheung et al., 2000). Furthermore, Matsumura et al. (2005) showed that MMP-2-KO mice were protected in a LAD ligation model of MI by preventing cardiac rupture, and reduced macrophage infiltration. This regulation, combined with the fact that miR-30d expression is decreased in the three cardiac dysfunction models performed in the present investigation (ISO infusion, LAD ligation and Ang II infusion), suggests that miR-30d upregulation could be a therapeutic modality in regulating pathological remodelling.

We have demonstrated that miR-30d overexpression decreases expression of *ITGA5* mRNA. This activity of miR-30d has been demonstrated previously in the literature, with Croset et al. (2018) identifying *ITGA5* downregulation after overexpression of the entire miR-30 family in a human breast cancer line but more importantly, by Li et al. (2021) who confirmed by luciferase reporter assay that miR-30d, specifically, directly targeted *ITGA5* in HEK293 cells. In fact, the latter publication demonstrated that miR-30d overexpression in mouse CFs attenuated a TGFβ1 mediated increase in *Itga5*. The functional effect of this targeting in CFs was decreased activation of the TGFβ pathway, decreased proliferation and decreased fibrosis. This highlights an important role for miR-30d in regulating how CFs respond to the ECM and the

pathways it then regulates. More recent work by Hu et al. (2022) found that miR-30d also decreases expression of GALNT2 which subsequently prevents its ability to glycosylate ITGA5 and resulted in similar suppresssion of proliferation, migration, and invasion but also induced apoptosis and cell-cycle arrest. As proliferation, migration and invasion are behaviours that are increased in MyoFbs during cardiac remodelling, this demonstrates that miR-30d regulates gene expression to suppress behaviours that would induce pathological remodelling.

Finally, we saw that inhibition of miR-30d resulted in a decrease in mRNA expression of *ACTA2*, the gene coding for α-SMA. This was a 12% decrease in expression and so it is questionable whether this has biological relevance for either CF behaviour or cardiac remodelling as a whole. *ACTA2* is used as a marker of MyoFb differentiation and upregulation is associated with an increase in the activation of CFs and occurs in response to injury and ther release of proinflammatory cytokines (Bachmann et al., 2022). Very interestingly, the downregulation of *ITGA5* and upregulation of *ACTA2* appear to be related. Shochet et al. (2020) found that silencing of *ITGA5* resulted in an increase in *ACTA2* and differentiation to a MyoFb phenotype and this has led to ITGA5 being considered as a therapeutic target in idiopathic pulmonary fibrosis (IPF). The inhibition of miR-30d leading to a decrease in *ACTA2* could be because its activity in decreasing the expression of *ITGA5* has been lost and this would be suggestive of a role for miR-30d in inducing a MyoFb phenotype in CFs.

We found that the secretion of IL-6 protein was not changed after overexpression or inhibition of any of the four miRNAs. This was despite overexpression of miR-21a, -214 and -224 all decreasing the expression of *IL6* mRNA. The reason for this could be that secreted IL-6 should be measured at a different time point than 72 hours post-transfection or that the post-transcriptional regulation of *IL6* mRNA does not necessarily manifest in an affect on protein translation and/or secretion. In regards to miR-21a specifically, Ge et al. (2020) and Lu et al. (2020) found that miR-21a inhibition reduced IL-6 secretion when challenged with LPS. Similarly, Hu et al. (2018) desmonstrated that miR-214 overexpression increased IL-6 secretion in response to LPS. This finding demonstrates that miRNA induced changes on gene expression do not necessarily reflect in changes in protein expression. Tasaki et al. (2022) developed a model for predicting protein expression based on the transcriptome profile of a cell with the underlying hypothesis that protein expression is not just determined by mRNA expression coding the protein itself but also the entire transcriptomic profile of the tissue. This is particularly relevant for IL-6 as it is a proinflammatory cytokine and its expression after challenge with DAMPs could be regulated differently by miRNAs than its expression at basal levels.

We have discovered for the first time that miR-214 overexpression leads to increased secretion of MMP-2. Although the effect of miR-214 on *MMP2* mRNA and MMP-2 protein expression has been demonstrated, this is the first time that effects on secretion have been detected. This finding, along with the miR-214 mediated increase in *TNC* mRNA expression, demonstrates that miR-214 upregulates the expression of mRNA and/or protein important for ECM regulation. This has functional effects on cell migration and invasion and Zhang et al. (2019) found that inhibiting miR-214 led to a decrease in MMP-2 expression and decreased the viability, migration and invasion of cells in triple negative breast cancer. The mechanism for this upregulation was elucidated then by Wang et al. (2015) who found that miR-214 increased MMP-2 expression by targeting the tumour suppressor protein, p53, in breast cancer and interestingly we found in our TMT proteomics screen that miR-214 overexpresssion decreased the protein, TP53 regulated inhibitor of apoptosis 1 (TRIAP1), which is dependent upon p53 activity. The activity of miR-214 has been implicated in migration and invasion extensively in cancer (Yang et al., 2013) and because cardiac injury increases migration and invasion in CFs and MyoFbs, this provides support for a role of miR-214 in inducing these activities through its epigenetic regulation (Souders et al., 2009b).

In summary, transfections have allowed us to artificially increase or inhibit endogenous miRNAs to explore the role that each plays in the regulation of gene expression and protein expression and secretion, relevant to cardiac remodelling. We have found a variety of changes induced, with each miRNA regulating expression of different targets. MiR-21a regulated the expression of the IL6 family, by decreasing expression of *IL6* and *IL6R* mRNA and increasing expression of *IL11*, with no effect on IL-6 secretion and miR-224 decreased expression of *IL6* mRNA and the ECM protein *MMP3* whilst increasing mRNA expression of the ECM binding integrin, *ITGA5*. The most interesting findings involved miR-214 and miR-30d which regulated expression of ECM or ECM-related genes in opposing directions. MiR-214 increased the expression of *TNC* and increased secretion of MMP-2 whereas miR-30d decreased the expression of *MMP2* and *ITGA5*. As neither of these miRNAs are well understood in CVD, they were selected for further investigation. The following chapter (Chapter 5) describes a TMT proteomics driven approach to identify the effect of miR-214 or miR-30d overexpression on cellular protein expression.

Chapter 5 A proteomics approach to identify targets of miR-214 and miR-30d in human cardiac fibroblasts

5.1 Introduction

In the previous chapters miR-21a, -214, -224 and -30d were investigated regarding their regulation of the known genes, proteins, and behaviours relevant to CFs during cardiac remodelling. To investigate the novel and unknown regulatory behaviours of these miRNAs, a proteomics screening-based approach was taken. Due to financial and time constraints, only two of the candidate miRNAs were selected for the screen. These miRNAs were miR-214-3p and miR-30d-5p, where their overexpression through transfection with pre-miRs was compared to transfection with pre-miR-NC (negative control). Following this screening, multiple bioinformatics tools were used to analyse the dataset and the findings, and this was combined with what is known in the literature regarding CFs in cardiac remodelling, to identify important and interesting targets to validate at mRNA and protein expression levels, and importantly at a functional level.

MiR-214 and miR-30d were chosen as candidate miRNAs because they represented pathologically relevant miRNAs (in CVD) of which there is not yet a clear consensus in the literature as to their roles. Any findings about the targets by which they may act and the subsequent pathways that they modulate could hold the potential for therapeutic applications in treating CVD. These miRNAs were also chosen since they were modulated in opposing directions in the ISO infusion model of cardiac dysfunction performed by Bageghni et al. (2018). Firstly, miR-214, which was increased following ISO infusion, has been investigated in multiple publications allied to CVD. In a literature analysis of miR-214 it was found that it is both increased and decreased in *in vivo* and *in vitro* models of cardiac dysfunction, specifically in CFs. For example, Sun et al. (2015) found that in a rat model of ISO induced cardiac dysfunction, miR-214 was upregulated in both fibrotic heart tissue and in cultured CFs, and downregulation of miR-214 with antagonists attenuated both CF proliferation and collagen synthesis. The authors discovered through bioinformatics analysis and luciferase reporter assays that miR-214 bound to the mRNA encoding MFN2, a critical regulator of proliferation and fibrosis. They also found that downregulating miR-214 led to inhibition of ERK1/2 MAPK signalling which is otherwise increased by ISO treatment. Conversely, Yang et al. (2019) found that miR-214$^{flox/flox}$/FSP1-cre mice (fibroblast-specific miR-214 KO mice) demonstrated aggravated cardiac fibrosis in a transverse aortic constriction (TAC) model of pressure overload-induced cardiac hypertrophy and heart failure. Similarly, the authors also found that murine myofibroblasts treated with TGFβ-1 had a downregulation of miR-214. Pivotally, Yang et al. (2019) suggest that miR-214 is a repressor of CF proliferation and FMT by targeting

NOD-like receptor family CARD domain containing 5 (NLRC5). These conflicting conclusions on the role of miR-214 in the context of CF behaviour, relevant to cardiac remodelling therefore poses miR-214 as an important miRNA for further research to clarify its role in this area. This research particularly addresses this importance for human disease as previous published research to date has only looked at animal models and cell lines, whereas this project looked at human primary cells.

Conversely, relatively little is known about the role of miR-30d, especially in CFs. The research by Bageghni et al. (2018) indicates that lower levels of miR-30d may be important in cardiac dysfunction, whether this just be a correlation or with a mechanistic underpinning. One important recent publication however by Li et al. (2021) found that miR-30d appears to play a cardioprotective role in MI and ischemia-reperfusion (I/R). MiR-30d overexpression, in mouse models of ischemic HF, was shown to ameliorate CM apoptosis and myocardial fibrosis and improve cardiac function whereas loss of function mouse models showed the opposite, with pathological left ventricular remodelling, fibrosis and CM death. Interestingly, miR-30d appears to play two distinct roles depending on its cellular context (i.e. CMs or CFs). Hypoxic stress selectively enriched miR-30d in CMs, where it was acutely protective by targeting mitogen-associated protein kinase kinase kinase kinase 4 (MAP4K4) to inhibit apoptosis. MiR-30d is also however secreted in EVs by CMs and inhibits CF proliferation and activation by directly targeting integrin α5 (ITGA5) via paracrine signalling. To summarise, this research found that lower expression of miR-30d (both in the heart and EVs) in the chronic phase of ischemic remodelling is associated with adverse remodelling.

Proteomics screening of transfected samples was performed by TMT proteomics. This technology utilises amine-specific isobaric tags to label peptides and then measure any upregulation or downregulation of protein expression (relative to pre-miR-NC transfection) by acidic RP nano-LC MSMS. STRING and IPA analysis was vital in predicting the pathways modulated by each miRNA by assessing for shared connections between the specific proteins changed by each miRNA. This screening led to theoretical analysis of the pathways that could be modulated by miR-30d and how they are relevant to cardiac remodelling based on previous investigations by other groups. For miR-214, interesting predictions were generated concerning mitochondrial dysfunction, ECM organisation and regulation of the expression of PIEZO1, a mechanosensitive cation channel expressed in CF (Blythe et al., 2019) and implicated in CVD (Beech and Kalli, 2019) (Stewart and Turner, 2021). PIEZO1 has been identified as an important ion channel in CVD and Bartoli et al. (2022) recently showed that a gain of function mutation of PIEZO1 in mice resulted in cardiac hypertrophy and cardiac fibrosis, the two main presentations of cardiac remodelling. Moreso, they found that PIEZO1 overexpression in CFs resulted in increased calcium entry in response to the PIEZO1 agonist,

YODA1. Blythe et al. (2019) had previously drawn a connection between PIEZO1 and release of the profibrotic cytokine, IL-6 in human and mouse CF. This work demonstrated that IL-6 mRNA expression and secretion is increased by PIEZO1 activation, via p38α MAPK activation. These investigations clarify PIEZO1 as an important mediator of cardiac remodelling by influencing CF behaviour. This screening has therefore led to a two-pronged approach, investigating that which is known to be important in CVD and that which was not.

5.2 Aims

The main aims of this chapter were:

- Perform a tandem mass tagging proteomics screen of human cardiac fibroblasts transfected with pre-miR-214 or pre-miR-30d;
- Utilise the findings of the proteomics screen to validate our cultured human cells as fibroblast populations;
- Analyse the shared networks that exist in CFs overexpressing miR-214 or miR-30d;
- Investigate the effect of miR-214 overexpression on mitochondrial activity;
- Investigate the effect of miR-214 on LOX mRNA and protein expression and enzymatic activity and determine whether an axis linked to MFN2 exists;
- Investigate the effect of miR-214 on PIEZO1 mRNA expression and function.

5.3 Methods

5.3.1 Generic methods

Human CFs were isolated from RAA biopsies as described in Section 2.2 and were transfected with pre-miRNA and anti-miRNA as described in Section 2.8. Protein lysates were obtained, and TMT proteomics (including analysis) performed as described in Section 2.13. RNA was isolated as described in Section 2.3 and mRNA levels quantified by qRT-PCR as described in Section 2.6. Protein lysates were obtained, and western blotting performed as described in Section 2.12. The citrate synthase assay was undertaken as described in Section 2.14, and the Flex station assay for the measurement of intracellular calcium signalling performed as described in Section 2.16.

5.4 Results

5.4.1 Assessing the levels of cell-type specific markers in cultured human cardiac fibroblasts

A large-scale proteomics screen was performed to measure the effect of miR-214 and miR-30d on all cellular protein expression in human CFs. The purpose of this was to identify any direct or indirect targets that each miRNA is modulating at the protein level. Human CFs from

6 patients were transfected with pre-miR-NC (negative control), -214 and -30d and protein was isolated after 72 hours of incubation before analysis by TMT proteomics. The TMT proteomics screen identified over 8,500 proteins. The expression levels of cell-type specific markers were evaluated to assess the homogeneity of the population of human CFs from the 6 different donors. The cultures were negative for markers of ECs (platelet endothelial cell adhesion molecule-1; PECAM-1/CD31), CMs (myosin heavy chain 6; MYH6/α-MHC) and SMCs (myosin heavy chain 11; MYH11) (Table 5.1). Finally, ACTA2 (α-SMC) was identified in our cultures which is a marker for MyoFbs or SMCs. However, as the SMC marker MYH11 was undetectable, this most likely indicates the presence of MyoFbs. A range of fibroblast-specific markers were also investigated which were all readily detectable, including discoidin domain receptor tyrosine kinase 2 (DDR2), platelet derived growth factor receptor alpha (PDGFRA), S100 calcium binding protein A4 (S100A4) and Thy-1 membrane glycoprotein (THY1 / CD90) which was increased by a LogFC of 0.52 by pre-miR-214 transfection. Three collagen types were also assessed, each of which were detectable and conversely modulated by miR-214 and miR-30d. Both alpha 1 and 2 chains of collagen 1 (COL1A1 and COL1A2) and alpha 1 of collagen 3 (COL3A1) were decreased by miR-214 and increased by miR-30d. We previously found that miR-214 overexpression resulted in decreased expression of *COL1A1* (Figure 4.20). Both of these analyses demonstrate that there is a strong regulation of ECM proteins by miR-214 and its activity in this regulation should be explored further. Thus, the data within the proteomics screen established that our cultures are composed of human CFs and not contaminated by other cardiac cell types such as ECs, CMs or SMCs.

Cell-type	Marker Protein	Mean Normalised abundance (and SEM)	Pre-miR-214 LogFC	Pre-miR-30d transfection
Endothelial cells	PECAM1 (Platelet endothelial cell adhesion molecule-1)	Undetectable		
Cardiomyocytes	MYH6 (Myosin Heavy Chain 6 / Alpha-Myosin Heavy Chain)	Undetectable		
Smooth muscle cells	MYH11 (Myosin Heavy Chain 11 / Smooth Muscle Myosin Heavy Chain)	Undetectable		
Smooth muscle cells/myofibroblasts	ACTA2 (smooth muscle alpha (α)-2 actin)	88.5	No change	No change
Fibroblasts	DDR2 (Discoidin Domain Receptor Tyrosine Kinase 2)	1303.7	No change	No change
	PDGFRA (Platelet Derived Growth Factor Receptor Alpha)	2176.3	No change	No change
	S100A4 (S100 Calcium Binding Protein A4)	3140.4	No change	No change
	THY1 (Thy-1 membrane glycoprotein)	465.7	0.52	No change
	COL1A1 (Collagen, type I, alpha I)	126	-1.01	0.80

	COL1A2 (Collagen, type I, alpha II)	231.2	-0.28	0.71
	COL3A1 (Collagen, type III, alpha I)	8409.7	-0.49	0.32

Table 5.1 Identification of cardiac cell specific markers in our tandem mass tagging screen of human cardiac fibroblasts. The scaled abundance values for cell-type markers of endothelial cells, cardiomyocytes, smooth muscle cells, myofibroblasts and fibroblasts were measured in human cardiac fibroblasts from 6 donors, as well as any Log fold-changes (LogFC) mediated by transfection with pre-miR-214 or pre-miR-30d for 72 h.

5.4.2 Investigating the effect of pre-miR-214 and pre-miR-30d on protein expression in human cardiac fibroblasts using tandem mass tagging proteomics

Amine-specific isobaric tags labelling peptides were measured to investigate the abundance of specific proteins. The LogFC of each protein was calculated between pre-miR-NC (negative control) and pre-miR-214 or pre-miR-30d transfected human CFs. A total of 8,792 proteins were investigated as being at detectable levels. For pre-miR-214, 4,162 proteins were significantly different to the pre-miR-NC transfection ($P<0.05$) (Figure 5.1). Of these, 3,387 proteins passed the false discovery rate (FDR); 2,058 proteins were significantly increased and 2,226 were significantly decreased by pre-miR-214. For pre-miR-30d, 3,622 proteins were significantly different to the pre-miR-NC transfection (Figure 5.2). Of these, 2,534 proteins passed the FDR; 1,784 proteins were significantly increased and 1,838 were significantly decreased by pre-miR-30d transfection.

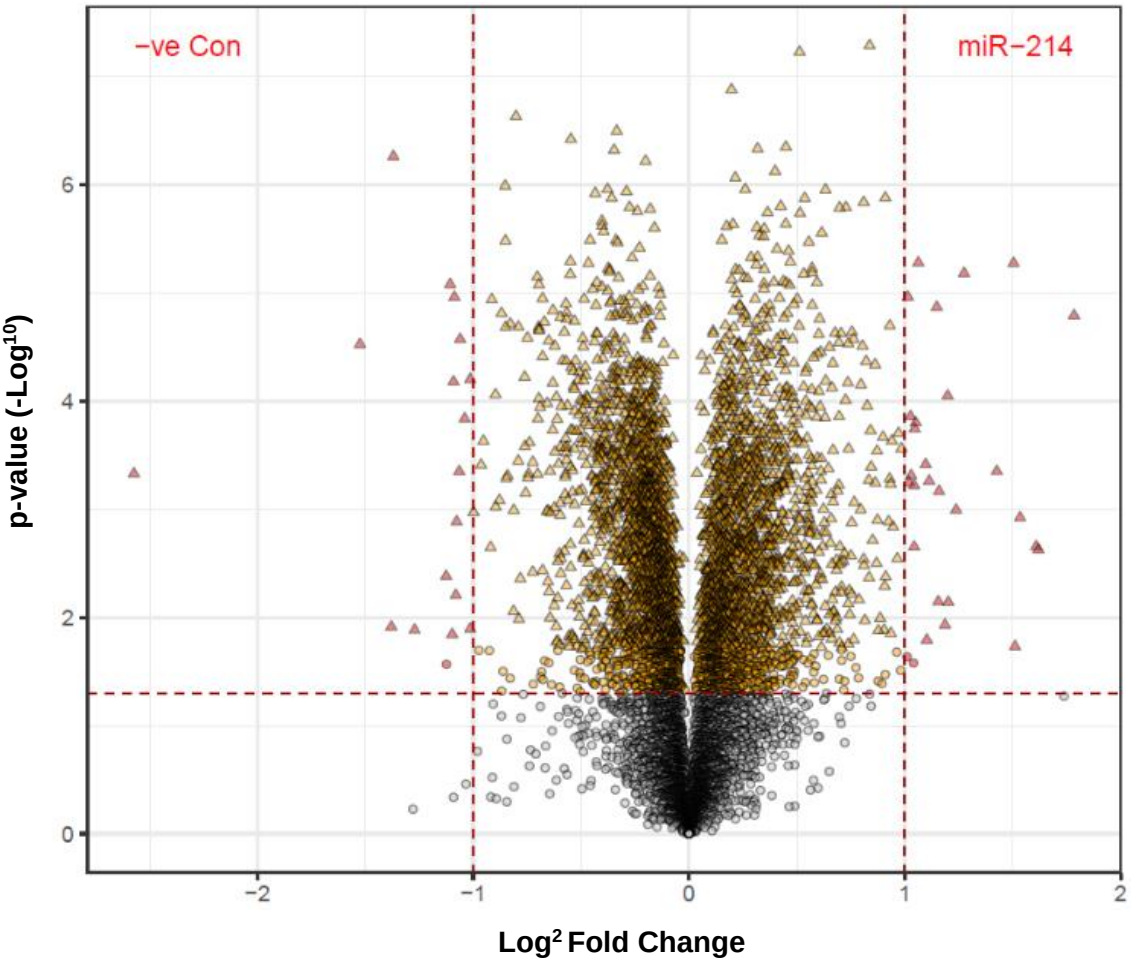

Figure 5.1 Volcano plot showing protein expression LogFC in pre-miR-214 transfected human cardiac fibroblasts. 8,792 proteins were measured at detectable levels in human cardiac fibroblasts cultured from 6 donors and the LogFC between pre-miR-NC and pre-miR-214 transfected cells is displayed here as Log^2 fold. Significance of difference in protein expression plotted by the log^{10} of p-value. Key: grey = NS, yellow = P<0.05, pink = P<0.05 and >1LogFC, circle = FDR fail and triangle = FDR pass.

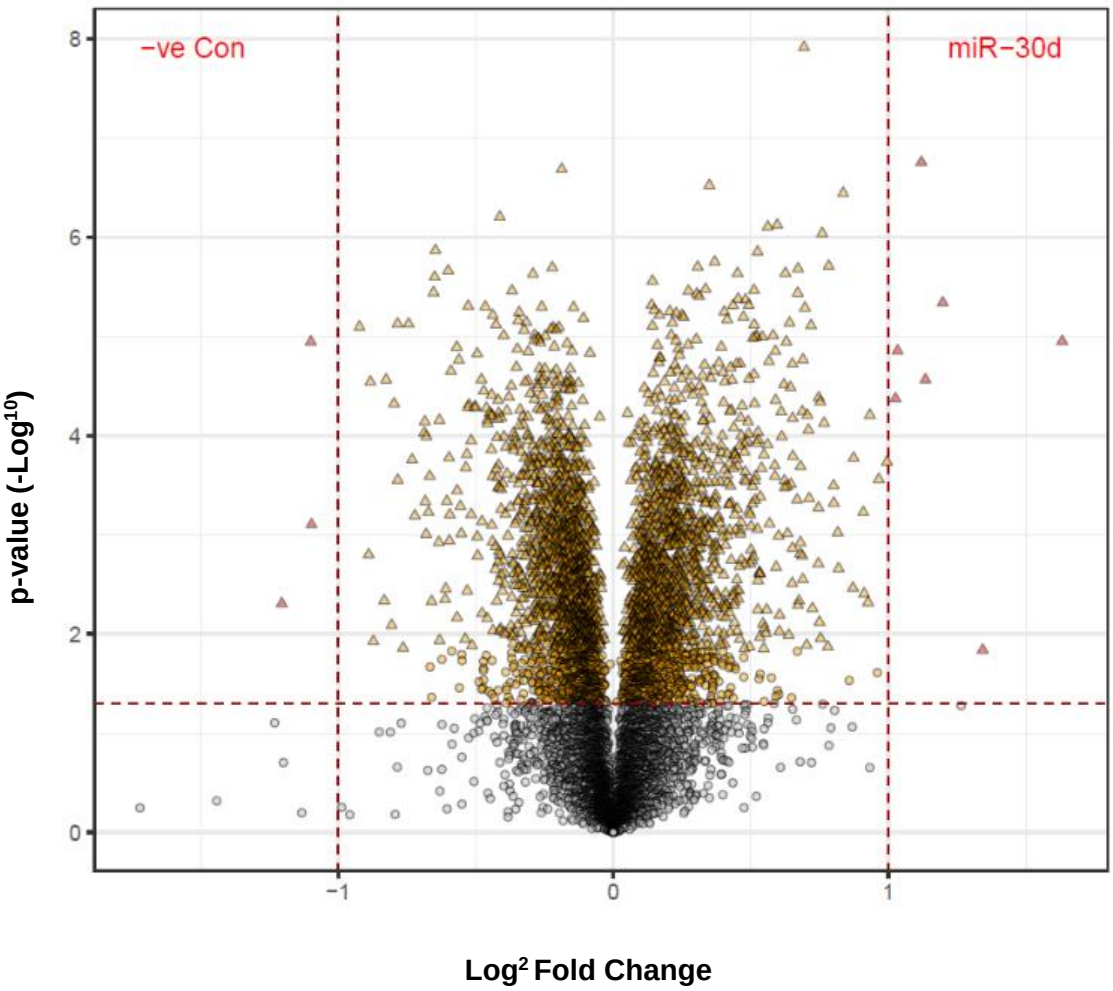

Figure 5.2 Volcano plot showing protein expression LogFC in pre-miR-30d transfected human cardiac fibroblasts. 8,792 proteins were measured at detectable levels in n=6 human cardiac fibroblasts (CFs) and the LogFC between pre-miR-NC and pre-miR-30d transfected cells is displayed here as Log^2 fold. Significance of difference in protein expression plotted by the log^{10} of p-value. Group sizes; n=6. Key: grey = NS, yellow = P<0.05, pink = P<0.05 and >1LogFC, circle = FDR fail and triangle = FDR pass.

The difference between the modulation of protein expression by pre-miR-214 or pre-miR-30d transfection (compared to pre-miR-NC transfection) was assessed by investigating the LogFC of the 15 most increased and the 15 most decreased proteins by each pre-miR transfection, relative to pre-miR-NC transfection. This data was displayed as heat maps in Figure 5.3 and Figure 5.4 for pre-miR-214 and pre-miR-30d transfection respectively. The heat map displays a colour range for the level of protein expression in each of the 6 patients investigated, for either pre-miR-214 or -30d transfection. Each miRNA regulates their own pattern of protein expression by inhibiting their own direct targets and affecting the expression of the targets they indirectly affect. For this reason, there are some proteins that have similar changes for both miRNAs, some that are unchanged by both and some that change conversely. For this reason, the right-hand side of the heat maps (Figures 5.3 and 5.4) are mixed in the colours rather than the uniformity seen on the left-hand side.

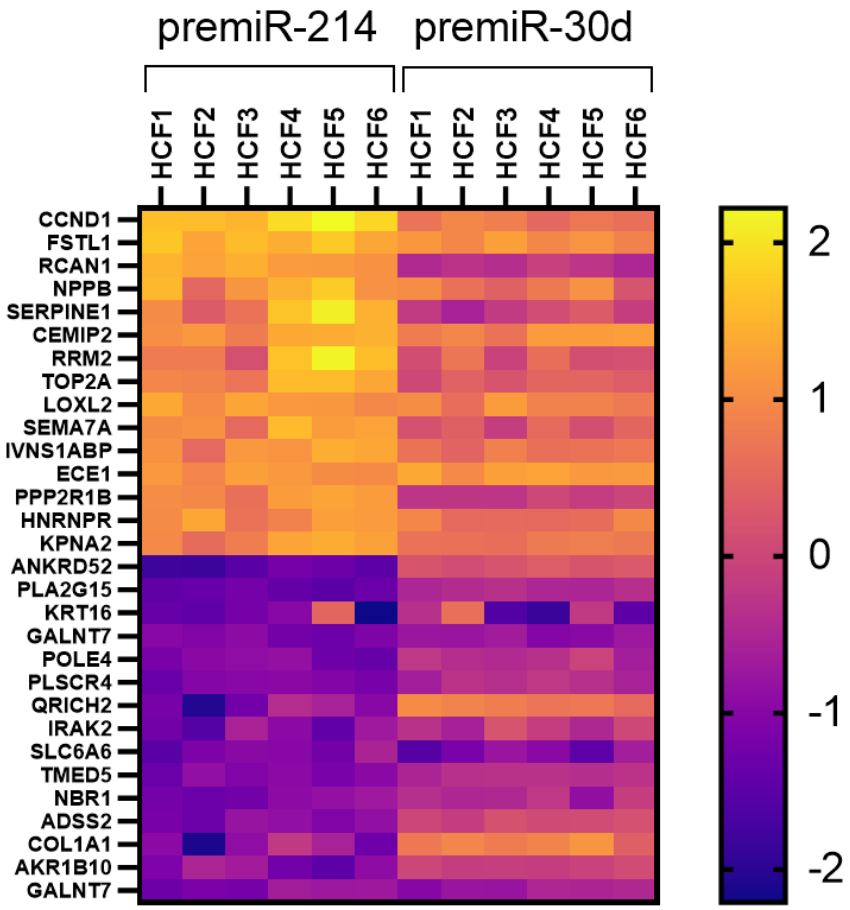

Figure 5.3 The top 15 most increased and decreased proteins by pre-miR-214 transfection in human cardiac fibroblasts. The log fold change (LogFC) is displayed as a colour code from yellow (largest increase) to dark blue (largest decrease) for each human CF patient (HCF1-HCF6) following pre-miR-214 or pre-miR-30d transfection. The proteins selected were the top 15 most increased and top 15 most decreased proteins by pre-miR-214 transfection.

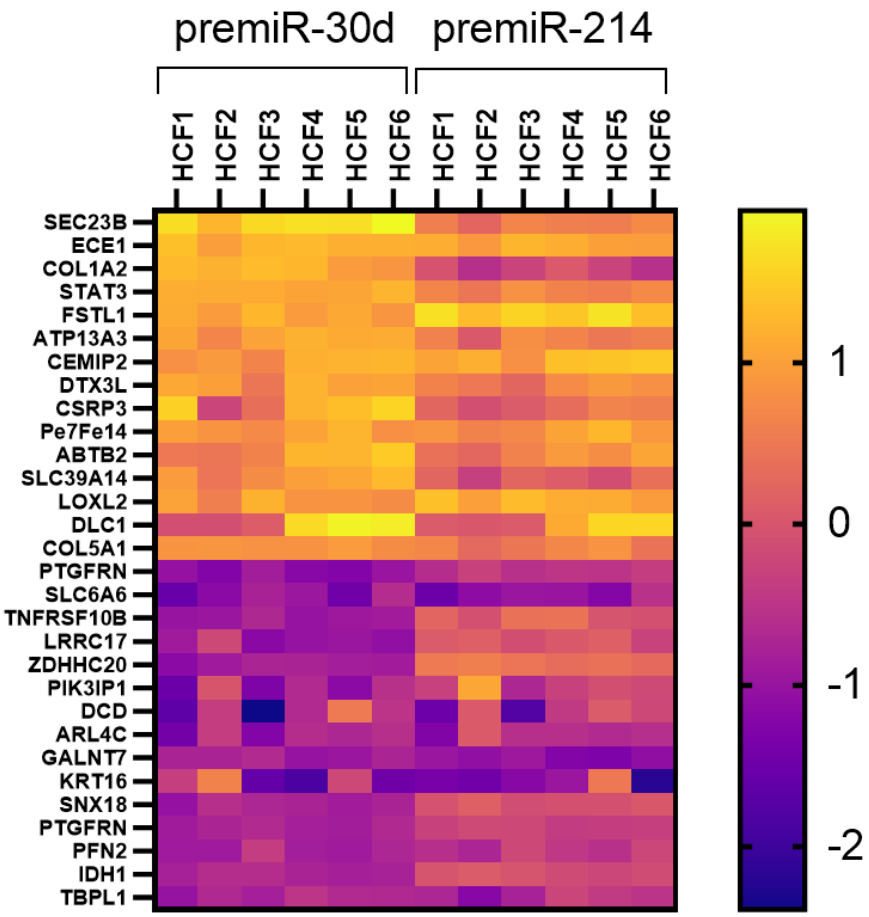

Figure 5.4 The top 15 most increased and decreased proteins by pre-miR-30d transfection in human cardiac fibroblasts. The log fold change (LogFC) is displayed for each human CF patient for pre-miR-214 or pre-miR-30d transfection, with the proteins selected being the top 15 most increased and top 15 most decreased proteins by pre-miR-30d transfection. Group sizes; n=6.

5.4.3 STRING functional analysis of pre-miR-214 or pre-miR-30d modulated protein expression in human cardiac fibroblasts

Using the data from the TMT proteomics screen, the effect of pre-miR-214 on canonical pathways was predicted through functional analysis, predicted by STRING. STRING is a freely available, online database that makes predictions on shared protein to protein interactions. By entering a list of proteins, STRING will draw interactions between known interactive proteins and compile a list of canonical pathways that those proteins are likely to be shared members of. One of the limitations is that LogFC is not considered, however this can generate different lists of canonical pathways to resources like IPA and therefore represents another useful way of analysing large proteomics datasets. Due to this being a large dataset of >8000 proteins and STRING being limited to analysis of 2000 proteins, for the analysis to cover the most interesting and important findings, the largest changes mediated by each miRNA (measured by LogFC) and the most reproducible changes (measured by P value) were both investigated. Any analysis of the most “significantly” modulated proteins therefore refers to most statistically significant (by P value). The first analysis was performed by entering the 100, 50 and 30 most modulated proteins by LogFC (both increased and decreased) by pre-miR-214 transfection, shown in Figure 5.5. For these proteins, the most shared networks exist between COL1A1, MMP-1, LOXL2, LOXL3, LOXL4, MAPK3 and cyclin D1 (CCND1). The next STRING analysis then looked for shared networks between the 100, 50 and 30 most significantly modulated proteins by P value (both increased and decreased) (Figure 5.6). The proteins with the most shared networks in this analysis were tight junction protein-1 (TJP1), catenin alpha-1 (CTNNA1), pyruvate dehydrogenase kinase 1 (PDK1) and MAPK10. Finally, STRING analysis was performed on the 50 most significantly modulated proteins, 50 most increased proteins and 50 most decreased proteins for pre-miR-214 transfection by removing any disconnected nodes and highlighting the most significant predicted canonical pathways (Figure 5.7). For the 50 most significantly modulated proteins, the most significant canonical pathway was “acetylation”. For the 50 most significantly increased proteins, no prediction could be made on a shared pathway. For the 50 most significantly decreased proteins, the most significant canonical pathways were “ECM organisation”, “protein lysine 6 oxidase activity” and “peptidyl lysine oxidation”.

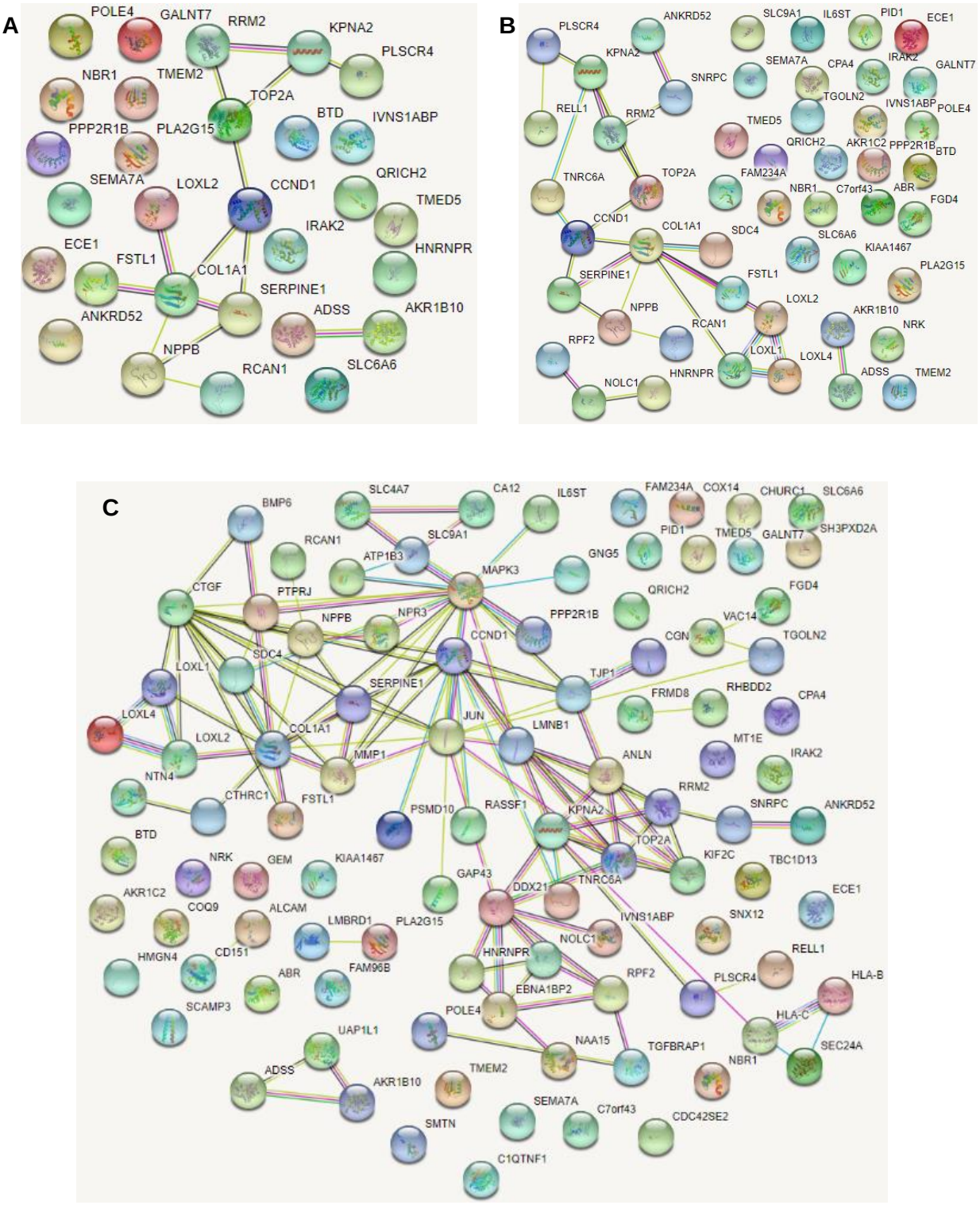

Figure 5.5 STRING predictive analysis of shared networks between the most increased and decreased proteins by miR-214. The 30 **(A)**, 50 **(B)** and 100 **(C)** most increased and decreased proteins (by fold change) in pre-miR-214 transfected samples were inputted for STRING analysis and shared networks that exist between these proteins are presented for each analysis.

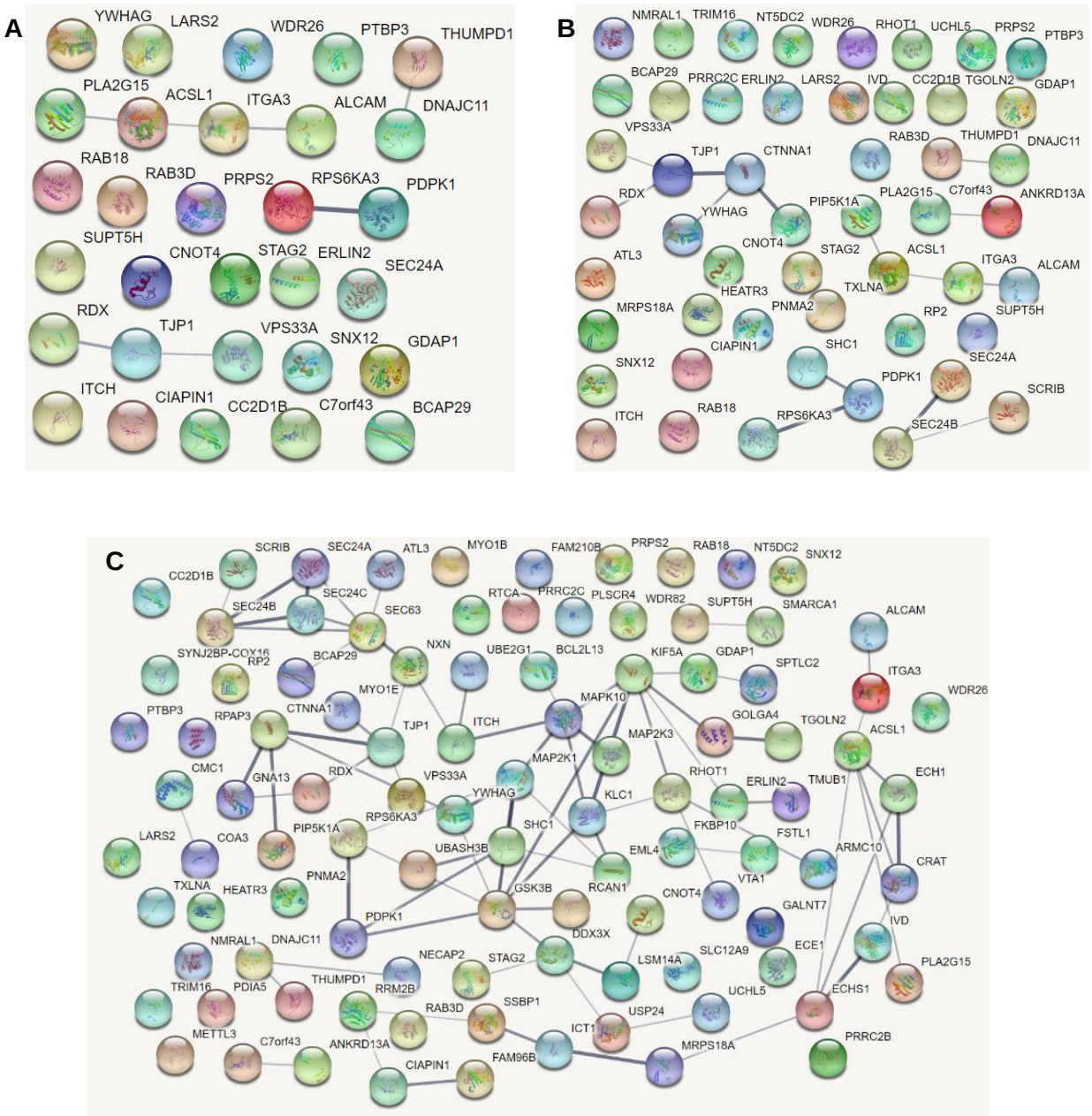

Figure 5.6 STRING predictive analysis of shared networks between the most statistically significantly modulated proteins by miR-214. The 30 **(A)**, 50 **(B)** and 100 **(C)** most significantly modulated proteins (by P value) in pre-miR-214 transfected samples were inputted for STRING analysis and shared networks that exist between these proteins are presented for each analysis.

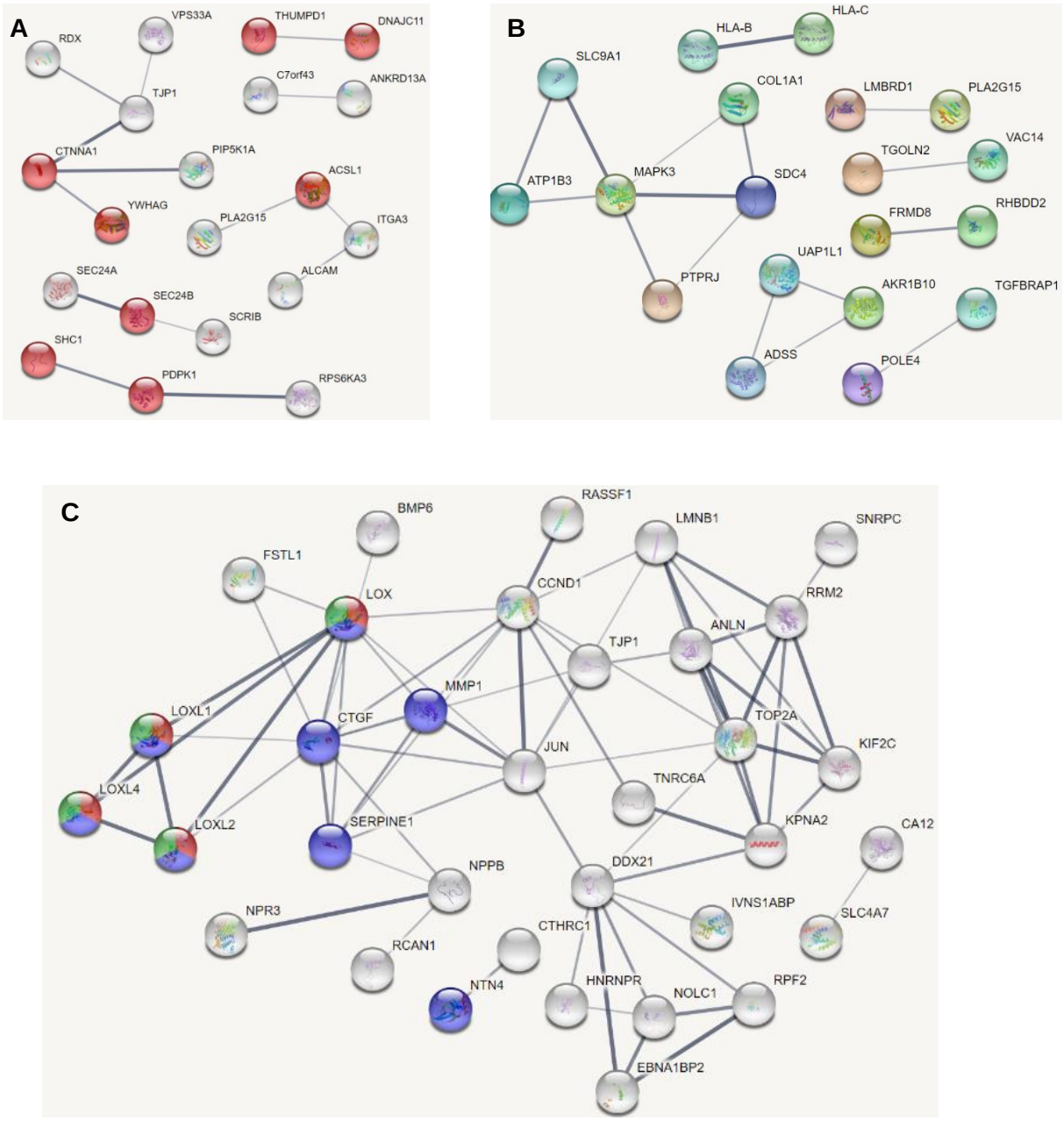

Figure 5.7 STRING predictive analysis of shared networks between the 50 most: significantly modulated proteins, increased proteins, and decreased proteins by miR-214. The 50 most significantly modulated proteins (by P value), most increased proteins and most decreased proteins (by fold change) in pre-miR-214 transfected samples were inputted for STRING analysis and any disconnected nodes were eliminated. The most enriched pathway for significantly changed proteins **(A)** was “acetylation” (red), there was no enriched pathways for decreased proteins **(B)** and the most enriched pathways for increased proteins **(C)** were “ECM organisation” (blue), “protein lysine 6 oxidase activity” (green) and “peptidyl lysine oxidation” (red).

For pre-miR-30d transfection, the first analysis on the 100, 50 and 30 most modulated proteins by LogFC (both increased and decreased) is shown in Figure 5.8. The proteins with the most shared networks in this analysis included COL5A1, COL1A1, COL1A2, CCND1, signal transducer and activator of transcription 3 (STAT3) and bone morphogenetic protein 6 (BMP6). The next STRING analysis then looked for shared networks between the 100, 50 and 30 most significantly modulated proteins by P value (both increased and decreased) (Figure 5.9). The proteins with the most shared networks in this analysis were STAT3, caspase 1 (CASP1) and protein transport protein Sec24A (SEC24A). Finally, STRING analysis was performed on the 50 most significantly modulated proteins, 50 most increased proteins and 50 most decreased proteins for pre-miR-30d transfection by removing any disconnected nodes and highlighting the most significant predicted canonical pathways (Figure 5.10). For the 50 most significantly modulated proteins, the most significant canonical pathway was “protein binding”. For the 50 most significantly increased proteins, no prediction could be made on a shared pathway. For the 50 most significantly decreased proteins, the most significant canonical pathways were “platelet derived growth factor binding”.

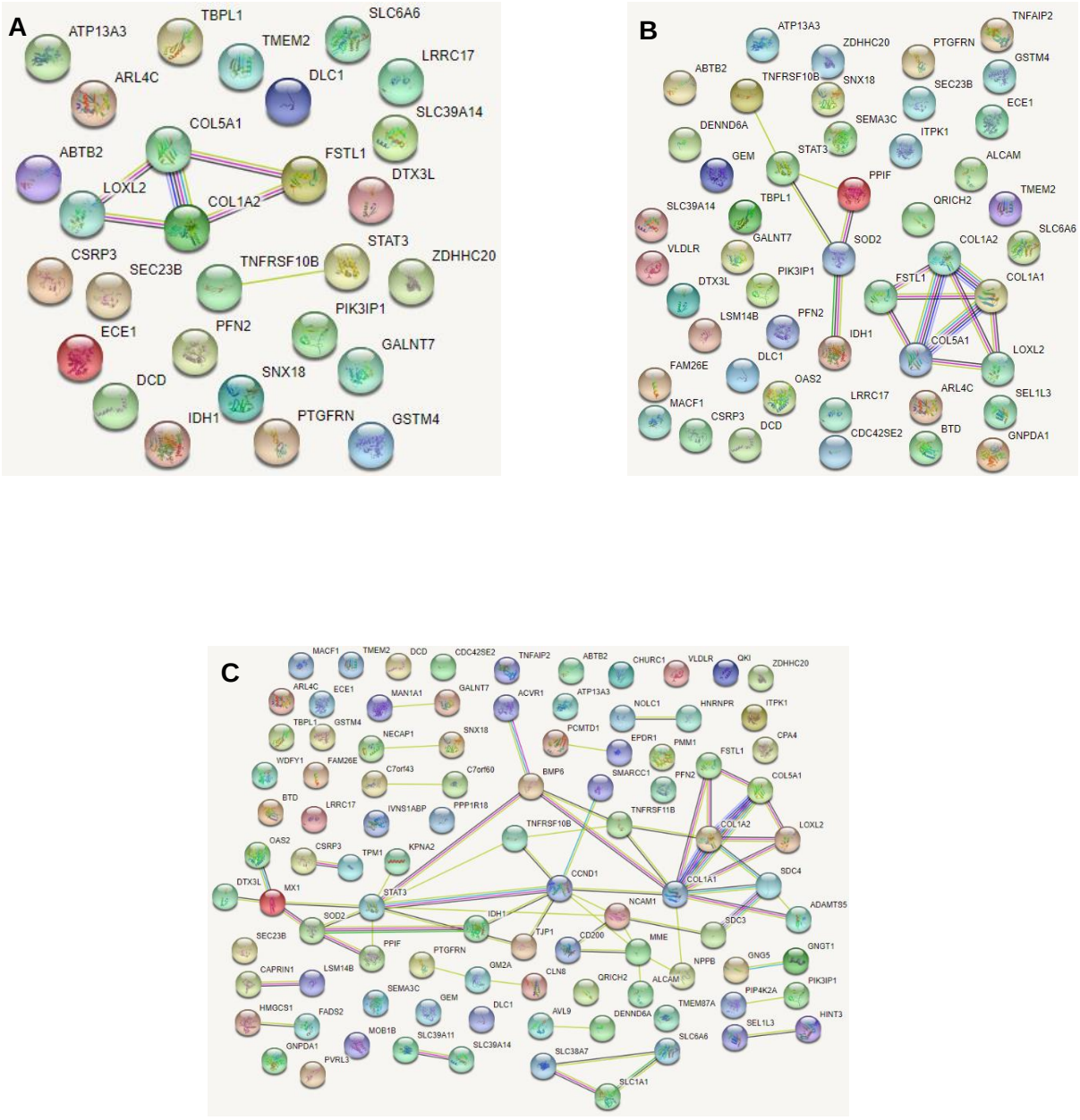

Figure 5.8 STRING predictive analysis of shared networks between the most increased and decreased proteins by miR-30d. The 30 **(A)**, 50 **(B)** and 100 **(C)** significantly most increased and decreased proteins (by fold change) in pre-miR-30d transfected samples were inputted for STRING analysis and shared networks that exist between these proteins are presented for each analysis.

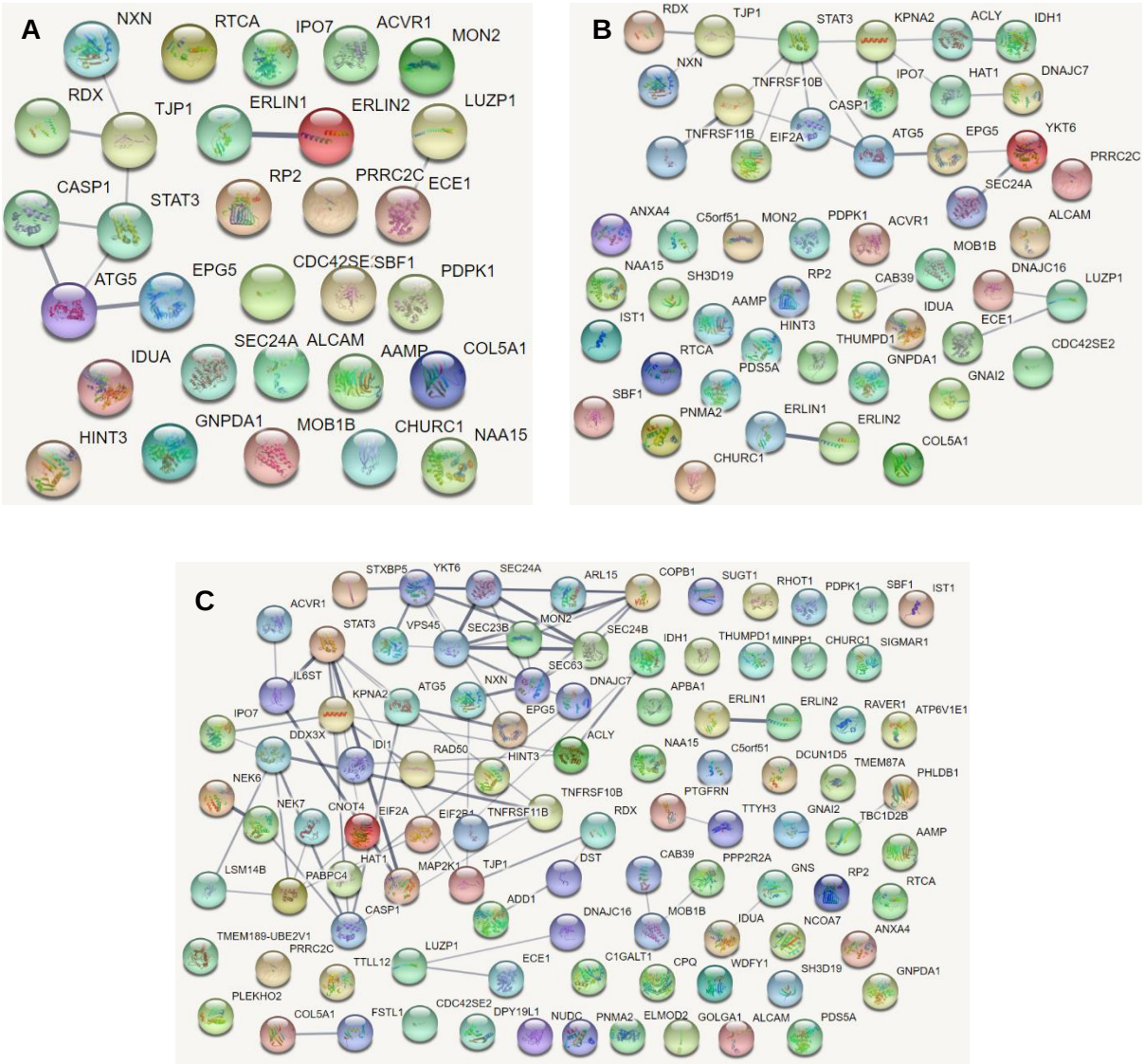

Figure 5.9 STRING predictive analysis of shared networks between the most statistically significantly modulated proteins by miR-30d. The 30 **(A)**, 50 **(B)** and 100 **(C)** most significantly modulated proteins (by P value) in pre-miR-30d transfected samples were inputted for STRING analysis and shared networks that exist between these proteins are presented for each analysis.

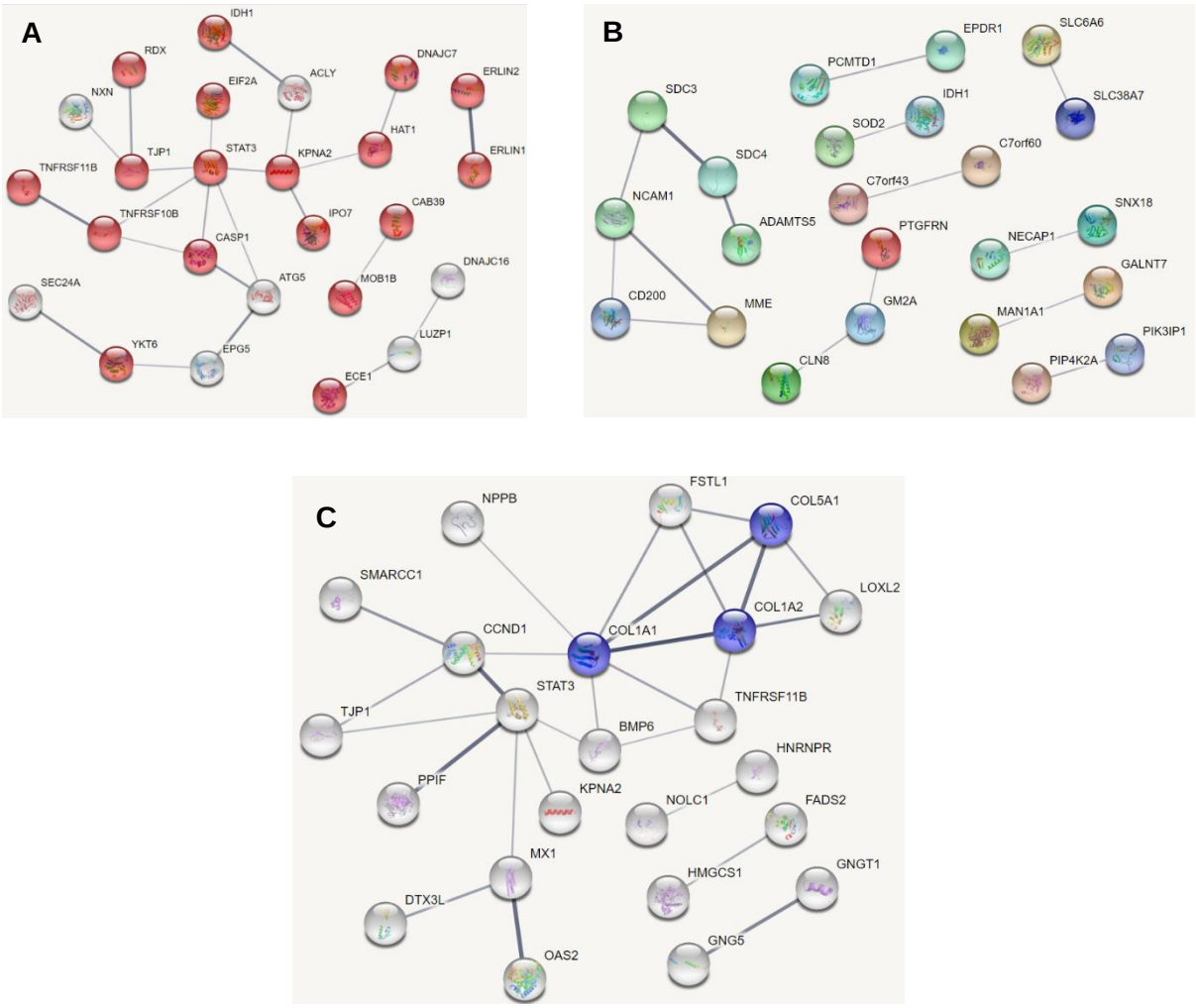

Figure 5.10 STRING predictive analysis of shared networks between the 50 most: significantly modulated proteins, increased proteins, and decreased proteins by miR-30d. The 50 most significantly modulated proteins (by P value), most increased proteins and most decreased proteins (by fold change) in pre-miR-30d transfected samples were inputted for STRING analysis and any disconnected nodes were eliminated. The most enriched pathway for significantly changed proteins **(A)** was “protein binding” (red), there was no enriched pathways for decreased proteins **(B)** and the most enriched pathways for increased proteins **(C)** was “platelet derived growth factor binding” (blue).

5.4.4 Ingenuity pathway analysis of pre-miR-214 or pre-miR-30d modulated protein expression in human cardiac fibroblasts

The next bioinformatics analysis performed on the proteomics dataset was Ingenuity Pathway Analysis (IPA). IPA is a licensed software, unlike STRING, and the major benefit of it is that it processes the LogFC of each protein in a list, as well as the directional change of those proteins. This means that whereas STRING might suggest a pathway in which all the listed proteins would normally be increased, IPA would consider that some may be decreased and predicts pathways with greater statistical strength. IPA also generates graphical figures containing each protein within a pathway and a colour code indicating whether proteins are increased, decreased, or predicted to be inhibited or activated, something that will be covered in this section. IPA was performed to analyse the LogFC values of each protein and make predictions on the canonical pathways affected by each pre-miR transfection.

Firstly, IPA was used to analyse all proteins that were significantly modulated (by P value) by pre-miR-214 transfection (Figure 5.11). Of the canonical pathways predicted to be modulated, there were 27 with a -log(p-value) >10 and 8 with a -log(p-value) >15. The most significant of these pathways was “mitochondrial dysfunction” and interestingly, there were other pathways that are comprised of mitochondrial proteins such as “oxidative phosphorylation”, “sirtuin signalling pathway” and “Huntington’s disease signalling” and these pathways likely occurred due to many mitochondrial proteins being affected by miR-214. There were also other pathways that are important to CVD and CF behaviour that were identified including “autophagy” and “AMPK signalling”. Some other pathways that occurred appeared less relevant to CFs or even the heart, including “estrogen receptor signalling” and “CLEAR signalling pathway”.

The next IPA analysis of pre-miR-214 transfection involved analysing all decreased proteins or all increased proteins (by fold-change) by pre-miR-214 transfection (Figure 5.12). There were 10 canonical pathways for each of the decreased proteins and the increased proteins analysis, with a -log(p-value) >6. For the significantly decreased proteins, the most significant pathway again was “mitochondrial dysfunction” and both “oxidative phosphorylation” and “autophagy” was also predicted. "Insulin receptor signalling” was also predicted which could be important as CFs can respond to insulin and subsequently modulates their function (Levick and Widiapradja, 2020). There was a larger amount of seemingly non-relevant pathways implicated in this method of analysis however, including “synaptogenesis signalling pathway”, “amyloid processing”, “CLEAR signalling pathway”, “melatonin signalling”, “estrogen receptor signalling” and “synaptic long term potentiation”. As these pathways are largely neuronal in their activity, this could be an argument that simply analysing increased or decreased proteins,

and not taking into account which are most statistically significant, can produce non-specific results. The proteins implicated in these pathways may be modulated, but their relevance to CF behaviour is likely lacking. For the significantly increased proteins, the most significant pathways appeared to show no relevance to CFs or cardiac remodelling and included pathways such as “ephrin B signalling”, “molecular mechanisms of cancer” and “colorectal cancer metastasis signalling”. This lack of specificity to CVD could point to the downregulation of pathways by miR-214 for CF regulation which is not surprising considering that miRNAs act directly by preventing protein translation.

The most significantly predicted affected pathway, “mitochondrial dysfunction”, is shown in Figure 5.13. All the proteins that make up this pathway, including all the proteins that make up oxidative phosphorylation and the electron transport chain (ETC) are displayed here. It is most noticeable, that most of the proteins in this pathway are decreased by miR-214. Any proteins that are not decreased by miR-214 are simply because they are not present in our proteomics screen however due to the action of miR-214 on other proteins, they are predicted to be inhibited. MiR-214 is seen to be decreasing proteins in all four of the complexes of the ETC which would have large implications for the generation of adenosine triphosphate (ATP), the hydrolysis of which is required for many cellular processes. Some of the most noticeable decreases mediated by miR-214 in this pathway are decreases in the NADH-ubiquinone oxidoreductase proteins (NDUFs) which make up a large part of complex I of the ETC. In fact, this decrease of almost all the proteins in each complex continues and in complex II, all four of the succinate dehydrogenase (SDH) proteins that make up this complex (SDHA, B, C and D) are decreased by miR-214. MiR-214 therefore shows marked dysregulation and decreases in almost all proteins that regulate healthy mitochondrial function.

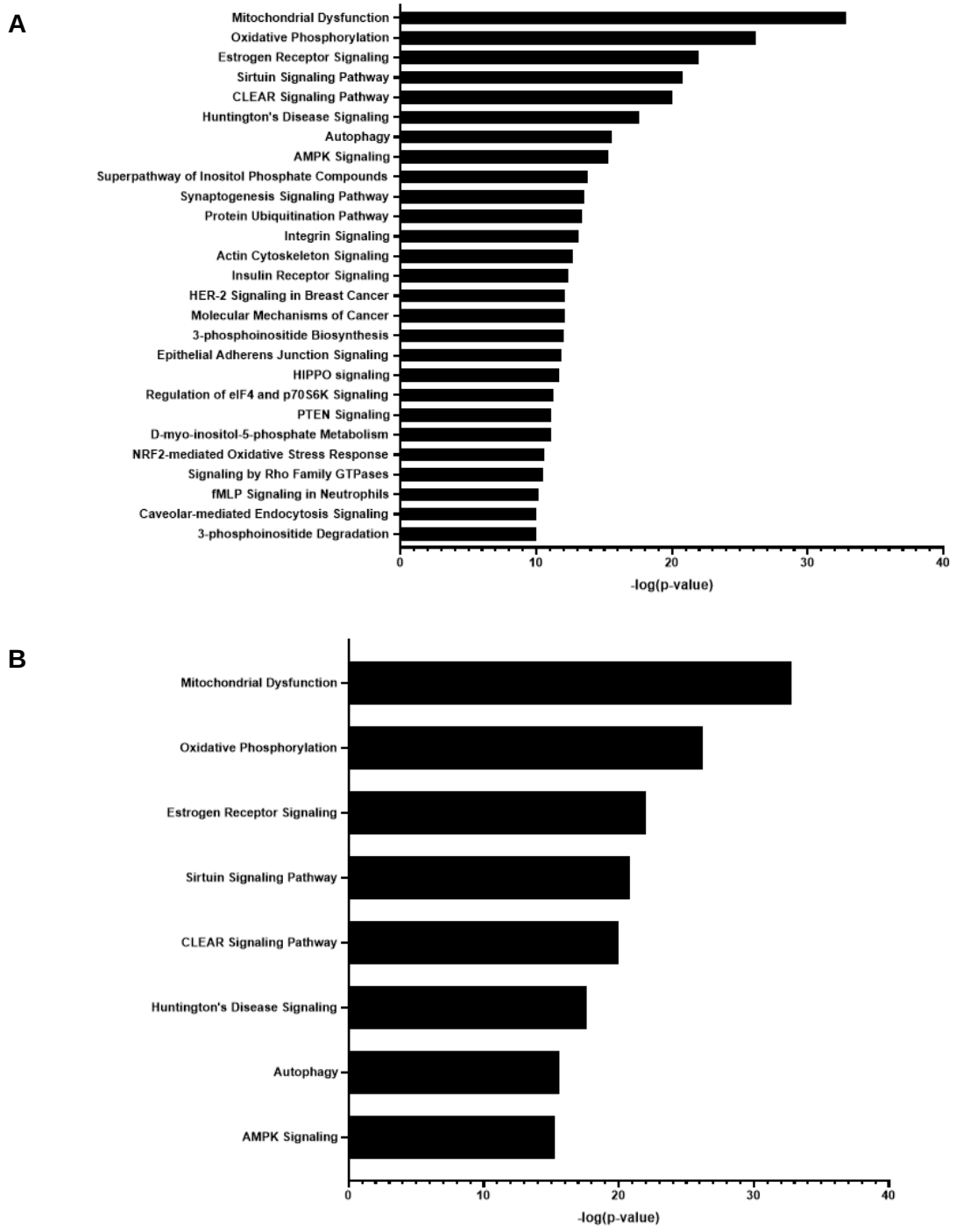

Figure 5.11 The most significantly predicted canonical pathways to be affected by pre-miR-214 transfection in human cardiac fibroblasts, when analysing all significantly modulated proteins. Ingenuity pathway analysis (IPA) was used to make predictions of modulated canonical pathways based on the fold change and direction of change of proteins in a TMT proteomics screen. The data that was entered was filtered by inputting all significantly changed proteins and then filtering the predictions by a -log(p-value) of >10 **(A)** or >15 **(B).**

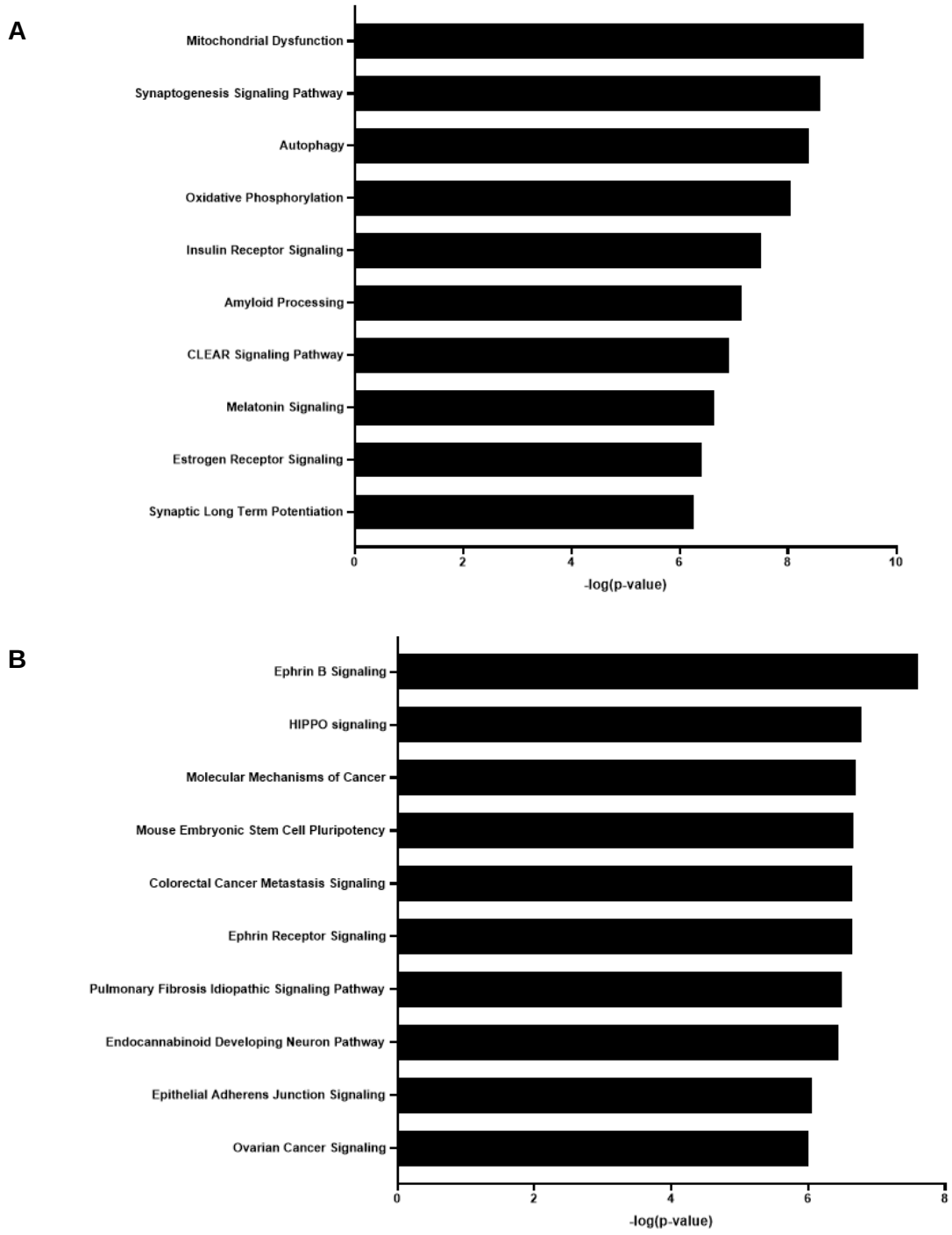

Figure 5.12 The most significantly predicted canonical pathways to be affected by pre-miR-214 transfection in human cardiac fibroblasts, when analysing all proteins based on fold change. Ingenuity pathway analysis (IPA) was used to make predictions of modulated canonical pathways based on the fold change and direction of change of proteins in a TMT proteomics screen. The data that was entered was filtered by inputting all significantly decreased proteins **(A)** or increased proteins **(B)** and then filtering the predictions by a -log(p-value) of >6.

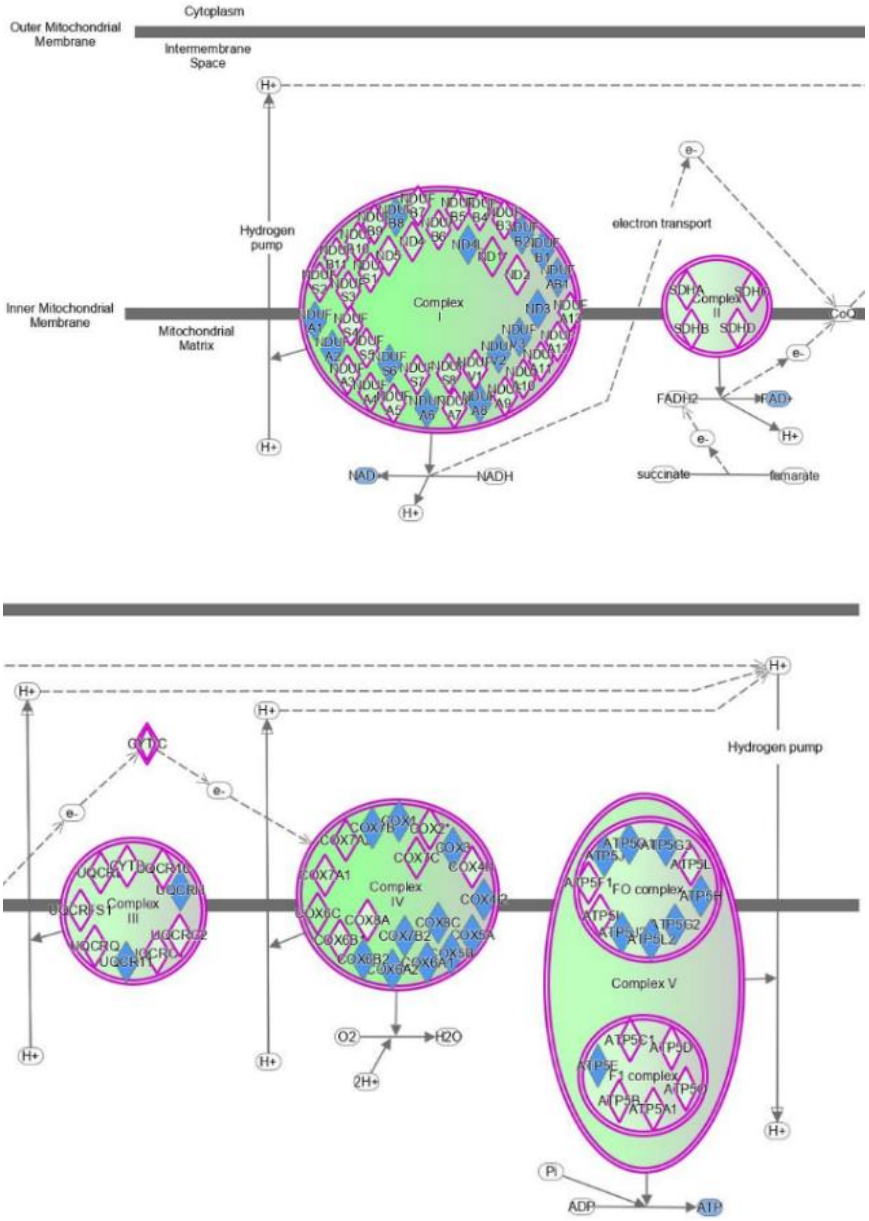

Figure 5.13 Proteins within the mitochondrial dysfunction canonical pathway that are significantly modulated by pre-miR-214 transfection. All proteins significantly modulated by pre-miR-214 were entered into ingenuity pathway analysis (IPA) and any proteins within the most significantly predicted modulated canonical pathway (mitochondrial dysfunction) have been mapped to their location within the mitochondria, their relationship with other proteins part of this pathway and indicated whether they are increased, decreased or unchanged by pre-miR-214 transfection. Key: pink = increased proteins, green = decreased proteins, blue = predicted inhibition, orange = predicted activation, white = no predicted effect.

IPA analysis of pre-miR-30d significantly modulated proteins (by P value) produced 11 canonical pathways with a -log(p-value) of >10 and 3 with a -log(p-value) >15 (Figure 5.14). The most significant of these pathways was “regulation of eIF4 and p70S6K signalling” and “EIF2 signalling”. It is interesting that both of these pathways are predicted as they have crossover considering that EIF proteins are eukaryotic initiation factors and these pathways are both concerned with eukaryotic protein translation via the recruitment of ribosomal proteins (Amorim et al., 2018).

The next IPA analysis of pre-miR-30d transfection involved analysing all decreased proteins or all increased proteins (by fold-change) by pre-miR-30d transfection (Figure 5.15). There were 8 canonical pathways for the decreased proteins with a -log(p-value) >5 and 9 canonical pathways for the increased proteins with a -log(p-value) >4. For the decreased proteins, the most significant pathway was “phagosome maturation”. This is particularly interesting as phagocytosis is a behaviour of MyoFbs (but not fibroblasts) where MyoFbs have been shown to phagocytose apoptotic cells following MI and then secrete anti-inflammatory cytokines, very similar to how macrophages act (Kurose, 2021). For the increased proteins, the most significant pathways were “EIF2 signalling” and “regulation of eIF4 and p70S6K signalling”. It is of note for miR-30d, that the pathways identified when looking at the most statistically significant proteins, are also predicted when looking at the most increased proteins (this was the other way round for miR-214). The identification of these pathways in both analyses gives them more reliability in those pathways being modulated by miR-30d. The most significantly predicted affected pathway, “regulation of eIF4 and p70S6K signalling pathway”, is shown in Figure 5.16. This pathway shows a mixture of proteins both increased and decreased rather than the entire pathway being “switched off”. Interestingly, some EIF proteins such as EIF4A and EIF4G are decreased but then others such as EIF3 are increased. The net result of these changes are predicted activation of translation. This is the importance of undertaking IPA analysis, by processing the increases and decreases of proteins within the same pathway and joining these findings together to decipher the overall affected pathways.

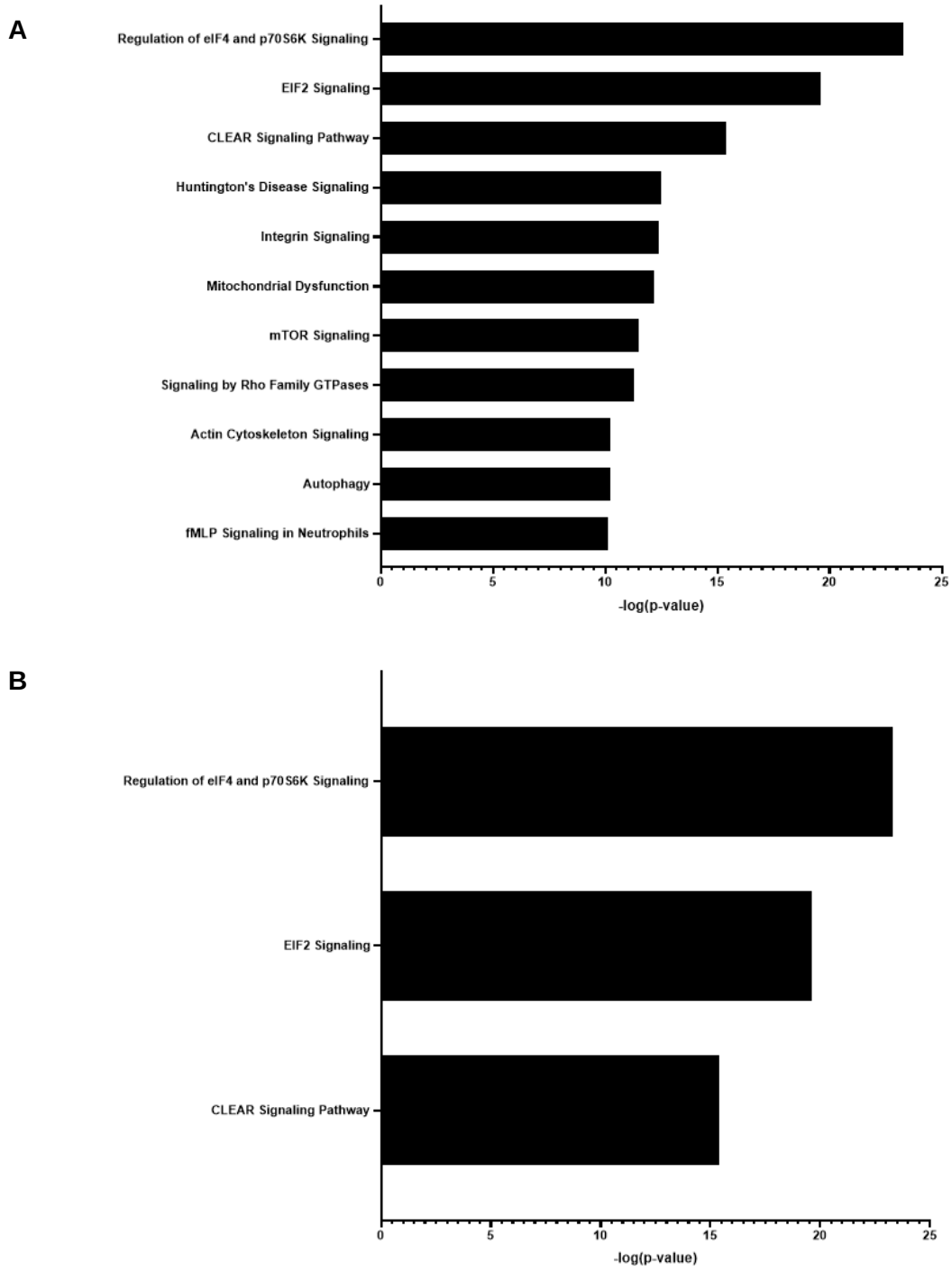

Figure 5.14 The most significantly predicted canonical pathways to be affected by pre-miR-30d transfection in human cardiac fibroblasts, when analysing all significantly modulated proteins. Ingenuity pathway analysis (IPA) was used to make predictions of modulated canonical pathways based on the fold change and direction of change of proteins in a TMT proteomics screen. The data that was entered was filtered by inputting all significantly changed proteins and then filtering the predictions by a -log(p-value) of >10 **(A)** or >15 **(B).**

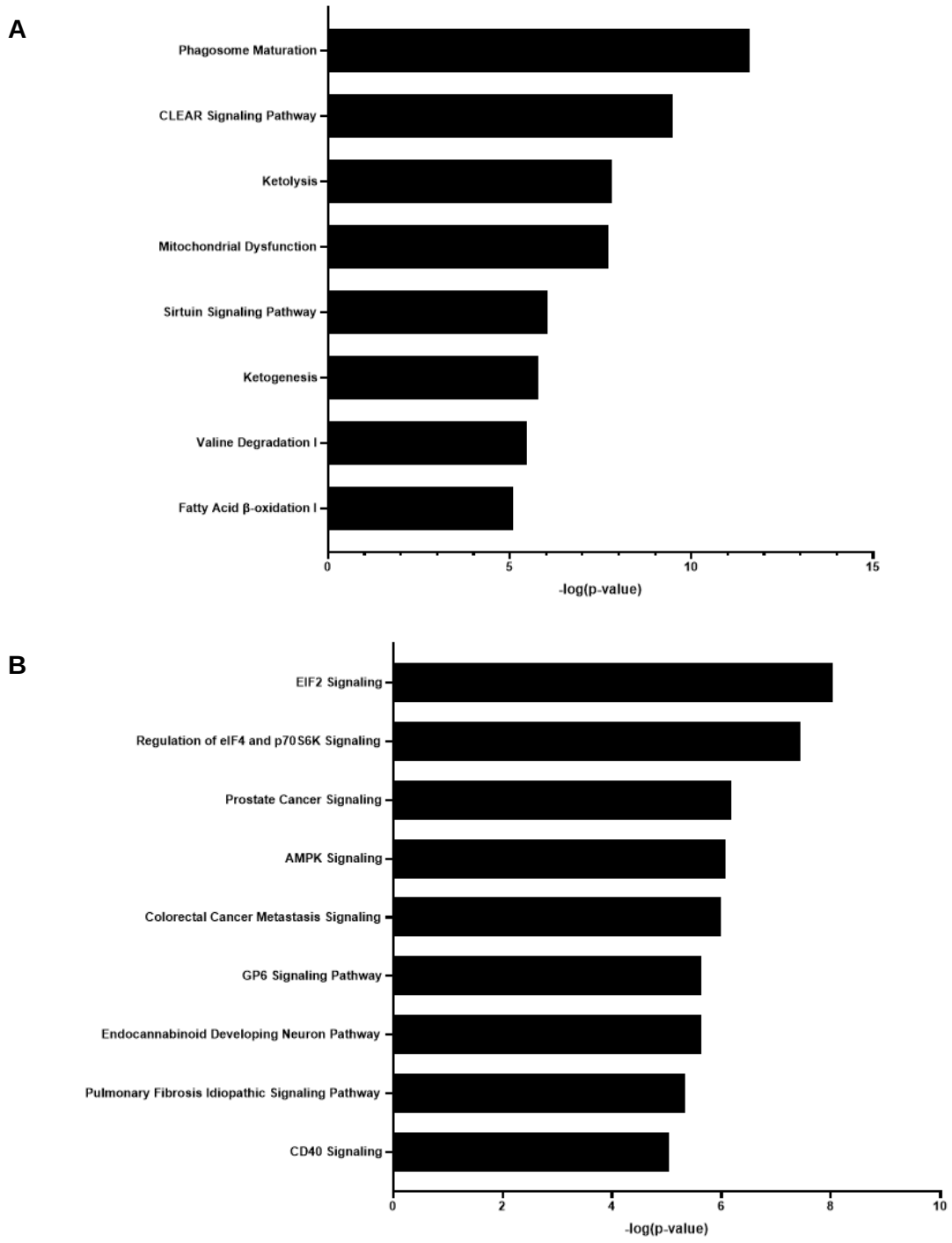

Figure 5.15 The most significantly predicted canonical pathways to be affected by pre-miR-30d transfection in human cardiac fibroblasts, when analysing all proteins based on fold change. Ingenuity pathway analysis (IPA) was used to make predictions of modulated canonical pathways based on the fold change and direction of change of proteins in a TMT proteomics screen. The data that was entered was filtered by inputting all significantly increased proteins **(A)** or decreased proteins **(B)** and then filtering the predictions by a -log(p-value) of >5.

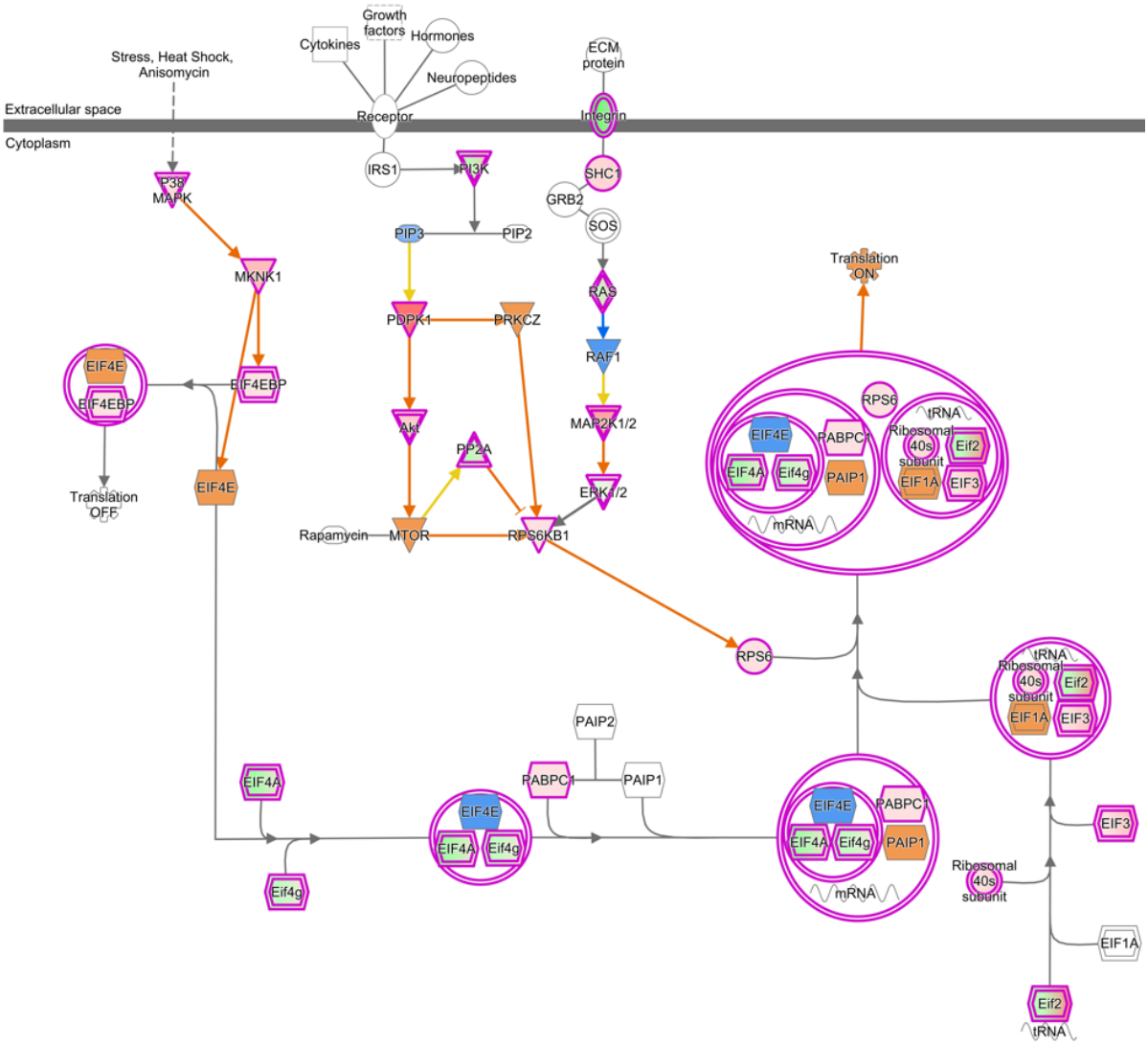

Figure 5.16 Proteins within the regulation of eIF4 and p70S6K signalling canonical pathway that are modulated by pre-miR-30d transfection. All proteins significantly modulated by pre-miR-30d were entered into ingenuity pathway analysis (IPA) and any proteins within the most significantly predicted modulated canonical pathway (regulation of eIF4 and p70S6K signalling) have been mapped to their location within the cytoplasm, their relationship with other proteins part of this pathway and indicated whether they are increased, decreased or unchanged by pre-miR-30d transfection. Key: pink = increased proteins, green = decreased proteins, blue = predicted inhibition, orange = predicted activation, white = no predicted effect.

5.4.5 Investigating the predicted effect of pre-miR-214 transfection on mitochondrial activity

Mitochondrial dysfunction was the most significantly predicted pathway to be affected when looking at all statistically significantly changed proteins (Figure 5.11) and all decreased proteins (Figure 5.12) by miR-214. In Table 5.2, a range of important proteins for mitochondrial activity have been listed along with their LogFC after pre-miR-214 and -30d transfection. The enzyme citrate synthase can be used to measure mitochondrial function. The citrate synthase assay measures the enzymatic reaction between acetyl coenzyme A (acetyl CoA) and oxaloacetic acid to form citric acid and CoA. Citrate synthase is located within the mitochondrial matrix and therefore this assay measures mitochondrial inner membrane integrity and therefore, mitochondrial health. The results of this assay are displayed in Figure 5.17. It was demonstrated that protein lysates obtained from pre-miR-214 transfected human CFs, showed significantly lower absorbance per minute per mg (absorbance/min/mg) of protein compared to protein lysates from pre-miR-NC transfection. This means that there was a decrease in the enzymatic reaction catalysed by citrate synthase and is used as a measure that mitochondrial activity is decreased in these cells. This absorbance and therefore citrate synthase activity, was 58.5% lower in pre-miR-214 compared to pre-miR-NC transfection. There was no difference in the absorbance observed between anti-miR-NC and anti-miR-214 transfection. This suggests that increased levels of miR-214 leads to mitochondrial dysfunction, however, inhibiting basal and endogenous levels of miR-214 (and therefore a decrease in miR-214) does not have the converse affect meaning this induction of mitochondrial dysfunction is something caused by increased miR-214 only.

Mitochondrial protein	Pre-miR-214 LogFC	Pre-miR-30d LogFC
MFN2	-0.41	-0.06 (not significant)
NDUFAF4	-0.38	0.02 (not significant)
NDUFC2	-0.35	-0.04 (not significant)
NDUFA4	-0.34	-0.05 (not significant)
SDHA	-0.19	-0.14
SDHB	-0.12	-0.07 (not significant)
SDHC	-0.19	-0.09 (not significant)
SDHD	-0.15	-0.15

Table 5.2 Changes in mitochondrial protein expression mediated by miR-214 and miR-30d. The LogFC of different, important mitochondrial proteins have been listed here, either after pre-miR-214 or -30d transfection. Group sizes; n=6.

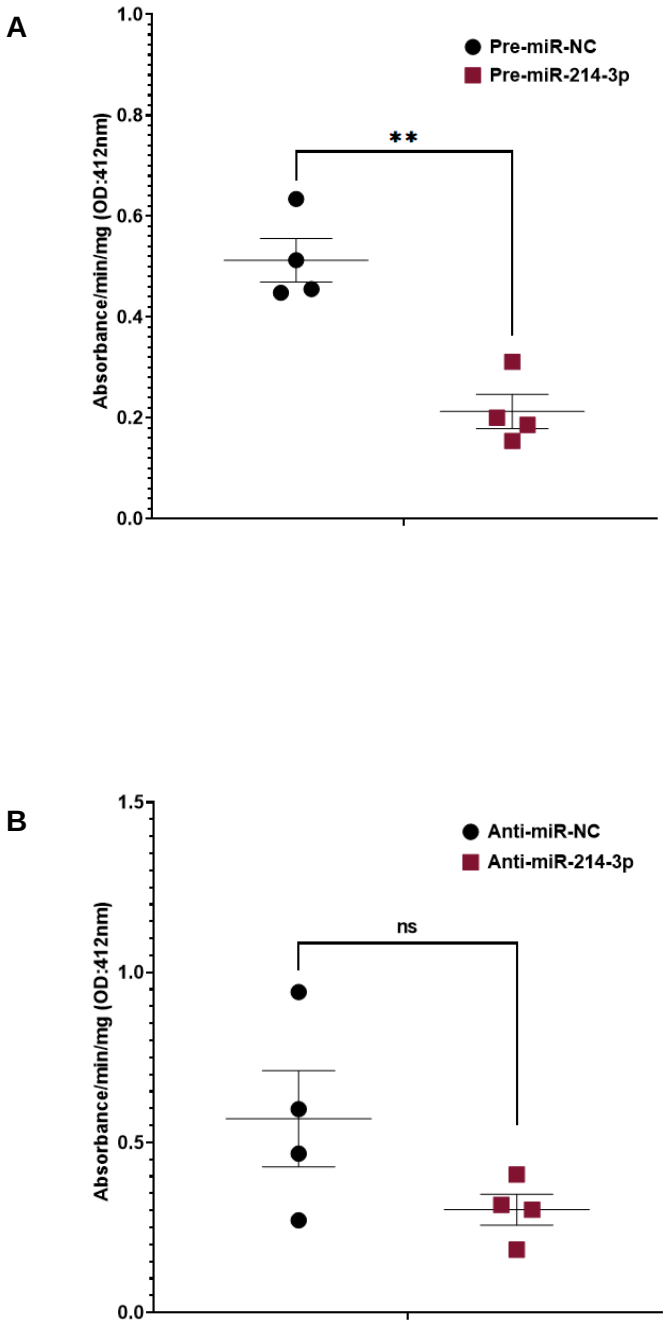

Figure 5.17 Mitochondrial function measured following miR-214 overexpression or inhibition. A citrate synthase (CS) assay was performed to measure CS activity as an indicator of mitochondrial activity in human cardiac fibroblasts, 72 hours post-transfection with pre-miR-NC or pre-miR-214 **(A)** and anti-miR-NC or anti-miR-214 **(B)**. Group sizes; n=4. One-tailed, parametric t test performed. **P<0.01 and ns=not significant.

A major protein for mitochondrial integrity and health is the mitochondrial fusion protein, MFN2. The fusion and fission mechanics of mitochondria is a regulated process that has implications for mitochondrial activity and health of the organism. Fusion helps to combine the contents of partially damaged mitochondria so that they complement each other (Youle and van der Bliek, 2012). The expression levels of (MFN2) (which showed a LogFC of -0.41, as displayed with other mitochondrial proteins in Table 5.2) was then further investigated by measuring mRNA and protein expression. Even though MFN2 downregulation has been shown at the protein level in the proteomics screen, it was important to measure the effect on the mRNA level as miRNAs act post-transcriptionally by binding to and either blocking or degrading mRNA. Therefore, this would confirm whether miR-214 is acting directly on MFN2 (post-transcriptional regulation) or indirectly by degrading regulators of MFN2 transcription. In the qRT-PCR analysis, pre-miR-214 transfected CFs showed significantly lower levels (43.3% lower) of MFN2 than pre-miR-NC transfected CFs (Figure 5.18). Anti-miR-214 transfected CFs meanwhile showed no difference in mRNA expression compared to anti-miR-NC transfection. Again, this could suggest that miR-214 mediates its effects on the mitochondria through overexpression only. Interestingly, the miRNA binding prediction database (miRdb.org) was used to investigate the presence of a miR-214 binding site in the 3' UTR of the human MFN2 gene, and MFN2 is ranked as the 11th strongest mRNA target for miR-214, with a prediction target score of 97/100. It was also found that there are three miR-214 seed binding sequences at locations 177, 622 and 1786 within the 3' UTR of the human MFN2 gene, shown in Figure 5.19. In subsequent Western Blot analysis, protein expression of MFN2 was also significantly reduced by pre-miR-214, but not by anti-miR-214 transfection (Figure 5.20). Therefore, overexpression by miR-214 decreases the mRNA expression levels and protein expression levels of MFN2, suggesting that there is direct regulation at the post-transcriptional level, that translates to the protein level.

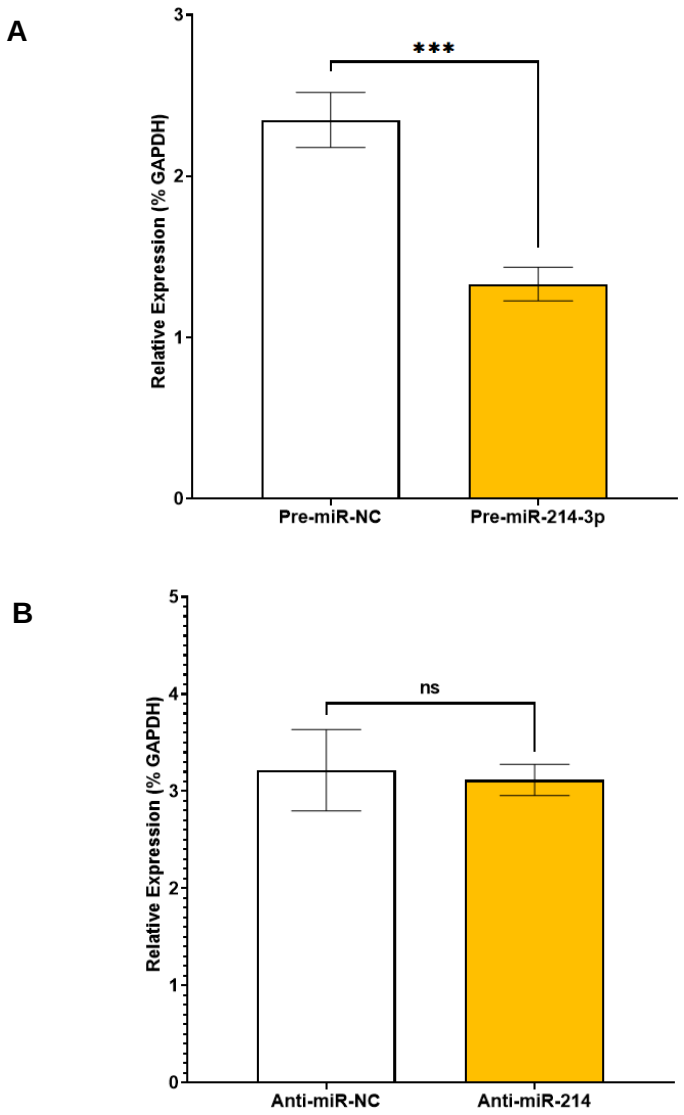

Figure 5.18 The gene expression levels of Mitofusin 2 in pre-miR-214 or anti-miR-214 transfected human cardiac fibroblasts. Human cardiac fibroblasts (CFs) were transfected with pre-miR-NC or pre-miR-214 **(A)** or anti-miR-NC or anti-miR-214 **(B)** and gene expression levels of Mitofusin 2 (MFN2) were measured at 48 hours post-transfection. Gene expression levels calculated by performing qRT-PCR and normalising levels relative to the housekeeping control, GAPDH. Horizontal bars indicate the mean value and error bars represent SEM. Group sizes; n=4. One-tailed, parametric t test performed. ***P<0.001. ns=not significant.

3' UTR Sequence

```
   1 tgggcacctg aggcggagtc tgcgtggaga ggggcggtgc tgccagccct aagtgccatg
  61 tgggctcccc caggggcacg tgtggctcct gccccctggc cactgccaag agaatgaagc
 121 acccagtctc gtaccatttt gagccctcca gcactactta ttttccccca cctttgcctg
 181 ctgttgctgg aagagctggc tcataccccc aaaggacact ttcagcgaca gctatggaca
 241 gcatggtacc aaggagttaa gttgaggctt tttccagctt tctctggttc atttgattgc
 301 ttgataaggc ctcaggatct cagcattgca caatgcctca tggaagcctt tgagggtatc
 361 acacagacac ccccaccttc ctccagcctg tgcgcacctg ccctccttgc agcccagcac
 421 acctgcaggt gtaagggacg attggagttt cttcccagag agtctgtccc agaaggactg
 481 tggcttgtgt gtgtccatct cgcctgttgg ctcagtgctt catcccattt gcagagcctc
 541 agacacgtct tggtggtgag gctcagttac ccctgggctt aggctgaggc gggccctgtg
 601 ctgggggtgg tagaaaggat gctgctgagg cagctggagg agtgggagta gctcagaggg
 661 gagggctgtt ggatgtatgg ggagctggca gagcaggtgg cagtcactgg gacaaggagg
 721 gacttgcctc tcttctcatt attgtgtcct ttgctttagt gtcagtcctg gacttgtgca
 781 ggcctgtttt gtgtagatct gttttggaag atggcatggt ctaggtggtt gaaggatgta
 841 gtagaaggat ggatggtgga aggtggggac gttggtggct ggctgaggtg catgggcccc
 901 acacaggaca gctggagaat gggccgtcca cttggcctcg ttctgcgagg ggctcatggg
 961 tctgagagcc cccacccact aggcttgatt gcatccctgt tgtgcccttt aagagacatg
1021 tttccacccc acccccaacc ttgtcccaag tgccctggac taaatttcct gtgccagtga
1081 ctgcagttgg ccaagggaca atgtggaaaa cccagtgtcc atctttccac cctccctgat
1141 ctccagaacc ttcgactgac ccccttgtct ttatgctgat gttgagtttt gggattgtta
1201 ctggttgaag tgggggcaga tgcctgtcac caaggtgttg actgtgtgag aaaagcagtt
1261 tgggtgacaa atcctgtgtg gcacaagttg gatcgcttcc tagaaataag caacacctct
1321 cccaaaaagc agcccacaag gcaggggccc agcagcccag ccatcactca tctttgagga
1381 aatgagttgg tagcctctgt gcactgtttg gtggccacat cacaggtgat gtcctgttca
1441 catacctgct tgtatttaaa gccctcagtc tgtcctgttg tgtggggcga agtgatggac
1501 tctgccaggt ggacatgctg tgggtggatg ttcccggcgt gtgccgggcc tgaatggaca
1561 ggggccactt cacagcatgt cagggaaaat cactgtcaca caattccaat ggattttgtg
1621 ctctttttga aaaaaaaaaa ttctttagcg taaacatgaa tttttttca atgtagcccc
1681 tggggaatga atgaaatttt gagcttcttc aatacgtaaa attaaattta taccactgag
1741 ggagagaccc tttctgaaag aagtatggcc aaaagcactt taatgctgct gacattgttg
1801 tttttatgtt catttgctgg agcgcaagac gtgctgacac agtgagtttt ctctgatgta
1861 tttaaggtga tgtatttgct tgagttactc ctgtatcatt gctcataata ttggaaacta
1921 aaataaaacc tagttggaaa tcctttgtga aaaaaaaa
```

Figure 5.19 The seed sequences for miR-214 binding in the 3' untranslated region of Mitofusin 2. The miRNA binding prediction database miRdb (miRdb.org) was used to identify 3 miR-214 seed sequences in the 3' UTR of the human MFN gene (marked in blue text).

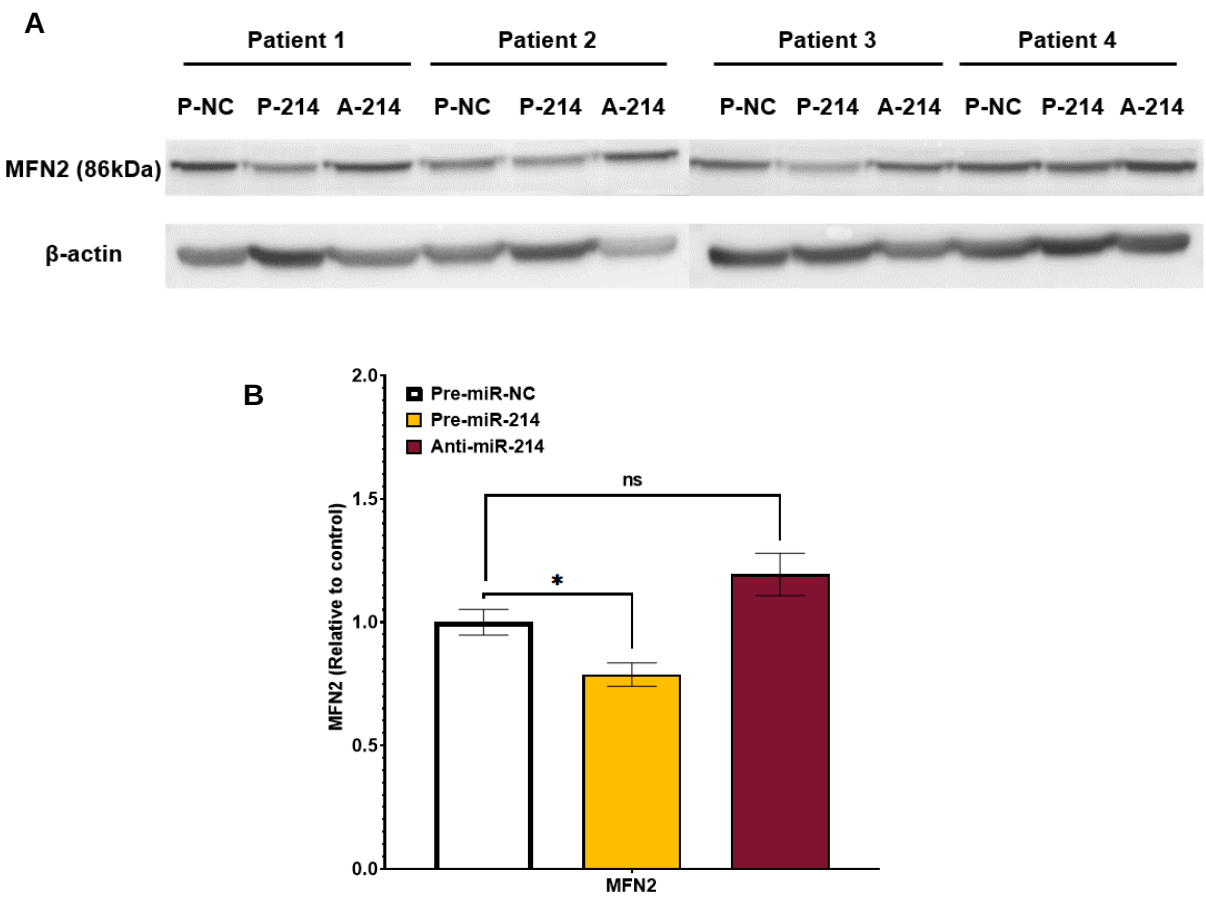

Figure 5.20 Western Blots showing the effect of pre-miR-214 and anti-miR-214 transfection on Mitofusin 2 protein expression in human cardiac fibroblasts. Protein lysates were extracted at 72 hours post-transfection and resolved by SDS-PAGE before blotting for Mitofusin 2 (MFN2) and beta-actin (β-actin) **(A).** The band intensities of MFN2 were plotted relative to the band intensities of β-actin, for each sample **(B).** Group sizes; n=4. One-tailed t test performed on log transformed data (Y=Log(Y)). *P<0.05. ns=not significant.

5.4.6 Investigating the predicted effect of pre-miR-214 transfection on lysyl oxidase

The LOX family of proteins are an important family of proteins that mediate collagen crosslinking. In doing so, they are important enzymes in the regulation of the ECM, which becomes dysregulated during cardiac fibrosis and cardiac remodelling. As the STRING analysis of the miR-214 proteomics dataset suggested that “ECM organisation”, “protein lysine 6 oxidase activity” (also known as LOXL1) and “peptidyl lysine oxidation” would be modulated pathways (Figure 5.7), this family of proteins was examined in more detail in the proteomics dataset. It was discovered that LOX and all four members of the LOX-like family (LOXL1, LOXL2, LOXL3 and LOXL4) were significantly increased by miR-214 (Table 5.3).

As miRNAs regulate activity through the negative regulation of their target mRNAs, and as the LOX proteins are increased, it was hypothesised that miR-214 regulates a negative regulator of the LOX family. To investigate this, the miRNA binding database (miRdb.org) was used to investigate the presence of a miR-214 binding site in the 3’ UTR of the LOXL1-antisense-1 (LOXL1-AS1). Antisense molecules work by binding to the mRNA for their target mRNA and so the hypothesis was that miR-214 inhibited this negative regulation. LOXL1-AS1 was not predicted as a miR-214 target by miRdb but as the predictions are based upon existing research and other researchers identifying seed sequences, a manual approach was also taken. The freely available search tool on miRbase (miRbase.org; powered by RNAcentral) was used to search for miRNA seed sequences in the RNA transcript of LOXL1-AS1, however no miR-214 seed sequence was detected. Nonetheless, as miRNAs usually bind to the 3’ UTR of RNA transcripts, and as the entirety of an antisense is untranslated and does not become protein, LOXL1-AS1 was still investigated at the mRNA level. It was found, however, that rather than decreasing LOXL1-AS1 mRNA, miR-214 treatment actually increased the mRNA levels of LOXL1-AS1 by 43.5% (Figure 5.21). This finding indicated that any miR-214 mediated increases in the LOX proteins was not via degradation of LOXL1-AS1.

The levels of each member of the LOX family were then also investigated at the mRNA level. It was found that pre-miR-214 transfection resulted in significantly higher levels of LOX (40%), LOXL1 (43%), LOXL2 (43%), LOXL3 (37%) and LOXL4 (52%) (Figure 5.21). This could be suggestive that the activity of miR-214 degrades a negative regulator of the entire LOX family at the transcriptional level, other than LOXL1-AS1.

The LOX family protein expression was then investigated by Western Blot, following pre-miR-214 treatment, to further confirm the TMT proteomics data. The Western Blot used a pan-LOX antibody which stained for several isoforms of LOX and LOXL proteins. Interestingly, it was found that while pre-miR-214 transfection had no effect on the expression of the mature 32 kDa LOX protein, it did influence both the glycosylated form of LOX (pro-LOX; 50 kDa) and

members of the LOXL family (Figure 5.22). Surprisingly, pre-miR-214 transfection led to significantly lower levels of pro-LOX however, it did result in significantly higher levels of LOXL. The effect of miR-214 on LOX expression therefore could perhaps be related to an effect on processing and glycosylation of the LOX protein.

LOX family protein	Pre-miR-214 LogFC	Pre-miR-214 FC
LOX	0.80	-0.57
LOXL1	1.03	-0.49
LOXL2	1.15	-0.45
LOXL3	0.48	-0.72
LOXL4	1.04	-0.49

Table 5.3 The effect of pre-miR-214 transfection on LOX family proteins in human cardiac fibroblasts. The LogFC measured in a TMT proteomics screen of each member of the LOX family of proteins, following pre-miR-214 transfection for 72 hours, were identified. Group sizes; n=6.

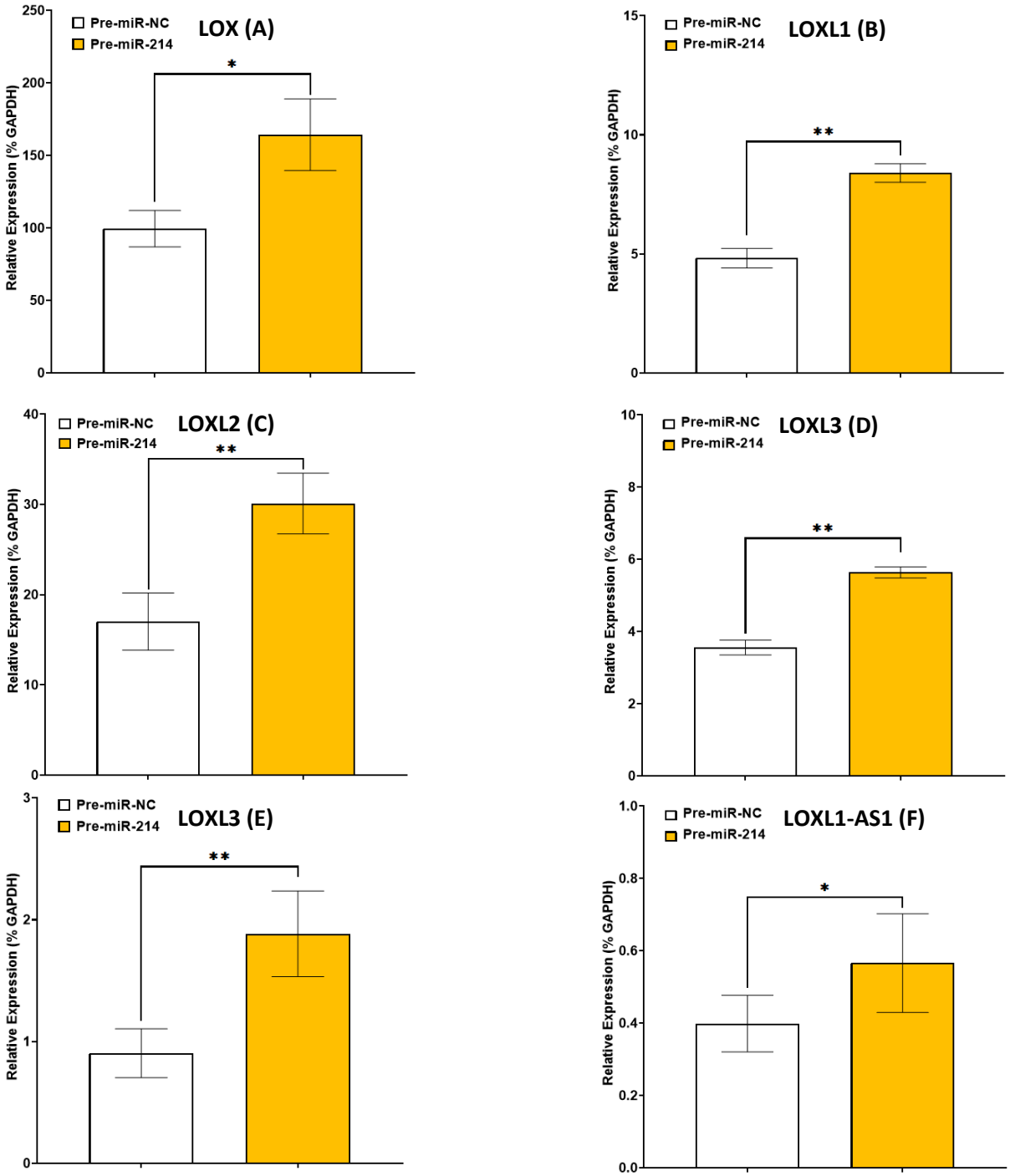

Figure 5.21 Gene expression levels of LOX, LOXL1-4 and LOXL1-AS1 following pre-miR-214 transfection. Human cardiac fibroblasts (CFs) were transfected with pre-miR-NC or pre-miR-214 and gene expression levels of lysyl oxidase (LOX) **(A),** lysyl oxidase like family members 1-4 (LOXL-1-4 **(B-E))** and lysyl oxidase like-1 antisense-1 (LOXL1-AS-1) **(F)** were measured at 48 hours post-transfection. Gene expression levels calculated by performing qRT-PCR and normalising levels relative to the housekeeping control, GAPDH. Horizontal bars indicate the mean value and error bars represent SEM. Group sizes; n=4. One-tailed parametric t test performed. **P<0.01 and *P<0.05.

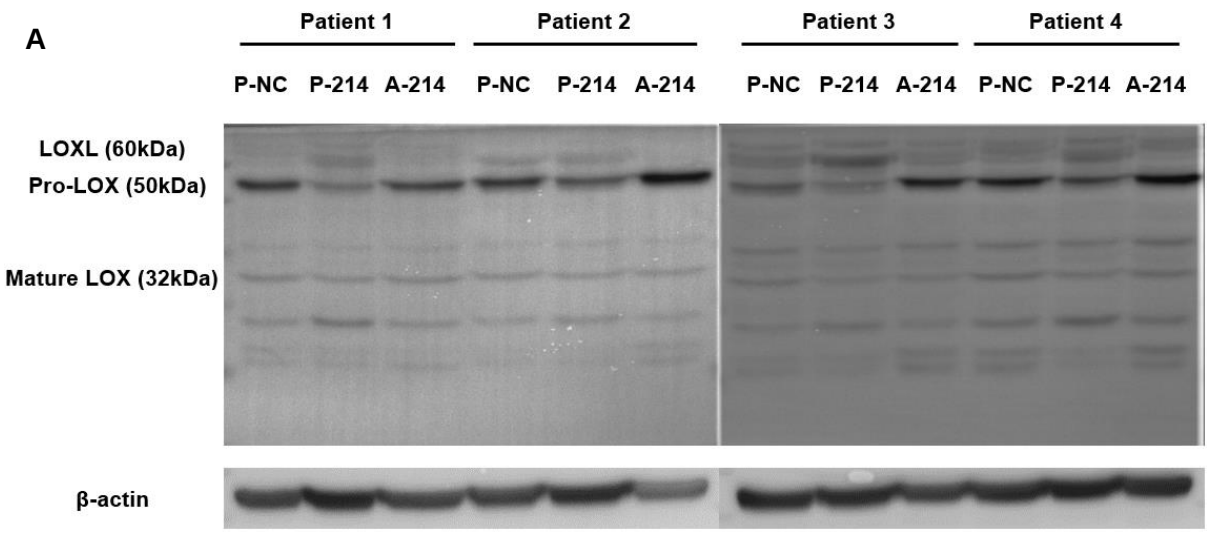
A
Patient 1
Patient 2
Patient 3
Patient 4
P-NC
P-214
A-214
P-NC
P-214
A-214
P-NC
P-214
A-214
P-NC
P-214
A-214
LOXL (60kDa)
Pro-LOX (50kDa)
Mature LOX (32kDa)
β-actin

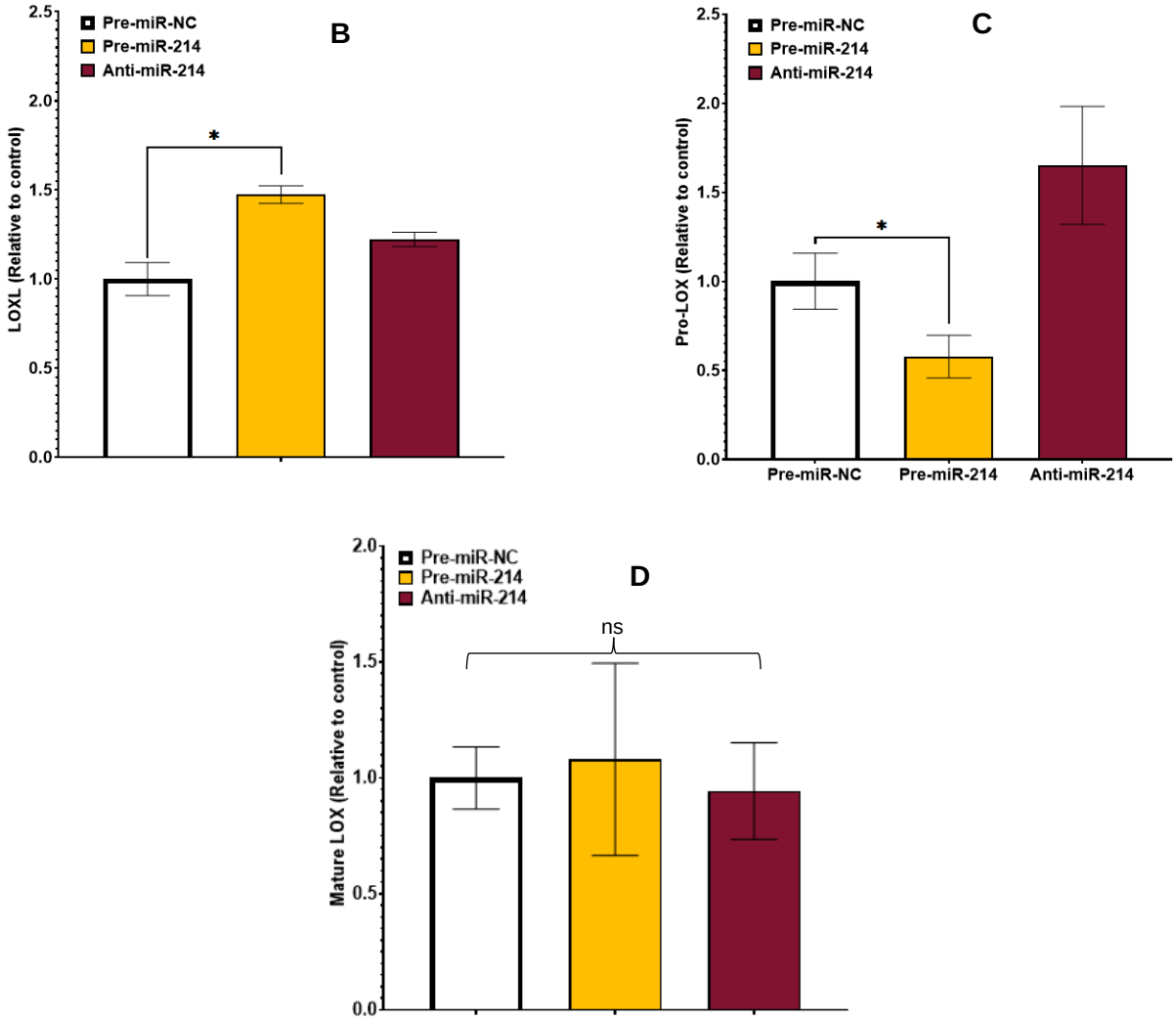

Figure 5.22 Western Blot data of beta-actin and LOXL, Pro-LOX and mature LOX in pre-miR-214 and anti-miR-214 transfected human cardiac fibroblasts. Protein lysates were extracted at 72 hours post-transfection and ran by SDS-PAGE gel electrophoresis by blotting for beta-actin (β-actin), lysyl oxidase-like proteins (LOXL), Pro-LOX and mature LOX **(A)**. The band intensities of LOXL, Pro-LOX and mature LOX were plotted relative to the band intensities of β-actin, for each sample **(B, C and D)**. Group sizes; n=4. One and two tailed parametric t tests performed. *P<0.05. ns=not significant.

5.4.7 Investigating the potential regulation of MFN2 on LOX expression

The potential regulation of MFN2 on the expression of the LOX family was then investigated to see if a regulatory network exists based on existing literature. Firstly, LOX family members have been shown to catalyse protein deacetylation (Ma et al., 2017a). Secondly, MFN2 has been demonstrated to attenuate histone acetylation of collagen IV (Mi et al., 2016). As CFs are known to secrete collagen during ECM remodelling, the potential of MFN2 to regulate LOX and LOXL family expression was explored. CFs were transfected with silencing RNA specific for MFN2 (MFN2 siRNA) and then mRNA and protein levels for LOX family members were measured. Firstly, to validate that the siRNA transfection was successful, qRT-PCR analysis was performed for MFN2 mRNA in negative control siRNA (NC siRNA) compared to MFN2 siRNA (Figure 5.23). It was identified that MFN2 siRNA successfully decreased the mRNA expression levels of MFN2 by 84.2% 48 hours after transfection.

To ensure that MFN2 siRNA transfection successfully decreased the protein expression of MFN2, Western Blot analysis was performed 72 hours after transfection (Figure 5.24). Transfection to silence MFN2 mRNA did successfully lead to a 45% reduction in MFN2 protein expression compared to NC siRNA. This means that any effect of reduced MFN2 protein on LOX expression would be detectable.

Experiments were then performed to investigate whether MFN2 knockdown could increase expression of the LOX family at the mRNA and protein levels. However, gene expression analysis found that MFN2 siRNA transfection resulted in significantly lower levels of mRNA for LOXL1 (25% decrease), LOXL2 (18.4% decrease), LOXL3 (34.1% decrease) and LOXL4 (37.9% decrease) (Figure 5.25). Like the effect of miR-214 overexpression on LOX protein expression (Figure 5.22), the knockdown of MFN2 did not affect LOXL or mature LOX expression but it did significantly decrease the expression of pro-LOX (Figure 5.26). This change was contradictory to what was hypothesised about potential MFN2 regulation of LOX, however, the fact that both miR-214 overexpression and MFN2 knockdown decrease the levels of pro-LOX, means that MFN2 could play a role in post-translational regulation of LOX.

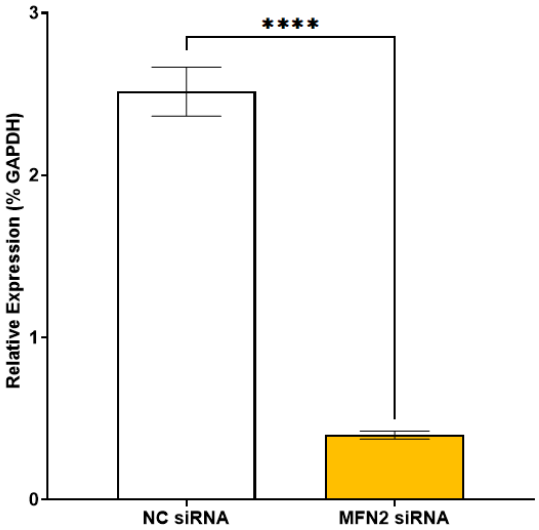

Figure 5.23 The effect of MFN2 siRNA on MFN2 mRNA levels in human cardiac fibroblasts. Human cardiac fibroblasts (CFs) were transfected with negative control siRNA (NC siRNA) or Mitofusin 2 siRNA (MFN2 siRNA) and gene expression levels of MFN2 were measured at 48 hours post-transfection. Gene expression levels calculated by performing qRT-PCR and normalising levels relative to the housekeeping control, GAPDH. Horizontal bars indicate the mean value and error bars represent SEM. Group sizes; n=4. One-tailed, parametric paired t test performed on log transformed data (Y=Log(Y)). ****P<0.0001.

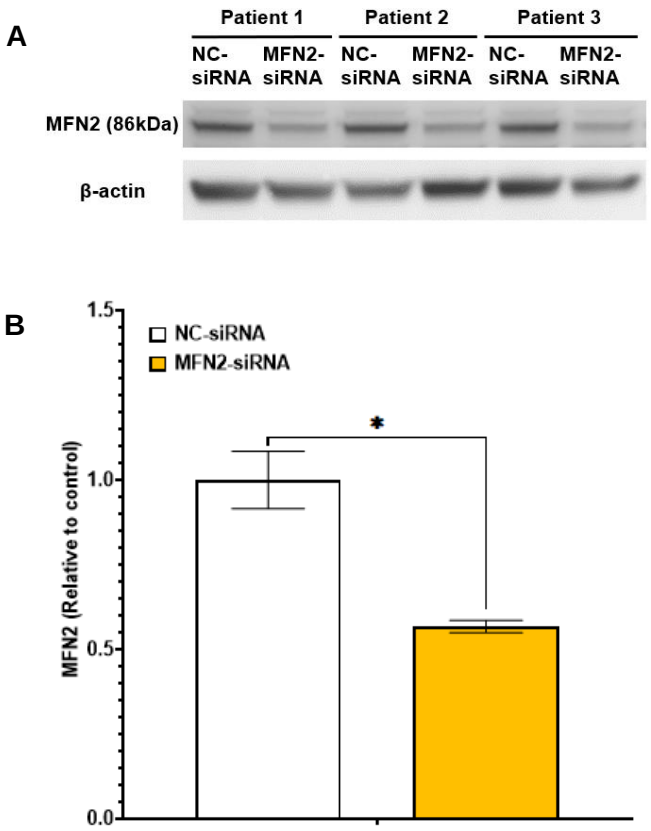

Figure 5.24 The effect of MFN2 siRNA on MFN2 protein levels in human cardiac fibroblasts. Protein lysates were extracted at 72 hours post-transfection and ran by SDS-PAGE gel electrophoresis by blotting for beta-actin (β-actin) and Mitofusin 2 (MFN2) **(A)**. The band intensities of MFN2 were plotted relative to the band intensities of β-actin, for each sample **(B).** Group sizes; n=3. One tailed, parametric, paired t test. *P<0.05.

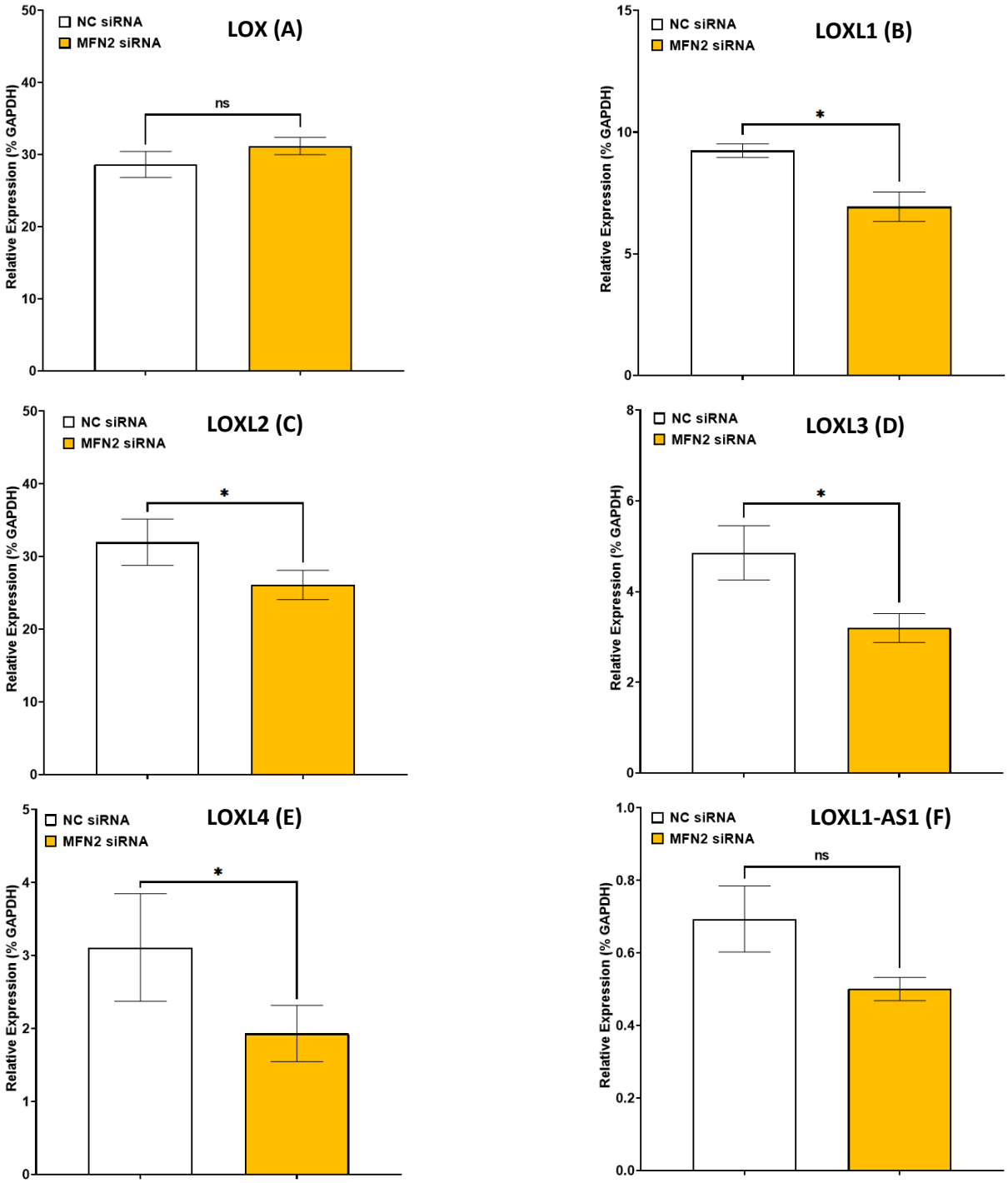

Figure 5.25 Gene expression levels of LOX, LOXL1-4 and LOXL1-AS1 following MFN2 knockdown Human cardiac fibroblasts (CFs) were transfected with NCsiRNA or MFN2siRNA and gene expression levels of lysyl oxidase (LOX) **(A),** lysyl oxidase like family members 1-4 (LOXL-1-4 (**B-E**)) and lysyl oxidase like-1 antisense-1 (LOXL1-AS-1) (F) were measured at 48 hours post-transfection. Gene expression levels calculated by performing qRT-PCR and normalising levels relative to the housekeeping control, GAPDH. Horizontal bars indicate the mean value and error bars represent SEM. Group sizes; n=4. One-tailed parametric t test performed. *P<0.05. ns=not significant.

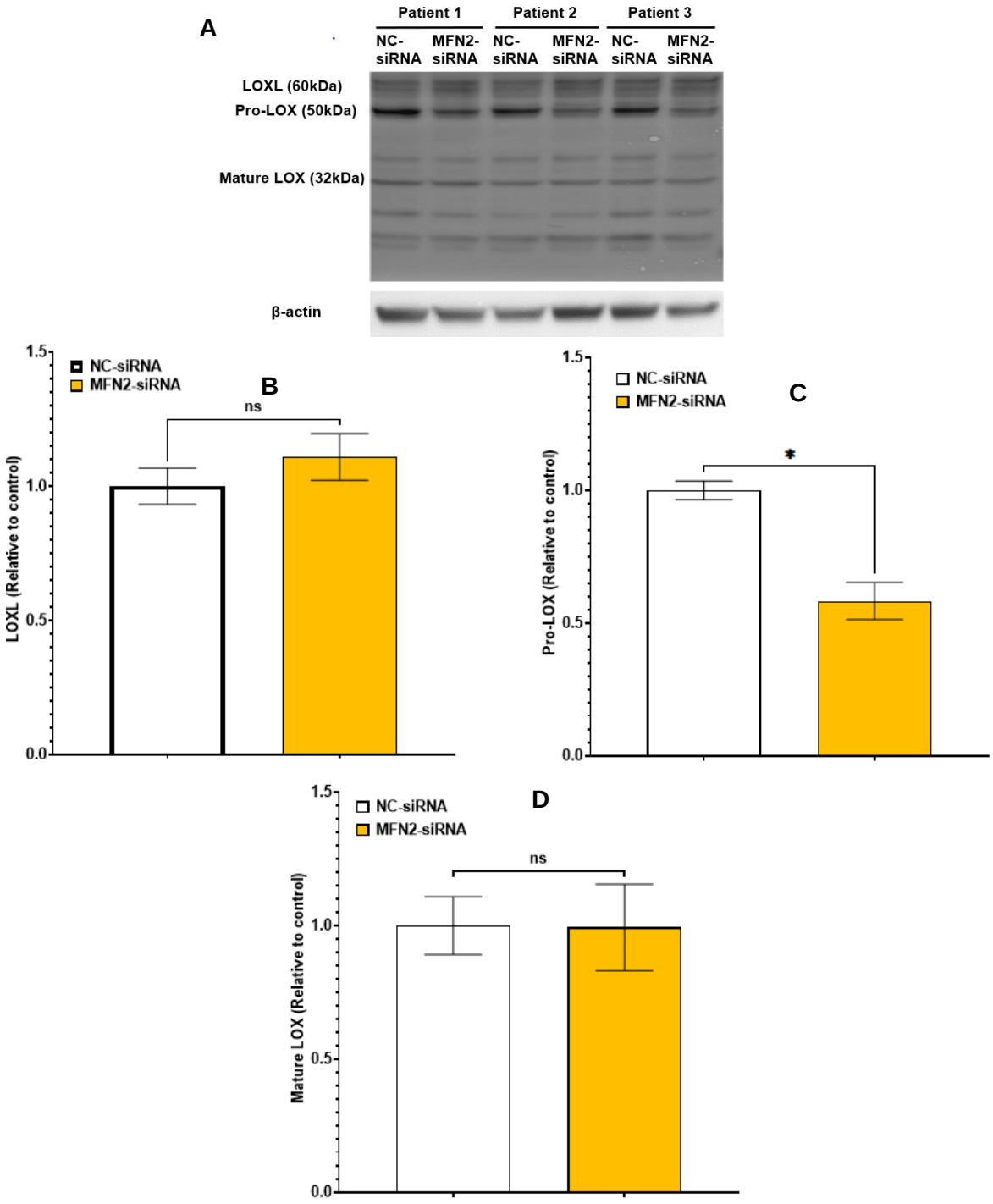

Figure 5.26 Western Blot data of LOXL, Pro-LOX and mature LOX in MFN2-siRNA transfected human cardiac fibroblasts. Protein lysates were extracted at 72 hours post-transfection and ran by SDS-PAGE gel electrophoresis by blotting for beta-actin (β-actin), lysyl oxidase-like proteins (LOXL), Pro-LOX and mature LOX **(A).** The band intensities of LOXL, Pro-LOX and mature LOX were plotted relative to the band intensities of β-actin, for each sample (**B, C and D**). Group sizes; n=3. Two tailed, parametric, paired t test. *P<0.05 and ns=not significant.

5.4.8 Investigating the effect of pre-miR-214 transfection on PIEZO1 expression and activity in human cardiac fibroblasts

The final potential miR-214 target investigated was PIEZO1 which was selected as a miRNA target due to it being a protein of interest in ongoing studies on cardiac fibroblasts within our laboratory (Blythe et al 2019; Bartoli et al 2022) (see Section 5.1). PIEZO1 levels showed a LogFC decrease of 79% in human CFs when transfected with pre-miR-214 (Table 5.4). The effect of pre-miR-214 transfection on the mRNA expression levels of PIEZO1 was investigated to determine whether miR-214 regulates PIEZO1 directly by binding to the mRNA. Pre-miR-214 transfection demonstrated significantly lower levels of PIEZO1 compared to pre-miR-NC transfection, with 40.3% lower expression (Figure 5.27A). Anti-miR-214 transfection did not show significantly different expression levels to anti-miR-NC transfection (Figure 5.27B).

The effect of pre-miR-214 and anti-miR-214 transfection on the activity of PIEZO1 was also investigated. It was demonstrated that transfection of human CFs with pre-miR-214 resulted in a significant reduction in intracellular calcium measurements (when treated with the PIEZO1 agonist, YODA), compared to pre-miR-NC, anti-miR-NC and anti-miR-214 transfection (Figure 5.28A-C). Therefore, miR-214 overexpression reduced PIEZO1 protein expression (measured by TMT proteomics), reduced PIEZO1 mRNA levels (measured by qRT-PCR) and reduced PIEZO1 activity (measured by intracellular calcium) and so miR-214 appears to directly inhibit PIEZO1 translation and thus activity in human CFs. The effect of pre-miR-214 on intracellular calcium influx was determined to be an effect specifically on PIEZO1 (rather than a non-specific effect due to altered cell viability or cell number for example) by confirming that ATP evoked intracellular calcium signalling in pre-miR-214 transfected cells that was not significantly different to the anti-miR or pre-miR-NC transfected CFs (Figure 5.28D).

Ion channel protein	Pre-miR-214 Log2FC	Pre-miR-214 FC
PIEZO1	-0.68	-0.6242

Table 5.4 The LogFC in PIEZO1 protein expression following pre-miR-214 transfection. The LogFC of PIEZO1, identified following a TMT proteomics screen after transfection with pre-miR-214 for 72 hours. Group sizes; n=6.

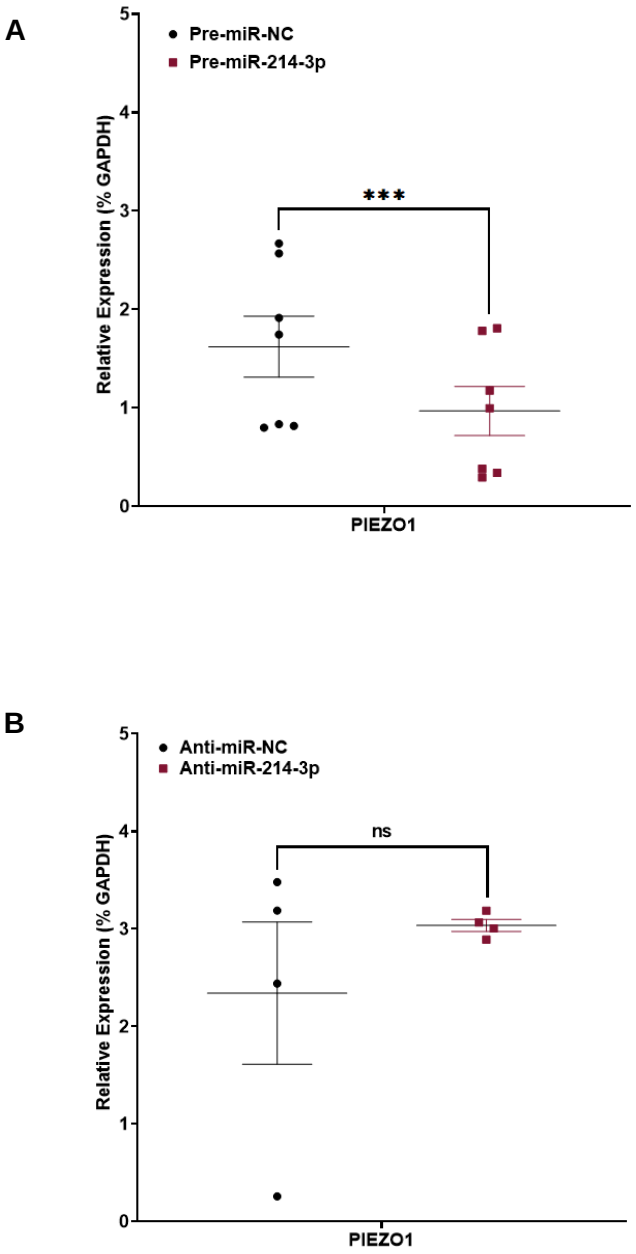

Figure 5.27 Gene expression levels of PIEZO1 following pre-miR-214 or anti-miR-214 transfection. Human cardiac fibroblasts were transfected with pre-miR-NC or pre-miR-214 **(A)** and anti-miR-NC or anti-miR-214 **(B)** and gene expression levels of PIEZO1 were measured at 48 hours post-transfection. Gene expression levels calculated by performing qRT-PCR and normalising levels relative to the housekeeping control, GAPDH. Horizontal bars indicate the mean value and error bars represent SEM. Group sizes; n=6 for pre-miR transfection and n=4 for anti-miR transfection. Two-tailed parametric t test performed on log transformed data (Y=Log(Y)). ***P<0.001 and ns=not significant.

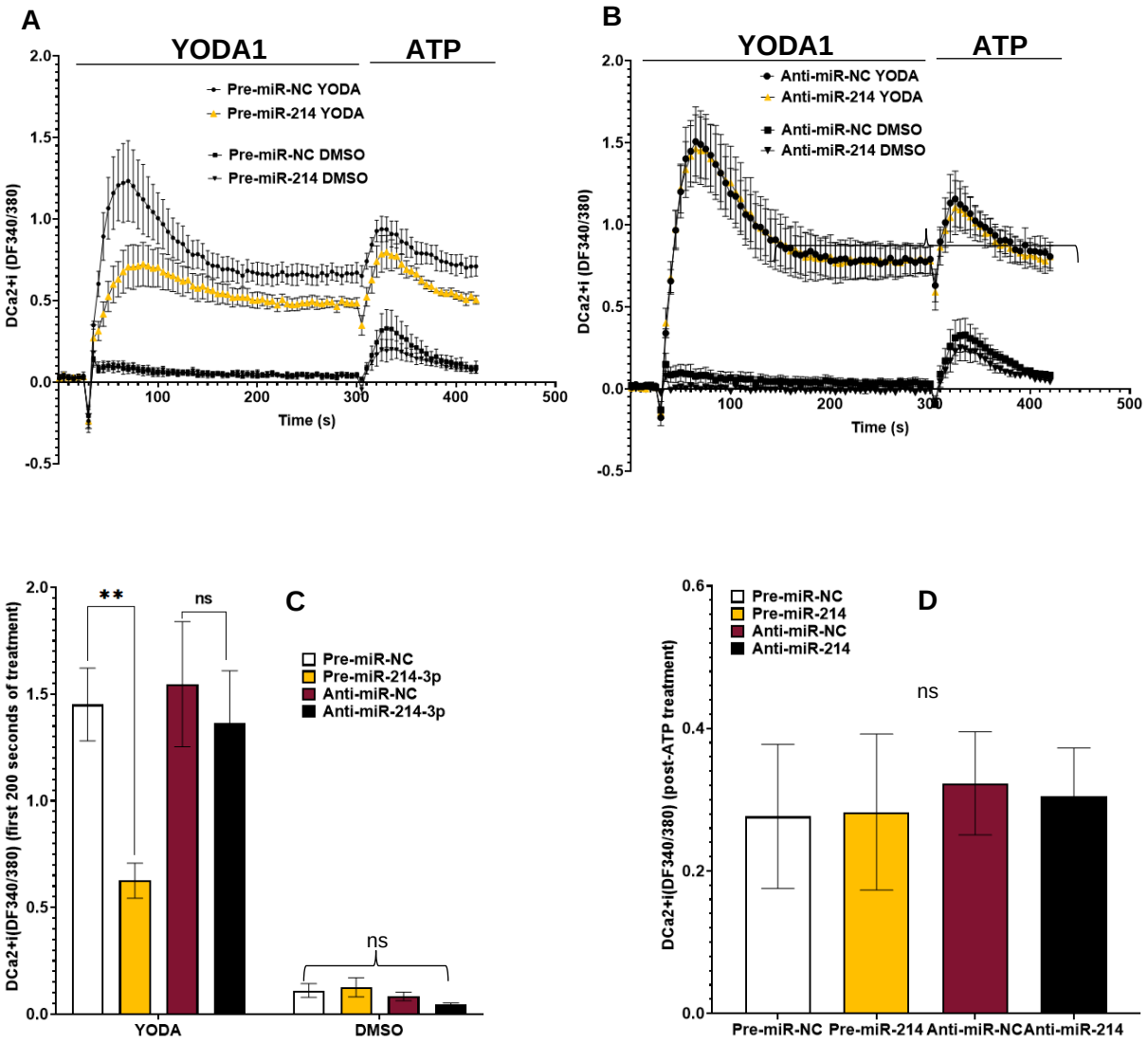

Figure 5.28 Yoda1-induced intracellular calcium measurements from human cardiac fibroblasts following pre-miR-214 or anti-miR-214 transfection. Representative calcium (Ca^{2+}) traces were taken from human cardiac fibroblasts, 72 hours post-transfection with pre-miR-NC or pre-miR-214 **(A)** and anti-miR-NC or anti-miR-214 **(B)**, when treated with 5µM YODA or 0.1% DMSO (vehicle control). Intracellular Ca^{2+} measurements were taken from the first 200 seconds of YODA or DMSO treatment and compared for significance **(C)**, as well as the remaining time, post-ATP injection (5µM at 300 seconds) **(D).** Group sizes; n=4. Two-way repeated measures ANOVA, with a Tukey multiple comparisons test. **P<0.01, *P<0.05 and ns=not significant.

5.5 Discussion

The aim of this chapter was to investigate the effect of overexpressing miR-214-3p or miR-30d-5p on protein expression in human cardiac fibroblasts and to pursue specific targets for downstream functional analyses, selected either as targets of interest in CVD or based on bioinformatics analyses.

MiR-214 and miR-30d were selected for TMT proteomics screening, out of our original panel of four miRNAs (miR-21a, -214, -224 and -30d) because they were differentially expressed in our ISO infusion model (miR-214 increased and miR-30d decreased) and our LAD ligation model (miR-214 increased at 3 days and miR-30d decreased at 4 weeks) and they showed opposing effects on the expression of related genes such as *MMP2*. It was encouraging that the proteomics screen found opposing fold changes for proteins changed by each miRNA, with many of the most increased proteins by miR-214 being decreased by miR-30d and vice versa (Figure 5.3 and 5.4). It was also encouraging to find that markers of ECs (PECAM-1), CMs (MYH6) and SMCs (MYH11) could not be detected in any of our 6 populations of human CFs treated in this screen (Table 5.1). Conversely, we were able to detect expression of markers for MyoFbs (ACTA2) or fibroblasts (DDR2, PDGFRA, S100A4, THY1, COL1A1, COL1A2 and COL3A1) at high levels in all 6 of our populations. This result is important because it means that we know that any miRNA regulation of gene expression that we detect is happening within human CFs and not in any contaminating cell types. Interestingly, three proteins that miR-214 and miR-30d show opposing regulation of are the collagens: COL1A1, COL1A2 and COL3A1, with miR-214 decreasing expression by 51%, 18% and 29% and miR-30d increasing expression 1.7-fold, 1.6-fold, and 1.2-fold respectively. The activity of each miRNA in regulating ECM related genes and proteins (such as collagen subtypes, MMP-2 mRNA, and protein and *TNC*) suggests that these miRNAs exhibit opposing effects on ECM regulation.

We used the bioinformatics tools, STRING, and IPA to infer shared networks that exist between the proteins changed by each miRNA and to generate lists of pathways that consist of those proteins. IPA was a more powerful tool than STRING as it considers the degree of fold-change and the direction of that change when it infers predictions. STRING was still valuable however for making graphical representations of proteins that share networks with each other and this was especially useful in identifying proteins that were at the centre of networks and therefore any change in these would be particularly influential. The first miRNA analysed by bioinformatics was miR-214, which, by its overexpression, modulated 4,162 proteins. We found that the proteins that shared the most connections with each other included: COL1A1, MMP-1, LOXL2, LOXL3, LOXL4, MAPK3, cyclin D1 (CCND1), tight

junction protein-1 (TJP1), catenin alpha-1 (CTNNA1), pyruvate dehydrogenase kinase 1 (PDK1) and MAPK10. We already knew from our qRT-PCR analysis that miR-214 decreased expression of *COL1A1* so it is not surprising to see protein expression of COL1A1 similarly decreased and Li et al. (2017) has previously shown that inhibition of miR-214 causes an increase in COL1A1. MMP-1 is upregulated by miR-214 and it is an interstitial collagenase that degrades collagen types 1 and 3. This is interesting because miR-214 is therefore inhibiting expression of collagen I and III and promoting expression of enzymes that degrade these collagens, demonstrating a very strong anti-fibrotic activity. The expression levels of MMP-1 have also been associated with different types of CVD, for example Lehrke et al. (2009) showed serum levels of MMP-1 are associated with total plaque burden in atherosclerosis and Picard et al. (2006) showed higher *MMP1* expression in the endomyocardial biopsies of patients with dilated cardiomyopathy.

We were also particularly interested by miR-214 increased expression of LOXL2, LOXL3 and LOXL4 and found that there were also increases in LOX and LOXL1, meaning the entire LOX family was upregulated. LOX enzymes act by oxidative deamination of collagen fibrils to form covalent cross-links and this leads to stiff collagen fibres that could underpin myocardial fibrosis (Kumari et al., 2017) (López et al., 2010). In fact, Adam et al. (2011) found that the left atrial myocardium of patients with AF is characterised by increased LOX expression and collagen cross-linking and that inhibition of LOX was found to prevent an Ang II induced increase in fibronectin, thus suggesting LOX as a therapeutic target in the prevention of myocardial fibrosis. Therefore, increased miR-214 in the acute phase of MI could be important for collagen cross-linking in scar formation, however, increases in HF models (such as our finding at 3 weeks post-ISO infusion) could be detrimental and promote long term fibrosis and remodelling.

When the results of the miR-214 proteomics screen were investigated by IPA, different results were generated compared to STRING. The results of this analysis found that mitochondrial dysfunction was predicted to be the most significantly affected pathway by miR-214, along with other related pathways including oxidative phosphorylation, sirtuin signalling and Huntington's disease signalling. The similarity between all these pathways was the significant dysregulation of mitochondrial proteins by miR-214 overexpression. In the case of oxidative phosphorylation specifically, there was decreased expression of a wide array of proteins across all four complexes of the ETC. Mitochondrial dysfunction has been identified as a driver in multiple types of CVD including ischemia-reperfusion injury, hypertension, and HF, and one of the principal components of this is the production of ROS which induce damage, necrosis and mutations (Poznyak et al., 2020). This damage ultimately leads to the release of DAMPs from necrotic cells or from phagocytes after engulfing said necrotic cells. Oxidative metabolism

by mitochondria is also the main energy source for the heart and the CMs, and dysfunction has been shown to reduce the contractile function of the heart as well as impairing calcium homeostasis (Zhou and Tian, 2018). The regulation of mitochondrial fusion and fission proteins is important for mitochondrial function, with fusion proteins mediating the convergence of impaired mitochondria, and fission proteins mediating the breakdown of mitochondria into smaller organelles. One of the major fusion proteins is MFN2, and miR-214 was found to decrease the expression of MFN2 in the TMT proteomics screen. It was also discovered through the predictive miR binding database, miRdb, that MFN2 contains three different potential miR-214 binding seed sequences in its 3' UTR. This regulation of MFN2 has been demonstrated to promote apoptosis in ischemic acute kidney injury where miR-214 overexpression decreased MFN2 expression and resulted in mitochondrial dysfunction (Yan et al., 2020). Moreover, MFN2 has been validated as a direct target of miR-214 in an investigation that showed miR-214 overexpression decreased MFN2 expression in the fibrotic heart and CFs (Sun et al., 2015). The latter investigation found that miR-214 overexpression induced CF proliferation and collagen synthesis via inhibition of MFN2 and activation of ERK1/2 MAPK signalling, which results in cardiac fibrosis.

Our next aim was to investigate whether miR-214 regulates LOX mRNA expression and we found that miR-214 overexpression increased the LOX family mRNA and decreased MFN2 mRNA expression (Figure 5.18 and 5.21). This indicates that miR-214 regulates the LOX family indirectly to increase its expression. We hypothesised that miR-214 regulated the expression of the LOXL1 antisense RNA 1 (LOXL1-AS1) to alleviate repression of the LOX family transcription. Overexpression did not decrease LOXL1-AS1 expression however, and instead it was increased which confirmed that miR-214 is not increasing the LOX family via this mechanism (Figure 5.21). We then hypothesised that LOX expression could be regulated by miR-214's effect on the mitochondria and on MFN2 specifically. Research shows that a decrease in expression of mitochondrial respiratory chain genes (as was observed in the present study with miR-214 overexpression at the protein level) is associated with an increase in collagen crosslinking and ECM stiffness and that ETC dysfunction can promote ECM integrity (Bubb et al., 2021). To test this, we transfected human CF with an *MFN2* siRNA, but found that LOX mRNA expression was not increased and LOXL1, -2, -3 and -4 mRNA were all decreased. Similarly, MFN2 inhibition did not increase LOX protein expression in Western blot experiments. Interestingly, we did find that miR-214 overexpression increased the expression of the LOXL family, decreased expression of pro-LOX and did not change the expression of mature LOX, when analysing by Western Blot (Figure 5.22). Similarly, inhibition of MFN2 decreased the expression of pro-LOX. The pro-LOX is an inactive, glycosylated proenzyme that first requires processing in the ER before its release as the mature LOX

enzyme (Grimsby et al., 2010). The importance of MFN2 expression in ER-mitochondrial tethering has been demonstrated by Han et al. (2021) and overexpression increased tethering in mice and a loss of MFN2 promotes ER stress (Ngoh et al., 2012). It is hypothesised therefore that miR-214 inhibition of MFN2 results in a decrease in the glycosylated pro-LOX by inducing ER stress and proteolytic processing of the proenzyme. Further studies are required to investigate the functional effect of miR-214 overexpression on collagen crosslinking.

We demonstrated for the first time that the overexpression of miR-214 induces mitochondrial dysfunction in CFs (Figure 5.17). The overexpression of miR-214 leading to mitochondrial dysfunction has been demonstrated *in vivo* by Bai et al. (2019) who also found that apoptosis was induced and disrupted oxidative phosphorylation. This regulation had not been explored in CFs until the current investigation. Mitochondrial dysfunction was one of the most significant pathways identified by IPA analysis because of the large number of mitochondrial proteins that were downregulated. These proteins included the NDUFs which are NADH dehydrogenases, (including NDUFAF4 (24% decrease), NDUFC2 (22% decrease) and NDUFA4 (21% decrease)) which catalyse the transfer of electrons from NADH to ubiquinone and are required for proper mitochondrial function. There were also decreases in all four of the succinate dehydrogenase proteins (SDHA, SDHB, SDHC and SDHD) that make up complex II and dysregulation of this complex is associated with the pathology of multiple types of cancer (Zhao et al., 2017b). The citrate synthase assay was performed as a measure of mitochondrial function as citrate synthase is localised to the inner mitochondrial membrane and the assay measures the integrity of the membrane (D'Souza and Srere, 1983). Mitochondrial dysfunction has been demonstrated as central to cardiac fibrosis and targeting this process has gained attention as a therapeutic modality. Dai et al. (2011) found that overexpression of the antioxidant enzyme, catalase, attenuated mitochondrial oxidative damage, cardiac fibrosis and hypertrophy that was induced by Ang II infusion in mice. Furthermore, Goh et al. (2019) found that Mitoquinone, a mitochondrial targeted antioxidant, inhibited fibrosis in an ascending aortic constriction pressure overload model by targeting ROS-mediated signalling of TGF-β1. Particularly relevant to CF behaviour, mitochondrial dysfunction and ROS signalling have been shown to increase transcription of MMPs, activate MMPs, decrease TIMP levels and decrease collagen synthesis (Siwik and Colucci, 2004), interestingly regulation that we have identified through our own investigation.

The current investigation is the first to demonstrate that miR-214 regulates the expression and function of the mechanosensitive ion channel, PIEZO1, in CFs. Indeed, this is the first time miR-214 has been shown to regulate PIEZO1 in any cells, and miRNA targeting has only been described once before by Huang et al. (2016) who found miR-103a targeted PIEZO1 in

endothelial cells to inhibit capillary tube formation. PIEZO1 was selected as a candidate target as it has been increasingly demonstrated as important in CVD at the level of the CF. Blythe et al. (2019) originally demonstrated that chronic PIEZO1 activation increased the expression and release of the pleiotropic cytokine, IL-6 in human and mouse CFs, via p38α MAPK activation. Subsequently, Bartoli et al. (2022) reported that a global gain-of-function mutation in PIEZO1 resulted in both cardiac hypertrophy and increased cardiac fibrosis (with increased expression of pro-fibrotic genes such as *Col3a1*) and up-regulation of PIEZO1 responses in CF. Although PIEZO1 expression was clearly decreased by miR-214 overexpression in the TMT proteomics screen, it was important to identify whether this was due to regulation at the mRNA level. miR-214 was found to decrease mRNA expression of PIEZO1, demonstrating that miR-214 may directly regulate PIEZO1 (Figure 5.27). Next, to confirm functional impact, the effect of miR-214 overexpression on the activity of PIEZO1 was established by measuring intracellular calcium in the presence of the PIEZO1 agonist, Yoda1 (Figure 5.28). Importantly, it was confirmed that the decreases in PIEZO1 mRNA and protein expression induced by miR-214 translated to a functional effect whereby Yoda1-induced intracellular calcium signalling was decreased significantly. Reassuringly, intracellular calcium signalling was not affected by miR-214 when CFs were stimulated with ATP only, demonstrating that miR-214 mediated this affect by decreasing expression of PIEZO1 specifically. Future investigations should establish what effect this inhibition has on the levels of fibrosis and hypertrophy *in vivo* through fibroblast-specific overexpression of miR-214.

Bioinformatics analysis was also performed on the proteomics screen following miR-30d overexpression. Firstly, STRING analysis revealed that the most shared pathways existed between the proteins; COL5A1, COL1A1, COL1A2, cyclin D1 (CCND1), STAT3, bone morphogenetic protein 6 (BMP6), caspase 1 (CASP1) and protein transport protein Sec24A (SEC24A). The most central protein to these shared networks was STAT3 and this signalling pathway has multiple roles, including promotion of cell proliferation, survival and migration and interesting it plays a key role in the IL-6 signalling pathway, downstream of IL-6R (Yu et al., 2009). STAT3 expression is increased by miR-30d (2.2-fold increase) and the activation of STAT3 integrates profibrotic pathways to activate fibroblasts. Hence, the inhibition of STAT3 has been suggested as a therapeutic option by inhibiting TGFβ activation of MyoFbs (Chakraborty et al., 2017). Interestingly, we also found that miR-30d increased the expression of *COL1A1* mRNA and in Chapter 4, we found that inhibition of miR-30d decreased the expression of *ACTA2* mRNA (encoding α-SMA) which suggests that miR-30d regulates the expression of genes and proteins that would promote differentiation to a MyoFb phenotype. This is in opposition to the findings of Li et al. (2021) who found that miR-30d overexpression decreased ACTA2 expression. However, Han et al. (2018) made findings that support our

work by showing miR-30d increased STAT3 activation to induce epithelial to mesenchymal transition (EMT), migration and invasion by increasing the expression of Krüppel-like transcription factor 11 (KLF11) in breast cancer. Interestingly, increased expression of KLF-11 protected against hypertrophy and fibrosis in a TAC mouse model and KLF-11 activators have been proposed as a candidate drug in HF patients which adds to the cardioprotective role suggested for miR-30d (Zheng et al., 2014).

IPA analysis predicted that miR-30d overexpression significantly affects the eIF4 and p70S6K signalling pathway and the second most significant pathway was eIF2 signalling, demonstrating a strong role between miR-30d and eukaryotic initiation factors (eIF). Translation initiation requires at least nine eIFs (Jackson et al., 2010). MiR-30d has been predicted to modulate eIF2 and eIF4. Firstly, eIF2 is responsible for the ribosomal recruitment of the initiator of translation, methionyl-tRNA, and miR-30d increases the expression of all 3 eIF2 subunits (eIF2S1, eIF2S2 and eIF2S3). The overall effect of miR-30d on eIF4 and p70S6K signalling was predicted as activation of translation through the inhibition of EIF4A2 and EIF4G2. This pathway is highly regulated with a wide array of initiation factor proteins that regulate the different steps of translation. MiR-30d upregulates and downregulates these proteins in a pattern that promotes overall protein translation. EIF signalling has been implicated in CVD as part of the mammalian target of rapamycin (mTOR) pathway where mTORC1 signalling initiates protein translation in response to growth factors and inhibits translation in response to stress (Sciarretta et al., 2014). Interestingly, miR-30d is implicated in an mTOR signalling pathway, where cerebral ischemia-reperfusion injury leads to inhibition of miR-30d to prevent its negative regulation of DNA damage-inducible transcript 4 (DDIT4), which is in itself a negative regulator of mTOR (Xu et al., 2021). The overall effect is that inhibition of miR-30d prevents protein translation and promotes autophagy and apoptosis induced by cerebral ischemia-reperfusion injury.

In summary, analysis of proteomics data by bioinformatics analysis has allowed the translation of miRNA effects on protein expression into effects on pathways and protein networks. This analysis has contextualised the activity of miR-214 and miR-30d to reveal what the overall effect of the miRNAs are in human CFs, rather than simply focusing on specific genes or proteins. The bioinformatics analysis followed by targeted downstream experiments revealed that miR-214 overexpression results in mitochondrial dysfunction. Protein targets across the entire ETC were decreased by miR-214 and this translated to mitochondrial dysfunction when assessed by a citrate synthase assay for mitochondrial integrity. We also found that miR-214 upregulated all members of the LOX family and, combined with our findings in Chapter 4, this demonstrates that miR-214 significantly affects expression of various ECM proteins including the LOX family, COL1A1, TNC and MMP-2. Finally, we found through candidate target

selection, that miR-214 decreases the expression of the mechanosensitive ion channel, PIEZO1 and that this decrease resulted in PIEZO1 specific dysregulation of calcium entry. Our analysis of miR-30d overexpression found that miR-30d significantly increases the expression of the master regulator, STAT3, which has been shown to promote proliferation, migration, and invasion, via miR-30d activity. We also found that miR-30d is predicted to activate protein translation and that miR-30d has been found to be inhibited in cardiac dysfunction models such as cerebral ischemia-reperfusion injury, leading to autophagy and apoptosis, and that miR-30d activity may inhibit apoptotic signals in response to stress. To establish the importance of these miRNAs in CVD, future work should involve overexpression or inhibition of each miRNA in animal models of disease to assess the effect of each on processes such as hypertrophy and fibrosis, the hallmarks of cardiac remodelling.

Chapter 6 Final discussion, future directions, and conclusion

6.1 Summary of results

Using whole heart RNA from *in vivo* cardiac dysfunction models in mice and patient derived, primary human cardiac fibroblasts cultured *in vitro*, it has been demonstrated that:

Chapter 3

- Cultured murine cardiac fibroblasts express miR-21a, -214, -224 and -30d
- MiR-21a, -214 and -224 were enriched in murine cardiac fibroblasts compared with other freshly isolated cardiac cell types
- Cultured human cardiac fibroblasts express miR-21a, -214, -224 and -30d
- Chronic isoproterenol infusion induced increases in miR-21a, -214 and -224 and decreased miR-30d expression at 3 weeks in whole heart murine RNA
- Fibroblast-specific p38α MAPK deletion reversed isoproterenol-induced expression changes in miR-21a, -214, -224 and -30d
- Experimental MI (permanent LAD ligation) increased miR-21a and -214 expression at 3 days and decreased miR-30d expression at 4 weeks in whole heart murine RNA
- Chronic angiotensin II infusion decreased miR-30d expression at 4 weeks in whole heart murine RNA
- TNFα treatment decreased miR-21a expression in cultured human CF
- Pharmacological inhibition of p38 MAPK decreased miR-224 expression in cultured human CF

Chapter 4

In cultured human CF:

- MiR-21a overexpression decreased mRNA expression of *IL6* and *IL6R* and increased expression of *IL11*, whereas miR-21a inhibition increased expression of *EDN1*
- MiR-214 overexpression decreased mRNA expression of *IL6* and *COL1A1* and increased expression of *TNC*, whereas miR-214 inhibition increased expression of *AGTR1*
- MiR-224 overexpression decreased mRNA expression of *IL6* and *MMP3*, and increased expression of *ITGA5*
- MiR-30d overexpression decreased mRNA expression of *MMP2* and *ITGA5*, and inhibition of miR-30d decreased expression of *ACTA2*
- MiR-214 overexpression increased the secretion of MMP-2 protein

Chapter 5

Following TMT proteomics analysis of cultured human CF transfected with pre-miR-214 or pre-miR-30d:

- STRING analysis predicted miR-214 regulation of ECM regulation
- IPA analysis predicted miR-214 regulation of mitochondrial dysfunction and oxidative phosphorylation
- MiR-214 overexpression increased lysyl oxidase (LOX), LOXL1, LOXL2, LOXL3 and LOXL4 mRNA and protein expression
- MiR-214 overexpression decreased mitofusin2 mRNA and protein expression
- MiR-214 overexpression decreased mitochondrial function
- MiR-214 decreased *PIEZO1* mRNA and protein expression in human cardiac fibroblasts
- MiR-214 decreased intracellular calcium signalling in human CF following treatment with the PIEZO1 agonist, Yoda1
- STRING analysis predicted miR-30d regulation of STAT3
- IPA analysis predicted miR-30d regulation of protein translation by targeting eIF4 and p70s6k signalling and eIF2 signalling

6.2 Final discussion

This investigation found that the expression of miR-21a, -214, -224 and -30d are dysregulated in *in vivo* mouse models of CVD and that the modulation of their expression following ISO infusion is dependent upon p38α MAPK expression in fibroblasts. The increase of miR-21a, -214 and -224 and decrease in -30d have been identified in *in vivo* models of cardiac dysfunction but their roles in regulating human CF behaviour are not fully understood (Thum et al., 2008) (Duan et al., 2015) (Zheng et al., 2021) (Roca-Alonso et al., 2015). The inhibition of p38 MAPK with the drug losmapimod however did not reduce the risk of major ischemic cardiovascular events in a multi-centre randomised clinical trial (O'Donoghue et al., 2016). The regulation of and the regulatory activities of miR-21a, -214, -224 and -30d were therefore investigated in human CFs as miRNAs and their downstream activity represent potential novel therapeutic targets (Nouraee and Mowla, 2015).

This study found that miR-21a overexpression decreased the mRNA expression of *IL6* and *IL6R* and increased the expression of *IL11*. This finding is supported by Liu et al. (2021) who found that miR-21a expression negatively correlated with *IL6* mRNA and that miR-21a mimic treatment was able to reverse an increase in *IL6* caused by lipopolysaccharide (LPS).

Moreover, Yang et al. (2018) found that miR-21a mimics decreased *IL6* in response to the DAMPs, high mobility group protein B1 (HMGB1) and heat shock protein 60 (HSP60) that were released in an MI model. The direct targeting of *IL6R* by miR-21a was identified by Wang et al. (2018b) through a luciferase reporter assay and they demonstrated this degradation suppresses proliferation, migration and invasion. Our investigation is the first to discover that miR-21a increases the expression of *IL11* mRNA and it was found that miR-21a can increase the expression of AP-1 for which there are two binding sites in the promoter of *IL11*, demonstrating a potential miR-21a/AP-1/IL-11 signalling axis (Zhou et al., 2011) (Cook and Schafer, 2020).

MiR-224 expression was decreased by pharmacological inhibition of p38 (SB203580) which is supported by previous work from our group that saw miR-224 expression was decreased in an ISO infusion model by fibroblast specific p38α MAPK KO (Bageghni et al., 2018). MiR-224 overexpression was found to decrease the mRNA expression of *IL6* and *MMP3* and increase expression of *ITGA5*. This is the first time that miR-224 overexpression has been found to decrease *IL6*, however An et al. (2021) demonstrated that IL-6 can induce miR-224 expression and miR-224 directly targets and decreases expression of SMAD4 which is interesting because inhibition of SMAD4 by siRNA reduced IL-6 expression (Yamada et al., 2013). SMAD4 has been validated as a target of miR-224 by several studies and so a potential regulatory axis could exist whereby miR-224 regulates IL6 through a negative feedback loop (Yao et al., 2010) (Zhang et al., 2013) (Ma et al., 2018).

MiR-214 and miR-30d were selected for further investigation due to their differential expression in our *in vivo* cardiac dysfunction models, differential regulation of cardiac remodelling genes and proteins, and a lack of understanding or consensus in the literature. MiR-214 overexpression decreased the mRNA expression of *IL6* and *COL1A1*, increased the expression of *TNC* and increased the secretion of MMP-2. TMT proteomic screening of miR-214 overexpression in human CFs found increases in the LOX family and qRT-PCR analysis confirmed miR-214 increased expression of the LOX family at the mRNA level. These miR-214-induced increases in ECM proteins were predicted by STRING analysis which predicted ECM regulation as a miR-214 impacted pathway. IPA analysis predicted miR-214 regulation of mitochondrial dysfunction, and this was confirmed by finding mitochondrial function was decreased by miR-214 in a citrate synthase assay and qRT-PCR, TMT proteomics and Western Blot demonstrated the decrease of MFN2 by miR-214. Finally, PIEZO1 was selected as a candidate target based on its implication in CVD and expression in human CFs (Blythe

et al., 2019, Bartoli et al., 2022) and it was found that miR-214 decreased PIEZO1 mRNA and protein expression and decreased intracellular calcium signalling specific to PIEZO1 activity.

Finally, miR-30d was the only miRNA to be decreased in our cardiac dysfunction models, with decreased expression 3 weeks following ISO infusion, at 4 weeks post-LAD ligation and at 4 weeks post-Ang II infusion. MiR-30d overexpression decreased the mRNA expression of *MMP2* and *ITGA5*, which was expected as Li et al. (2021) demonstrated miR-30d decreased expression of *ITGA5* in human CFs to decrease myocardial fibrosis. In the proteomics screen, miR-30d was found to increase the expression of STAT3 which has been shown to promote proliferation, migration, and invasion in the context of breast cancer but not yet in CVD (Han et al., 2018). Bioinformatics analysis of this proteomics dataset predicted that miR-30d would activate protein translation through modulation of eIF4 and eIF2 signalling pathways and similarly, this has been demonstrated in response to cerebral ischemic reperfusion injury (Xu et al., 2021).

In summary, this study has assessed the effects of miRNAs on human CF gene expression, protein expression and predicted modulation of pathways relevant to cardiac remodelling. To fully understood the effect of these miRNAs in regulating CF behaviour, it will be necessary to perform fibroblast- and CF-specific miRNA overexpression and inhibition in *in vivo* models of cardiac dysfunction.

6.3 Clinical relevance

CVD is the leading cause of mortality worldwide, with 17.9 million deaths per annum (Kim, 2021). In the UK, 168,000 people die each year from CVD (ONS, 2021), and the disease costs the UK economy £9 billion each year. According to the World Health Organization (2022), there were 58,332 clinical trials in CVD between 1999 and 2021, accounting for 10.4% of all clinical trials globally for this time period, yet CVD remains the world's biggest killer and the number of cases and deaths increase each year. As previously mentioned, large multi-centre, randomised clinical trials have failed to meet primary endpoints, such as in the trial of p38 MAPK inhibitors (O'Donoghue et al., 2016). The potential of RNA modulation, either as targets or as modalities has been realised recently and medicine is said to be in the midst of an RNA therapeutic "revolution" (Damase et al., 2021). The importance of RNA therapeutics has been born partly out of a lack of protein targets, given that only ~12% of proteins have active binding sites that can be targeted by small molecules (Hopkins and Groom, 2002).

RNA therapeutics can be divided into two different approaches; RNA interference (RNAi) where antisense oligonucleotides (ASOs) are synthesised to bind with complementarity to

endogenous RNA and inhibit their translation (Rinaldi and Wood, 2018), or mRNA where mRNAs are delivered with the purpose of transient expression of protein which has been demonstrated in vaccine technology for the expression of viral proteins (Baden et al., 2021). There are currently 15 ASO therapeutics approved by the Food and Drug Administration (FDA) (Igarashi et al., 2022) and the disease Duchenne Muscular Dystrophy (DMD) has received particular attention for the use of ASOs such as Eteplirsen (Sarepta therapeutics) to interfere with pre-mRNA splicing (Lim et al., 2017) and Revenko et al. (2022) (AstraZeneca and Ionis) demonstrated that ASO directed targeting of the previously thought “undruggable target”, FOXP3, in T-regulatory cells resulted in anti-tumour immunity.

Of course, endogenous inhibitors of mRNA translation exist in the form of microRNAs. As has been demonstrated in the current investigation, the overexpression of miRNAs and the inhibition of miRNAs each modulate gene expression and therefore increases, and decreases could equally be exploited as therapeutic options. To date, there are currently no clinically approved miRNA therapeutics, however there are many in clinical trials. One such therapeutic is anti-miR-17 oligonucleotide RGLS4326 (Regulus Therapeutics) where inhibition of miR-17 was found to attenuate cyst growth in autosomal dominant polycystic kidney disease (ADPKD). There is mixed success however, as a phase II clinical trial of the miR-21 inhibitor Lademirsen was terminated by Sanofi after meaningful improvement in kidney function was not achieved in kidney disease (Trials.gov, 2022).

In the field of CVD, the most recent drug discovery company to develop miRNA-based therapeutics is Cardior. This company possesses a drug pipeline with five programmes focused on either interaction with noncoding-RNA (ncRNA) or modulation of ncRNA. At least one of these is an ASO anti-miR directed against miR-132 (called CDR132L). This compound exemplifies how research on miRNA activity in disease can lead to the development of a compound for treatment of said disease. MiR-132 activation was found to induce cardiac hypertrophy and autophagy in CMs and hypertrophic stimuli increased its expression, and injection with antagomir reduced both cardiac hypertrophy and HF in mice (Ucar et al., 2012). Following this, improved cardiac function and reversed cardiac remodelling as well as tolerability and safety was demonstrated in pig models (Batkai et al., 2020) and more recently, this compound passed a phase 1b randomised, double-blind, placebo-controlled study in human patients and is currently in phase 2 clinical trials (Täubel et al., 2021).

Regarding the delivery of miRNA mimics to overexpress miRNAs, there are currently no such compounds in clinical trials. One compound that failed phase 1 clinical trials was MRX34, which was a liposomal miR-34a, intended for the treatment of patients with primary liver cancer (Christopher et al., 2016). This trial involved intravenous delivery of a liposomal miR-34 mimic

however the trial was terminated early due to major immune mediated adverse events and the deaths of four patients (Hong et al., 2020). This result demonstrates that, as with all types of drugs, there are safety concerns attached with the delivery of increased levels of miRNAs into the human body.

Of course, an important clinical application of miRNAs that could be much more easily achieved is the validation and clinical approval of miRNAs as biomarkers in human disease. To date there are no clinically approved miRNA biomarkers despite numerous publications demonstrating their differential expression in patient samples. MiRNAs hold promise as successful biomarkers as they are found circulating, they are present in liquid biopsies that can be easily taken from patients (urine, saliva, plasma etc.), they are biologically stable and their expression has been shown to correlate with extent of pathology (tumour burden, level of fibrosis etc.) (Gayosso-Gómez and Ortiz-Quintero, 2021). In CVD, Watson et al. (2015) demonstrated that the expression of miR-30c, −146a, −221, −328, and −375 could be used to differentiate HFrEF from HFpEF and that any of these miRNAs could be used in combination with detection of BNP to improve diagnosis compared to BNP alone. Similarly, miRNAs have been demonstrated as biomarkers in acute MI, including; miR-21 (Liu et al., 2015), miR-29b (Grabmaier et al., 2017) and miR-208b (Lv et al., 2014). One of the miRNAs from our investigation that holds promise as a biomarker that is decreased in CVD is miR-30d. We found that miR-30d was decreased at 3-weeks post-ISO infusion, 4-weeks post-LAD ligation and 4-weeks post-Ang II infusion, meaning it has been decreased in a HF model, an MI model and a hypertensive model and Xiao et al. (2017) found serum miR-30d expression was significantly lower in acute HF patients who did not survive the 1-year follow up.

6.4 Limitations

One limitation of this study is that most of the experiments were performed in cultured human CFs which differ from *in vivo* experiments due to the impact of culture conditions and a lack of cellular heterogeneity, for example there are no CMs or ECs impacting CFs or engaging in crosstalk. However, human CFs were used *in vitro* to simplify the system and to look at the mechanics of these miRNAs in CFs. A strength of this is that human CFs were used as opposed to animal CFs but importantly it was shown that the expression profile of cultured human CFs was like murine CFs for these miRNAs. Proteomics analysis confirmed the cultures of human CFs were pure and free from contamination by other cardiac cell types.

One of the limitations of the investigation was the scope of the TMT proteomics screen. The study began with analysing the role of all four miRNAs, miR-21a, -214, -224 and -30d but only miR-214 and -30d were selected for proteomics analysis due to financial and time constraints. Analysis of all four miRNAs would have been of great interest. Similarly, our screen could have

been more reflective of the directional changes seen in cardiac dysfunction had we inhibited miR-30d by transfecting with anti-miRs for proteomics analysis, rather than overexpressing it. This is because as explained previously, miR-30d was decreased in all the *in vivo* mouse models of cardiac dysfunction. Nevertheless, our proteomics study provided important novel information on the regulation of the cellular proteome by these miRNAs.

Another limitation however is that our proteomics screen only looked at cellular and ECM proteins whereas there are many important proteins synthesised by CFs that are present in the secretome. This could be investigated in future studies, however.

One other limitation to be considered is that pre-miR transfection resulted in increases of miRNA expression by hundreds or thousands of folds, depending on the miRNA. As has been explained previously, this does not reflect the increases detected in murine models of dysfunction, where increases are <10-fold compared to controls. This is something that should be considered when designing any potential mouse models of miRNA overexpression. Another consideration is that Khan et al. (2009) found that miRNA targets actually increase in expression following transfection and they hypothesise that pre-miRs could actually compete with endogenous miRNAs for RISC machinery and prevent binding to target mRNA.

6.5 Future directions

6.5.1 Do miR-21a, -214, -224 or -30d regulate human cardiac fibroblast migration?

Our investigation sought to determine what role miR-21a, -214, -224 and -30d play in the regulation of human CF behaviours relevant to cardiac remodelling, with a focus on cell proliferation. However, another important behaviour of activated CFs and MyoFbs is cell migration, which is increased upon activation and differentiation. Mitchell et al. (2007) demonstrated that IL-1β stimulated a dose dependent increase in migration of rat CFs and Siddesha et al. (2013) showed that Ang II treatment led to increased migration of adult mouse CFs as well as activation of MMP-2, -14 and -9 via NF-κB and AP-1 activation. MiR-21 has been shown to promote CF to MyoFb transition but the effect on migration has not been investigated (Zhou et al., 2018). Similarly, miR-214, -224 and -30d have not shown regulation of CF migration although miR-214 inhibition was found to attenuate migration of a triple negative breast cancer cell line (Zhang et al., 2019). In other studies, miR-224 overexpression promoted migration by targeting *PTEN* (Peng et al., 2021), and miR-30d mimics increased migration and invasion in a breast cancer cell line (Han et al., 2018). Future investigations would involve transfection of human CFs with specific pre-miRs or anti-miRs and then measurement of migration using a Boyden chamber assay or scratch wound assay (Riches et al., 2009).

6.5.2 Are miR-21a, -214, -224 or -30d differentially expressed in patient clinical samples?

One important investigation in the future would be to measure the expression levels of miR-21a, -214, -224 and -30d in clinical samples taken from patients with different types of CVD, whether this be acute MI, hypertension, stroke, HFpEF or HFrEF. Samples should include both human tissue biopsies and liquid biopsies such as serum. The purpose of this would be to assess for any associations between the expression levels of these miRNAs and the type of disease, the extent of disease, diabetic status, sex and any future changes such as mortality. The extent of disease would include measurements such as degree of fibrosis or cardiac output. Importantly, if any associations are found, especially in liquid biopsies, then this could lead to the validation of any of these miRNAs as potential biomarkers for CVD.

6.5.3 What is the effect of miRNA overexpression or inhibition on coculturing human cardiac fibroblasts and cardiomyocytes?

The heart is a dynamic organ, with regulation of ECM turnover and any dysregulation can result in disease, but another dynamic process that occurs here that has not been mentioned is crosstalk between CFs and CMs. This has been described by Bageghni et al. (2018) where CFs release IL-6 to induce cardiac hypertrophy in CMs by paracrine signalling and the expression of receptors such as integrins allow CFs to sense changes in the ECM such as mechanical transduction and MMP and TIMP balance and then communicate these changes to CMs and vice versa (Civitarese et al., 2017). Importantly, miRNAs can be released in extracellular vesicles (EVs) by cells and then act on mRNA expression in other cell types (Mills et al., 2019). Indeed, this has been demonstrated in CVD where Li et al. (2021) found that miR-30d is released by CMs in EVs and then acts on CFs to target and decrease the expression of *ITGA5*; supporting our finding that miR-30d expression was not enriched in murine CFs. A future direction would therefore involve; 1) modulating the expression of these miRNAs in human CFs and then co-culturing with CMs to investigate effect on CMs (including hypertrophy, contraction and calcium signalling), 2) culture CFs in conditioned media obtained from CMs to investigate influence on miRNA expression and 3) culture CMs in conditioned media obtained from CFs where miRNA expression has been modulated to investigate the influence on CM behaviour/gene and protein expression.

6.5.4 Does miR-214 regulate LOX activity?

We found that miR-214 overexpression increased the mRNA and protein expression of LOX, LOXL1, LOXL2, LOXL3 and LOXL4 but we do not yet know the effect on LOX activity. LOX enzymatic activity can be measured by a LOX activity assay where hydrogen peroxide is released by LOX catalysis of a LOX substrate and fluorescence is then measured. We

hypothesise that miR-214 overexpression would similarly lead to an increase in LOX activity and this assay would confirm this effect.

6.5.5 Does miR-214 regulate collagen gel contraction?

The key role of the LOX family of proteins is the deamination of specific lysine and hydroxylysine residues in collagen to form stable crosslinks between collagen fibres, which results in thicker collagen fibrils (Herchenhan et al., 2015). As well as the synthesis and release of collagen, CFs regulate contraction of collagen which is important for contraction of the scar produced in wound healing post-MI, and collagen gel contraction can be induced by mediators of cardiac dysfunction such as Ang II which induces contraction via integrins (Burgess et al., 1994). As we know that miR-214 increases LOX expression, and LOX acts by forming collagen cross-linking, it would be interesting to know what the effect is on collagen gel contraction and therefore learn what role miR-214 may play in wound healing post-MI. Collagen gel contraction assays could be performed as described previously (van Nieuwenhoven et al., 2013).

6.5.6 Does miR-214 directly target *PIEZO1*?

The present study provided evidence of the first time that miR-214 decreases the expression of PIEZO1 mRNA and protein and decreased intracellular calcium signalling after treatment with the PIEZO1 specific agonist, Yoda1. However, we have not confirmed yet whether miR-214 directly binds to the 3' UTR of *PIEZO1* or whether it indirectly inhibits its expression by binding to an upstream regulator of *PIEZO1*. This would be identified by performing a luciferase reporter assay to see whether luciferase activity is affected and determine whether miR-214 binds to *PIEZO1* mRNA.

6.5.7 What is the effect of miRNA transgenic inhibition or mimic delivery of miR-214 or miR-30d in mouse models of cardiac dysfunction?

Finally, the most important consideration on the effect of these miRNAs in CFs is how this translates to an *in vivo* model. This is essential because, as we have described, there are a multitude of factors that influence cell behaviour in the heart, whether this be communication with the ECM, paracrine signalling with other cells, responding to stress and DAMPs and even intracellular signalling. There are different methods by which miRNA activity can be modulated *in vivo*, for example transgenic mouse models for inhibition in specific cell types (Park et al., 2010) and overexpression (Fornari et al., 2019). One important mouse model to investigate would be the effect of miR-214 on cardiac dysfunction in mice, specifically focusing on its role in decreasing the expression of PIEZO1. The current investigation found that miR-214 expression was increased at 3 weeks post-ISO infusion and at 3 days post-LAD ligation and

it would be interesting to determine what effect this increase has on PIEZO1 expression at these time points. Similarly, an investigation could look at the effect of overexpression of miR-214 in mice at later time points such as 4 weeks post-LAD ligation and 4 weeks post-Ang II infusion when miR-214 levels are unchanged. This is relevant because Bartoli et al. (2022) showed that a global PIEZO1 gain of function mutation caused fibrosis and hypertrophy in mice, with hyperactivation of PIEZO1 evident in CF, and so it would be particularly interesting to investigate what effect miR-214 overexpression specifically in fibroblasts would have on hypertrophy and fibrosis.

6.6 Conclusion

MiRNAs have been implicated in human health and disease and importantly play pathological and cardioprotective roles in cardiovascular disease. The overall aim of this study was to gain an understanding of the roles of miR-21a-5p, -214-3p, -224-5p and -30d-5p in human CF. Investigation revealed expression of each miRNA in mouse and human CF and that *in vivo* models of cardiac dysfunction affected their expression levels. Overexpression of miR-21a regulated mRNA expression of the proinflammatory IL6 family, by decreasing *IL6* and *IL6R* expression and increasing *IL11* expression. MiR-214 overexpression decreased mRNA expression of *IL6* and *COL1A1* and increased expression of *TNC* and secretion of MMP-2. Overexpression of miR-224 decreased gene expression of *IL6* and *MMP3* and increased expression of *ITGA5*. MiR-30d overexpression decreased mRNA expression of *MMP2* and *ITGA5*. MiR-214 and -30d were selected for further analysis by performing proteomics analysis following their overexpression. MiR-30d was predicted to significantly modulate eIF2 and eIF4 signalling pathways and protein translation as well as increase STAT3 expression. MiR-214 led to significant mitochondrial dysfunction and targeted the mitochondrial fission protein, MFN2. MiR-214 was found to regulate expression of various ECM proteins and upregulated expression of the LOX family. Finally, miR-214 decreased mRNA and protein expression of PIEZO1 and functional analysis demonstrated miR-214 mediated PIEZO1-specific downregulation in intracellular calcium signalling. These novel findings provide more understanding of the role that these miRNAs play in the regulation of human cardiac fibroblasts, relevant to cardiac remodelling, and pave the way for future therapeutic and biomarker studies focused on these miRNAs.

List of References

AMERICAN HEART ADAM, O., LÖHFELM, B., THUM, T., GUPTA, S. K., PUHL, S. L., SCHÄFERS, H. J., BÖHM, M. & LAUFS, U. 2012. Role of miR-21 in the pathogenesis of atrial fibrosis. *Basic Res Cardiol,* 107**,** 278.

ADAM, O., THEOBALD, K., LAVALL, D., GRUBE, M., KROEMER, H. K., AMELING, S., SCHÄFERS, H. J., BÖHM, M. & LAUFS, U. 2011. Increased lysyl oxidase expression and collagen cross-linking during atrial fibrillation. *J Mol Cell Cardiol,* 50**,** 678-85.

ALBERT, N. M. 2004. Ventricular dysrhythmias in heart failure. *J Cardiovasc Nurs,* 19**,** S11-26.

ALMEIDA, M. I., SILVA, A. M., VASCONCELOS, D. M., ALMEIDA, C. R., CAIRES, H., PINTO, M. T., CALIN, G. A., SANTOS, S. G. & BARBOSA, M. A. 2016. miR-195 in human primary mesenchymal stromal/stem cells regulates proliferation, osteogenesis and paracrine effect on angiogenesis. *Oncotarget,* 7**,** 7-22.

AMIN, M. M. J., TREVELYAN, C. J. & TURNER, N. A. 2021. MicroRNA-214 in Health and Disease. *Cells,* 10.

AMORIM, I. S., LACH, G. & GKOGKAS, C. G. 2018. The Role of the Eukaryotic Translation Initiation Factor 4E (eIF4E) in Neuropsychiatric Disorders. *Front Genet,* 9**,** 561.

AN, F., WU, X., ZHANG, Y., CHEN, D., LIN, Y., WU, F., DING, J., XIA, M. & ZHAN, Q. 2021. miR-224 Regulates the Aggressiveness of Hepatoma Cells Through the IL-6/STAT3/SMAD4 Pathway. *Turk J Gastroenterol,* 32**,** 532-542.

ANTOON, J. W., NITZCHKE, A. M., MARTIN, E. C., RHODES, L. V., NAM, S., WADSWORTH, S., SALVO, V. A., ELLIOTT, S., COLLINS-BUROW, B., NEPHEW, K. P. & BUROW, M. E. 2013. Inhibition of p38 mitogen-activated protein kinase alters microRNA expression and reverses epithelial-to-mesenchymal transition. *Int J Oncol,* 42**,** 1139-50.

ARMADA, A., GOMES, B. C., VIVEIROS, M., RUEFF, J. & RODRIGUES, A. S. 2019. Regulation of ABCB1 activity by microRNA-200c and microRNA-203a in breast cancer cells: the quest for microRNAs' involvement in cancer drug resistance. *Cancer Drug Resist,* 2**,** 897-911.

ARPINO, V., BROCK, M. & GILL, S. E. 2015. The role of TIMPs in regulation of extracellular matrix proteolysis. *Matrix Biol,* 44-46**,** 247-54.

ASSOCIATION, A. H. 2017. *Classes of Heart Failure* [Online]. https://www.heart.org/en/health-topics/heart-failure/what-is-heart-failure/classes-of-heart-failure: American Heart Association. [Accessed 05/10/2022 2022].

AURORA, A. B., MAHMOUD, A. I., LUO, X., JOHNSON, B. A., VAN ROOIJ, E., MATSUZAKI, S., HUMPHRIES, K. M., HILL, J. A., BASSEL-DUBY, R., SADEK, H. A. & OLSON, E. N. 2012. MicroRNA-214 protects the mouse heart from ischemic injury by controlling Ca^{2+} overload and cell death. *J Clin Invest,* 122**,** 1222-32.

AZEVEDO, P. S., POLEGATO, B. F., MINICUCCI, M. F., PAIVA, S. A. & ZORNOFF, L. A. 2016. Cardiac Remodeling: Concepts, Clinical Impact, Pathophysiological Mechanisms and Pharmacologic Treatment. *Arq Bras Cardiol,* 106**,** 62-9.

BACHMANN, J. C., BAUMGART, S. J., URYGA, A. K., BOSTEEN, M. H., BORGHETTI, G., NYBERG, M. & HERUM, K. M. 2022. Fibrotic Signaling in Cardiac Fibroblasts and Vascular Smooth Muscle Cells: The Dual Roles of Fibrosis in HFpEF and CAD. *Cells,* 11.

BADEN, L. R., EL SAHLY, H. M., ESSINK, B., KOTLOFF, K., FREY, S., NOVAK, R., DIEMERT, D., SPECTOR, S. A., ROUPHAEL, N., CREECH, C. B., MCGETTIGAN, J., KHETAN, S., SEGALL, N., SOLIS, J., BROSZ, A., FIERRO, C., SCHWARTZ, H., NEUZIL, K., COREY, L., GILBERT, P., JANES, H., FOLLMANN, D., MAROVICH, M., MASCOLA, J., POLAKOWSKI, L., LEDGERWOOD, J., GRAHAM, B. S., BENNETT, H., PAJON, R., KNIGHTLY, C., LEAV, B., DENG, W., ZHOU, H., HAN, S., IVARSSON, M., MILLER, J. & ZAKS, T. 2021. Efficacy and Safety of the mRNA-1273 SARS-CoV-2 Vaccine. *N Engl J Med,* 384**,** 403-416.

BADIMON, L., PADRÓ, T. & VILAHUR, G. 2012. Atherosclerosis, platelets and thrombosis in acute ischaemic heart disease. *Eur Heart J Acute Cardiovasc Care,* 1**,** 60-74.

BAGEGHNI, S. A., HEMMINGS, K. E., ZAVA, N., DENTON, C. P., PORTER, K. E., AINSCOUGH, J. F. X., DRINKHILL, M. J. & TURNER, N. A. 2018. Cardiac fibroblast-specific p38α MAP kinase promotes cardiac hypertrophy via a putative paracrine interleukin-6 signaling mechanism. *The FASEB Journal,* 32**,** 4941-4954.

BAI, M., CHEN, H., DING, D., SONG, R., LIN, J., ZHANG, Y., GUO, Y., CHEN, S., DING, G., ZHANG, Y., JIA, Z., HUANG, S., HE, J. C., YANG, L. & ZHANG, A. 2019. MicroRNA-214 promotes chronic kidney disease by disrupting mitochondrial oxidative phosphorylation. *Kidney Int,* 95**,** 1389-1404.

BAR-ELI, M. 2011. Searching for the 'melano-miRs': miR-214 drives melanoma metastasis. *Embo j,* 30**,** 1880-1.

BARCELLOS-HOFF, M. H. & BISSELL, M. J. 1989. A Role for the Extracellular Matrix in Autocrine and Paracrine Regulation of Tissue-Specific Functions. *In:* KREY, L. C., GULYAS, B. J. & MCCRACKEN, J. A. (eds.) *Autocrine and Paracrine Mechanisms in Reproductive Endocrinology.* Boston, MA: Springer US.

BARTOLI, F., EVANS, E. L., BLYTHE, N. M., STEWART, L., CHUNTHARPURSAT-BON, E., DEBANT, M., MUSIALOWSKI, K. E., LICHTENSTEIN, L., PARSONAGE, G., FUTERS, T. S., TURNER, N. A. & BEECH, D. J. 2022. Global PIEZO1 Gain-of-Function Mutation Causes Cardiac Hypertrophy and Fibrosis in Mice. *Cells,* 11.

BATKAI, S., GENSCHEL, C., VIERECK, J., RUMP, S., BÄR, C., BORCHERT, T., TRAXLER, D., RIESENHUBER, M., SPANNBAUER, A., LUKOVIC, D., ZLABINGER, K., HAŠIMBEGOVIĆ, E., WINKLER, J., GARAMVÖLGYI, R., NEITZEL, S., GYÖNGYÖSI, M. & THUM, T. 2020. CDR132L improves systolic and diastolic function in a large animal model of chronic heart failure. *European Heart Journal,* 42**,** 192-201.

BAUM, J. & DUFFY, H. S. 2011. Fibroblasts and myofibroblasts: what are we talking about? *J Cardiovasc Pharmacol,* 57**,** 376-9.

BEECH, D. J. & KALLI, A. C. 2019. Force Sensing by Piezo Channels in Cardiovascular Health and Disease. *Arterioscler Thromb Vasc Biol,* 39**,** 2228-2239.

BERTERO, T., GROSSO, S., ROBBE-SERMESANT, K., LEBRIGAND, K., HÉNAOUI, I. S., PUISSÉGUR, M. P., FOURRE, S., ZARAGOSI, L. E., MAZURE, N. M., PONZIO, G., CARDINAUD, B., BARBRY, P., REZZONICO, R. & MARI, B. 2012. "Seed-Milarity" confers to hsa-miR-210 and hsa-miR-147b similar functional activity. *PLoS One,* 7**,** e44919.

BHUIYAN, T. & MAURER, M. S. 2011. Heart Failure with Preserved Ejection Fraction: Persistent Diagnosis, Therapeutic Enigma. *Curr Cardiovasc Risk Rep,* 5**,** 440-449.

BLYTHE, N. M., MURAKI, K., LUDLOW, M. J., STYLIANIDIS, V., GILBERT, H. T. J., EVANS, E. L., CUTHBERTSON, K., FOSTER, R., SWIFT, J., LI, J., DRINKHILL, M. J., VAN NIEUWENHOVEN, F. A., PORTER, K. E., BEECH, D. J. & TURNER, N. A. 2019. Mechanically activated Piezo1 channels of cardiac fibroblasts stimulate p38 mitogen-activated protein kinase activity and interleukin-6 secretion. *J Biol Chem,* 294**,** 17395-17408.

BONNANS, C., CHOU, J. & WERB, Z. 2014. Remodelling the extracellular matrix in development and disease. *Nat Rev Mol Cell Biol,* 15**,** 786-801.

BORZI, C., CALZOLARI, L., CENTONZE, G., MILIONE, M., SOZZI, G. & FORTUNATO, O. 2017. mir-660-p53-mir-486 Network: A New Key Regulatory Pathway in Lung Tumorigenesis. *Int J Mol Sci,* 18.

BRANCACCIO, M., HIRSCH, E., NOTTE, A., SELVETELLA, G., LEMBO, G. & TARONE, G. 2006. Integrin signalling: The tug-of-war in heart hypertrophy. *Cardiovascular Research,* 70**,** 422-433.

BRETHERTON, R., BUGG, D., OLSZEWSKI, E. & DAVIS, J. 2020. Regulators of cardiac fibroblast cell state. *Matrix Biol,* 91-92**,** 117-135.

BREW, K. & NAGASE, H. 2010. The tissue inhibitors of metalloproteinases (TIMPs): an ancient family with structural and functional diversity. *Biochim Biophys Acta,* 1803**,** 55-71.

BUBB, K., HOLZER, T., NOLTE, J. L., KRÜGER, M., WILSON, R., SCHLÖTZER-SCHREHARDT, U., BRINCKMANN, J., ALTMÜLLER, J., ASZODI, A., FLEISCHHAUER, L., CLAUSEN-SCHAUMANN, H.,

PROBST, K. & BRACHVOGEL, B. 2021. Mitochondrial respiratory chain function promotes extracellular matrix integrity in cartilage. *Journal of Biological Chemistry,* 297.

BUJAK, M., DOBACZEWSKI, M., GONZALEZ-QUESADA, C., XIA, Y., LEUCKER, T., ZYMEK, P., VEERANNA, V., TAGER, A. M., LUSTER, A. D. & FRANGOGIANNIS, N. G. 2009. Induction of the CXC chemokine interferon-gamma-inducible protein 10 regulates the reparative response following myocardial infarction. *Circ Res,* 105**,** 973-83.

BURGESS, M. L., CARVER, W. E., TERRACIO, L., WILSON, S. P., WILSON, M. A. & BORG, T. K. 1994. Integrin-mediated collagen gel contraction by cardiac fibroblasts. Effects of angiotensin II. *Circulation Research,* 74**,** 291-298.

CAO, W., SHI, P. & GE, J.-J. 2017. miR-21 enhances cardiac fibrotic remodeling and fibroblast proliferation via CADM1/STAT3 pathway. *BMC Cardiovascular Disorders,* 17**,** 88.

CAO, Y., TANG, S., NIE, X., ZHOU, Z., RUAN, G., HAN, W., ZHU, Z. & DING, C. 2021. Decreased miR-214-3p activates NF-κB pathway and aggravates osteoarthritis progression. *EBioMedicine,* 65**,** 103283.

CATANESI, M., D'ANGELO, M., TUPONE, M. G., BENEDETTI, E., GIORDANO, A., CASTELLI, V. & CIMINI, A. 2020. MicroRNAs Dysregulation and Mitochondrial Dysfunction in Neurodegenerative Diseases. *Int J Mol Sci,* 21.

CHAKRABORTY, D., ŠUMOVÁ, B., MALLANO, T., CHEN, C.-W., DISTLER, A., BERGMANN, C., LUDOLPH, I., HORCH, R. E., GELSE, K., RAMMING, A., DISTLER, O., SCHETT, G., ŠENOLT, L. & DISTLER, J. H. W. 2017. Activation of STAT3 integrates common profibrotic pathways to promote fibroblast activation and tissue fibrosis. *Nature Communications,* 8**,** 1130.

CHAN, J. A., KRICHEVSKY, A. M. & KOSIK, K. S. 2005. MicroRNA-21 is an antiapoptotic factor in human glioblastoma cells. *Cancer Res,* 65**,** 6029-33.

CHEN, H., ZHANG, F., ZHANG, Y. L. & YANG, X. C. 2021. Relationship between circulating miRNA-21, atrial fibrosis, and atrial fibrillation in patients with atrial enlargement. *Ann Palliat Med,* 10**,** 12742-12749.

CHEN, W., HARBECK, M. C., ZHANG, W. & JACOBSON, J. R. 2013. MicroRNA regulation of integrins. *Transl Res,* 162**,** 133-43.

CHEN, Z., YUAN, Y. C., WANG, Y., LIU, Z., CHAN, H. J. & CHEN, S. 2015. Down-regulation of programmed cell death 4 (PDCD4) is associated with aromatase inhibitor resistance and a poor prognosis in estrogen receptor-positive breast cancer. *Breast Cancer Res Treat,* 152**,** 29-39.

CHENG, Y., HE, Q., JIN, T. & LI, N. 2022. miR-214-3p Protects and Restores the Myocardial Tissue of Rat Myocardial Infarction Model by Targeting PTEN. *Evid Based Complement Alternat Med,* 2022**,** 1175935.

CHENG, Y., JI, R., YUE, J., YANG, J., LIU, X., CHEN, H., DEAN, D. B. & ZHANG, C. 2007. MicroRNAs are aberrantly expressed in hypertrophic heart: do they play a role in cardiac hypertrophy? *Am J Pathol,* 170**,** 1831-40.

CHENG, Y. & ZHANG, C. 2010. MicroRNA-21 in cardiovascular disease. *J Cardiovasc Transl Res,* 3**,** 251-5.

CHEUNG, P.-Y., SAWICKI, G., WOZNIAK, M., WANG, W., RADOMSKI, M. W. & SCHULZ, R. 2000. Matrix Metalloproteinase-2 Contributes to Ischemia-Reperfusion Injury in the Heart. *Circulation,* 101**,** 1833-1839.

CHIONG, M., WANG, Z. V., PEDROZO, Z., CAO, D. J., TRONCOSO, R., IBACACHE, M., CRIOLLO, A., NEMCHENKO, A., HILL, J. A. & LAVANDERO, S. 2011. Cardiomyocyte death: mechanisms and translational implications. *Cell Death & Disease,* 2**,** e244-e244.

CHIPMAN, L. B. & PASQUINELLI, A. E. 2019. miRNA Targeting: Growing beyond the Seed. *Trends Genet,* 35**,** 215-222.

CHRISTOPHER, A. F., KAUR, R. P., KAUR, G., KAUR, A., GUPTA, V. & BANSAL, P. 2016. MicroRNA therapeutics: Discovering novel targets and developing specific therapy. *Perspect Clin Res,* 7**,** 68-74.

CIVITARESE, R. A., KAPUS, A., MCCULLOCH, C. A. & CONNELLY, K. A. 2017. Role of integrins in mediating cardiac fibroblast-cardiomyocyte cross talk: a dynamic relationship in cardiac biology and pathophysiology. *Basic Res Cardiol,* 112**,** 6.

COOK, S. A. & SCHAFER, S. 2020. Hiding in Plain Sight: Interleukin-11 Emerges as a Master Regulator of Fibrosis, Tissue Integrity, and Stromal Inflammation. *Annu Rev Med,* 71**,** 263-276.

CROSET, M., PANTANO, F., KAN, C. W. S., BONNELYE, E., DESCOTES, F., ALIX-PANABIÈRES, C., LECELLIER, C. H., BACHELIER, R., ALLIOLI, N., HONG, S. S., BARTKOWIAK, K., PANTEL, K. & CLÉZARDIN, P. 2018. miRNA-30 Family Members Inhibit Breast Cancer Invasion, Osteomimicry, and Bone Destruction by Directly Targeting Multiple Bone Metastasis-Associated Genes. *Cancer Res,* 78**,** 5259-5273.

CUI, N., HU, M. & KHALIL, R. A. 2017. Biochemical and Biological Attributes of Matrix Metalloproteinases. *Prog Mol Biol Transl Sci,* 147**,** 1-73.

D'ALESSANDRO, E., SCAF, B., MUNTS, C., VAN HUNNIK, A., TREVELYAN, C. J., VERHEULE, S., SPRONK, H. M. H., TURNER, N. A., TEN CATE, H., SCHOTTEN, U. & VAN NIEUWENHOVEN, F. A. 2021. Coagulation Factor Xa Induces Proinflammatory Responses in Cardiac Fibroblasts via Activation of Protease-Activated Receptor-1. *Cells,* 10.

D'SOUZA, S. F. & SRERE, P. A. 1983. Binding of citrate synthase to mitochondrial inner membranes. *J Biol Chem,* 258**,** 4706-9.

DAI, B., WANG, F., NIE, X., DU, H., ZHAO, Y., YIN, Z., LI, H., FAN, J., WEN, Z., WANG, D. W. & CHEN, C. 2020. The Cell Type-Specific Functions of miR-21 in Cardiovascular Diseases. *Front Genet,* 11**,** 563166.

DAI, D. F., JOHNSON, S. C., VILLARIN, J. J., CHIN, M. T., NIEVES-CINTRÓN, M., CHEN, T., MARCINEK, D. J., DORN, G. W., 2ND, KANG, Y. J., PROLLA, T. A., SANTANA, L. F. & RABINOVITCH, P. S. 2011. Mitochondrial oxidative stress mediates angiotensin II-induced cardiac hypertrophy and Galphaq overexpression-induced heart failure. *Circ Res,* 108**,** 837-46.

DAMASE, T. R., SUKHOVERSHIN, R., BOADA, C., TARABALLI, F., PETTIGREW, R. I. & COOKE, J. P. 2021. The Limitless Future of RNA Therapeutics. *Frontiers in Bioengineering and Biotechnology,* 9.

DARBY, I. A., LAVERDET, B., BONTÉ, F. & DESMOULIÈRE, A. 2014. Fibroblasts and myofibroblasts in wound healing. *Clin Cosmet Investig Dermatol,* 7**,** 301-11.

DASEKE, M. J., 2ND, TENKORANG, M. A. A., CHALISE, U., KONFRST, S. R. & LINDSEY, M. L. 2020. Cardiac fibroblast activation during myocardial infarction wound healing: Fibroblast polarization after MI. *Matrix Biol,* 91-92**,** 109-116.

DAVIS, B. N., HILYARD, A. C., LAGNA, G. & HATA, A. 2008. SMAD proteins control DROSHA-mediated microRNA maturation. *Nature,* 454**,** 56-61.

DE SOUZA, R. R. 2002. Aging of myocardial collagen. *Biogerontology,* 3**,** 325-35.

DELEON-PENNELL, K. Y., MESCHIARI, C. A., JUNG, M. & LINDSEY, M. L. 2017. Matrix Metalloproteinases in Myocardial Infarction and Heart Failure. *Prog Mol Biol Transl Sci,* 147**,** 75-100.

DESVIGNES, T., CONTRERAS, A. & POSTLETHWAIT, J. H. 2014. Evolution of the miR199-214 cluster and vertebrate skeletal development. *RNA Biol,* 11**,** 281-94.

DÍEZ, J., GONZÁLEZ, A. & KOVACIC, J. C. 2020. Myocardial Interstitial Fibrosis in Nonischemic Heart Disease, Part 3/4: JACC Focus Seminar. *J Am Coll Cardiol,* 75**,** 2204-2218.

DING, H., WANG, Y., HU, L., XUE, S., WANG, Y., ZHANG, L., ZHANG, Y., QI, H., YU, H., AUNG, L. H. H., AN, Y. & LI, P. 2020. Combined detection of miR-21-5p, miR-30a-3p, miR-30a-5p, miR-155-5p, miR-216a and miR-217 for screening of early heart failure diseases. *Biosci Rep,* 40.

DING, Y. Q., ZHANG, Y. H., LU, J., LI, B., YU, W. J., YUE, Z. B., HU, Y. H., WANG, P. X., LI, J. Y., CAI, S. D., YE, J. T. & LIU, P. Q. 2021. MicroRNA-214 contributes to Ang II-induced cardiac hypertrophy by targeting SIRT3 to provoke mitochondrial malfunction. *Acta Pharmacol Sin,* 42**,** 1422-1436.

DONG, H., DONG, S., ZHANG, L., GAO, X., LV, G., CHEN, W. & SHAO, S. 2016. MicroRNA-214 exerts a Cardio-protective effect by inhibition of fibrosis. *Anat Rec (Hoboken),* 299**,** 1348-57.

DONG, S., CHENG, Y., YANG, J., LI, J., LIU, X., WANG, X., WANG, D., KRALL, T. J., DELPHIN, E. S. & ZHANG, C. 2009. MicroRNA expression signature and the role of microRNA-21 in the early phase of acute myocardial infarction. *J Biol Chem,* 284**,** 29514-25.

DUAN, Q., YANG, L., GONG, W., CHAUGAI, S., WANG, F., CHEN, C., WANG, P., ZOU, M. H. & WANG, D. W. 2015. MicroRNA-214 Is Upregulated in Heart Failure Patients and Suppresses XBP1-Mediated Endothelial Cells Angiogenesis. *J Cell Physiol,* 230**,** 1964-73.

DUNLAY, S. M., WESTON, S. A., REDFIELD, M. M., KILLIAN, J. M. & ROGER, V. L. 2008. Tumor necrosis factor-alpha and mortality in heart failure: a community study. *Circulation,* 118**,** 625-31.

FAN, D., TAKAWALE, A., LEE, J. & KASSIRI, Z. 2012. Cardiac fibroblasts, fibrosis and extracellular matrix remodeling in heart disease. *Fibrogenesis Tissue Repair,* 5**,** 15.

FELKIN, L. E., LARA-PEZZI, E., GEORGE, R., YACOUB, M. H., BIRKS, E. J. & BARTON, P. J. 2009. Expression of extracellular matrix genes during myocardial recovery from heart failure after left ventricular assist device support. *J Heart Lung Transplant,* 28**,** 117-22.

FORNARI, F., GRAMANTIERI, L., CALLEGARI, E., SHANKARAIAH, R. C., PISCAGLIA, F., NEGRINI, M. & GIOVANNINI, C. 2019. MicroRNAs in Animal Models of HCC. *Cancers (Basel),* 11.

FRANCULA-ZANINOVIC, S. & NOLA, I. A. 2018. Management of Measurable Variable Cardiovascular Disease' Risk Factors. *Curr Cardiol Rev,* 14**,** 153-163.

FRANGOGIANNIS, N. G. 2020. Cardiac fibrosis. *Cardiovascular Research,* 117**,** 1450-1488.

FRANTZ, C., STEWART, K. M. & WEAVER, V. M. 2010. The extracellular matrix at a glance. *J Cell Sci,* 123**,** 4195-200.

FREED, D. H., CHILTON, L., LI, Y., DANGERFIELD, A. L., RAIZMAN, J. E., RATTAN, S. G., VISEN, N., HRYSHKO, L. V. & DIXON, I. M. 2011. Role of myosin light chain kinase in cardiotrophin-1-induced cardiac myofibroblast cell migration. *Am J Physiol Heart Circ Physiol,* 301**,** H514-22.

FREY, N., KATUS, H. A., OLSON, E. N. & HILL, J. A. 2004. Hypertrophy of the Heart. *Circulation,* 109**,** 1580-1589.

GAYOSSO-GÓMEZ, L. V. & ORTIZ-QUINTERO, B. 2021. Circulating MicroRNAs in Blood and Other Body Fluids as Biomarkers for Diagnosis, Prognosis, and Therapy Response in Lung Cancer. *Diagnostics (Basel),* 11.

GE, J., YAO, Y., JIA, H., LI, P. & SUN, W. 2020. Inhibition of miR-21 ameliorates LPS-induced acute lung injury through increasing B cell lymphoma-2 expression. *Innate Immun,* 26**,** 693-702.

GOH, K. Y., HE, L., SONG, J., JINNO, M., ROGERS, A. J., SETHU, P., HALADE, G. V., RAJASEKARAN, N. S., LIU, X., PRABHU, S. D., DARLEY-USMAR, V., WENDE, A. R. & ZHOU, L. 2019. Mitoquinone ameliorates pressure overload-induced cardiac fibrosis and left ventricular dysfunction in mice. *Redox Biol,* 21**,** 101100.

GONG, R., JIANG, Z., ZAGIDULLIN, N., LIU, T. & CAI, B. 2021. Regulation of cardiomyocyte fate plasticity: a key strategy for cardiac regeneration. *Signal Transduction and Targeted Therapy,* 6**,** 31.

GRABMAIER, U., CLAUSS, S., GROSS, L., KLIER, I., FRANZ, W. M., STEINBECK, G., WAKILI, R., THEISS, H. D. & BRENNER, C. 2017. Diagnostic and prognostic value of miR-1 and miR-29b on adverse ventricular remodeling after acute myocardial infarction - The SITAGRAMI-miR analysis. *Int J Cardiol,* 244**,** 30-36.

GRIMSBY, J. L., LUCERO, H. A., TRACKMAN, P. C., RAVID, K. & KAGAN, H. M. 2010. Role of lysyl oxidase propeptide in secretion and enzyme activity. *J Cell Biochem,* 111**,** 1231-43.

HALL, C., GEHMLICH, K., DENNING, C. & PAVLOVIC, D. 2021. Complex Relationship Between Cardiac Fibroblasts and Cardiomyocytes in Health and Disease. *J Am Heart Assoc,* 10**,** e019338.

HAN, M., WANG, Y., GUO, G., LI, L., DOU, D., GE, X., LV, P., WANG, F. & GU, Y. 2018. microRNA-30d mediated breast cancer invasion, migration, and EMT by targeting KLF11 and activating STAT3 pathway. *J Cell Biochem,* 119**,** 8138-8145.

HAN, S., ZHAO, F., HSIA, J., MA, X., LIU, Y., TORRES, S., FUJIOKA, H. & ZHU, X. 2021. The role of Mfn2 in the structure and function of endoplasmic reticulum-mitochondrial tethering in vivo. *J Cell Sci,* 134.

HAYASHI, T., KOYAMA, N., AZUMA, Y. & KASHIMATA, M. 2011. Mesenchymal miR-21 regulates branching morphogenesis in murine submandibular gland in vitro. *Dev Biol,* 352**,** 299-307.

HE, S., YANG, F., YANG, M., AN, W., MAGUIRE, E. M., CHEN, Q., XIAO, R., WU, W., ZHANG, L., WANG, W. & XIAO, Q. 2020. miR-214-3p-Sufu-GLI1 is a novel regulatory axis controlling inflammatory smooth muscle cell differentiation from stem cells and neointimal hyperplasia. *Stem Cell Research & Therapy,* 11**,** 465.

HEERKENS, E. H. J., IZZARD, A. S. & HEAGERTY, A. M. 2007. Integrins, Vascular Remodeling, and Hypertension. *Hypertension,* 49**,** 1-4.

HERCHENHAN, A., UHLENBROCK, F., ELIASSON, P., WEIS, M., EYRE, D., KADLER, K. E., MAGNUSSON, S. P. & KJAER, M. 2015. Lysyl Oxidase Activity Is Required for Ordered Collagen Fibrillogenesis by Tendon Cells. *J Biol Chem,* 290**,** 16440-50.

HIGASHIKUNI, Y., TANAKA, K., KATO, M., NUREKI, O., HIRATA, Y., NAGAI, R., KOMURO, I. & SATA, M. 2013. Toll-like receptor-2 mediates adaptive cardiac hypertrophy in response to pressure overload through interleukin-1β upregulation via nuclear factor κB activation. *J Am Heart Assoc,* 2**,** e000267.

HONG, D. S., KANG, Y.-K., BORAD, M., SACHDEV, J., EJADI, S., LIM, H. Y., BRENNER, A. J., PARK, K., LEE, J.-L., KIM, T.-Y., SHIN, S., BECERRA, C. R., FALCHOOK, G., STOUDEMIRE, J., MARTIN, D., KELNAR, K., PELTIER, H., BONATO, V., BADER, A. G., SMITH, S., KIM, S., O'NEILL, V. & BEG, M. S. 2020. Phase 1 study of MRX34, a liposomal miR-34a mimic, in patients with advanced solid tumours. *British Journal of Cancer,* 122**,** 1630-1637.

HOPKINS, A. L. & GROOM, C. R. 2002. The druggable genome. *Nat Rev Drug Discov,* 1**,** 727-30.

HSUEH, W. A., LAW, R. E. & DO, Y. S. 1998. Integrins, Adhesion, and Cardiac Remodeling. *Hypertension,* 31**,** 176-180.

HU, Q., TIAN, T., LENG, Y., TANG, Y., CHEN, S., LV, Y., LIANG, J., LIU, Y., LIU, T., SHEN, L. & DONG, X. 2022. The O-glycosylating enzyme GALNT2 acts as an oncogenic driver in non-small cell lung cancer. *Cell Mol Biol Lett,* 27**,** 71.

HU, Y., LI, G., ZHANG, Y., LIU, N., ZHANG, P., PAN, C., NIE, H., LI, Q. & TANG, Z. 2018. Upregulated TSG-6 Expression in ADSCs Inhibits the BV2 Microglia-Mediated Inflammatory Response. *BioMed Research International,* 2018**,** 7239181.

HUA, X., WANG, Y. Y., JIA, P., XIONG, Q., HU, Y., CHANG, Y., LAI, S., XU, Y., ZHAO, Z. & SONG, J. 2020. Multi-level transcriptome sequencing identifies COL1A1 as a candidate marker in human heart failure progression. *BMC Med,* 18**,** 2.

HUANG, L., LI, L., CHEN, X., ZHANG, H. & SHI, Z. 2016. MiR-103a targeting Piezo1 is involved in acute myocardial infarction through regulating endothelium function. *Cardiol J,* 23**,** 556-562.

HUMERES, C. & FRANGOGIANNIS, N. G. 2019. Fibroblasts in the Infarcted, Remodeling, and Failing Heart. *JACC Basic Transl Sci,* 4**,** 449-467.

HUMPHREYS, D. T., WESTMAN, B. J., MARTIN, D. I. K. & PREISS, T. 2005. MicroRNAs control translation initiation by inhibiting eukaryotic initiation factor 4E/cap and poly(A) tail function. *Proceedings of the National Academy of Sciences,* 102**,** 16961-16966.

HUO, K. G., RICHER, C., BERILLO, O., MAHJOUB, N., FRAULOB-AQUINO, J. C., BARHOUMI, T., OUERD, S., COELHO, S. C., SINNETT, D., PARADIS, P. & SCHIFFRIN, E. L. 2019. miR-431-5p Knockdown Protects Against Angiotensin II-Induced Hypertension and Vascular Injury. *Hypertension,* 73**,** 1007-1017.

IGARASHI, J., NIWA, Y. & SUGIYAMA, D. 2022. Research and development of oligonucleotide therapeutics in Japan for rare diseases. *Future Rare Diseases,* 2**,** FRD19.

IMANAKA-YOSHIDA, K., HIROE, M., NISHIKAWA, T., ISHIYAMA, S., SHIMOJO, T., OHTA, Y., SAKAKURA, T. & YOSHIDA, T. 2001. Tenascin-C modulates adhesion of cardiomyocytes to extracellular matrix during tissue remodeling after myocardial infarction. *Lab Invest,* 81**,** 1015-24.

IMANAKA-YOSHIDA, K., TAWARA, I. & YOSHIDA, T. 2020. Tenascin-C in cardiac disease: a sophisticated controller of inflammation, repair, and fibrosis. *Am J Physiol Cell Physiol,* 319**,** C781-c796.

IVEY, M. J. & TALLQUIST, M. D. 2016. Defining the Cardiac Fibroblast. *Circ J,* 80**,** 2269-2276.
JACKSON, B. M., GORMAN, J. H., 3RD, SALGO, I. S., MOAINIE, S. L., PLAPPERT, T., ST JOHN-SUTTON, M., EDMUNDS, L. H., JR. & GORMAN, R. C. 2003. Border zone geometry increases wall stress after myocardial infarction: contrast echocardiographic assessment. *Am J Physiol Heart Circ Physiol,* 284**,** H475-9.
JACKSON, R. J., HELLEN, C. U. & PESTOVA, T. V. 2010. The mechanism of eukaryotic translation initiation and principles of its regulation. *Nat Rev Mol Cell Biol,* 11**,** 113-27.
JAFARI, N., ABEDIANKENARI, S. & HOSSEIN-NATAJ, H. 2021. miR-34a mimic or pre-mir-34a, which is the better option for cancer therapy? KatoIII as a model to study miRNA action in human gastric cancer cells. *Cancer Cell Int,* 21**,** 178.
JAMES, K., BRYL-GORECKA, P., OLDE, B., GIDLOF, O., TORNGREN, K. & ERLINGE, D. 2022. Increased expression of miR-224-5p in circulating extracellular vesicles of patients with reduced coronary flow reserve. *BMC Cardiovasc Disord,* 22**,** 321.
JAVADOV, S., KOZLOV, A. V. & CAMARA, A. K. S. 2020. Mitochondria in Health and Diseases. *Cells,* 9.
JAZBUTYTE, V. & THUM, T. 2010. MicroRNA-21: from cancer to cardiovascular disease. *Curr Drug Targets,* 11**,** 926-35.
JIANG, X., NING, Q. & WANG, J. 2013. Angiotensin II induced differentially expressed microRNAs in adult rat cardiac fibroblasts. *J Physiol Sci,* 63**,** 31-38.
JUAN, A. H., KUMAR, R. M., MARX, J. G., YOUNG, R. A. & SARTORELLI, V. 2009. Mir-214-dependent regulation of the polycomb protein Ezh2 in skeletal muscle and embryonic stem cells. *Mol Cell,* 36**,** 61-74.
KAKKAR, R. & LEE, R. T. 2010. Intramyocardial Fibroblast Myocyte Communication. *Circulation Research,* 106**,** 47-57.
KAMKIN, A., KISELEVA, I., ISENBERG, G., WAGNER, K. D., GÜNTHER, J., THERES, H. & SCHOLZ, H. 2003. Cardiac fibroblasts and the mechano-electric feedback mechanism in healthy and diseased hearts. *Prog Biophys Mol Biol,* 82**,** 111-20.
KEEPERS, B., LIU, J. & QIAN, L. 2020. What's in a cardiomyocyte - And how do we make one through reprogramming? *Biochim Biophys Acta Mol Cell Res,* 1867**,** 118464.
KHAN, A. A., BETEL, D., MILLER, M. L., SANDER, C., LESLIE, C. S. & MARKS, D. S. 2009. Transfection of small RNAs globally perturbs gene regulation by endogenous microRNAs. *Nat Biotechnol,* 27**,** 549-55.
KIM, H. C. 2021. Epidemiology of cardiovascular disease and its risk factors in Korea. *Global health & medicine,* 3**,** 134-141.
KIM, P., CHU, N., DAVIS, J. & KIM, D. H. 2018. Mechanoregulation of Myofibroblast Fate and Cardiac Fibrosis. *Adv Biosyst,* 2.
KIMURA, T., TAJIRI, K., SATO, A., SAKAI, S., WANG, Z., YOSHIDA, T., UEDE, T., HIROE, M., AONUMA, K., IEDA, M. & IMANAKA-YOSHIDA, K. 2019. Tenascin-C accelerates adverse ventricular remodelling after myocardial infarction by modulating macrophage polarization. *Cardiovasc Res,* 115**,** 614-624.
KUMAR, D., NARANG, R., SREENIVAS, V., RASTOGI, V., BHATIA, J., SALUJA, D. & SRIVASTAVA, K. 2020. Circulatory miR-133b and miR-21 as Novel Biomarkers in Early Prediction and Diagnosis of Coronary Artery Disease. *Genes (Basel),* 11.
KUMARI, S., PANDA, T. K. & PRADHAN, T. 2017. Lysyl Oxidase: Its Diversity in Health and Diseases. *Indian J Clin Biochem,* 32**,** 134-141.
KUROSE, H. 2021. Cardiac Fibrosis and Fibroblasts. *Cells,* 10.
LAGOS-QUINTANA, M., RAUHUT, R., LENDECKEL, W. & TUSCHL, T. 2001. Identification of novel genes coding for small expressed RNAs. *Science,* 294**,** 853-8.
LAI, E. C., WIEL, C. & RUBIN, G. M. 2004. Complementary miRNA pairs suggest a regulatory role for miRNA:miRNA duplexes. *Rna,* 10**,** 171-5.
LANDGRAF, P., RUSU, M., SHERIDAN, R., SEWER, A., IOVINO, N., ARAVIN, A., PFEFFER, S., RICE, A., KAMPHORST, A. O., LANDTHALER, M., LIN, C., SOCCI, N. D., HERMIDA, L., FULCI, V.,

CHIARETTI, S., FOÀ, R., SCHLIWKA, J., FUCHS, U., NOVOSEL, A., MÜLLER, R. U., SCHERMER, B., BISSELS, U., INMAN, J., PHAN, Q., CHIEN, M., WEIR, D. B., CHOKSI, R., DE VITA, G., FREZZETTI, D., TROMPETER, H. I., HORNUNG, V., TENG, G., HARTMANN, G., PALKOVITS, M., DI LAURO, R., WERNET, P., MACINO, G., ROGLER, C. E., NAGLE, J. W., JU, J., PAPAVASILIOU, F. N., BENZING, T., LICHTER, P., TAM, W., BROWNSTEIN, M. J., BOSIO, A., BORKHARDT, A., RUSSO, J. J., SANDER, C., ZAVOLAN, M. & TUSCHL, T. 2007. A mammalian microRNA expression atlas based on small RNA library sequencing. *Cell,* 129**,** 1401-14.

LATIJNHOUWERS, M., BERGERS, M., PONEC, M., DIJKMAN, H., ANDRIESSEN, M. & SCHALKWIJK, J. 1997. Human epidermal keratinocytes are a source of tenascin-C during wound healing. *J Invest Dermatol,* 108**,** 776-83.

LEE, Y. B., BANTOUNAS, I., LEE, D. Y., PHYLACTOU, L., CALDWELL, M. A. & UNEY, J. B. 2009. Twist-1 regulates the miR-199a/214 cluster during development. *Nucleic Acids Res,* 37**,** 123-8.

LEHRKE, M., GREIF, M., BROEDL, U. C., LEBHERZ, C., LAUBENDER, R. P., BECKER, A., VON ZIEGLER, F., TITTUS, J., REISER, M., BECKER, C., GÖKE, B., STEINBECK, G., LEBER, A. W. & PARHOFER, K. G. 2009. MMP-1 serum levels predict coronary atherosclerosis in humans. *Cardiovascular Diabetology,* 8**,** 50.

LEVICK, S. P. & WIDIAPRADJA, A. 2020. The Diabetic Cardiac Fibroblast: Mechanisms Underlying Phenotype and Function. *Int J Mol Sci,* 21.

LI, J., FAN, R., ZHAO, S., LIU, L., GUO, S., WU, N., ZHANG, W. & CHEN, P. 2011. Reactive oxygen species released from hypoxic hepatocytes regulates MMP-2 expression in hepatic stellate cells. *Int J Mol Sci,* 12**,** 2434-47.

LI, J., SALVADOR, A. M., LI, G., VALKOV, N., ZIEGLER, O., YERI, A., XIAO, C. Y., MEECHOOVET, B., ALSOP, E., RODOSTHENOUS, R. S., KUNDU, P., HUAN, T., LEVY, D., TIGGES, J., PICO, A. R., GHIRAN, I., SILVERMAN, M. G., MENG, X., KITCHEN, R., XU, J., KEUREN-JENSEN, K. V., SHAH, R., XIAO, J. & DAS, S. 2021. Mir-30d Regulates Cardiac Remodeling by Intracellular and Paracrine Signaling. *Circulation Research,* 128**,** e1-e23.

LI, J., SHA, Z., ZHU, X., XU, W., YUAN, W., YANG, T., JIN, B., YAN, Y., CHEN, R., WANG, S., YAO, J., XU, J., WANG, Z., LI, G., DAS, S., YANG, L. & XIAO, J. 2022a. Targeting miR-30d reverses pathological cardiac hypertrophy. *EBioMedicine,* 81**,** 104108.

LI, P., WANG, J., GUO, F., ZHENG, B. & ZHANG, X. 2020. A novel inhibitory role of microRNA-224 in particulate matter 2.5-induced asthmatic mice by inhibiting TLR2. *J Cell Mol Med,* 24**,** 3040-3052.

LI, Q. S., MENG, F. Y., ZHAO, Y. H., JIN, C. L., TIAN, J. & YI, X. J. 2017. Inhibition of microRNA-214-5p promotes cell survival and extracellular matrix formation by targeting collagen type IV alpha 1 in osteoblastic MC3T3-E1 cells. *Bone Joint Res,* 6**,** 464-471.

LI, X., GARCIA-ELIAS, A., BENITO, B. & NATTEL, S. 2022b. The effects of cardiac stretch on atrial fibroblasts: analysis of the evidence and potential role in atrial fibrillation. *Cardiovasc Res,* 118**,** 440-460.

LI, Y., ZHAO, L., QI, Y. & YANG, X. 2019. MicroRNA-214 upregulates HIF-1α and VEGF by targeting ING4 in lung cancer cells. *Mol Med Rep,* 19**,** 4935-4945.

LIANG, L., YANG, Z., DENG, Q., JIANG, Y., CHENG, Y., SUN, Y. & LI, L. 2021. miR-30d-5p suppresses proliferation and autophagy by targeting ATG5 in renal cell carcinoma. *FEBS Open Bio,* 11**,** 529-540.

LIM, G. B. 2020. Complexity and plasticity of cardiac cellular composition. *Nature Reviews Cardiology,* 17**,** 759-759.

LIM, K. R., MARUYAMA, R. & YOKOTA, T. 2017. Eteplirsen in the treatment of Duchenne muscular dystrophy. *Drug Des Devel Ther,* 11**,** 533-545.

LIM, L. P., GLASNER, M. E., YEKTA, S., BURGE, C. B. & BARTEL, D. P. 2003. Vertebrate microRNA genes. *Science,* 299**,** 1540.

LIN, Z. Y., CHEN, G., ZHANG, Y. Q., HE, H. C., LIANG, Y. X., YE, J. H., LIANG, Y. K., MO, R. J., LU, J. M., ZHUO, Y. J., ZHENG, Y., JIANG, F. N., HAN, Z. D., WU, S. L., ZHONG, W. D. & WU, C. L. 2017.

MicroRNA-30d promotes angiogenesis and tumor growth via MYPT1/c-JUN/VEGFA pathway and predicts aggressive outcome in prostate cancer. *Mol Cancer,* 16**,** 48.

LINDSEY, M. L., IYER, R. P., ZAMILPA, R., YABLUCHANSKIY, A., DELEON-PENNELL, K. Y., HALL, M. E., KAPLAN, A., ZOUEIN, F. A., BRATTON, D., FLYNN, E. R., CANNON, P. L., TIAN, Y., JIN, Y.-F., LANGE, R. A., TOKMINA-ROSZYK, D., FIELDS, G. B. & DE CASTRO BRÁS, L. E. 2015. A Novel Collagen Matricryptin Reduces Left Ventricular Dilation Post-Myocardial Infarction by Promoting Scar Formation and Angiogenesis. *Journal of the American College of Cardiology,* 66**,** 1364-1374.

LING, H., PICKARD, K., IVAN, C., ISELLA, C., IKUO, M., MITTER, R., SPIZZO, R., BULLOCK, M., BRAICU, C., PILECZKI, V., VINCENT, K., PICHLER, M., STIEGELBAUER, V., HOEFLER, G., ALMEIDA, M. I., HSIAO, A., ZHANG, X., PRIMROSE, J., PACKHAM, G., LIU, K., BOJJA, K., GAFÀ, R., XIAO, L., ROSSI, S., SONG, J. H., VANNINI, I., FANINI, F., KOPETZ, S., ZWEIDLER-MCKAY, P., WANG, X., IONESCU, C., IRIMIE, A., FABBRI, M., LANZA, G., HAMILTON, S. R., BERINDAN-NEAGOE, I., MEDICO, E., MIRNEZAMI, A., CALIN, G. A. & NICOLOSO, M. S. 2016. The clinical and biological significance of MIR-224 expression in colorectal cancer metastasis. *Gut,* 65**,** 977-989.

LIU, H., LEI, C., HE, Q., PAN, Z., XIAO, D. & TAO, Y. 2018. Nuclear functions of mammalian MicroRNAs in gene regulation, immunity and cancer. *Molecular Cancer,* 17**,** 64.

LIU, J., CHEN, W., ZHANG, H., LIU, T. & ZHAO, L. 2017. miR-214 targets the PTEN-mediated PI3K/Akt signaling pathway and regulates cell proliferation and apoptosis in ovarian cancer. *Oncol Lett,* 14**,** 5711-5718.

LIU, R., DU, J., ZHOU, J., ZHONG, B., BA, L., ZHANG, J., LIU, Y. & LIU, S. 2021. Elevated microRNA-21 Is a Brake of Inflammation Involved in the Development of Nasal Polyps. *Front Immunol,* 12**,** 530488.

LIU, X., DONG, Y., CHEN, S., ZHANG, G., ZHANG, M., GONG, Y. & LI, X. 2015. Circulating MicroRNA-146a and MicroRNA-21 Predict Left Ventricular Remodeling after ST-Elevation Myocardial Infarction. *Cardiology,* 132**,** 233-41.

LIU, Y., NIE, H., ZHANG, K., MA, D., YANG, G., ZHENG, Z., LIU, K., YU, B., ZHAI, C. & YANG, S. 2014. A feedback regulatory loop between HIF-1α and miR-21 in response to hypoxia in cardiomyocytes. *FEBS Lett,* 588**,** 3137-46.

LIU, Y. & ZHU, X. 2017. Endoplasmic reticulum-mitochondria tethering in neurodegenerative diseases. *Transl Neurodegener,* 6**,** 21.

LÖFFLER, D., BROCKE-HEIDRICH, K., PFEIFER, G., STOCSITS, C., HACKERMÜLLER, J., KRETZSCHMAR, A. K., BURGER, R., GRAMATZKI, M., BLUMERT, C., BAUER, K., CVIJIC, H., ULLMANN, A. K., STADLER, P. F. & HORN, F. 2007. Interleukin-6 dependent survival of multiple myeloma cells involves the Stat3-mediated induction of microRNA-21 through a highly conserved enhancer. *Blood,* 110**,** 1330-3.

LÓPEZ, B., GONZÁLEZ, A., HERMIDA, N., VALENCIA, F., DE TERESA, E. & DÍEZ, J. 2010. Role of lysyl oxidase in myocardial fibrosis: from basic science to clinical aspects. *Am J Physiol Heart Circ Physiol,* 299**,** H1-9.

LORENZEN, J. M., SCHAUERTE, C., HÜBNER, A., KÖLLING, M., MARTINO, F., SCHERF, K., BATKAI, S., ZIMMER, K., FOINQUINOS, A., KAUCSAR, T., FIEDLER, J., KUMARSWAMY, R., BANG, C., HARTMANN, D., GUPTA, S. K., KIELSTEIN, J., JUNGMANN, A., KATUS, H. A., WEIDEMANN, F., MÜLLER, O. J., HALLER, H. & THUM, T. 2015. Osteopontin is indispensible for AP1-mediated angiotensin II-related miR-21 transcription during cardiac fibrosis. *Eur Heart J,* 36**,** 2184-96.

LOTHER, A., BERGEMANN, S., DENG, L., MOSER, M., BODE, C. & HEIN, L. 2018. Cardiac Endothelial Cell Transcriptome. *Arteriosclerosis, Thrombosis, and Vascular Biology,* 38**,** 566-574.

LU, X., YU, Y. & TAN, S. 2020. The role of the miR-21-5p-mediated inflammatory pathway in ulcerative colitis. *Exp Ther Med,* 19**,** 981-989.

LU, X. X., CAO, L. Y., CHEN, X., XIAO, J., ZOU, Y. & CHEN, Q. 2016. PTEN Inhibits Cell Proliferation, Promotes Cell Apoptosis, and Induces Cell Cycle Arrest via Downregulating the

PI3K/AKT/hTERT Pathway in Lung Adenocarcinoma A549 Cells. *Biomed Res Int,* 2016**,** 2476842.

LV, L., LI, T., LI, X., XU, C., LIU, Q., JIANG, H., LI, Y., LIU, Y., YAN, H., HUANG, Q., ZHOU, Y., ZHANG, M., SHAN, H. & LIANG, H. 2018. The lncRNA Plscr4 Controls Cardiac Hypertrophy by Regulating miR-214. *Mol Ther Nucleic Acids,* 10**,** 387-397.

LV, P., ZHOU, M., HE, J., MENG, W., MA, X., DONG, S., MENG, X., ZHAO, X., WANG, X. & HE, F. 2014. Circulating miR-208b and miR-34a are associated with left ventricular remodeling after acute myocardial infarction. *Int J Mol Sci,* 15**,** 5774-88.

MA, J., HUANG, K., MA, Y., ZHOU, M. & FAN, S. 2018. The TAZ–miR-224–SMAD4 axis promotes tumorigenesis in osteosarcoma. *Cell Death & Disease,* 8**,** e2539-e2539.

MA, L., HUANG, C., WANG, X. J., XIN, D. E., WANG, L. S., ZOU, Q. C., ZHANG, Y. S., TAN, M. D., WANG, Y. M., ZHAO, T. C., CHATTERJEE, D., ALTURA, R. A., WANG, C., XU, Y. S., YANG, J. H., FAN, Y. S., HAN, B. H., SI, J., ZHANG, X., CHENG, J., CHANG, Z. & CHIN, Y. E. 2017a. Lysyl Oxidase 3 Is a Dual-Specificity Enzyme Involved in STAT3 Deacetylation and Deacetylimination Modulation. *Mol Cell,* 65**,** 296-309.

MA, Y., IYER, R. P., JUNG, M., CZUBRYT, M. P. & LINDSEY, M. L. 2017b. Cardiac Fibroblast Activation Post-Myocardial Infarction: Current Knowledge Gaps. *Trends Pharmacol Sci,* 38**,** 448-458.

MALIZIA, A. P. & WANG, D. Z. 2011. MicroRNAs in cardiomyocyte development. *Wiley Interdiscip Rev Syst Biol Med,* 3**,** 183-90.

MAO, L., LIU, S., HU, L., JIA, L., WANG, H., GUO, M., CHEN, C., LIU, Y. & XU, L. 2018. miR-30 Family: A Promising Regulator in Development and Disease. *Biomed Res Int,* 2018**,** 9623412.

MAQBOOL, A., SPARY, E. J., MANFIELD, I. W., RUHMANN, M., ZULIANI-ALVAREZ, L., GAMBOA-ESTEVES, F. O., PORTER, K. E., DRINKHILL, M. J., MIDWOOD, K. S. & TURNER, N. A. 2016. Tenascin C upregulates interleukin-6 expression in human cardiac myofibroblasts via toll-like receptor 4. *World J Cardiol,* 8**,** 340-50.

MATSUMURA, S., IWANAGA, S., MOCHIZUKI, S., OKAMOTO, H., OGAWA, S. & OKADA, Y. 2005. Targeted deletion or pharmacological inhibition of MMP-2 prevents cardiac rupture after myocardial infarction in mice. *J Clin Invest,* 115**,** 599-609.

MELMAN, Y. F., SHAH, R., DANIELSON, K., XIAO, J., SIMONSON, B., BARTH, A., CHAKIR, K., LEWIS, G. D., LAVENDER, Z., TRUONG, Q. A., KLEBER, A., DAS, R., ROSENZWEIG, A., WANG, Y., KASS, D., SINGH, J. P. & DAS, S. 2015. Circulating MicroRNA-30d Is Associated With Response to Cardiac Resynchronization Therapy in Heart Failure and Regulates Cardiomyocyte Apoptosis: A Translational Pilot Study. *Circulation,* 131**,** 2202-2216.

MI, X., TANG, W., CHEN, X., LIU, F. & TANG, X. 2016. Mitofusin 2 attenuates the histone acetylation at collagen IV promoter in diabetic nephropathy. *J Mol Endocrinol,* 57**,** 233-249.

MILLS, J., CAPECE, M., COCUCCI, E., TESSARI, A. & PALMIERI, D. 2019. Cancer-Derived Extracellular Vesicle-Associated MicroRNAs in Intercellular Communication: One Cell's Trash Is Another Cell's Treasure. *Int J Mol Sci,* 20.

MILUTINOVIĆ, A., ŠUPUT, D. & ZORC-PLESKOVIČ, R. 2020. Pathogenesis of atherosclerosis in the tunica intima, media, and adventitia of coronary arteries: An updated review. *Bosn J Basic Med Sci,* 20**,** 21-30.

MIRBASE. 2022a. *Mature sequence hsa-miR-21-5p* [Online]. https://www.mirbase.org/cgi-bin/mature.pl?mature_acc=MIMAT0000076: University of Manchester. [Accessed 12/10/2022 2022].

MIRBASE. 2022b. *Mature sequence hsa-miR-30d-3p* [Online]. mirbase.org: University of Manchester. Available: https://www.mirbase.org/cgi-bin/mirna_entry.pl?acc=MI0000255 [Accessed 19/10/2022 2022].

MIRBASE. 2022c. *Mature sequence hsa-miR-214-3p* [Online]. mirbase.org. Available: https://www.mirbase.org/cgi-bin/mature.pl?mature_acc=MIMAT0000271 [Accessed 18/10/22 2022].

MIRBASE. 2022d. *Mature sequence hsa-miR-224-5p* [Online]. mirbase.org: University of Manchester. Available: https://www.mirbase.org/cgi-bin/mirna_entry.pl?acc=MI0000301 [Accessed 19/10/2022 2022].

MIRNA, M., PAAR, V., TOPF, A., KRAUS, T., SOTLAR, K., AIGNER, A., EWE, A., WATZINGER, S., PODESSER, B. K., HACKL, M., PISTULLI, R., HOPPE, U. C., KISS, A. & LICHTENAUER, M. 2022. A new player in the game: treatment with antagomiR-21a-5p significantly attenuates histological and echocardiographic effects of experimental autoimmune myocarditis. *Cardiovasc Res,* 118**,** 556-572.

MIROSHNIKOVA, Y. A., MOUW, J. K., BARNES, J. M., PICKUP, M. W., LAKINS, JOHNATHAN N., KIM, Y., LOBO, K., PERSSON, A. I., REIS, G. F., MCKNIGHT, T. R., HOLLAND, ERIC C., PHILLIPS, J. J. & WEAVER, V. M. 2016. Tissue mechanics promote IDH1-dependent HIF1α–tenascin C feedback to regulate glioblastoma aggression. *Nature Cell Biology,* 18**,** 1336-1345.

MITCHELL, M. D., LAIRD, R. E., BROWN, R. D. & LONG, C. S. 2007. IL-1beta stimulates rat cardiac fibroblast migration via MAP kinase pathways. *Am J Physiol Heart Circ Physiol,* 292**,** H1139-47.

MØLLER, T., JAMES, J. P., HOLMSTRØM, K., SØRENSEN, F. B., LINDEBJERG, J. & NIELSEN, B. S. 2019. Co-Detection of miR-21 and TNF-α mRNA in Budding Cancer Cells in Colorectal Cancer. *Int J Mol Sci,* 20.

MORISHIMA, M. & ONO, K. 2021. Serum microRNA-30d is a sensitive biomarker for angiotensin II-induced cardiovascular complications in rats. *Heart Vessels,* 36**,** 1597-1606.

MURPHY, S. P., IBRAHIM, N. E. & JANUZZI, J. L., JR. 2020. Heart Failure With Reduced Ejection Fraction: A Review. *JAMA,* 324**,** 488-504.

MYLONAS, K. J., TURNER, N. A., BAGEGHNI, S. A., KENYON, C. J., WHITE, C. I., MCGREGOR, K., KIMMITT, R. A., SULSTON, R., KELLY, V., WALKER, B. R., PORTER, K. E., CHAPMAN, K. E. & GRAY, G. A. 2017. 11β-HSD1 suppresses cardiac fibroblast CXCL2, CXCL5 and neutrophil recruitment to the heart post MI. *J Endocrinol,* 233**,** 315-327.

NAGASE, H., VISSE, R. & MURPHY, G. 2006. Structure and function of matrix metalloproteinases and TIMPs. *Cardiovascular Research,* 69**,** 562-573.

NAGPAL, V., RAI, R., PLACE, A. T., MURPHY, S. B., VERMA, S. K., GHOSH, A. K. & VAUGHAN, D. E. 2016. MiR-125b Is Critical for Fibroblast-to-Myofibroblast Transition and Cardiac Fibrosis. *Circulation,* 133**,** 291-301.

NGOH, G. A., PAPANICOLAOU, K. N. & WALSH, K. 2012. Loss of mitofusin 2 promotes endoplasmic reticulum stress. *J Biol Chem,* 287**,** 20321-32.

NICOLSON, G. L. 2014. Mitochondrial Dysfunction and Chronic Disease: Treatment With Natural Supplements. *Integr Med (Encinitas),* 13**,** 35-43.

NIELSEN, S. H., MOUTON, A. J., DELEON-PENNELL, K. Y., GENOVESE, F., KARSDAL, M. & LINDSEY, M. L. 2019. Understanding cardiac extracellular matrix remodeling to develop biomarkers of myocardial infarction outcomes. *Matrix Biol,* 75-76**,** 43-57.

NING, Q. & JIANG, X. 2013. Angiotensin II upregulated the expression of microRNA-224 but not microRNA-21 in adult rat cardiac fibroblasts. *Biomed Rep,* 1**,** 776-780.

NOURAEE, N. & MOWLA, S. J. 2015. miRNA therapeutics in cardiovascular diseases: promises and problems. *Front Genet,* 6**,** 232.

O'BRIEN, J., HAYDER, H., ZAYED, Y. & PENG, C. 2018. Overview of MicroRNA Biogenesis, Mechanisms of Actions, and Circulation. *Front Endocrinol (Lausanne),* 9**,** 402.

O'DONOGHUE, M. L., GLASER, R., CAVENDER, M. A., AYLWARD, P. E., BONACA, M. P., BUDAJ, A., DAVIES, R. Y., DELLBORG, M., FOX, K. A., GUTIERREZ, J. A., HAMM, C., KISS, R. G., KOVAR, F., KUDER, J. F., IM, K. A., LEPORE, J. J., LOPEZ-SENDON, J. L., OPHUIS, T. O., PARKHOMENKO, A., SHANNON, J. B., SPINAR, J., TANGUAY, J. F., RUDA, M., STEG, P. G., THEROUX, P., WIVIOTT, S. D., LAWS, I., SABATINE, M. S. & MORROW, D. A. 2016. Effect of Losmapimod on Cardiovascular Outcomes in Patients Hospitalized With Acute Myocardial Infarction: A Randomized Clinical Trial. *Jama,* 315**,** 1591-9.

OLSON, E. R., NAUGLE, J. E., ZHANG, X., BOMSER, J. A. & MESZAROS, J. G. 2005. Inhibition of cardiac fibroblast proliferation and myofibroblast differentiation by resveratrol. *Am J Physiol Heart Circ Physiol,* 288**,** H1131-8.

ORGANIZATION, W. H. 2022. *Number of clinical trial registrations by location, disease, phase of development, age and sex of trial participants (1999-2021)* [Online]. https://www.who.int/observatories/global-observatory-on-health-research-and-development/monitoring/number-of-trial-registrations-by-year-location-disease-and-phase-of-development: World Health Organization. [Accessed 29/11/2022 2022].

PAGE-MCCAW, A., EWALD, A. J. & WERB, Z. 2007. Matrix metalloproteinases and the regulation of tissue remodelling. *Nat Rev Mol Cell Biol,* 8**,** 221-33.

PALOMER, X., CAPDEVILA-BUSQUETS, E., BOTTERI, G., DAVIDSON, M. M., RODRÍGUEZ, C., MARTÍNEZ-GONZÁLEZ, J., VIDAL, F., BARROSO, E., CHAN, T. O., FELDMAN, A. M. & VÁZQUEZ-CARRERA, M. 2015. miR-146a targets Fos expression in human cardiac cells. *Dis Model Mech,* 8**,** 1081-91.

PARK, C. Y., CHOI, Y. S. & MCMANUS, M. T. 2010. Analysis of microRNA knockouts in mice. *Hum Mol Genet,* 19**,** R169-75.

PARK, S., RANJBARVAZIRI, S., LAY, F. D., ZHAO, P., MILLER, M. J., DHALIWAL, J. S., HUERTAS-VAZQUEZ, A., WU, X., QIAO, R., SOFFER, J. M., RAU, C., WANG, Y., MIKKOLA, H. K. A., LUSIS, A. J. & ARDEHALI, R. 2018. Genetic Regulation of Fibroblast Activation and Proliferation in Cardiac Fibrosis. *Circulation,* 138**,** 1224-1235.

PAUSCHINGER, M., CHANDRASEKHARAN, K. & SCHULTHEISS, H. P. 2004. Myocardial remodeling in viral heart disease: possible interactions between inflammatory mediators and MMP-TIMP system. *Heart Fail Rev,* 9**,** 21-31.

PENG, X., GUO, C., WU, Y., YING, M., CHANG, R., SONG, L., ZHAN, L. & ZHAN, X. 2021. miR-224-5p regulates the proliferation, migration and invasion of pancreatic mucinous cystadenocarcinoma by targeting PTEN. *Mol Med Rep,* 23.

PENNA, E., ORSO, F. & TAVERNA, D. 2015. miR-214 as a key hub that controls cancer networks: small player, multiple functions. *J Invest Dermatol,* 135**,** 960-969.

PHILIPPE, L., ALSALEH, G., SUFFERT, G., MEYER, A., GEORGEL, P., SIBILIA, J., WACHSMANN, D. & PFEFFER, S. 2012. TLR2 expression is regulated by microRNA miR-19 in rheumatoid fibroblast-like synoviocytes. *J Immunol,* 188**,** 454-61.

PICARD, F., BREHM, M., FASSBACH, M., PELZER, B., SCHEURING, S., KÜRY, P., STRAUER, B. E. & SCHWARTZKOPFF, B. 2006. Increased cardiac mRNA expression of matrix metalloproteinase-1 (MMP–1) and its inhibitor (TIMP–1) in DCM patients. *Clinical Research in Cardiology,* 95**,** 261-269.

PIPERIGKOU, Z. & KARAMANOS, N. K. 2019. Dynamic Interplay between miRNAs and the Extracellular Matrix Influences the Tumor Microenvironment. *Trends Biochem Sci,* 44**,** 1076-1088.

POLYAKOVA, E. A., MIKHAYLOV, E. N., SONIN, D. L., CHEBURKIN, Y. V. & GALAGUDZA, M. M. 2021. Neurohumoral, cardiac and inflammatory markers in the evaluation of heart failure severity and progression. *J Geriatr Cardiol,* 18**,** 47-66.

POLYTARCHOU, C., HOMMES, D. W., PALUMBO, T., HATZIAPOSTOLOU, M., KOUTSIOUMPA, M., KOUKOS, G., VAN DER MEULEN-DE JONG, A. E., OIKONOMOPOULOS, A., VAN DEEN, W. K., VORVIS, C., SEREBRENNIKOVA, O. B., BIRLI, E., CHOI, J., CHANG, L., ANTON, P. A., TSICHLIS, P. N., POTHOULAKIS, C., VERSPAGET, H. W. & ILIOPOULOS, D. 2015. MicroRNA214 Is Associated With Progression of Ulcerative Colitis, and Inhibition Reduces Development of Colitis and Colitis-Associated Cancer in Mice. *Gastroenterology,* 149**,** 981-92.e11.

PORTER, K. E. & TURNER, N. A. 2009. Cardiac fibroblasts: at the heart of myocardial remodeling. *Pharmacol Ther,* 123**,** 255-78.

POZNYAK, A. V., IVANOVA, E. A., SOBENIN, I. A., YET, S. F. & OREKHOV, A. N. 2020. The Role of Mitochondria in Cardiovascular Diseases. *Biology (Basel),* 9.

PRABHU, S. D. & FRANGOGIANNIS, N. G. 2016. The Biological Basis for Cardiac Repair After Myocardial Infarction: From Inflammation to Fibrosis. *Circ Res,* 119**,** 91-112.

RAFIEIAN-KOPAEI, M., SETORKI, M., DOUDI, M., BARADARAN, A. & NASRI, H. 2014. Atherosclerosis: process, indicators, risk factors and new hopes. *Int J Prev Med,* 5**,** 927-46.

RAMACHANDRA, R. K., SALEM, M., GAHR, S., REXROAD, C. E., 3RD & YAO, J. 2008. Cloning and characterization of microRNAs from rainbow trout (Oncorhynchus mykiss): their expression during early embryonic development. *BMC Dev Biol,* 8**,** 41.

REVENKO, A., CARNEVALLI, L. S., SINCLAIR, C., JOHNSON, B., PETER, A., TAYLOR, M., HETTRICK, L., CHAPMAN, M., KLEIN, S., SOLANKI, A., GATTIS, D., WATT, A., HUGHES, A. M., MAGIERA, L., KAR, G., IRELAND, L., MELE, D. A., SAH, V., SINGH, M., WALTON, J., MAIRESSE, M., KING, M., EDBROOKE, M., LYNE, P., BARRY, S. T., FAWELL, S., GOLDBERG, F. W. & MACLEOD, A. R. 2022. Direct targeting of FOXP3 in Tregs with AZD8701, a novel antisense oligonucleotide to relieve immunosuppression in cancer. *J Immunother Cancer,* 10.

RICHES, K., MORLEY, M. E., TURNER, N. A., O'REGAN, D. J., BALL, S. G., PEERS, C. & PORTER, K. E. 2009. Chronic hypoxia inhibits MMP-2 activation and cellular invasion in human cardiac myofibroblasts. *J Mol Cell Cardiol,* 47**,** 391-9.

RINALDI, C. & WOOD, M. J. A. 2018. Antisense oligonucleotides: the next frontier for treatment of neurological disorders. *Nature Reviews Neurology,* 14**,** 9-21.

ROCA-ALONSO, L., CASTELLANO, L., MILLS, A., DABROWSKA, A. F., SIKKEL, M. B., PELLEGRINO, L., JACOB, J., FRAMPTON, A. E., KRELL, J., COOMBES, R. C., HARDING, S. E., LYON, A. R. & STEBBING, J. 2015. Myocardial MiR-30 downregulation triggered by doxorubicin drives alterations in β-adrenergic signaling and enhances apoptosis. *Cell Death & Disease,* 6**,** e1754-e1754.

ROSELL-GARCÍA, T., PARADELA, A., BRAVO, G., DUPONT, L., BEKHOUCHE, M., COLIGE, A. & RODRIGUEZ-PASCUAL, F. 2019. Differential cleavage of lysyl oxidase by the metalloproteinases BMP1 and ADAMTS2/14 regulates collagen binding through a tyrosine sulfate domain. *J Biol Chem,* 294**,** 11087-11100.

ROY, S., KHANNA, S., HUSSAIN, S. R., BISWAS, S., AZAD, A., RINK, C., GNYAWALI, S., SHILO, S., NUOVO, G. J. & SEN, C. K. 2009. MicroRNA expression in response to murine myocardial infarction: miR-21 regulates fibroblast metalloprotease-2 via phosphatase and tensin homologue. *Cardiovasc Res,* 82**,** 21-9.

SAADAT, S., NOUREDDINI, M., MAHJOUBIN-TEHRAN, M., NAZEMI, S., SHOJAIE, L., ASCHNER, M., MALEKI, B., ABBASI-KOLLI, M., RAJABI MOGHADAM, H., ALANI, B. & MIRZAEI, H. 2020. Pivotal Role of TGF-β/Smad Signaling in Cardiac Fibrosis: Non-coding RNAs as Effectual Players. *Front Cardiovasc Med,* 7**,** 588347.

SAMNEGÅRD, A., SILVEIRA, A., TORNVALL, P., HAMSTEN, A., ERICSSON, C. G. & ERIKSSON, P. 2006. Lower serum concentration of matrix metalloproteinase-3 in the acute stage of myocardial infarction. *J Intern Med,* 259**,** 530-6.

SAVARY, G., BUSCOT, M., DEWAELES, E., HENAOUI, I. S., QUARRÉ, S., COURCOT, E., CAUFFIEZ, C., BARBRY, P., PERRAIS, M., MARI, B. & POTTIER, N. 2014. MiR-214-3p, a new fibromiR involved in the pathogenesis of idiopathic pulmonary fibrosis. *European Respiratory Journal,* 44**,** 1731.

SAYED, D., HONG, C., CHEN, I. Y., LYPOWY, J. & ABDELLATIF, M. 2007. MicroRNAs play an essential role in the development of cardiac hypertrophy. *Circ Res,* 100**,** 416-24.

SAYED, D., RANE, S., LYPOWY, J., HE, M., CHEN, I. Y., VASHISTHA, H., YAN, L., MALHOTRA, A., VATNER, D. & ABDELLATIF, M. 2008. MicroRNA-21 targets Sprouty2 and promotes cellular outgrowths. *Mol Biol Cell,* 19**,** 3272-82.

SCHAFER, S., VISWANATHAN, S., WIDJAJA, A. A., LIM, W. W., MORENO-MORAL, A., DELAUGHTER, D. M., NG, B., PATONE, G., CHOW, K., KHIN, E., TAN, J., CHOTHANI, S. P., YE, L., RACKHAM, O. J. L., KO, N. S. J., SAHIB, N. E., PUA, C. J., ZHEN, N. T. G., XIE, C., WANG, M., MAATZ, H., LIM, S., SAAR, K., BLACHUT, S., PETRETTO, E., SCHMIDT, S., PUTOCZKI, T., GUIMARÃES-CAMBOA, N., WAKIMOTO, H., VAN HEESCH, S., SIGMUNDSSON, K., LIM, S. L., SOON, J. L., CHAO, V. T. T.,

CHUA, Y. L., TAN, T. E., EVANS, S. M., LOH, Y. J., JAMAL, M. H., ONG, K. K., CHUA, K. C., ONG, B. H., CHAKARAMAKKIL, M. J., SEIDMAN, J. G., SEIDMAN, C. E., HUBNER, N., SIN, K. Y. K. & COOK, S. A. 2017. IL-11 is a crucial determinant of cardiovascular fibrosis. *Nature,* 552**,** 110-115.

SCHULTZ, W. M., KELLI, H. M., LISKO, J. C., VARGHESE, T., SHEN, J., SANDESARA, P., QUYYUMI, A. A., TAYLOR, H. A., GULATI, M., HAROLD, J. G., MIERES, J. H., FERDINAND, K. C., MENSAH, G. A. & SPERLING, L. S. 2018. Socioeconomic Status and Cardiovascular Outcomes. *Circulation,* 137**,** 2166-2178.

SCHUMACHER, S., DEDDEN, D., NUNEZ, R. V., MATOBA, K., TAKAGI, J., BIERTÜMPFEL, C. & MIZUNO, N. 2021. Structural insights into integrin α(5)β(1) opening by fibronectin ligand. *Sci Adv,* 7.

SCHWARTZ, M. A. 2010. Integrins and extracellular matrix in mechanotransduction. *Cold Spring Harb Perspect Biol,* 2**,** a005066.

SCIARRETTA, S., VOLPE, M. & SADOSHIMA, J. 2014. Mammalian target of rapamycin signaling in cardiac physiology and disease. *Circ Res,* 114**,** 549-64.

SEDGWICK, B., RICHES, K., BAGEGHNI, S. A., O'REGAN, D. J., PORTER, K. E. & TURNER, N. A. 2014. Investigating inherent functional differences between human cardiac fibroblasts cultured from nondiabetic and Type 2 diabetic donors. *Cardiovasc Pathol,* 23**,** 204-10.

SHI, H., ZHANG, X., HE, Z., WU, Z., RAO, L. & LI, Y. 2017. Metabolites of Hypoxic Cardiomyocytes Induce the Migration of Cardiac Fibroblasts. *Cell Physiol Biochem,* 41**,** 413-421.

SHIN, S. Y., CHOI, C., LEE, H. G., LIM, Y. & LEE, Y. H. 2012. Transcriptional regulation of the interleukin-11 gene by oncogenic Ras. *Carcinogenesis,* 33**,** 2467-76.

SHINDE, A. V., HUMERES, C. & FRANGOGIANNIS, N. G. 2017. The role of α-smooth muscle actin in fibroblast-mediated matrix contraction and remodeling. *Biochimica et Biophysica Acta (BBA) - Molecular Basis of Disease,* 1863**,** 298-309.

SHOCHET, G. E., BROOK, E., BARDENSTEIN-WALD, B., GROBE, H., EDELSTEIN, E., ISRAELI-SHANI, L. & SHITRIT, D. 2020. Integrin alpha-5 silencing leads to myofibroblastic differentiation in IPF-derived human lung fibroblasts. *Ther Adv Chronic Dis,* 11**,** 2040622320936023.

SIDDESHA, J. M., VALENTE, A. J., SAKAMURI, S. S., YOSHIDA, T., GARDNER, J. D., SOMANNA, N., TAKAHASHI, C., NODA, M. & CHANDRASEKAR, B. 2013. Angiotensin II stimulates cardiac fibroblast migration via the differential regulation of matrixins and RECK. *J Mol Cell Cardiol,* 65**,** 9-18.

SIEGEL, R. C. & FU, J. C. 1976. Collagen cross-linking. Purification and substrate specificity of lysyl oxidase. *Journal of Biological Chemistry,* 251**,** 5779-5785.

SIWIK, D. A. & COLUCCI, W. S. 2004. Regulation of matrix metalloproteinases by cytokines and reactive oxygen/nitrogen species in the myocardium. *Heart Fail Rev,* 9**,** 43-51.

SOUDERS, C. A., BOWERS, S. L. & BAUDINO, T. A. 2009a. Cardiac fibroblast: the renaissance cell. *Circ Res,* 105**,** 1164-76.

SOUDERS, C. A., BOWERS, S. L. K. & BAUDINO, T. A. 2009b. Cardiac Fibroblast. *Circulation Research,* 105**,** 1164-1176.

STAVAST, C. J. & ERKELAND, S. J. 2019. The Non-Canonical Aspects of MicroRNAs: Many Roads to Gene Regulation. *Cells,* 8.

STEWART, L. & TURNER, N. A. 2021. Channelling the Force to Reprogram the Matrix: Mechanosensitive Ion Channels in Cardiac Fibroblasts. *Cells,* 10.

SUN, M., YU, H., ZHANG, Y., LI, Z. & GAO, W. 2015. MicroRNA-214 Mediates Isoproterenol-induced Proliferation and Collagen Synthesis in Cardiac Fibroblasts. *Scientific Reports,* 5**,** 18351.

SUNDSTRÖM, J., EVANS, J. C., BENJAMIN, E. J., LEVY, D., LARSON, M. G., SAWYER, D. B., SIWIK, D. A., COLUCCI, W. S., SUTHERLAND, P., WILSON, P. W. & VASAN, R. S. 2004. Relations of plasma matrix metalloproteinase-9 to clinical cardiovascular risk factors and echocardiographic left ventricular measures: the Framingham Heart Study. *Circulation,* 109**,** 2850-6.

SWEENEY, M., CORDEN, B. & COOK, S. A. 2020. Targeting cardiac fibrosis in heart failure with preserved ejection fraction: mirage or miracle? *EMBO Mol Med,* 12**,** e10865.

TANG, C. M., LIU, F. Z., ZHU, J. N., FU, Y. H., LIN, Q. X., DENG, C. Y., HU, Z. Q., YANG, H., ZHENG, X. L., CHENG, J. D., WU, S. L. & SHAN, Z. X. 2016. Myocyte-specific enhancer factor 2C: a novel target gene of miR-214-3p in suppressing angiotensin II-induced cardiomyocyte hypertrophy. *Sci Rep,* 6**,** 36146.

TASAKI, S., XU, J., AVEY, D. R., JOHNSON, L., PETYUK, V. A., DAWE, R. J., BENNETT, D. A., WANG, Y. & GAITERI, C. 2022. Inferring protein expression changes from mRNA in Alzheimer's dementia using deep neural networks. *Nat Commun,* 13**,** 655.

TÄUBEL, J., HAUKE, W., RUMP, S., VIERECK, J., BATKAI, S., POETZSCH, J., RODE, L., WEIGT, H., GENSCHEL, C., LORCH, U., THEEK, C., LEVIN, A. A., BAUERSACHS, J., SOLOMON, S. D. & THUM, T. 2021. Novel antisense therapy targeting microRNA-132 in patients with heart failure: results of a first-in-human Phase 1b randomized, double-blind, placebo-controlled study. *Eur Heart J,* 42**,** 178-188.

TAYLOR, H. A., SIMMONS, K. J., CLAVANE, E. M., TREVELYAN, C. J., BROWN, J. M., PRZEMYŁSKA, L., WATT, N. T., MATTHEWS, L. C. & MEAKIN, P. J. 2022. PTPRD and DCC Are Novel BACE1 Substrates Differentially Expressed in Alzheimer's Disease: A Data Mining and Bioinformatics Study. *Int J Mol Sci,* 23.

THUM, T., GROSS, C., FIEDLER, J., FISCHER, T., KISSLER, S., BUSSEN, M., GALUPPO, P., JUST, S., ROTTBAUER, W., FRANTZ, S., CASTOLDI, M., SOUTSCHEK, J., KOTELIANSKY, V., ROSENWALD, A., BASSON, M. A., LICHT, J. D., PENA, J. T., ROUHANIFARD, S. H., MUCKENTHALER, M. U., TUSCHL, T., MARTIN, G. R., BAUERSACHS, J. & ENGELHARDT, S. 2008. MicroRNA-21 contributes to myocardial disease by stimulating MAP kinase signalling in fibroblasts. *Nature,* 456**,** 980-4.

TRIALS.GOV, C. 2022. *Study of Lademirsen (SAR339375) in Patients With Alport Syndrome (HERA)* [Online]. https://clinicaltrials.gov/ct2/show/NCT02855268: Clinical Trials.gov. [Accessed 29/11/2022 2022].

TURCHINOVICH, A., WEIZ, L., LANGHEINZ, A. & BURWINKEL, B. 2011. Characterization of extracellular circulating microRNA. *Nucleic Acids Res,* 39**,** 7223-33.

TURNER, N. A. 2011. Therapeutic regulation of cardiac fibroblast function: targeting stress-activated protein kinase pathways. *Future Cardiology,* 7**,** 673-691.

TURNER, N. A. 2014. Effects of interleukin-1 on cardiac fibroblast function: relevance to post-myocardial infarction remodelling. *Vascul Pharmacol,* 60**,** 1-7.

TURNER, N. A. 2016. Inflammatory and fibrotic responses of cardiac fibroblasts to myocardial damage associated molecular patterns (DAMPs). *J Mol Cell Cardiol,* 94**,** 189-200.

TURNER, N. A. & BLYTHE, N. M. 2019. Cardiac Fibroblast p38 MAPK: A Critical Regulator of Myocardial Remodeling. *J Cardiovasc Dev Dis,* 6.

TURNER, N. A., DAS, A., O'REGAN, D. J., BALL, S. G. & PORTER, K. E. 2011. Human cardiac fibroblasts express ICAM-1, E-selectin and CXC chemokines in response to proinflammatory cytokine stimulation. *Int J Biochem Cell Biol,* 43**,** 1450-8.

TURNER, N. A. & PORTER, K. E. 2012. Regulation of myocardial matrix metalloproteinase expression and activity by cardiac fibroblasts. *IUBMB Life,* 64**,** 143-50.

TURNER, N. A. & PORTER, K. E. 2013. Function and fate of myofibroblasts after myocardial infarction. *Fibrogenesis Tissue Repair,* 6**,** 5.

UCAR, A., GUPTA, S. K., FIEDLER, J., ERIKCI, E., KARDASINSKI, M., BATKAI, S., DANGWAL, S., KUMARSWAMY, R., BANG, C., HOLZMANN, A., REMKE, J., CAPRIO, M., JENTZSCH, C., ENGELHARDT, S., GEISENDORF, S., GLAS, C., HOFMANN, T. G., NESSLING, M., RICHTER, K., SCHIFFER, M., CARRIER, L., NAPP, L. C., BAUERSACHS, J., CHOWDHURY, K. & THUM, T. 2012. The miRNA-212/132 family regulates both cardiac hypertrophy and cardiomyocyte autophagy. *Nature Communications,* 3**,** 1078.

VAN BALKOM, B. W., DE JONG, O. G., SMITS, M., BRUMMELMAN, J., DEN OUDEN, K., DE BREE, P. M., VAN EIJNDHOVEN, M. A., PEGTEL, D. M., STOORVOGEL, W., WÜRDINGER, T. & VERHAAR, M. C. 2013. Endothelial cells require miR-214 to secrete exosomes that suppress senescence

and induce angiogenesis in human and mouse endothelial cells. *Blood,* 121**,** 3997-4006, s1-15.

VAN LINTHOUT, S., MITEVA, K. & TSCHÖPE, C. 2014. Crosstalk between fibroblasts and inflammatory cells. *Cardiovasc Res,* 102**,** 258-69.

VAN NIEUWENHOVEN, F. A., HEMMINGS, K. E., PORTER, K. E. & TURNER, N. A. 2013. Combined effects of interleukin-1α and transforming growth factor-β1 on modulation of human cardiac fibroblast function. *Matrix Biol,* 32**,** 399-406.

VAN NIEUWENHOVEN, F. A. & TURNER, N. A. 2013. The role of cardiac fibroblasts in the transition from inflammation to fibrosis following myocardial infarction. *Vascul Pharmacol,* 58**,** 182-8.

VAN ROOIJ, E., SUTHERLAND, L. B., LIU, N., WILLIAMS, A. H., MCANALLY, J., GERARD, R. D., RICHARDSON, J. A. & OLSON, E. N. 2006. A signature pattern of stress-responsive microRNAs that can evoke cardiac hypertrophy and heart failure. *Proc Natl Acad Sci U S A,* 103**,** 18255-60.

VISSE, R. & NAGASE, H. 2003. Matrix Metalloproteinases and Tissue Inhibitors of Metalloproteinases. *Circulation Research,* 92**,** 827-839.

WANG, B., YAO, K., HUUSKES, B. M., SHEN, H. H., ZHUANG, J., GODSON, C., BRENNAN, E. P., WILKINSON-BERKA, J. L., WISE, A. F. & RICARDO, S. D. 2016. Mesenchymal Stem Cells Deliver Exogenous MicroRNA-let7c via Exosomes to Attenuate Renal Fibrosis. *Mol Ther,* 24**,** 1290-301.

WANG, F., LV, P., LIU, X., ZHU, M. & QIU, X. 2015. microRNA-214 enhances the invasion ability of breast cancer cells by targeting p53. *Int J Mol Med,* 35**,** 1395-402.

WANG, H., PENG, R., WANG, J., QIN, Z. & XUE, L. 2018a. Circulating microRNAs as potential cancer biomarkers: the advantage and disadvantage. *Clin Epigenetics,* 10**,** 59.

WANG, W., SCHULZE, C. J., SUAREZ-PINZON, W. L., DYCK, J. R., SAWICKI, G. & SCHULZ, R. 2002. Intracellular action of matrix metalloproteinase-2 accounts for acute myocardial ischemia and reperfusion injury. *Circulation,* 106**,** 1543-9.

WANG, W., YUAN, X., XU, A., ZHU, X., ZHAN, Y., WANG, S. & LIU, M. 2018b. Human cancer cells suppress behaviors of endothelial progenitor cells through miR-21 targeting IL6R. *Microvasc Res,* 120**,** 21-28.

WANG, Y. C. A. X. 2022. *hsa-miR-224-5p* [Online]. mirdb.org: Yuhao Chen and Xiaowei Wang. Available: https://mirdb.org/cgi-bin/search.cgi?searchType=miRNA&full=mirbase&searchBox=MIMAT0000281 [Accessed 19/10/2022 2022].

WATANABE, K., NARUMI, T., WATANABE, T., OTAKI, Y., TAKAHASHI, T., AONO, T., GOTO, J., TOSHIMA, T., SUGAI, T., WANEZAKI, M., KUTSUZAWA, D., KATO, S., TAMURA, H., NISHIYAMA, S., TAKAHASHI, H., ARIMOTO, T., SHISHIDO, T. & WATANABE, M. 2020. The association between microRNA-21 and hypertension-induced cardiac remodeling. *PLoS One,* 15**,** e0226053.

WATSON, C. J., GUPTA, S. K., O'CONNELL, E., THUM, S., GLEZEVA, N., FENDRICH, J., GALLAGHER, J., LEDWIDGE, M., GROTE-LEVI, L., MCDONALD, K. & THUM, T. 2015. MicroRNA signatures differentiate preserved from reduced ejection fraction heart failure. *Eur J Heart Fail,* 17**,** 405-15.

WHITMARSH, A. J. 2010. A central role for p38 MAPK in the early transcriptional response to stress. *BMC Biol,* 8**,** 47.

WIDJAJA, A. A., VISWANATHAN, S., JINRUI, D., SINGH, B. K., TAN, J., WEI TING, J. G., LAMB, D., SHEKERAN, S. G., GEORGE, B. L., SCHAFER, S., CARLING, D., ADAMI, E. & COOK, S. A. 2021. Molecular Dissection of Pro-Fibrotic IL11 Signaling in Cardiac and Pulmonary Fibroblasts. *Front Mol Biosci,* 8**,** 740650.

WIGHT, T. N. & POTTER-PERIGO, S. 2011. The extracellular matrix: an active or passive player in fibrosis? *Am J Physiol Gastrointest Liver Physiol,* 301**,** G950-5.

XIAO, J., GAO, R., BEI, Y., ZHOU, Q., ZHOU, Y., ZHANG, H., JIN, M., WEI, S., WANG, K., XU, X., YAO, W., XU, D., ZHOU, F., JIANG, J., LI, X. & DAS, S. 2017. Circulating miR-30d Predicts Survival in Patients with Acute Heart Failure. *Cell Physiol Biochem,* 41**,** 865-874.

XU, F., ZHANG, L., KODER, R. L. & NANDA, V. 2010. De novo self-assembling collagen heterotrimers using explicit positive and negative design. *Biochemistry,* 49**,** 2307-16.

XU, Q., GUOHUI, M., LI, D., BAI, F., FANG, J., ZHANG, G., XING, Y., ZHOU, J., GUO, Y. & KAN, Y. 2021. lncRNA C2dat2 facilitates autophagy and apoptosis via the miR-30d-5p/DDIT4/mTOR axis in cerebral ischemia-reperfusion injury. *Aging (Albany NY),* 13**,** 11315-11335.

XU, Y., HUANG, Y., ZHANG, S., GUO, L., WU, R., FANG, X., CHEN, X., XU, H. & NIE, Q. 2022. CircDCLRE1C Regulated Lipopolysaccharide-Induced Inflammatory Response and Apoptosis by Regulating miR-214b-3p/STAT3 Pathway in Macrophages. *Int J Mol Sci,* 23.

YAMADA, D., KOBAYASHI, S., WADA, H., KAWAMOTO, K., MARUBASHI, S., EGUCHI, H., ISHII, H., NAGANO, H., DOKI, Y. & MORI, M. 2013. Role of crosstalk between interleukin-6 and transforming growth factor-beta 1 in epithelial-mesenchymal transition and chemoresistance in biliary tract cancer. *Eur J Cancer,* 49**,** 1725-40.

YAN, L., QIU, J. & YAO, J. 2017. Downregulation of microRNA-30d promotes cell proliferation and invasion by targeting LRH-1 in colorectal carcinoma. *Int J Mol Med,* 39**,** 1371-1380.

YAN, Y., MA, Z., ZHU, J., ZENG, M., LIU, H. & DONG, Z. 2020. miR-214 represses mitofusin-2 to promote renal tubular apoptosis in ischemic acute kidney injury. *Am J Physiol Renal Physiol,* 318**,** F878-f887.

YANG, K., SHI, J., HU, Z. & HU, X. 2019. The deficiency of miR-214-3p exacerbates cardiac fibrosis via miR-214-3p/NLRC5 axis. *Clinical Science,* 133**,** 1845-1856.

YANG, L., WANG, B., ZHOU, Q., WANG, Y., LIU, X., LIU, Z. & ZHAN, Z. 2018. MicroRNA-21 prevents excessive inflammation and cardiac dysfunction after myocardial infarction through targeting KBTBD7. *Cell Death Dis,* 9**,** 769.

YANG, T. S., YANG, X. H., WANG, X. D., WANG, Y. L., ZHOU, B. & SONG, Z. S. 2013. MiR-214 regulate gastric cancer cell proliferation, migration and invasion by targeting PTEN. *Cancer Cell Int,* 13**,** 68.

YANG, X., QIN, Y., SHAO, S., YU, Y., ZHANG, C., DONG, H., LV, G. & DONG, S. 2016. MicroRNA-214 Inhibits Left Ventricular Remodeling in an Acute Myocardial Infarction Rat Model by Suppressing Cellular Apoptosis via the Phosphatase and Tensin Homolog (PTEN). *Int Heart J,* 57**,** 247-50.

YANG, X., YU, T. & ZHANG, S. 2020. MicroRNA-489 suppresses isoproterenol-induced cardiac fibrosis by downregulating histone deacetylase 2. *Exp Ther Med,* 19**,** 2229-2235.

YAO, G., YIN, M., LIAN, J., TIAN, H., LIU, L., LI, X. & SUN, F. 2010. MicroRNA-224 is involved in transforming growth factor-beta-mediated mouse granulosa cell proliferation and granulosa cell function by targeting Smad4. *Mol Endocrinol,* 24**,** 540-51.

YE, C., YU, X., LIU, X., DAI, M. & ZHANG, B. 2018. miR-30d inhibits cell biological progression of Ewing's sarcoma by suppressing the MEK/ERK and PI3K/Akt pathways in vitro. *Oncol Lett,* 15**,** 4390-4396.

YIN, Y., LV, L. & WANG, W. 2019. Expression of miRNA-214 in the sera of elderly patients with acute myocardial infarction and its effect on cardiomyocyte apoptosis. *Exp Ther Med,* 17**,** 4657-4662.

YOULE, R. J. & VAN DER BLIEK, A. M. 2012. Mitochondrial fission, fusion, and stress. *Science,* 337**,** 1062-5.

YU, H., PARDOLL, D. & JOVE, R. 2009. STATs in cancer inflammation and immunity: a leading role for STAT3. *Nature Reviews Cancer,* 9**,** 798-809.

YUAN, J., CHEN, H., GE, D., XU, Y., XU, H., YANG, Y., GU, M., ZHOU, Y., ZHU, J., GE, T., CHEN, Q., GAO, Y., WANG, Y., LI, X. & ZHAO, Y. 2017. Mir-21 Promotes Cardiac Fibrosis After Myocardial Infarction Via Targeting Smad7. *Cell Physiol Biochem,* 42**,** 2207-2219.

YUE, B. 2014. Biology of the extracellular matrix: an overview. *J Glaucoma,* 23**,** S20-3.

ZHANG, G. J., ZHOU, H., XIAO, H. X., LI, Y. & ZHOU, T. 2013. Up-regulation of miR-224 promotes cancer cell proliferation and invasion and predicts relapse of colorectal cancer. *Cancer Cell Int,* 13**,** 104.

ZHANG, H. J., ZHAO, W., VENKATARAMAN, S., ROBBINS, M. E., BUETTNER, G. R., KREGEL, K. C. & OBERLEY, L. W. 2002. Activation of matrix metalloproteinase-2 by overexpression of manganese superoxide dismutase in human breast cancer MCF-7 cells involves reactive oxygen species. *J Biol Chem,* 277**,** 20919-26.

ZHANG, J., XING, Q., ZHOU, X., LI, J., LI, Y., ZHANG, L., ZHOU, Q. & TANG, B. 2017. Circulating miRNA-21 is a promising biomarker for heart failure. *Mol Med Rep,* 16**,** 7766-7774.

ZHANG, Y., ZHAO, Z., LI, S., DONG, L., LI, Y., MAO, Y., LIANG, Y., TAO, Y. & MA, J. 2019. Inhibition of miR-214 attenuates the migration and invasion of triple-negative breast cancer cells. *Mol Med Rep,* 19**,** 4035-4042.

ZHAO, B., HU, M., WU, H., REN, C., WANG, J. & CUI, S. 2017a. Tenascin-C expression and its associated pathway in BMSCs following co-culture with mechanically stretched ligament fibroblasts. *Mol Med Rep,* 15**,** 2465-2472.

ZHAO, Q., YUAN, X., ZHENG, L. & XUE, M. 2022. miR-30d-5p: A Non-Coding RNA With Potential Diagnostic, Prognostic and Therapeutic Applications. *Front Cell Dev Biol,* 10**,** 829435.

ZHAO, S., XIAO, X., SUN, S., LI, D., WANG, W., FU, Y. & FAN, F. 2018. MicroRNA-30d/JAG1 axis modulates pulmonary fibrosis through Notch signaling pathway. *Pathol Res Pract,* 214**,** 1315-1323.

ZHAO, T., MU, X. & YOU, Q. 2017b. Succinate: An initiator in tumorigenesis and progression. *Oncotarget,* 8**,** 53819-53828.

ZHENG, H., SHI, L., TONG, C., LIU, Y. & HOU, M. 2021. circSnx12 Is Involved in Ferroptosis During Heart Failure by Targeting miR-224-5p. *Front Cardiovasc Med,* 8**,** 656093.

ZHENG, Y., KONG, Y. & LI, F. 2014. Krüppel-like transcription factor 11 (KLF11) overexpression inhibits cardiac hypertrophy and fibrosis in mice. *Biochem Biophys Res Commun,* 443**,** 683-8.

ZHOU, B. & TIAN, R. 2018. Mitochondrial dysfunction in pathophysiology of heart failure. *J Clin Invest,* 128**,** 3716-3726.

ZHOU, J., HU, M., WANG, F., SONG, M., HUANG, Q. & GE, B. 2017. miR-224 Controls Human Colorectal Cancer Cell Line HCT116 Proliferation by Targeting Smad4. *Int J Med Sci,* 14**,** 937-942.

ZHOU, J., WANG, K. C., WU, W., SUBRAMANIAM, S., SHYY, J. Y., CHIU, J. J., LI, J. Y. & CHIEN, S. 2011. MicroRNA-21 targets peroxisome proliferators-activated receptor-alpha in an autoregulatory loop to modulate flow-induced endothelial inflammation. *Proc Natl Acad Sci U S A,* 108**,** 10355-60.

ZHOU, P. & PU, W. T. 2016. Recounting Cardiac Cellular Composition. *Circ Res,* 118**,** 368-70.

ZHOU, X.-L., XU, H., LIU, Z.-B., WU, Q.-C., ZHU, R.-R. & LIU, J.-C. 2018. miR-21 promotes cardiac fibroblast-to-myofibroblast transformation and myocardial fibrosis by targeting Jagged1. *Journal of Cellular and Molecular Medicine,* 22**,** 3816-3824.

ZHU, W. S., TANG, C. M., XIAO, Z., ZHU, J. N., LIN, Q. X., FU, Y. H., HU, Z. Q., ZHANG, Z., YANG, M., ZHENG, X. L., WU, S. L. & SHAN, Z. X. 2016. Targeting EZH1 and EZH2 contributes to the suppression of fibrosis-associated genes by miR-214-3p in cardiac myofibroblasts. *Oncotarget,* 7**,** 78331-78342.

ZILE, M. R., MEHURG, S. M., ARROYO, J. E., STROUD, R. E., DESANTIS, S. M. & SPINALE, F. G. 2011. Relationship between the temporal profile of plasma microRNA and left ventricular remodeling in patients after myocardial infarction. *Circ Cardiovasc Genet,* 4**,** 614-9.

ZOU, Y. C., YAN, L. M., GAO, Y. P., WANG, Z. Y. & LIU, G. 2020. miR-21 may Act as a Potential Mediator Between Inflammation and Abnormal Bone Formation in Ankylosing Spondylitis Based on TNF-α Concentration-Dependent Manner Through the JAK2/STAT3 Pathway. *Dose Response,* 18**,** 1559325819901239.